Laporan Akhir Projek Penyelidikan Jangka Pendek

Development of Novel Silica/HT Nanocore Multishell Particles for Transesterification of Jatropha Curcas Oil

By
Assoc. Prof. Mohd Roslee Othman
Assoc. Prof. Ahmad Zuhairi Abdullah
Assoc. Prof. Norashid Aziz

2012

Fuel Processing Technology 90 (2009) 1502–1514

Contents lists available at ScienceDirect

Fuel Processing Technology

journal homepage: www.elsevier.com/locate/fuproc

Technologies for production of biodiesel focusing on green catalytic techniques: A review

Z. Helwani [a,b], M.R. Othman [b,*], N. Aziz [b], W.J.N. Fernando [b], J. Kim [c,*]

[a] Department of Chemical Engineering, Riau University, Pekanbaru 28293, Indonesia
[b] School of Chemical Engineering, Universiti Sains Malaysia, 14300 Nibong Tebal, Penang, Malaysia
[c] Department of Chemical Engineering, Kyung Hee University, Yongin, 446-701, Republic of Korea

ARTICLE INFO

Article history:
Received 3 February 2009
Received in revised form 25 June 2009
Accepted 25 July 2009

Keywords:
Biodiesel
Transesterification
Heterogeneous catalyst
Hydrotalcite

ABSTRACT

Biodiesel production is undergoing rapid technological reforms in industries and academia. This has become more obvious and relevant since the recent increase in the petroleum prices and the growing awareness relating to the environmental consequences of the fuel overdependency. In this paper, various technological methods to produce biodiesel being used in industries and academia are reviewed. Catalytic transesterification, the most common method in the production of biofuel, is emphasized in the review. The two most common types of catalysts; homogeneous liquids and heterogeneous solids, are discussed at length in the paper. Two types of processes; batch and continuous processes, are also presented. Although batch production of biodiesel is favored over continuous process in many laboratory and larger scale efforts, the latter is expected to gain wider acceptance in the near future, considering its added advantages associated with higher production capacity and lower operating costs to ensure long term supply of biodiesel.

1. Introduction

Biodiesel is a fuel derived from the transesterification of fats and oils [1–6]. This fuel has similar properties to that of diesel produced from crude oil and can be used directly to run existing diesel engines or as a mixture with crude oil diesel. The main advantages of using biodiesel is that it is biodegradable, can be used without modifying existing engines, and produces less harmful gas emissions such as sulfur oxide [3–5]. Biodiesel reduces net carbon dioxide emissions by 78% on a life-cycle basis when compared to conventional diesel fuel [7]. It has also been shown to have dramatic improvements on engine exhaust emissions. For instance, combustion of neat biodiesel decreases carbon monoxide (CO) emissions by 46.7%, particulate matter emissions by 66.7% and unburned hydrocarbons by 45.2% [8]. Additionally, biodiesel is non-toxic, making it useful for transportation applications in highly sensitive environments, such as marine ecosystems and mining enclosures.

The predominant base-catalyzed production process requires the use of high quality, high purity virgin oils. The chemistry of the base transesterification reaction in use limits feedstock flexibility due to unwanted side reactions (neutralization reactions) [9,10] and the currently employed catalysts are not reused so they must be neutralized and discarded as an aqueous salt waste stream. Furthermore, the predominant production mode is a batch or semi-continuous process (reactants added continuously to a flow reactor). Operational problems in the conventional production process are typically linked to the catalyst (e.g. potassium and sodium hydroxide) because they are hazardous, caustic, and hygroscopic.

However, biodiesel is still far more expensive than conventional petroleum-derived diesel due to the higher feedstock and processing costs. By creating a continuous process it may be possible to reduce the production cost and hence lower the overall cost of biodiesel, making the price of biodiesel more competitive [1–5]. At present several countries such as Brazil, United States, Germany, Australia, Italy and Austria are already using bioethanol or blended/diesel and biodiesel. Other countries such as Malaysia use blend fuel (5% palm oil, 95% regular diesel). It is expected that this trend will grow and more countries will use biofuels [10–14] as a complementary strategy for sustainability.

This paper reviews biodiesel production by transesterification of triglycerides from a catalytic standpoint since there is a need to use heterogeneous catalysts and to replace or complement the current homogeneous catalysts with the heterogeneous ones, to incorporate catalysts that are effective for a broader spectrum of reactants that can tolerate higher levels of impurities [15–17] and to develop improved continuous processing technologies rather than batch processing. The first half of the paper includes the most important aspects of the current biodiesel production schemes that employ homogeneous

* Corresponding authors. Othman is to be contacted at Tel.: +60 45996426; fax: +60 45941013. Kim, Tel.: +82 31 201 2492; fax: +82 31 202 1946.
E-mail addresses: chroslee@eng.usm.my (M.R. Othman), jkim21@khu.ac.kr (J. Kim).

0378-3820/$ - see front matter © 2009 Elsevier B.V. All rights reserved.
doi:10.1016/j.fuproc.2009.07.016

liquid alkali and acid catalysts. The second half of the paper reviews biodiesel production using heterogeneous solid catalysts, such as metals, anchored metal complexes, solid bases and solid acids.

2. Current biodiesel production technologies using liquid catalysts

There are different methods of biodiesel production and application such as direct use and blending, microemulsions, thermal cracking (Pyrolysis) of vegetable oil and transesterification [18]. Some methodologies proposed in the past, such as pyrolysis and cracking of oils and fats, can produce compounds that are smaller than their triglyceride (TG) source and, therefore, suitable to be used as a fuel [1,16]. However, pyrolysis is not very selective and a wide range of compounds is usually obtained. Depending on the TG source and the pyrolytic method employed, alkanes, alkenes, aromatic compounds, esters, CO_2, CO, water, and H_2 are produced in varying proportions. Oxygen removal from substrate molecules is another downside of pyrolytic production methods. Fuels obtained by pyrolysis of TGs are less environmentally pleasant than petroleum-derived fuels in terms of oxygen content. In addition, solid residues of ash and carbon that are created during TG pyrolysis require additional separation steps. Catalytic cracking has been used in an effort to control the types of products generated by TG cracking, using a vast variety of catalysts [19,20], including: SiO_2/Al_2O_3 [21], NiMo/g-Al_2O_3 [22], $NiSiO_2$ [23], Al_2O_3 [24], MgO [24], composites of zeolites [25], and Al-MCM-41 [26,27]. However, a gasoline-like fuel is more likely to be formed than a diesel-like fuel [28].

The most common method of biodiesel production is transesterification (alcoholysis) of oil (triglycerides) with methanol in the presence of a catalyst which gives biodiesel (fatty acid methyl esters, FAME) and glycerol (by-product). The selection of catalyst depends on the amount of free fatty acid (FFA) present in the oil. Generally, the catalysts are base, acid, or enzyme. For triglyceride stock having lower amount of FFAs, base-catalyzed reaction gives a better conversion in a relatively short time while for higher FFAs containing stock, acid-catalyzed esterification followed by transesterification is suitable [17]. The stoichiometric reaction requires 1 mol of triglyceride and 3 mol of alcohol. However, excess alcohol is used to drive the reversible reaction forward in order to increase the yields of the alkyl esters and to assist phase separation from the glycerol. Fig. 1 shows the reaction of triglyceride with alcohol in the presence of a catalyst producing biodiesel (mixture of alkyl esters) and glycerol [17].

Most biodiesel production of today utilizes batch reactors. Biodiesel plants using batch reactors can produce between 500 and 10,000 tons of biodiesel per year. This number can be increased if continuous processing technology is applied. A number of successful experiments resulting in increased biodiesel production form continuous processes have been reported in the literature [29–34].

Although continuous production plants can achieve higher biodiesel throughputs and are less costly to operate per biodiesel unit, batch plants are less expensive to build and can more easily be adapted to changing raw materials and reaction conditions. This flexibility is particularly important given the economic impetus to use diverse TG feedstock for biodiesel production. Nevertheless, current trend is leaning toward the construction of continuous production plants to ensure sustainability of biodiesel supply [15,35] and lower operational cost by increasing the volume.

2.1. Homogeneous base-catalyzed transesterification

The transesterification process is catalyzed by alkaline metal alkoxides [36,37] and hydroxides [38–41], as well as sodium or potassium carbonates [42]. The alkaline catalysts normally show high performance when vegetable oils with high quality is used. However, when the oils contain significant amounts of free fatty acids, they cannot be converted into biodiesels but to a lot of soap [43]. These free fatty acids react with the alkaline catalyst to produce soaps that inhibit the separation of biodiesel, glycerin and wash water [44]. Triglycerides are readily transesterified batchwise in the presence of alkaline catalyst at atmospheric pressure and at a temperature of approximately 60–70 ° C with an excess of methanol [2]. It often takes at least several hours to ensure the alkali (NaOH or KOH) catalytic transesterification reaction is complete. Removal of these catalysts is technically difficult and it brings extra cost to the final product [45,46].

Alkaline metal alkoxides (as CH_3ONa for the methanolysis) are most active catalysts, since they give very high yields (>98%) in short reaction times (30 min) even if they are applied at low molar concentrations (0.5 mol%). Alkaline metal hydroxides (KOH and NaOH) are cheaper than metal alkoxides, but less active. Nevertheless, they are a good alternative since they can give the same high conversions of vegetable oils simply by increasing the catalyst concentration to 1 or 2 mol% [17]. It was reported that 100 g of vegetable oil is transesterified in methanol (200 ml) containing fresh sodium (0.8 g) for the purpose of sodium methoxide-catalyzed transesterification. The reaction was quite fast between a vegetable oil and sodium methoxide in methanol. The triglycerides were completely transesterified in 2–5 min at room temperature (293–298 K) through sodium methoxide-catalyzed transesterification compared to 60–360 min in acid- and alkali-catalyzed processes at higher temperature of 303–338 K [47].

During transesterification, the glycerin that is formed needs to be removed so that it is not converted into formaldehyde or acetaldehyde when burned because both would pose a health hazard [48]. Base-catalyzed transesterification is much faster than acid-catalyzed transesterification and is the most commonly used method commercially [18]. Putting that together with the fact that the alkaline catalysts are

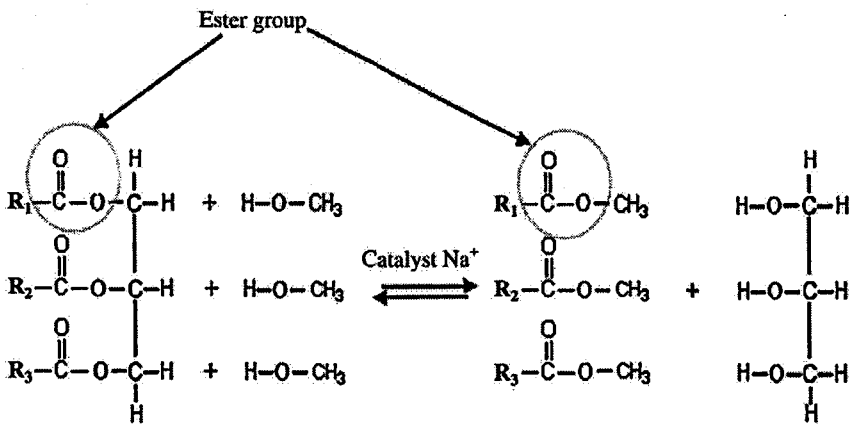

Fig. 1. Overall scheme of the triglycerides transesterification.

Table 1
Typical reaction conditions for biodiesel synthesis using homogeneous base catalysis [29].

	Base-catalyzed biodiesel synthesis
Feedstocks	Triglyceride mixtures with low free fatty acid contents (<0.5%) e.g. Refined vegetable oils + anhydrous short chain alcohol (generally, methanol)
Alcohol-to-oil molar ratio (recommended)	6:1
Temperature	60–65 °C
Pressure	1.4–4.1 bar
Catalyst	NaOH (most common)
Catalyst concentration (by weight of lipid feedstock)	0.5–2 wt.%
Conversions ≥95% can be expected after 1 h reaction	

less corrosive than acidic compounds, industrial processes usually favor base catalysts such as alkaline metal alkoxides and hydroxides as well as sodium or potassium carbonates.

Table 1 shows typical reaction conditions for base-catalyzed transesterification in biodiesel synthesis. Fig. 2 depicts a simplified block flow diagram (BFD) for a typical biodiesel production process using base catalysis [29].

2.2. Homogeneous acid-catalyzed transesterification

One advantage of acid catalysts over base catalysts is their low susceptibility to the presence of FFA in the starting feedstock. However, acid-catalyzed transesterification is especially sensitive to water concentration. It was demonstrated, previously, that as little as 0.1 wt.% water in the reaction mixture was able to affect ester yields in transesterification of vegetable oil with methanol, with the reaction almost completely inhibited at 5 wt.% water concentration [49]. Water content should be kept under 0.5 wt.% to achieve higher than 90% ester yield under their reaction conditions (60 ° C, methanol-to-oil molar ratio 6:1, 3 wt.% sulfuric acid and 96 h). Similar condition also applies for methyl ester formation by the transesterification of rapeseed oil with methanol using base and acid catalysts (1.5 wt.% NaOH and 3 wt.% H_2SO_4). Previous study shows that water concentration was more critical in acid catalysis than in base catalysis [50]. However, none addresses the cause for the observed difference in transesterification sensitivity to water using either base or acid catalysts.

The transesterification of small esters under acid-catalyzed conditions can be retarded by the presence of spectator polar compounds. Given that water can form water-rich clusters around protons (solvent–proton complexes) with less acid strength than methanol-only proton complexes [51–52], some catalyst deactivation may be expected with increased water concentrations. Water-rich methanol proton complexes that are less hydrophobic than methanol-only clusters can make it more difficult for the catalytic species (H^+) to approach the hydrophobic TG (and possibly DG) molecules that eventually contributes to catalyst deactivation. In the presence of water in the feedstock or when water is produced in significant quantities, some catalyst can be deactivated by hydration. Increased water concentration was found to affect transesterification more than it affects esterification [49,53]. This is due to the presence of polar carboxylic functional groups in FFAs that allows FFAs to interact readily with polar compounds, promoting the alcoholysis reaction.

In general, acid-catalyzed reactions are performed at high alcohol-to-oil molar ratios, low-to-moderate temperatures and pressures, and high acid catalyst concentrations. Table 2 summarizes reaction conditions in order to obtain biodiesel from waste cooking oil using sulfuric acid as the catalyst [29]. A simplified BFD of the acid process is shown in Fig. 3.

2.3. Transesterification and reaction variables

The transesterification reaction is normally a sequence of three consecutive reversible reactions [54]. In this process triglyceride is converted stepwise into diglyceride, monoglyceride, and, finally, glycerol in which 1 mol of alkyl esters is formed in each step. Several aspects, including the type of catalyst (alkaline or acid), alcohol/vegetable oil molar ratio, temperature, purity of the reactants (mainly water content), and free fatty acid content, influence the transesterification rates [17,46]. If a glyceride contains high free fatty acid and water, acid-catalyzed transesterification is suitable [1]. Nevertheless, there are some limitations. The alkali-catalyzed process is sensitive to both water and FFA content due to occurrence of saponification reaction under alkaline conditions. On the other hand, the reaction rate

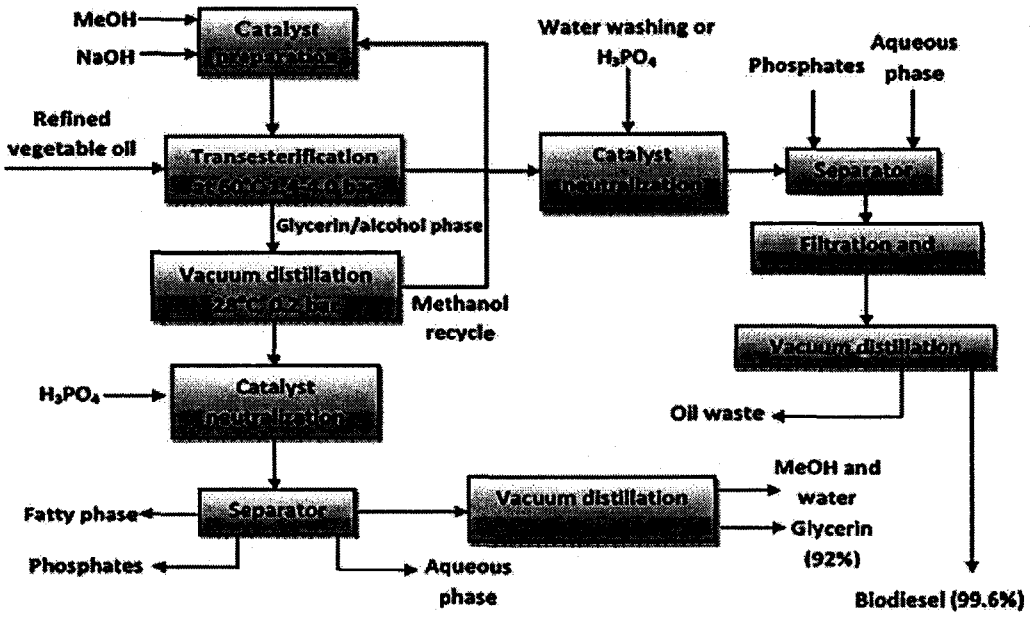

Fig. 2. A simplified block flow diagram for a typical base-catalyzed process for the production of biodiesel.

Table 2
Reaction conditions used by Zhang et al. in the acid-catalyzed synthesis of biodiesel from waste cooking oil [29].

	Acid-catalyzed biodiesel synthesis
Feedstocks	Triglyceride mixtures with high free fatty acid contents (>4%) e.g., waste cooking oil oil + methanol
Alcohol-to-oil molar ratio (recommended)	50:1
Temperature	80 °C
Pressure	4 bar
Catalyst	H_2SO_4
Catalyst load	1:3:1 molar ratio of sulfuric acid to waste oil
An oil conversion of 97% is expected after 4 h of reaction	

of the acid-catalyzed process is relatively slower [55]. A remedial measure to minimize or prevent the soap formation is by using 2 or 3 mol% K_2CO_3. The key role of K_2CO_3 in this example is the formation of corresponding bicarbonate salt instead of water. Similarly, during the production of non digestible polyol polyesters through interesterification of fatty acids with polyols, e.g. sucrose, the application of low temperature and/or high pressure to increase the mass transfer area, using back mixing in the initial stages, and plug-flow conditions in the final stages can be exercised [46].

The overall reaction is also controlled by three mechanisms: mass transfer, kinetic and equilibrium. The mass transfer becomes slow if the immiscibility of the two reactants (i.e. methanol and triglycerides) is poor. On the completion of the mass transfer, the ensuing process is controlled by the kinetic. The forward and reverse reactions can either follow a second order reaction based on an alcohol-to-oil mole ratio of 6:1 or a pseudo-first order for higher alcohol-to-oil mole ratio such as 30:1 [37,56]. A higher reaction rate can be obtained when higher alcohol-to-oil ratio is used. However, the alcohol separation and purification at the end of the esterification process is complicated and costly. In addition, at higher alcohol–oil ratios the separation of glycerol from ester becomes difficult [39]. Due to these limitations, majority of batch processes use a 6:1 alcohol-to-oil mole ratio.

Both kinetic and mass transfer of the reaction can be improved by increasing the reaction temperatures and vigorous mixing [56–58]. As in any reaction, increase in temperature increases reaction rate exponentially. An increase in temperature also allows the reactants to be more miscible, allowing a higher rate of reaction to take place. The solubility of methanol and ethanol in beef tallow at different temperatures reveals that the solubility of the alcohols increased in the triglyceride phase as the temperature was increased [18]. However, the operating temperature is limited by the boiling point of the alcohol used as a reactant (e.g. 67 °C at atmospheric pressure if methanol is used).

In the study of the kinetics of palm oil transesterification in a batch reactor, it was demonstrated that, while the overall conversion of the process did not change with temperature, the rate of the transesterification process was increased with temperature [58]. The overall reaction kinetics is dependent on the individual rate constants for the conversion of triglyceride to diglyceride, monoglyceride and alcohol ester. The conversion of triglyceride to diglyceride was reportedly the slowest in the transesterification based on the rate constants [57,58]. The time needed for the mass transfer to occur was shortened as temperature was increased, leading to a higher rate of transesterification.

Alternatively, vigorous mixing can be utilized to increase the rate of collision between the reactants and to homogenize the reaction mixture. The alcohol (e.g. methanol) and the triglyceride source (typically vegetable oil/animal fat) are immiscible and tend to form two layers. Vigorous mixing increases the mass transfer rate by dispersing the alcohol as fine droplets in the triglyceride phase, thereby increasing the contact surface area between the two immiscible reactants [59]. In a study on the effect of impeller speed (300–700 rpm) and reaction temperature (25 and 65 °C) on the transesterification of sunflower oil over a 1-min period [56], it was found that the formation of methyl ester increased as the impeller speed was increased from 300 to 600 rpm. The triglyceride conversion reached its maximum value at 600 rpm. The rate of methyl ester formation was also increased as the reaction temperature increased from 25 to 65 °C.

A secondary solvent (co-solvent) which is soluble in both reactants (i.e. alcohol and triglyceride) can also be used as an alternative to create a homogeneous phase. A common co-solvent for this application has been THF (tetrahydrofuran), with a boiling point of 67 °C [18,56,60–62]. A study on the effects of using a secondary solvent (THF) on the transesterification of soybean oil to biodiesel shows that the reaction yield was increased due to the reduction of mass transfer resistance [60]. The co-solvent improved the solubility of the alcohol in the triglyceride phase, allowing better mixing of the two phases and hence more reactions to take place. However, it should be noted that when co-solvent is used, the processing cost is higher due to the extra processing equipment required for the separation of the co-solvent and the cost of the co-solvent itself.

Most biodiesel production processes using alkali-catalyzed approach require that the oils be pre-treated in order to achieve the required FFAs of ±0.5 wt.% . In the US, most biodiesel is produced from refined soybean oil, which accounts for 60–75% of the total cost of biodiesel [63].

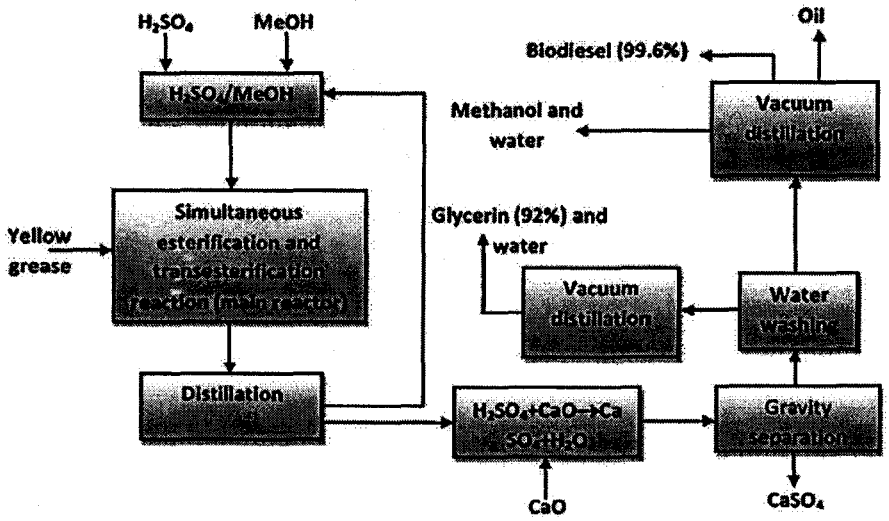

Fig. 3. A simplified block flow diagram of the acid-catalyzed process for the production of biodiesel.

Even though inedible animal fats, waste cooking oil, and brown grease can sell for significantly less than refined vegetable oils, elevated FFA concentrations are becoming a major issue. Processing alternatives like acid–base integrated process allows for the use of low cost, low quality feedstocks, but these technologies still require additional catalyst, processing steps and time, thereby eliminating some of the gains obtained by the use of lower cost feedstocks.

2.4. Reactor design

The operation and design of reactor is one of the important issues in catalytic biorenewable processes. A number of catalytic processes need multiphase reactor systems with catalyst geometries that accommodate for the attributes of renewable feedstocks: low volatility, thermal stability and multiple reaction phases. The reactions that occur not only take place within a single fluid phase (such as acid–base-catalyzed condensation), but there are also multiphase reactions (liquid–gas–solid catalyst) which are affected by diffusional and thermal effects. These reactions need heterogeneous reactors like fluidized bed, entrained flow, trickle bed, slurry phase, bubbling bed and fixed bed reactors to facilitate adequate contact between fluid phases and catalyst [64].

Reactors are usually characterized as batch or continuous. Both can be either a continuous stirred tank reactors (CSTRs) or plug flow reactors (PFRs) [3,34,65–67]. The most important consideration in reactor design is the extent of product conversion. Key reactor variables that dictate conversion and selectivity are temperature, pressure, reaction time (residence time in continuous reactors), and degree of mixing. In transesterification, the selectivity of the reaction is not adversely affected by the increase in temperature. However, an increase in the reaction temperature does impact the operating pressure.

Since this reaction is usually conducted in liquid phase, the pressure in the reactor must be maintained at a sufficient level that keeps the methanol in the liquid phase. Depending on the reactor type, this can render the production cost of biodiesel unnecessarily higher. The conversion rate can be improved by increasing the reaction time. However, increasing the reaction time can decrease the chemical throughput or increase the reactor size. Another important parameter in the reactor design is the degree of mixing. For batch reactors and CSTRs the degree of mixing is directly related to the amount of energy introduced through the impeller. However, a threshold exists where additional mixing will not provide any performance enhancement. For PFRs, the degree of mixing is dictated by the design of the reactor (i.e. length and the use of static mixers) and the flow pattern created within the reactor (i.e. turbulence or laminar) [5,65–68]. The common continuous reactors investigated for the production of biodiesel are: plug flow reactor [34], oscillatory flow reactor [66], reactive distillation column [69], continuous high temperature gas–liquid reactor [Patent WO 01/88072 A1] [70], and combined plug flow/CSTR arrangement [65]. The overall objectives of these continuous reactors are to reduce post reaction cleaning and total processing time.

With the exception of the patented reactor, all biodiesel reactors have the underlying similarity in that they operate in a liquid/liquid phase [34,65–71]. The major limitation of the CSTR or tubular reactors is that the reaction temperature is limited to alcohol boiling point of 65 ° C (for methanol) if the reactor is to be operated at atmospheric pressure and significant mass transfer resistance is expected in the industrial size reactor even when using higher shear mixing.

The process design, reactor design and catalyst design should be considered in an integrated manner to optimize the operation of the catalytic processes in a biorefinery. Mass and heat transfer as well as residence time and flow patterns should be considered properly during a reactor design so that the catalyst performs to its maximum designed capacity [64].

2.5. Biodiesel purification process

The use of homogeneous catalysts in biodiesel synthesis presents separation and catalyst recovery issues. For instance, process methodologies using homogeneous alkali catalysts necessitate a multi-step preparation and purification protocol since such catalysts tolerate neither moisture nor FFAs. As previously mentioned, presence of water can constitute a major problem. It was reported that water and FFA contents of beef tallow were maintained below 0.06 wt.% and 0.5 wt.%, respectively, in order to yield effective transesterification reaction under alkaline conditions [18]. Thus, low water levels appear to be even more critical than FFA levels.

Crude biodiesel is initially purified by thoroughly washing the ester phase with water or by neutralization with a polyprotic mineral acid to eliminate base catalyst residues. Next, in a settling tank, an aqueous phase, salt precipitates, and biodiesel are separated. Another water washing step follows to further remove polar compounds that might still be present in the biodiesel product. Finally, the biodiesel is vacuum distillated at moderate-to-high temperatures (around 190–270 ° C) to comply with ASTM specifications (99.6% or purer) [29].

Vacuum distillation step is used for methanol recycle prior to glycerin purification. The remaining base catalyst in the crude glycerin is commonly neutralized with low cost mineral acids, such as phosphoric acid. This operation also converts the soaps back to FFAs. After neutralization, three distinct phases are formed: a low density (top) layer containing FFAs, a dense (bottom) liquid layer composed of glycerin, water and alcohol, and a third layer made of salt precipitates. These three phases are then separated with the non glycerin layers being treated as waste. Glycerin is further purified by distillation to remove water and alcohol. This procedure yields 90–95% pure glycerin for commercial use.

Even though the role of homogeneous catalysts are significant for the industrial or large scale production of biodiesel and for easy conversion at moderate temperatures (40 to 65 ° C), a major drawback is always present during separation and purification of the product. It was reported [72] that the solubility of homogeneous catalysts either in biodiesel layer and or in glycerin layer was possible only to a certain extent. Methods such as extensive bubble washing, spray washing, counter current washing, and agitation are used to wash and purify the contaminated products. However, these processes are considered time consuming and uneconomical. Besides, catalysts contaminated crude glycerol which is separated by gravitational settling or centrifuging can further compound the seriousness of the issue.

3. Potential technology using solid catalysts

Attempts at improving the process for biodiesel production have been ongoing for decades [73,74]. The ideal process would involve a continuous flow reaction that neither deactivate nor consume the catalyst and that minimizes or eliminates the need for multitudinous downstream separation and purification steps. Various approaches have been investigated including reactive distillation [75–77], continuous flow centrifugation [34], homogeneous catalysts overlaid on a bed of porous non-catalytic particles [78], and oscillatory flow reactors [66]. Microwave heating in conjunction with heterogeneous barium, alumina, silica, zinc aluminate, and zirconium-based catalysts have also been reported [79–81] with promising results.

Alternative production methods have also emerged from laboratory/bench-scale research aimed at reducing the cost of biodiesel [45,67]. One such method uses alcohol in its supercritical state that eliminates the need for a catalyst. The supercritical process requires only a short residence time to reach high conversion [53]. Another option is to use a solid catalyst [43,82,83] which simplifies downstream purification of the biodiesel. The catalyst can be separated by physical methods such as a hydrocyclone in the case

where a multiphase reactor is used. Alternatively, a fixed bed reactor would eliminate the catalyst removal step in entirety.

3.1. Heterogeneous solid catalysis in biodiesel production

Biodiesel production employing homogeneous base-catalyzed process is still favorable despite the issues discussed earlier. The main reason is due to the fact that it is kinetically much faster than heterogeneously catalyzed transesterification and is economically viable [84]. The high consumption of energy and costly separation of the homogeneous catalyst from the reaction mixture, however, have called for development of heterogeneous catalyst. The number of researches in the area of heterogeneous catalysts has increased recently. A great variety of catalysts in catalytic transesterification of vegetable oils have been used. These include zeolites, hydrotalcites, oxides, γ-alumina, etcetera. Table 3 lists different heterogenous catalysts for transesterification of vegetable oils reported in the literature. Most of these catalysts are alkali or alkaline oxides supported over large surface area supports. Similar to their homogeneous counterparts, solid basic catalysts are more active than solid acid catalysts [91,92]. CaO, used as a solid basic catalyst, possesses many advantages such as long catalyst lifetimes, higher activity and requirement of only mild reaction conditions. The reaction rate, however, was slow in producing biodiesel [98].

Despite lower activity, solid acid catalysts have been used in many industrial processes because they contain a variety of acid sites with different strength of Bronsted or Lewis acidity, compared to the homogenous acid catalysts. Solid acid catalysts, such as Nafion-NR50, sulfated zirconia and tungstated zirconia were chosen to catalyze biodiesel-forming transesterification due to the presence of sufficient acid site strength. Among the solid catalysts, Nafion demonstrated higher selectivity towards the production of methyl ester and glycerol due to its acid strength [101–103]. However, Nafion has disadvantages of high cost and lower activity compared to liquid acids [102].

Vegetable oil containing FFA was found to react with base catalyst forming soap which would deactivate the base catalyst and result in inefficient target reaction. It was reported that the transesterification of vegetable oil using sulfated zirconia as heterogeneous acid catalysts (SO_4^{-2}/ZrO_2) and tungstated zirconia (WO_3/ZrO_2) successfully converted the FFA to FAME prior to the biodiesel production. The pellet-type WO_3/ZrO_2 was used for the reaction with longer time and it was found that 65% conversion could be maintained for up to 140 h [96]. In another study [102], the production of high quality biodiesel fuel from vegetable oil using solid heteropolyacid ($Cs_{2.5}H_{0.5}PW_{12}O_{40}$) shows that the catalyst was capable of producing 99% yield using only low catalyst concentration (1.85×10^{-3}:1 weight ratio of catalyst to oil), low methanol-to-oil ratio (5.3:1) in a relatively short reaction time (45 min) at low temperature (338 K). The process was environmentally benign and economical since the activity of the $Cs_{2.5}PW$ was not considerably affected by the free fatty acid and moisture content in the vegetable oil, and the catalyst could be easily separated from the product mixture and reused number of times.

In general, the factors which govern the path of transesterification reactions are: the nature of the raw materials, types of catalysts and optimum experimental conditions (temperature, oil to methanol ratio and catalyst concentration). As far as experimental condition is concerned, for the generation of methyl ester with high yield, optimization of certain parameters or the application of optimized parameters is necessary. For example, a solid base catalyst, prepared under specified conditions of 3.5 wt.% KNO_3 loadings on Al_2O_3 substrate followed by calcinations at 773 K for 5 h produced the catalytic group of Al–O–K and favored the conversion of soybean oil into methyl esters [85] with a FAME yield of more than 75%. Similarly, a heterogeneous base catalyst (Na/NaOH/γ-Al_2O_3) used in the reaction at temperatures of 25–65 ° C and a catalyst concentration of 1–3% was found to achieve conversion rate that was over two orders of magnitude [83].

Compared to homogenously catalyzed process, the transesterification with solid catalyst can tolerate more extreme reaction conditions i.e. at higher temperatures and pressures. This is because of the fact that the solid catalyzed process is an immiscible liquid/liquid/solid 3-phase system (corresponding to oil, methanol and catalyst) that is highly mass transfer limited [104]. The temperature could go from 70 ° C to as high as 200 ° C to achieve more than 95% of yield using MgO, CaO, TiO_2 and CHT catalysts [105–107].

In biodiesel production of jatropha curcas oil [95] with CaO solid catalyst dipped in ammonium nitrate followed by calcination at 900 °C, it was shown than conversion of 93% was achieved after 3.5 h of transesterification at reaction temperature of 70 ° C, catalyst dosages and the oil to methanol ratio of 1.5% and 9:1, respectively. A yield in excess of 95% was observed below 70 °C within 30 min in soybean oil transesterification [99] with SrO as a heterogeneous catalyst. A long catalyst lifetime of SrO was also observed and it was able to sustain the activity after repeated usage for 10 cycles.

Heterogeneous catalyst is reportedly used in the fatty acid methyl esther (FAME) plant of Diester Industrie (Paris) at Sete, France. The Esterfip-H process produces FAME by esterification of plant oils such as that from rapeseed, soybean or sunflower. The heterogeneous catalyst is a spinel mixed oxide of two (non-noble) metals, which eliminate several neutralization and washing steps needed for processes using homogeneous catalysts. The purity of methyl esters exceed 99%, which yield close to 100%. In addition, the heterogeneous process produces glycerol as by-product with purity of better than 98% compared to about 80% from homogeneous process. The overall production economic improves through the utilization of the by-product [108].

Table 3
Different heterogeneous catalysts used for transesterification of vegetable oils.

Vegetable oil	Catalysts	Ratio MeOH/Oil	Reaction time, h	Temperature, °C	Conversion, %	References
Blended vegetable oil	Mesoporous silica loaded with MgO	8	5	220	96	[85]
Soybean oil	WO_3/ZrO_2, zirconia–alumina and sulfated tin oxide	40	20	200–300	90	[43]
Soybean oil	Calcined LDH (Li–Al)	15	1–6	65	71.9	[86]
Palm oil	Mg–Al–CO_3 (hydrotalcite)	30	6	100	86.6	[87,88]
Soybean oil	La/zeolite beta	14.5	4	160	48.9	[89]
Soybean oil	MgO $MgAl_2O_4$	3	10	65	57	[90]
Sunflower oil	NaOH/alumina	6–48	1	50	99	[91]
Soybean oil	MgO, ZnO, Al_2O_3	55	7	70, 100, 130	82	[92]
Soybean oil	Cu and Co	6	3	70		[93]
Sunflower oil	CaO/SBA-15	12	5	160	95	[94]
Jatropha Curcas oil	CaO	9	2.5	70	93	[95]
VO	Cs-heteropoly acid, SO_4^{2-}/ZrO_2, $SO4^{2-}/Al_2O_3$, $SO_4^{2-}/SiO2$, WO_3/ZrO_2	19.4	1	75	70	[96]
Rape oil	Mg–Al HT	6	4	65	90.5	[97]
Soybean oil	CaO, SrO	12	0.5–3	65	95	[98,99]
Soybean oil	ETS-10	6	24	120	94.6	[83]
Cotton seed oil	Mg–Al–CO_3 HT	6	12	180–210	87	[100]

In most of the solid catalyzed experiments, the reaction proceeds at a relatively slow rate [109]. The presence of heterogeneous catalysts turns the reaction mixture into a three-phase system, i.e., oil–methanol-catalyst, which protracts the reaction for the purpose of effective mass transfer. At the same time, heterogeneous catalysis requires relatively harsh reaction conditions in order to achieve the desirable conversion and yield. It was reported that temperatures as low as 78 K to as high as 1000 K were also used [110].

3.1.1. A special reference to hydrotalcites

Hydrotalcite-like compounds (HTlcs) are a class of anionic and basic clays known as layered double hydroxides (LDH) with the formula $Mg_6Al_2(OH)_{16}CO_3.4H_2O$ (Fig. 4). It presents a positively charged brucite-like layers ($Mg(OH)_2$) in which some of Mg^{2+} are replaced by Al^{3+} in the octahedral sites of hydroxide sheets. Interstitial layers formed by CO_3^{2-} anions and water molecules compensate the positive charge resulting from this substitution. Both magnesium and aluminum can be isomorphously substituted by other divalent or trivalent cations, and a wide range of compositions containing various combinations of M(II), M (III) and different anions A^{n-} can be synthesized [111].

In recent years these materials have received considerable attention because they are used in a wide range of application such as adsorbent for liquid ions [112] and gas molecules [113]. They also find use as catalyst [114], precursors [115] and other catalytic reactions [116]. Their most important applications are due to their permanent anion-exchange and adsorption capacity, the mobility of their interlayer anions and water molecules, their large surface areas and the stability and homogeneity of the materials formed by their thermal decomposition [117].

Decomposition of Mg–Al hydrotalcite yields a high surface area Mg–Al mixed oxide, which presumably exposes strong Lewis base sites [118–121]. The basic properties of these sites depend on the Mg–Al ratio in the precursor hydrotalcite [122]. Interestingly, the reconstruction of decomposed Mg–Al hydrotalcite by rehydration at room temperature has been reported to enhance the catalytic activity [123]. During rehydration, the brucite-like layers are reformed and the charge-compensating carbonate anions are replaced by hydroxyl anions, thus forming Brønsted base sites. The decomposed-rehydrated Mg–Al hydrotalcite with Brønsted base sites exhibits higher catalytic activity than the decomposed Mg–Al hydrotalcite with Lewis base sites for the aldol condensation of benzaldehyde with acetone [123], aldol condensation of citral with ketones, selfaldolization of acetone [124], Michael addition reactions [125], and the transesterification of oleic acid methyl ester with glycerol [121]. It was reported that thermally activated Mg–Al hydrotalcites with various Mg–Al ratios were effective catalysts for transesterification of tributyrin with methanol, with increasing catalytic activity as the Mg content in the Mg–Al hydrotalcite increased [126]. The catalytic transesterification of glyceryl tributyrate with methanol to form methyl butanoate was investigated using a series of Mg/Al hydrotalcites. Triglyceride conversion to methyl ester occurred immediately without an induction period with concomitant formation of glyceride. The yield of the primary products rose linearly with triglyceride consumption over the first 15 min of reaction, after which secondary transesterification of the diglyceride to monoglyceride initiated. The activities of higher Mg loading (21 and 24 wt.% Mg) in hydrotalcites were found comparable to those reported for the best alternative Li-doped CaO solid base catalysts of 2.5 mmol $min^{-1}g\ (cat)^{-1}$. Pure MgO showed lower activity and selectivity, attributed to reduced number of accessible basic sites. The catalytic activities of these hydrotalcites also showed stark correlation with their corresponding intralayer charge densities favoring tributyrate transesterification. This increased intralayer electron density of the Mg rich hydrotalcites was correlated with increase of basicity of these materials. All hydrotalcite materials are effective catalysts for the transesterification of glyceryl tributyrate with methanol. The rate of esterification normally increases steadily with Mg content and is reportedly 10 times more active than MgO.

In the methanolysis experiments using Mg–Al hydrotalcite (by co-precipitation method) catalysts [86,87,100,126], the optimum conversions of soybean oil and glyceryl tributyrate were 80%. In transesterification of rape oil with methanol using calcined Mg–Al hydrotalcite (that exhibited different properties than untreated hydrotalcite), about 90.5% conversion was achieved [97]. This demonstrates the importance of the micro-structural properties and the need to improve them. A convenient method to change the properties of LDH and their calcinations products can be made using sol–gel [127]. This method is favorable due to the ease of preparation, product's homogeneity at the molecular level, high deposition rate, easy introduction of the dopants and it does not involve expensive steps like in vacuum deposition [128]. Sol–gel processing can be applied at room temperature [129] and pressure by different but simple arrangements [130]. The specific surface area of the solids obtained with the sol–gel method was up to three times greater than that achieved by co-precipitation [131–134].

3.2. Enzyme catalyzed transesterification

Enzymatic methanolysis using lipases for biodiesel production is also increasingly researched. The main purpose is to overcome the issue involving recovery and treatment of the by-product that requires complex processing equipment [135]. The main drawback of enzyme catalyzed process stems from the high cost of the lipases as catalyst [136]. In order to reduce the cost, enzyme immobilization is introduced for ease of recovery and reused [137–142]. Although lipase catalyzed transesterification offers an attractive alternative, the industrial application of this technology has been slow due to feasibility aspects and some technical challenges.

Inactivation of enzyme that leads to the decrease of yields mostly stems from low solubility of methanol at moderate concentrations [143]. This problem can be resolved by stepwise addition of methanol [141]. Since the solubility of methanol in the alkyl esters is greater than in the oil, this procedure limits enzyme deactivation. The low solubility of glycerol in biodiesel also poses a challenge in enzymatic transesterification because it reduces the enzymes activity [142–146]. This problem can be overcome by simply using 1,4-dioxane as co-solvent to solubilize methanol. However, a high proportion of this solvent (90%) is necessary to obtain a reasonable conversion [147].

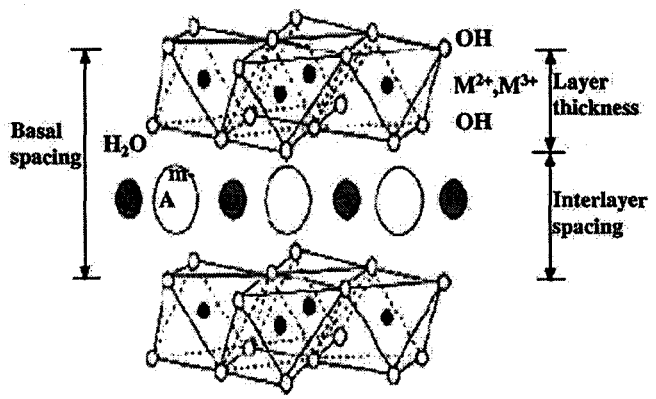

Fig. 4. Schematic representation of the hydrotalcite-type anionic clay structure.

4. Other potential technology for biodiesel production

An alternative technology for biodiesel production is non-catalytic transesterification with methanol under supercritical conditions (SC MeOH) [45,148]. The reaction is fast, conversion raises 50–95% for the first 10 min [84,149] but it requires temperature of 250–400 ° C and

pressures as high as 1200 psi [55,67], which leads to high production costs and energy consumption; the main obstacle to the commercialization. Other technologies that will be reviewed include hydrotreating and ESTERFIP Process.

4.1. Transesterification using supercritical fluids

In conventional transesterification of fats and vegetable oils for biodiesel production, the production free fatty acids and water are often undesirable because their presence causes soap to form and catalyst to deactivate. However, the presence of water has positive effects in non-catalytic supercritical method because it promotes the mechanisms of reaction. The technology is able to overcome the reaction initiation lag time caused by the extremely low solubility of the alcohol in the TG phase. Compared to chemical reactions using catalysts, the supercritical method offers 3 main advantages. First, it is environmentally friendly. Catalyst is not needed in the reaction, making the after-production process much simpler since the separating process of the catalyst and saponified products from methyl esters becomes unnecessary. The waste water containing acid or alkali resulted from the after-production process can also be avoided. Second, supercritical reaction takes a shorter reaction time than the traditional catalytic transesterification reaction, and the conversion rate is very high. The catalytic transesterification reaction requires several hours to reach reaction equilibrium, but the supercritical method only takes 2–4 min [148]. Third, neither acidity nor water content influences the reaction in supercritical method [53,150]. This allows a variety of resources to be used as feed materials. For instance, swill oil and frying oil having high acid value and water content and whose composition is complex, can be easily transformed into biodiesel in supercritical methanol. Table 4 provides comparison between catalytic commercial methanol process and supercritical methanol (SCM) method for biodiesel production from vegetable oils by transesterification.

The disadvantages of the supercritical methods stem mostly from high pressure and temperature requirement [151], high methanol-to-oil ratios (usually 42) that renders the production expensive and the process neither explain nor verify any compliance of free glycerol to less than 0.02% as established in the ASTM D6584 or other equivalent international standards.

4.2. Hydrotreating

Another route to the production of a diesel substitute from vegetable oils and fats is through hydrotreatment (HDT) of the triglyceride-containing feedstocks as shown in Fig. 5 [22,23,152]. The hydrocarbons are produced by two reaction pathways: (i) hydrodeoxygenation (HDO) and (ii) hydrodecarboxylation (HDC). n-Alkanes originating from HDO have the same carbon number as the original fatty acid chain, i.e. even carbon number, typically 16 or 18. The main reaction by-products of this route are water and propane. On the other hand, HDC yields hydrocarbons with an odd carbon number; they have one carbon atom less in the molecule than the original fatty acid chain. The dominant by-products are CO, CO_2 and propane [22,153,154].

Table 4
Comparisons between catalytic methanol (MeOH) process and supercritical methanol (SCM) method for biodiesel from vegetable oils by transesterification [148].

	Catalytic methanol process	SCM method
Methylating agent	Methanol	Methanol
Catalyst	Alkali	None
Reaction temperature (K)	303–338	523–573
Reaction pressure (Mpa)	0.1	10–25
Reaction time (min)	60–360	7–15
Methyl ester yield (%)	96	98
Removal for purification	Methanol, catalyst, glycerine, soaps	Methanol
Free fatty acid	Saponified products	Methyl ester, water

Hydrotreating is used in the petroleum refinery to remove S, N and metals from petroleum-derived feedstocks including heavy gas–oil or vacuum gas–oil [155]. Hydrotreating has been used to produce straight chain alkanes ranging from n-C_{15} to n-C_{18}, from a fatty acid fraction of tall oil (produced during kraft refining), and other vegetable oils [156–158]. The normal alkanes have a high cetane number (above 98) whereas typical diesel fuel has a cetane number around 45. The normal alkanes also have good cold flow properties. In fact a 10-month on-road test of six postal delivery vans showed that engine fuel economy was greatly improved by a blend of petro-diesel with hydrotreated tall oil. The advantages of hydrotreating over transesterification are that the former is compatible with the current infrastructure, the process leads to a deoxygenated and thus stable product that is fully compatible with petroleum-derived diesel fuels, the product exhibits high cetane number and low sulfur content [158–172].

Some petroleum refineries plan to annex hydrotreating facilities into their existing infrastructure with little capital investment. Others have begun to apply hydrotreatment technologies for the production of renewable diesel fuel from vegetable oils and animal fats. Neste Oil Corporation is currently adding 3500 barrels per day unit to their Porvoo Kilpilahti, Finland oil-refinery that produces diesel fuel from vegetable oil by a modified hydrotreating process [173]. They either take advantage of existing plants (oil refineries) by hydroconverting in HDT units blends of triglyceride-containing material with diesel

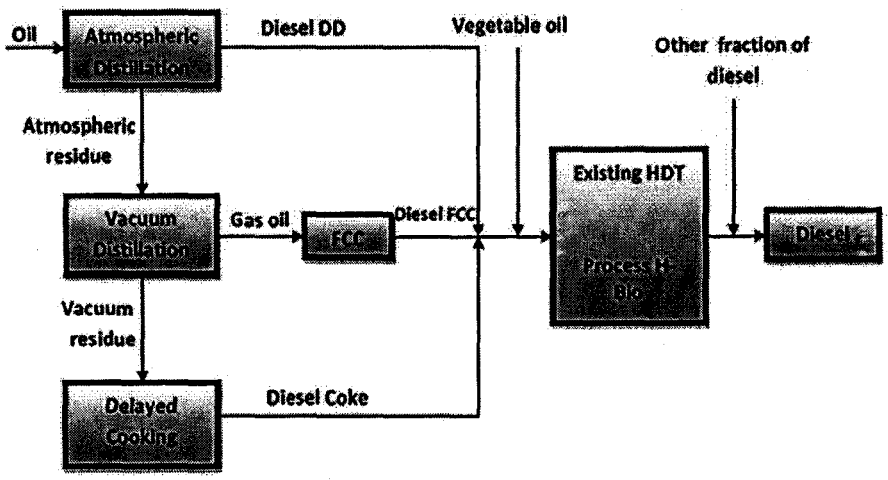

Fig. 5. Hydrotreating process.

streams derived from the various units of a refinery (atmospheric distillation, FCC, delayed coker, etc.) [174,175], or construct new plants for the production of neat renewable diesel fuel blending stock which can be used as cetane number improver of mineral diesel [176]. One of the major concerns for the application of the hydro-conversion process is the extent of the vegetable oil conversion at conventional hydroprocessing conditions. Blending of the hydrodesulfurized diesel with vegetable oils or fats and a subsequent hydrotreatment of the blend would offer flexibility in the production scheme and a very good alternative to the production of mixed petro-biodiesel.

In order to maintain the usefulness of the existing petroleum refinery infrastructure for vegetable oil conversion to diesel fuel, the vegetable oils need to be hydrotreated with petroleum-derived feedstocks such as heavy vacuum oil (HVO) with standard hydrotreating catalysts [177–182]. It is also possible to hydrotreat vegetable oils with petroleum feedstocks by diluting vegetable oils with HVO to increase the yield of straight chain alkanes. For example, a 5 wt.% sunflower oil to 95 wt.% HVO produces the maximum theoretical straight chain C_{15}–C_{18} yield of 87%. However, mixing the sunflower oil with HVO does not decrease the desulfurization.

4.3. Biodiesel via ESTERFIP process

Some solid metal oxides such as those of tin, magnesium, and zinc are known catalysts but they actually act according to a homogeneous mechanism and end up as metal soaps or metal glycerates. In this alternative process, transesterfication reaction is promoted by a completely heterogeneous catalyst. This catalyst consists of a mixed oxide of zinc and aluminum, which promotes the transesterification reaction without catalyst loss. The reaction is performed at higher temperature and pressure than homogeneous catalysis processes, with an excess of methanol. This excess is removed by vaporization and recycled to the process with fresh methanol [80].

The desired chemical conversion required to produce biodiesel is reached with two successive stages of reaction and glycerol separation in order to shift the equilibrium of methanolysis. The flow sheet of this process is presented in Fig. 6. The catalyst section includes two fixed bed reactors, fed with vegetable oil and methanol at a given ratio. Excess of methanol is removed after each reactor by partial evaporation. Then, esters and glycerol are separated in a settler. Glycerol outputs are gathered and the residual methanol is removed by evaporation. In order to obtain biodiesels that comply with the European specifications, the last traces of methanol and glycerol must be removed. The purification section of methyl ester coming from the second decanter consists of methanol vaporized under vacuum followed by a final purification in an adsorber for removing the soluble glycerol.

The main characteristics of the biodiesel fuels produced from rapeseed oil with the heterogeneous catalyst are summarized in Table 5. Glycerides content and methyl esters content determined by gas chromatography follows the European standard test methods (EN 14105/EN 14103). The main characteristics of the glycerin co-produced with methyl esters from rapeseed oil with the heterogeneous catalyst are presented in Table 6. The glycerin obtained is limpid and colorless. The glycerol content of the glycerin produced is at least 98%. Neither ash, nor inorganic compounds are detected in the glycerin produced. The major impurities of the glycerin are water, methanol and matter organic non-glycerol (MONG, such as methyl ester).

5. Future perspectives

Different technologies for the production of biodiesel are described and reviewed in the paper. Table 7 summarizes and compares these technologies. Current biodiesel production is in many aspects simple, operator friendly and, within their boundaries, efficient. Transesterification reaction is predominantly carried out in the presence of homogeneous catalyst. In this process, purification steps to isolate residual catalysts and soap need to be performed in order to remove the by-products from deactivating the catalysts. In addition, further neutralization and washing processing steps are required to eliminate catalysts residues, but this will increase the biodiesel production cost and raise environmental concerns.

A solid heterogeneous catalyst integrated with continuous processing technologies is expected to gain wider acceptance in the future due to its potential effectiveness and efficiency. The use of solid catalysts and continuous flow reactors may complement the existing

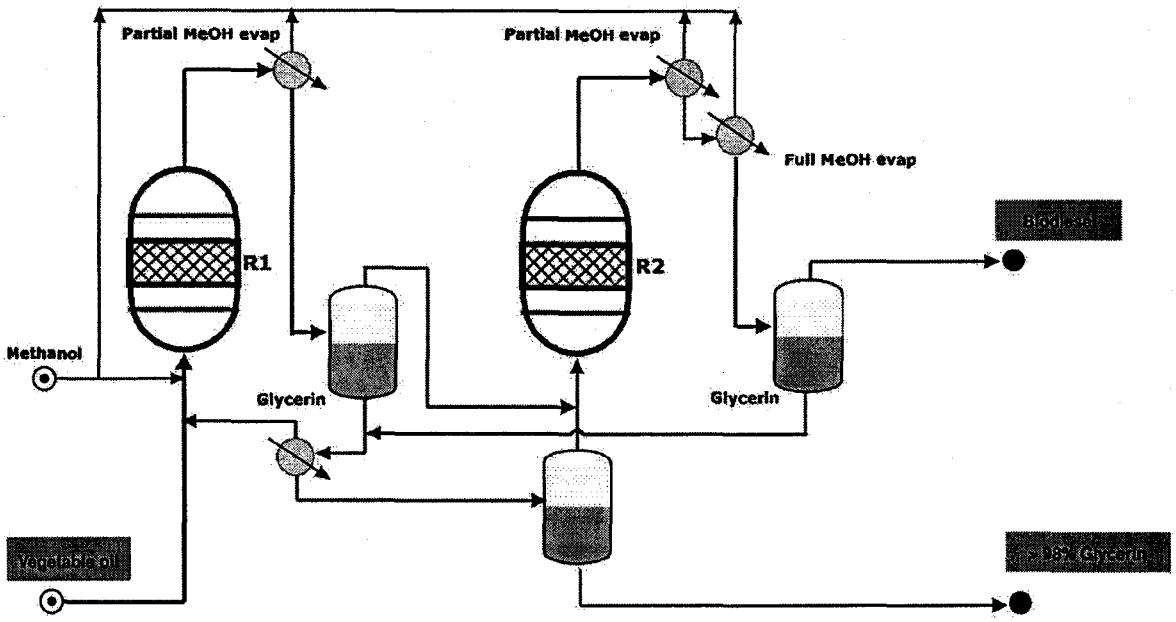

Fig. 6. Simplified flow sheet of the new heterogenous process, Esterfip-H.

Table 5
Main characteristics of biodiesel fuel obtained from rapeseed oil with heterogeneous catalyst [80].

	Biodiesel from reactor 1	Biodiesel from reactor 2	European specification
Weight composition (%)			
Methyl esters	94.1	98.3	>96.5
Monoglycerides	2.0	0.5	<0.8
Diglycerides	1.1	0.1	<0.2
Triglycerides	1.5	0.1	<0.2
Free glycerol	–	–	<0.02
Metal content (mg/kg)			
Group I (Na + K)	<2	<2	<5
Group II (Ca + Mg)	<2	<2	<5
Zn	<1	<1	–
Phosphorus content (mg/kg)	<10	<10	<10
Acid number (mg KOH/kg)	<0.3	<0.3	<0.3

Table 6
Main characteristic of glycerin obtained from rapeseed oil with heterogeneous catalyst [80].

Method		
Glycerol content (wt.%)	BS 5711-3	>98.0
Specific gravity 25 °C (kg/m³)	ISO 3675	1264
Refractive index, 20 °C	ASTM D1747	1.4735
Acidity (mg KOH/g)	EN 14104	0.1
Ash (wt.%)	ISO 6245	None
Chlorides (mg/kg)	EP5.0	<10
Chlorinated compounds (mg/kg)	EP5.0	<10
Halogenated compounds (mg/kg)	EP5.0	<10
Heavy metals (mg/kg)	ASTM D4951	None
Arsenic (mg/kg)	ISO 11969 D18	<0.1

batch homogeneous catalyst production technology to reduce the cost of production. While there are potential benefits that the solid heterogeneous catalyst can offer, issues relating to the low catalytic activity, leachates, reusability and regeneration should be addressed and emphasized in the future research in order to ensure the sustainability of the process.

Table 7
Comparison of the different technologies to produce Biodiesel.

Variable	Base catalyst	Acid catalyst	Lipase catalyst	Supercritical alcohol	Heterogeneous catalyst
Reaction temperature (°C)	60–70	55–80	30–40	239–385	180–220
Free fatty acid in raw materials	Saponified products	Esters	Methyl esters	Esters	Not sensitive
Water in raw materials	Interfere with reaction	Interfere with reaction	No influence		Not sensitive
Yields of methyl esters	Normal	Normal	Higher	Good	Normal
Recovery of glycerol	Difficult	Difficult	Easy		Easy
Purification of methyl esters	Repeated washing	Repeated washing	None		Easy
Production cost of catalyst	Cheap	Cheap	Relatively expensive	Medium	Potentially cheaper

Acknowledgement

The authors acknowledge financial supports from MOSTI and the Universiti Sains Malaysia.

References

[1] F.R. Ma, M.A. Hanna, Biodiesel production: a review, Bioresour. Technol. 70 (1999) 1–15.
[2] A. Srivastava, R. Prasad, Triglycerides-based diesel fuels, Renew. Sustain. Energy Rev. 4 (2000) 111–133.
[3] G. Knothe, J.H. Van Gerpen, J. Krahl, The Biodiesel Handbook, AOCS Press, Champaign, IL, 2005.
[4] G. Pahl, Biodiesel: Growing a New Energy Economy, Chelsea Green Publishers, White River Junction, VT, 2005.
[5] J.H. Van Gerpen, Biodiesel processing and production, Fuel Processing Tech. 86 (2005) 1097–1107.
[6] M. Mittelbach, C. Remschmidt, Biodiesel: the Comprehensive Handbook, M. Mittelbach, Austria, 2006.
[7] K.S. Tyson, Biodiesel Handling and Use Guidelines, NREL, Golden CO, 2001, p. 22.
[8] J.L.C. Shumaker, S.A. Crofcheck, E.S. Tackett, M. Jimenez, Crocker, Biodiesel production from soybean oil using calcined Li–Al layered double hydroxide catalysts, Catal. Lett. 115 (2007) 56–61.
[9] E. Lotero, Y. Liu, D.E. Lopez, K. Suwannakarn, D.A. Bruce, J.G.J. Goodwin, Synthesis of biodiesel via acid catalysis, Ind. Eng. Chem. Res. 44 (2005) 5353–5363.
[10] M.J. Haas, A.J. McAloon, W.C. Yee, T.A. Foglia, A process model to estimate biodiesel production costs, Bioresour. Tech. 97 (2006) 671–678.
[11] M. Bender, Economic feasibility review for community-scale farmer cooperatives for biodiesel, Bioresour. Tech. 70 (1999) 81–87.
[12] W. Korbitz, Biodiesel production in Europe and North America, an encouraging prospect, Renew, Energy 16 (1999) 1078–1083.
[13] International Energy Agency, Biofuels for Transport: an International Perspective, International Energy Agency, Paris, France, 2004.
[14] M.P. Dorado, F. Cruz, J.M. Palomar, F.J. Lopez, An approach to the economics of two vegetable oil-based biofuels in Spain, Renew, Energy 31 (2006) 1231–1237.
[15] E. Lotero, J.G. Goodwin Jr., D.A. Bruce, K. Suwannakarn, Y. Liu, D.E. Lopez, The catalysis of biodiesel synthesis, Catalysis, 19 (2006) 41–83.
[16] H. Fukuda, A. Konda, N. Noda, Biodiesel fuel production by transesterification of oils, J Biosci. Bioeng. 92 (2001) 405–416.
[17] U. Schuchardta, R. Serchelia, R.M. Vargas, Transesterification of vegetable oils: a review, J. Braz. Chem. Soc. 9 (1998) 199–210.
[18] F. Ma, L.D. Clements, M.A. Hanna, Biodiesel fuel from animal fat. Ancillary studies on transesterification of beef tallow, Ind. Eng. Chem. Res. 37 (1998) 3768–3771.
[19] F. Billaud, Y. Guitard, A.K.T. Minh, O. Zahraa, P. Lozano, D. Pioch, Kinetic studies of catalytic cracking of octanoic acid, J. Mol. Catal. A: Chem. 192 (2003) 281–288.
[20] G. Knothe, R.O. Dunn, M.O. Bagby, Biodiesel: the use of vegetable oils and their derivatives as alternative diesel fuels, in: B.C. Saha (Ed.), Fuels and Chemicals from Biomass, American Chemical Society, Washington, DC, 1997, pp. 172–208.
[21] D. Pioch, P. Lozano, M.C. Rasoanantoandro, J. Graille, P. Geneste, A. Guida, Biofuels from catalytic cracking of tropical vegetable oils, Oleagineux 48 (1993) 289–291.
[22] G.N. da Rocha Filho, D. Brodzki, G. Djega-Mariadassou, Formation of alkanes, alkylcycloalkanes and alkylbenzenes during the catalytic hydrocracking of vegetable oils, Fuel 72 (1993) 543–549.
[23] J. Gusmao, D. Brodzki, G. Djega-Mariadassou, R. Frety, Utilization of vegetable oils as an alternative source for diesel-type fuel: hydrocracking on reduced Ni/SiO_2 and sulphided $Ni–Mo/c-Al_2O_3$, Catal. Today 5 (1989) 533–544.
[24] J.R.S. Dos Anjos, W.D. Gonzalez, Y.L. Lam, R. Frety, Catalytic decomposition of vegetable oil, Appl. Catal. 5 (1983) 299–308.
[25] F.A.A. Twaiq, A.R. Mohamad, S. Bhatia, Performance of composite catalysts in palm oil cracking for the production of liquid fuels and chemicals, Fuel Process. Technol. 85 (2004) 1283–1300.
[26] F.A.A. Twaiq, A.R. Mohamed, S. Bhatia, Liquid hydrocarbon fuels from palm oil by catalytic cracking over aluminosilicate mesoporous catalysts with various Si/Al ratios, Micropor. Mesopor. Mater. 64 (2003) 95–107.
[27] F.A.A. Twaiq, N.A.M. Zabidi, A.R. Mohamed, S. Bhatia, Catalytic conversion of palm oil over mesoporous aluminosilicate MCM-41 for the production of liquid hydrocarbon fuels, Fuel Process. Technol. 84 (2003) 105–120.
[28] A.W. Schwab, G.J. Dykstra, E. Selke, S.C. Sorenson, E.H. Pryde, Diesel fuel from thermal-decomposition of soybean oil, J. Am. Oil Chem. Soc. 65 (1988) 1781–1786.
[29] Y. Zhang, M.A. Dube, D.D. McLean, M. Kates, Biodiesel production from waste cooking oil: 2. Economic assessment and sensitivity analysis, Bioresour Technol. 90 (2003) 229–240.
[30] Z. Helwani, M.R. Othman, N. Aziz, J. Kim, W.J.N. Fernando, Solid heterogeneous catalysts for transesterification of triglycerides with methanol: a review, Appl. Catal. A – Gen. 363 (2009) 1–10.
[31] D.G.B. Boocock, Process for Production of Fatty Acid Methyl Esters from Fatty Acid Triglycerides', US, 2004.
[32] H. Noureddini, D. Harkey, V. Medikonduru, Continuous process for the conversion of vegetable oils into methyl esters of fatty acids, J. Am. Oil Chem. Soc. 75 (12) (1998) 1775–1783.
[33] V. Jordan, B. Gutsche, Development of an environmentally benign process for the production of fatty acid methyl esters, Chemosphere, 43 (2001) 99.
[34] C.L. Peterson, J.L. Cook, J.C. Thompson, J.S. Taberski, Continuous flow biodiesel production, Appl. Eng. Agriculture 18 (1) (2002) 5–11.

[35] D. Anderson, D. Masterson, B. McDonald, L. Sullivan, Renewable energy management, International Palm Oil Conference, Putrajaya, Malaysia, 2003.
[36] A.W. Schwab, M.O. Bagby, B. Freedman, Preparation and properties of diesel fuels from vegetable oils, Fuel 66 (1987) 1372–1378.
[37] B. Freedman, R.O. Butterfield, E.H. Pryde, Transesterification kinetics of soybean oil, J. Am. Oil. Chem. Soc. 63 (10) (1986) 1375–1380.
[38] C. Stavarache, M. Vinatoru, R. Nishimura, Y. Maed, Fatty acids methyl esters from vegetable oil by means of ultrasonic energy, Ultrason Sonochem. 12 (2005) 367–372.
[39] L.C. Meher, M.G. Kulkarni, A.K. Dalai, S.N. Naik, Transesterification of karanja (*Pongamia pinnata*) oil by solid basic catalysts, Eur. J. Lipid Sci. Technol. 108 (2006) 389–397.
[40] A. Ohi, H. Aoyama, H. Ohuchi, A. Kato, M. Yamaoka, Fatty acid ester from palm oil as diesel fuel, Nenryo Kyokaishi 62 (1983) 24–31.
[41] H.A. Aksoy, I. Becerik, F. Karaosmanoglu, H.C. Yamaz, H. Civelekoglu, Utilization prospects of Turkish raisin seed oil as an alternative engine fuel, Fuel 69 (1990) 600–603.
[42] V. Varghaa, P. Truterb, Biodegradable polymers by reactive blending transesterification of thermoplastic starch with poly(vinyl acetate) and poly(vinyl acetate-co-butyl acrylate, Eur. Polymer J. 41 (2005) 715–726.
[43] S. Furuta, H. Matsuhasbi, K. Arata, Biodiesel fuel production with solid superacid catalysis in fixed bed reactor under atmospheric pressure, Catal. Commun. 5 (2004) 721–723.
[44] M. Canakci, J.V. Gerpen, A pilot plant to produce biodiesel from high free fatty acid feedstocks, Trans. ASAE 46 (2003) 945–955.
[45] A. Demirbas, Biodiesel from vegetable oils via transesterification in supercritical methanol, Energy Conv. Mgmt. 43 (2002) 2349–2356.
[46] A. Demirbas, Biodiesel fuels from vegetable oils via catalytic and non-catalytic supercritical alcohol transesterifications and other methods: a survey, Energy Conv. Mgmt. 44 (13) (2003) 2093–2109.
[47] A. Demirbas, Comparison of transesterification methods for production of biodiesel from vegetable oils and fats, Energy Conv. Mgmt. 49 (2008) 125–130.
[48] M. Freier, Medicinal Chemistry Symposium, September 2005, <www.nesacs.org/TheNucleus/Sep05>.
[49] M. Canakci, J. Van Gerpen, Biodiesel production via acid catalysis, Trans. ASAE 42 (1999) 1203–1210.
[50] D. Kusdiana, S. Saka, Effects of water on biodiesel fuel production by supercritical methanol treatment, Bioresour. Technol. 91 (2004) 289–295.
[51] R. Sridharan, I.M. Mathai, Transesterification reactions, Sci. Ind. Resource 33 (1974) 178–187.
[52] F. Rived, I. Canals, E. Bosch, M. Roses, Acidity in methanol–water, Anal. Chim. Acta 439 (2001) 315.
[53] D. Kusdiana, S. Saka, Two-step preparation for catalyst-free biodiesel fuel production: hydrolysis and methyl esterification, Appl Biochem Biotechnol. 115 (2004) 781–791.
[54] J.M. Marchetti, V.U. Miguel, A.F. Errazu, Possible methods for biodiesel production, Renew. Sustain. Energy Rev. 11 (6) (2007) 1300–1311.
[55] S. Al-Zuhair, Production of biodiesel: possibilities and challenges, Biofuels Bioprod. Bioref. 1 (2007) 57–66.
[56] G. Vicente, M. Martinez, J. Aracil, A. Esteban, Kinetics of sunflower oil methanolysis, Ind. Eng. Chem. Res. 44 (15) (2005) 5447–5454.
[57] H. Noureddini, D. Zhu, Kinetics of transesterification of soybean oil, J. Am. Oil. Chem. Soc. 74 (1997) 1457–1463.
[58] D. Darnoko, M. Cheryan, Continuous production of palm methyl esters, J. Am. Oil. Chem. Soc. 77 (12) (2000) 1269–1272.
[59] O.S. Stamenkovic, M.L. Lazic, Z.B. Todorovic, V.B. Veljkovic, D.U. Skala, The effect of agitation intensity on alkali-catalyzed methanolysis of sunflower oil, Bioresour. Tech. 98 (14) (2007) 2688–2699.
[60] D.G.B. Boocock, S.K. Konar, V. Mao, H. Sidi, Fast one-phase oil-rich processes for the preparation of vegetable oil methyl esters, Biomass and Bioenergy 11 (1) (1996) 43–50.
[61] D.G.B. Boocock, S.K. Konar, V. Mao, C. Lee, S. Buligan, Fast formation of high purity methyl esters from vegetable oils, J. Am. Oil. Chem. Soc. 75 (9) (1998) 1167–1172.
[62] D.G.B. Boocock, Single-Phase Process for Production of Fatty Acid Methyl Esters from Mixtures of Triglcerides and Fatty Acids, Boocock, David Gavin Broole, WO0112581, 2001.
[63] J.A. Kinast, K.S. Tyson, Production of biodiesel from multiple feedstocks and properties of biodiesel and biodiesel/diesel blends, Final report', NREL, Golden, CO, Volume, 2003, p. 57.
[64] D.J. Miller, J.E. Jackson, Catalysis for biorenewables conversion, National Science Foundation Workshop Report, Virginia, 2004.
[65] H. Noureddini, D. Harkey, V. Medikonduru, Continuous process for the conversion of vegetable oils into methyl esters of fatty acids, J. Am. Oil. Chem. Soc. 75 (1998) 1775.
[66] A.P. Harvey, M.R. Mackley, T. Seliger, Process intensification of biodiesel production using a continuous oscillatory flow reactor, J. Chem. Tech. Biotech. 78 (2003) 338–341.
[67] J. Van Gerpen, B. Shanks, R. Pruszko, D. Clements, G. Knothe, Biodiesel Production Technology, National Renewable Energy Laboratory, CO, USA, 2004.
[68] B.B. He, A.P. Singh, J.C. Thompson, Experimental optimization of a continuous flow reactive distillation reactor for biodiesel production, Trans. Am. Soc. Agri. Engineers 48 (6) (2005) 2237–2243.
[69] B.B. He, A.P. Singh, J.C. Thompson, A novel continuous-flow reactor using reactive distillation for biodiesel production, Trans. of the ASABE 49 (1) (2006) 107–112.
[70] D. Nimcevic, R.J. Gapes, in: Dragan Nimcevic, Richard J. Gapes (Eds.), Transesterification of Fat, vol. WO0188072, 2004.
[71] D. Darnoko, M. Cheryan, Kinetics of palm oil transesterification in a batch reactor, J. Am. Oil. Chem. Soc. 77 (12) (2000) 1263–1267.
[72] M.K. Certinkaya, Optimization of base-catalyzed reaction of used cooking oil, Energy & Fuels 18 (6) (2004) 1888–1895.
[73] U.F. Schuchardt, G.C. Lopes, Brazil Patent, (11)(21)PI8202429, Universidade Federal da Bahia, 1983.
[74] C. Weiliang, H. Hengwen, Z. Jinchang, Preparation of biodiesel from soybean oil using supercritical methanol and cosolvent, Fuel 84 (2005) 347–351.
[75] A.A. Kiss, A.C. Dimian, G. Rothenberg, Solid acid catalysts for biodiesel production — towards sustainable energy, Adv. Synth. Catal. 348 (2006) 75–81.
[76] A.A. Kiss, F. Omota, A.C. Dimian, G. Rothernberg, The heterogeneous advantage: biodiesel by catalytic reactive distillation, Topics in Cat. 40 (1–4) (2006) 141–150.
[77] A.A. Kiss, A.C. Dimian, G. Rothenberg, Biodiesel by catalytic reactive distillation powered by metal oxides, Energy and fuel 22 (2008) 598–604.
[78] T. Haas, US Patent 6,392,062 (2002), Degussa AG.
[79] M.A. Portnoff, D.A. Purta, M.A. Nasta, J. Zhang, F. Pourarian, US Patent Application 2005/0274065 (2005).
[80] L. Bournay, D. Casanave, B. Delfort, G. Hillion, J.A. Chodorge, New heterogeneous process for biodiesel production: a way to improve the quality and the value of the crude glycerin produced by biodiesel plants, Catal. Today 106 (2005) 190–192.
[81] G. Ondrey, Chementator IGCC, Chem. Eng. 10 (2004) 13.
[82] F. Abreu, F.B. Alves, C.C.S. Macêdo, L.F. Zara, P.A.Z. Suarez, New multi-phase catalytic systems based on tin compounds active for vegetable oil transesterificaton reaction, J. Mol. Catal. A: Chem. 227 (2005) 263–267.
[83] G.J. Suppes, M.A. Dasari, E.J. Doskocil, P.J. Mankidy, M.J. Goff, Transesterification of soybean oil with zeolite and metal catalysts, Appl. Catal. A: Gen. 257 (2004) 213–223.
[84] L.Y. Wang, J.C. Yang, Transesterification of soybean oil with nano-MgO or not in supercritical and subcritical methanol, Fuel 86 (3) (2007) 328–333.
[85] E. Li, V. Rudolph, Transesterification of vegetable oil to biodiesel over MgO-functionally mesoporous catalysts, Energy and Fuels 22 (2008) 143–149.
[86] J.L. Shumaker, C. Crofcheck, S.A. Tackett, E. Santillan-Jimenez, T. Morgan, Y. Ji, M. Crocker, T.J. Toops, Biodiesel synthesis using calcined layered double hydroxide catalysts, App. Catal. B: Env. 82 (2008) 120–130.
[87] W.L. Xie, H. Peng, L.G. Chen, Calcined Mg–Al hydrotalcites as solid base catalysts for methanolysis of soybean oil, J. Mol. Catal. A: Chem. 246 (2006) 24–32.
[88] W. Trakarnpruk, S. Porntangjitlikit, Palm oil biodiesel synthesized with potassium loaded calcined hydrotalcite and effect of biodiesel blend on elastomer properties, Renew. Energy 33 (2008) 1558–1563.
[89] Q. Shu, B. Yang, H. Yuan, S. Qing, G. Zhu, Synthesis of biodiesel from soybean oil and methanol catalyzed by zeolite beta modified with La^{3+}, Catal. Commun. 8 (2007) 2159–2165.
[90] Y. Wang, F. Zhang, S. Yu, L. Yang, D. Li, D.G. Evans, X. Duan, Preparation of macrospherical magnesia-rich magnesium aluminate spinel catalysts for methnolysis of soybean oil, Chem. Eng. Sci. 63 (17) (2008) 4306–4312.
[91] G. Arzamendi, I. Campoa, E. Arguinarena, M. Sanchez, M. Montes, L.M. Gandia, Synthesis of biodiesel with heterogeneous NaOH/alumina catalysts: comparison with homogeneous NaOH, Chem. Eng. J. 134 (2007) 123–130.
[92] W.M. Antunes, C.O. Veloso, C.A. Henriques, Transesterification of soybean oil with methanol catalyzed by basic solids, Catal. Today 133–135 (2008) 548–554.
[93] Y.D. Wang, T. Al-Shemmeri, P. Eames, J. McMullan, N. Hewitt, Y. Huang, et al., An experimental investigation of the performance and gaseous exhaust emissions of a diesel engine using blends of a vegetable oil, Appl. Thermal Eng. 26 (2006) 1684–1691.
[94] M.C.G. Albuquerque, I. Jimenez-Urbistondo, J. Santamaria-Gonzalez, J.M. Merida-Robles, et al., CaO supported on mesoporous silicas as basic catalysts for transesterification reactions, Appl. Catal. A: Gen. 334 (2008) 35–43.
[95] Z. Huaping, W. Zongbin, C. Yuanxiao, Z. Ping, D. Shije, L. Xiaohua, M. Zongqiang, Preparation of biodiesel catalyzed by solid super base of calcium oxide and its refining process, Chinese J. Catalysis 27 (5) (2006) 391–396.
[96] Y.-M. Park, D.-W. Lee, D.-K. Kim, J.-S. Lee, K.-Y. Lee, The heterogeneous catalyst system for the continuous conversion of free fatty acids in used vegetable oils for the production of biodiesel, Catal. Today 131 (2008) 238–243.
[97] H.-Y. Zeng, Z. Feng, X. Deng, Y.-Q. Li, Activation of Mg–Al hydrotalcite catalysts for transesterification of rape oil, Fuel 87 (13–14) (2008) 3071–3076.
[98] X. Liu, H. He, Y. Wang, S. Zhu, Transesterification of soybean oil to biodiesel using CaO as a solid base catalyst, Fuel 87 (2008) 216–221.
[99] X. Liu, H. He, Y. Wang, S. Zhu, X. Piao, Transesterification of soybean oil to biodiesel using CaO as a solid base catalyst, Cat. Commun. 8 (2007) 1107–1111.
[100] N. Barakos, S. Pasias, N. Papayannakos, Transesterification of triglycerides in high and low quality oil feeds over an HT2 hydrotalcite catalyst, Biosource Technol. 99 (2008) 5037–5042.
[101] D.E. Lopez, J.G. Goodwin Jr., D.A. Bruce, Transesterification of triacetin with methanol on Nafion-acid resins, J. Catal. 245 (2007) 381–391.
[102] F. Chai, F. Cao, F. Zhai, Y. Chen, X. Wang, Z. Su, Transesterification of vegetable oil to biodiesel using a heteropolyacid solid catalyst, Adv. Synth. Catal. 349 (2007) 1057–1065.
[103] J.H. Clark, Solid acids for green chemistry, Acc. Chem. Res. 35 (2002) 791–797.
[104] A.K. Singh, S.D. Fernando, Reaction kinetics of soybean oil transesterification using heterogeneous metal oxide catalysts, Chem. Eng. Tech. 30 (12) (2007) 1–6.
[105] Y. Wang, S.O.P. Liu, Z. Zhang, Preparation of biodiesel from waste cooking oil via two-step catalyzed process, Energy Conv. Mgmt. 48 (2007) 184–188.
[106] M. Di Serio, M. Ledda, M. Cozzolino, G. Minutillo, R. Tesser, E. Santacesaria, Transesterification of soybean oil to biodiesel by using heterogeneous basic catalysts, Ind. Eng. Chem. Res. 45 (2006) 3009–3014.
[107] M.S. Dean, E.J. Yoder, Doskocil, Nanocrystalline metal oxide-based catalysts for biodiesel production from soybean oil, Catal. Reaction Eng. 39 (2006) 1–10.

[108] Chementator, Biodiesel Production Using a Heterogeneous Catalyst, January 2008 <http://www.axens.net/upload/news/fichier/chemical_engineering.pdf> (2004).
[109] S. Gryglewicz, Rapeseed oil methyl esters preparation using heterogeneous catalysts, Bioresour. Technol. 70 (1999) 249–253.
[110] C.V. Mc Neff, L. Mc Neff, et al., A continuous system for biodiesel production, Appl. Catal. A: Gen. 343 (2008) 39–48.
[111] G. Carja, R. Nakamura, T. Aida, H. Niiyama, Textural properties of layered double hydroxides: effect og magnesium substitution by copper or iron, Microporous Mesoporous Mater. 47 (2001) 275–284.
[112] J. Das, D. Das, G.P. Dash, K.M. Parida, Studies on Mg/Fe hydrotalcite-like compound (HTlc): removal of inorganic selenite (SeO_3^{2-}), J. Colloidal Interface Sci. 251 (2002) 26–32.
[113] T. Yamamoto, T. Kodama, N. Hasegawa, M. Tsuji, T. Tamaura, Synthesis of hydrotalcite with high layer charge for CO_2 adsorbent, Energy Conv. Mgmt. 36 (1995) 637–640.
[114] K. Schulze, W. Makowski, R. Chyzy, R. Dziembaj, G. Geismar, Nickel doped hydrotalcites as catalyst precursors for the partial oxidation of light paraffins, Appl. Clay Sci. 18 (2001) 59–69.
[115] C. Morato, B. Alonso, F. Coq, F. Medina, Y. Cesteros, J.E. Sueiras, P. Salagre, D. Tichit, Palladium hydrotalcite as precursor for the catalytic hydroconversion of CCl_2F_2 (CFC-12) and $CHClF_2$ (HCFC-12), Appl. Catal. A: Gen. 32 (2001) 167–179.
[116] Y. Ding, E. Alpay, High temperature recovery of CO_2 from flue gases using hydrotalcite adsorbent, Process Saf. Environ. Prot. 79 (2) (2001) 45–51.
[117] J.W. Wang, A.G. Kalinichev, R.J. Kirkpatrick, X.Q. Hou, Molecular modeling of the structure and energetic of hydrotalcite hydration, Chem. Mater. 13 (1) (2001) 145–150.
[118] C.O. Veloso, C.N. Perez, B.M. de Souza, E.C. Lima, A.G. Dias, J.L.F. Monteiro, C.A. Henriques, Condensation of glyceraldehydes acetonide with ethyl acetoacetate over Mg, Al-mixed oxides derived from hydrotalcites, Micro. Meso. Mater. 107 (2008) 23–30.
[119] M.J. Climent, A. Corma, S. Iborra, K. Epping, A. Velty, Increasing the basicity and catalytic activity of hydrotalcites by different synthesis procedures, J. Catal. 225 (2004) 316–326.
[120] D. Tichit, M.H. Lhouty, A. Guida, B.H. Chiche, F. Figueras, A. Auroux, D. Bartalini, E. Garrone, Textural properties and catalytic activity of hydrotalcites, J. Catal. 151 (1995) 50–59.
[121] S. Corma, S. Abd Hamid, S. Iborra, A. Velty, Lewis and bronsted basic sites on solid catalysts and their role in the synthesis of monoglycerides, J. Catal. 234 (2005) 340–347.
[122] J.I. Di Cosimo, J.v. Díez, M. Xu, E. Iglesia, C.R. Apesteguía, Structure and surface and catalytic properties of Mg–Al basic oxides, J. Catal. 178 (1998) 499–510.
[123] K.K. Rao, M. Gravelle, J. Valente, F. Figueras, Activation of Mg–Al hydrotalcite catalysts for aldol condensation reaction, J. Catal. 173 (1998) 115–121.
[124] S. Abelló, J. Pérez-Ramírez, Nanoplatelet-based reconstructed hydrotalcites: towards more efficient solid base catalysts in aldol, Chem. Commun. (2005) 1453–1455.
[125] B.M. Choudary, M.L. Kantam, Ch.V. Reddy, S. Aranganathan, P.L. Santhia, F. Figueras, Mg–Al–O–t-Bu hydrotalcite: a new and effeicient heterogeneouos catalyst for transesterification, J. Mol. Catal. A: Chem. 159 (2000) 411–416.
[126] D.G. Cantrell, L.J. Gillie, A.F. Lee, K. Wilson, Structure-reactivity correlations in MgAl hydrotalcite catalysts for biodiesel synthesis, Appl. Catal. A: Gen. 287 (2005) 183–190.
[127] M.R. Othman, Z. Helwani, Martunus, W.J.N. Fernando, Synthetic hydrotalcites from different routes and their application as catalysts and gas adsorbents: a review, Appl. Organomet. Chem. 23 (2009) 335–346.
[128] J.D. Roy, T. Perkins, T. Kaydanova, D.L. Young, Preparation and characterization of sol–gel derived copper–stronsium-oxide thin film, Thin Solid Film, 516 (2008) 4093–4101.
[129] Q. Fu, C.-B. Cao, H.-S. Zhu, Preparation of alumina films from a new sol–gel route, Thin solid films 348 (2008) 99–102.
[130] M. Garcia-Heras, A. Jimenez-Morales, B. Casal, J.C. Galvan, S. Radzki, M.A. Villegas, Preparation and electrochemical study of cerium–silica sol–gel thin film, J. of Alloys and compounds 380 (2004) 219–224.
[131] M.A. Aramendia, V. Borau, C. Jimenez, J.M. Marinas, J.R. Ruiz, F.J. Urbano, Comparative study of Mg/M (III) (M=Al, Ga, In) layered double hydroxides obtained by coprecipitation and the sol–gel method, J. of Solid State Chemistry 168 (2002) 156–161.
[132] M. Jitianu, M. Zaharescu, M. Balasoiu, A. Ivanov, A. Jitianu, Comparative study of sol–gel and coprecipitated Ni–Al hydrotalcites, J. Sol–gel Sci. Tech. 19 (2000) 453–457.
[133] M. Bolognini, F. Cavani, D. Scagliarini, C. Flego, C. Perego, M. Saba, Mg/Al mixed oxides prepared by coprecipitation and sol–gel routes: a comparison of their physico-chemical features and performances in m-cresol methylation, Micro-porous Mesoporous Mater. 66 (2003) 77–89.
[134] M.R. Othman, N.M. Rasid, W.J.N. Fernando, Effect of thermal treatment on the micro-structures of co-precipitated and sol–gel synthesized Mg–Al hydrotalcites, J. Microporous Mesoporous Mater. 93 (2006) 23–28.
[135] S.H. Ha, M.N. Lan, S.H. Lee, S.M. Hwang, Y.-M. Koo, Lipase-catalyzed biodiesel production from soybean oil in ionic liquids, Enzyme Microbial Technol. 41 (2007) 480–483.
[136] Y. Wang, H. Wu, M.H. Zong, Improvement of biodiesel production by lipozyme TL IM-catalyzed methanolysis using response surface methodology and acyl migration enhancer, Bioresour. Techn. 99 (2008) 7232–7237.
[137] M.K. Modi, J.R.C. Reddy, B.V.S.K. Roa, R.B.N. Prasad, Lipase-mediated conversion of vegetable oils into biodiesel using ethyl acetate as acyl acceptor, Bioresour. Technol. 98 (2007) 1260–1264.
[138] Y. Watanabe, Y. Shimada, A. Sugihara, Y. Tominaga, Enzymatic conversion of waste edible oil to biodiesel fuel in a fixed-bed bioreactor, J. Am. Oil. Chem. Soc. 78 (2001) 7.
[139] K. Nie, F. Xie, F. Wang, T. Tan, Lipase catalyzed methanolysis to produce biodiesel: Optimization of the biodiesel production, J. Mol. Catal. B: Enzyme. 43 (2006) 142–147.
[140] L. Li, W. Du, D. Liu, L. Wang, Z. Li, Lipase-catalyzed transesterification of rapeseed oils for biodiesel production with a novel organic solvent as the reaction medium, J. Mol. Catal. B: Enzyme. 43 (2006) 58–62.
[141] Y. Shimada, Y. Watanabe, A. Sugihara, Y. Tominaga, Enzymatic alcoholysis for biodiesel fuel production and application of the reaction to oil processing, J. Mol. Catal. B: Enzyme. 17 (2002) 133–142.
[142] D. Royon, M. Daz, G. Ellenrieder, S. Locatelli, Enzymatic production of biodiesel from cotton seed oil using t-butanol as a solvent, Bioresour. Technol. 98 (2007) 648–653.
[143] Y. Shimada, Y. Watanabe, T. Samukawa, Conversion of vegetable oil to biodiesel using immobilized *Candida antarctica* lipase, J. Am. Oil. Chem. Soc. 76 (1999) 789–793.
[144] V. Dossat, D. Combes, A. Marty, Continuous enzymatic transesterification of high oleic sunflower oil in a packed beg reactor: influence of the glycerol production, Enzyme Microbial Technol. 25 (1999) 194–200.
[145] T.A. Foglia, L.A. Nelson, W.N. Marmer, Production of biodiesel, lubricants and fuel and lubricant additives. Patent [5,713,965], USA, 1998.
[146] D. Oliveira, J.D. Oliveira, Enzymatic alcoholysis of palm kernel oil in *n*-hexane and $SCCO_2$, J. Supercrit. Fluids 19 (2001) 141–148.
[147] M. Iso, B. Chen, M. Eguchi, T. Kudo, S. Shrestha, Production of biodiesel fuel from triglycerides and alcohol using immobilized lipase, J. Mol. Catal. B: Enzyme. 16 (2001) 53–58.
[148] S. Saka, D. Kusdiana, Biodiesel fuel from rapeseed oil as prepared in supercritical methanol, Fuel 80 (2001) 225–231.
[149] A. Demirbas, Biodiesel production from vegetable oils by supercritical methanol, J. Sci. Ind. Res. 64 (2005) 858–865.
[150] D. Kusdiana, S. Saka, Kinetics of transesterification in rapeseed oil to biodiesel fuels as treated in supercritical methanol, Fuel 80 (2001) 693–698.
[151] M. Balat, H. Balat, A critical review of bio-diesel as a vehicular fuel, Energy conv. Mgmt. 49 (10) (2008) 2727–2741.
[152] J. Kubička, P. Chudoba, Šimaček, Europacat VIII, Turku, Finland, , August 26–31 2007.
[153] G.W. Huber, J.A. Dumesic, An overview of aqueous-phase catalytic processes for production of hydrogen and alkanes in a biorefinery, Catal. Today 111 (2006) 119–132.
[154] G.W. Huber, P. O'Connor, A. Corma, Processing biomass in conventional oil refineries: production of high quality diesel by hydrotreating vegetable oils in heavy vacuum oil mixtures, Appl. Catal. A: Gen. 329 (2007) 120.
[155] R.J. Farrauto, C. Bartholomew, Introduction to Industrial Catalytic Processes, Chapman & Hall, London, UK, 1997.
[156] W. Craig, Production of hydrocarbons with a relatively high cetane rating. United States Patent 4,992,605, 1991.
[157] J. Monnier, G. Tourigny, D. Soveran, A. Wong, E. Hogan, Conversion of biomass feedstock to diesel fuel additive assigned to natural resources Canada, United Sates Patent 5,705,722, 1998.
[158] M. Stumborg, A. Wong, E. Hogan, Hydroprocessed vegetable oils for diesel fuel improvement, Bioresource Technol. 56 (1996) 13–18.
[159] O.I. Senol, T.R. Viljava, A.O.I. Krause, Hydrodeoxygenation of methyl esters on sulphided NiMo/c-Al_2O_3 and CoMo/c-Al_2O_3 catalysts, Catal. Today 100 (2005) 331–335.
[160] O.I. Senol, T.R. Viljava, A.O.I. Krause, Hydrodeoxygenation of aliphatic esters on sulphided NiMo/c-Al_2O_3 and CoMo/c-Al_2O_3 catalyst: the effect of water, Catal. Today 106 (2005) 186–189.
[161] O.I. Senol, E.M. Ryymin, T.R. Viljava, A.O.I. Krause, Reactions of methyl heptanoate hydrodeoxygenation on sulphided catalysts, J. Mol. Catal. A: Chem. 268 (2007) 1–8.
[162] O.I. Senol, T.R. Viljava, A.O.I. Krause, Effects of sulphiding agents on the hydrodeoxygenation of aliphatic esters on sulphided catalysts, Appl. Catal. A: Gen. 326 (2) (2007) 236–244.
[163] E. Laurent, B. Delmon, Study of the hydrodeoxygenation of carbonyl, carboxylic and guaiacyl groups over sulphided CoMo/c-Al_2O_3 and NiMo/c-Al_2O_3 catalysts. I. Catalytic reaction schemes, Appl. Catal. A: Gen. 109 (1994) 77–96.
[164] E. Laurent, B. Delmon, Study of the hydrodeoxygenation of carbonyl, carboxylic and guaiacyl groups over sulphided CoMo/c-Al_2O_3 and NiMo/c-Al_2O_3 catalysts. II. Influence of water, ammonia and hydrogen sulfide, Appl. Catal. A: Gen. 109 (1994) 97–115.
[165] A. Centeno, E. Laurent, B. Delmon, Influence of the support of CoMo sulfide catalysts and of the addition of potassium and platinum on the catalytic performances for the hydrodeoxygenation of carbonyl, carboxylic and guaiacol-type molecules, J. Catal. 154 (1995) 288–298.
[166] M. Ferrari, R. Maggi, B. Delmon, P. Grange, Influence of the hydrogen sulfide partial pressure and of a nitrogen compound on the hydrodeoxygenation activity of a CoMo/carbon catalyst, J. Catal. 198 (2001) 47–55.
[167] M. Ferrari, S. Bosmans, R. Maggi, B. Delmon, P. Grange, CoMo/Carbon hydrodeoxygenation catalysts: influence of the hydrogen sulfide partial pressure and of the sulfidation temperature, Catal. Today 65 (2001) 257–264.
[168] M. Snare, I. Kubičkova, P. Maki-Arvela, K. Eranen, D. Murzin, Heterogeneous catalytic deoxygenation of stearic acid for production of biodiesel, Ind. Eng. Chem. Res. 45 (2006) 5708–5715.
[169] I. Kubic˘kova, M. Snare, K. Eranen, P. Maki-Arvela, D. Murzin, Hydrocarbons for diesel fuel via decarboxylation of vegetable oils, Catal. Today 106 (2001) 197–200.

[170] P. Maki-Arvela, I. Kubic˘kova, M. Snare, K. Eranen, D. Murzin, Catalytic deoxygenation of fatty acids and their derivatives, Energy Fuels 21 (2007) 30–41.
[171] M. Snåre, I. Kubic˘ková, P. Mäki-Arvela, K. Eränen, J. Warna, D. Murzin, Production of diesel fuel from renewable feeds: kinetics of ethyl stearate decarboxylation, Chem. Eng. J. 134 (1–3) (2007) 29–34.
[172] M. Snåre, I. Kubic˘ková, P. Mäki-Arvela, D. Chichova, K. Eränen, D. Murzin, Catalytic deoxygenation of unsaturated renewable feedstocks for production of diesel fuel hydrocarbons, Fuel 87 (2008) 933–945.
[173] Neste oil website: <http://www.nesteoil.com/default.asp?path=1,41,539, 7516,7537>.
[174] Petrobras website: <http://www2.petrobras.com.br/tecnologia/ing/hbio.asp>.
[175] ConocoPhillips website: <http://www.conocophillips.com/Tech/emerging/Tyson/index.htm>.
[176] T. Kalnes, T. Marker, D. Shonnard, Green diesel: a second generation biofuel, Int. J. Chem. Reactor Eng. 5 (2007) Article A48.
[177] A. Corma, G.W. Huber, L. Sauvanaud, P. O'Connor, Processing biomass-derived oxygenates in the oil refinery: catalytic cracking (FCC) reaction pathways and role of catalyst, J. Catal. 247 (2) (2007) 307.
[178] G.W. Huber, A. Corma, Synergies between bio- and oil refineries for the production of fuels from biomass, Angew. Chem. Int. Ed. 46 (2007) 7184–7201.
[179] R. Marinangeli, T. Marker, J. Petri, T. Kalnes, M. McCall, D. Mackowiak, B. Jerosky, B. Reagan, L. Nemeth, M. Krawczyk, S. Czernik, D. Elliott, D. Shonnard, Opportunities for biorenewables in oil refineries, DOE Award #DE-FG36-05GO15085, UOP, 2006.
[180] R. Stern, G. Hillion, J.J. Rouxel, S. Leporq, US Patent 5,908,946 (1999).
[181] R. Stern, G. Hillion, J.J. Rouxel, US Patent 6,147,196 (2000).
[182] R.F. Vogel, R.J. Rennard, J.A. Tabacek, US patent 4,490,479 (1984).

AIP Conf. Proc. 1136: 454-458

Characteristics of Hydrotalcite Synthesized From A Solvothermal Method

M.K Hafiz*, [1]M.R Othman*, N. Aziz*

**School of Chemical Engineering, Universiti Sains Malaysia, 14300 Nibong Tebal Penang, Malaysia*
[1]*E-mail: chroslee@eng.usm.my*

Abstract. Hydrotalcite intercalated compounds (HT) was synthesized by solvothermal method using aluminum and magnesium alkoxides as precursors. Most of the solvothermal products were mesoporous structures with well-defined morphologies. The solvothermal samples from this study exhibited the characteristics of lamellar structures resembling hydrotalcite compounds even without calcination. The crystal size grew with increasing temperature during solvothermal process. While calcination increased crystallinity of samples in previous efforts, it did not improve the crystallinity level in this study.

Keywords: Layered double hydroxides, Solvothermal, Crystallization
PACS: 81.07.-b Nanoscale materials and structures: fabrication and characterization

INTRODUCTION

Hydrotalcite (HT), a magnesium–aluminum hydroxycarbonate is known as good adsorbents and anion exchangers [1]. Recently they have been used in the preparation of nanocomposite materials [2]. Ideal HT has a structural formula of $Mg_6Al_2(OH)16CO_3{\cdot}4H_2O$. There are extensive possibilities for solid solubility on both cation and anion sublattices. HT can more generally be formulated as $(M^{II}_{1-x}M^{III}_x)_8(OH)_{16}(X^{n-})_{8x/n}{\cdot}4H_2O$, where for example M^{II} is Mg^{2+}, Ni^{2+}, M^{III} is Al^{3+}, Ga^{3+}, Cr^{3+} or Fe^{3+}, and X^{n-} is CO_3^{2-}, NO_3^-, F^-, Cl^- or more complex inorganic and organic anions.

In this paper, HT is synthesized from a solvothermal method that requires hydrolysis and condensation of precursor materials be carried out at elevated temperature and autogeneous pressure. Solvothermal methods are convenient for their reactions usually produce crystallines that do not require post annealing treatments. In addition, most of the solvothermal products are nano or microparticles with well-defined morphologies [3].

EXPERIMENTAL

Methods: 0.15mol of magnesium methoxide, 9.5 mL potassium carbonate were dissolved in 100ml ethanol and stirred vigorously. A volume of 100mL ethanol containing 0.05mol aluminum tri-sec-butoxide and 2.1 mL PVA was added. An

appropriate amount of NaOH was used to catalyze the hydrolysis and maintain at pH≈10 under continuous stirring until homogeneity at room temperature. The mixture was sealed in a 100 ml Teflon-lined stainless steel autoclave and heated at 160°C, 180°C and 200°C for 2 h under continuous stirring. After cooling to room temperature, the solid product was isolated by distillation under vacuum and subsequently washed with absolute ethanol. After distillation the solid was then washed with absolute ethanol supersonically and followed by drying in an oven at 110°C. The resulting solids were labeled as HT-s1, HT-s2 and HT-s3 respectively. Then HT-s2 was calcined at 400°C and 800°C for 5 h. The resulting solids were labeled as HT-1, HT-2 and HT-3 to represent uncalcined, calcined at 400°C and calcined at 800°C, respectively.

RESULT AND DISCUSSION

FIGURE 1.a indicates that rhombus hydrotalcites are readily obtainable even at the lowest temperature of 160°C. At 180°C and 200°C, a marked increase of hydrotalcite content was observed in the samples manifested by the emergence of more distinguished peaks. According to XRD results, the higher the temperature and time of solvothermal treatment, the higher the hydrotalcite enrichment, leading to an increasing growth of crystallites [4]. At the elevated temperatures, the integral intensity values show a marked decrease in the upper 2θ angle. At lower angle, peaks intensity appeared to increase, signifying further development of the intercalated nature of the structures.

FIGURE 1.b suggests that impurity peaks were no longer observed, indicating that the high purity of HT crystalline was successfully synthesized by allowing it to sustain sufficient rehydration. For HT-2 and HT-3, the XRD patterns reveal that other phases started to appear. A single periclase MgO phase and an amorphous alumina phase, Al_2O_3 were produced. Other phases like brucite, $Mg(OH)_2$ and periclase, MgO phase were also observed.

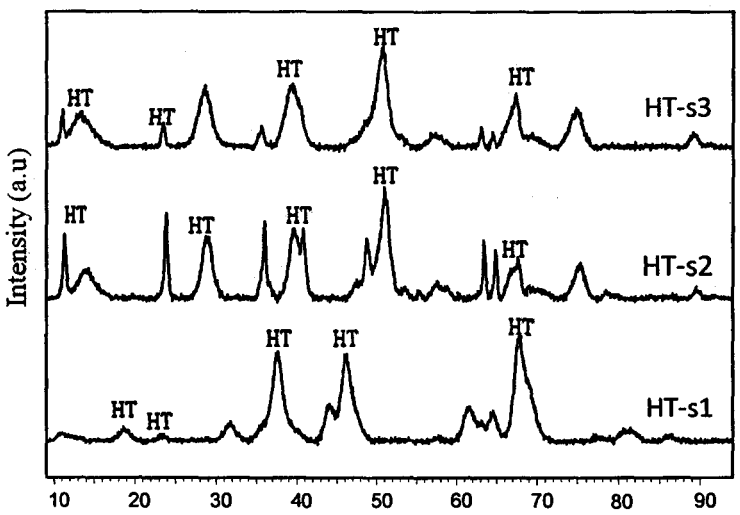

(a)

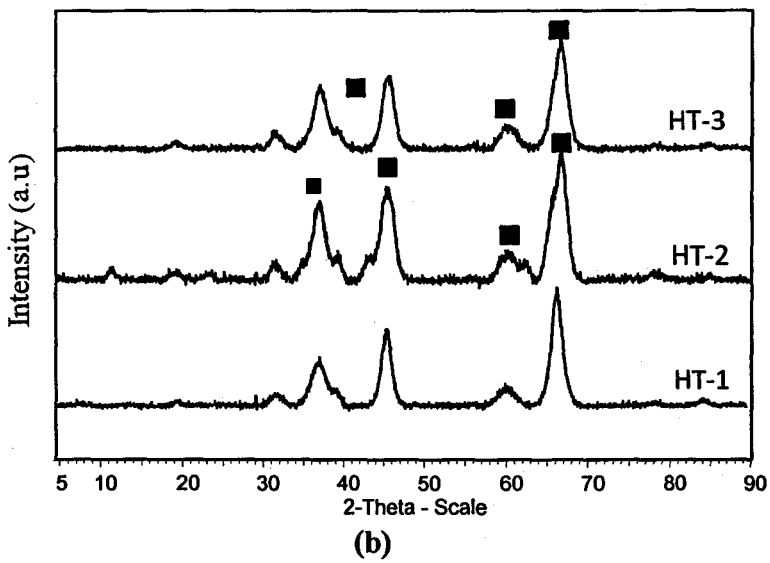

Fig. 1 XRD patterns for the (a) solvothermal samples at different temperatures and (b) calcined and uncalcined HTs. Symbols denote phase other than hydotalcite.

FIGURE 2 shows that HTs exhibited a broadband ranging from 3400 to 3500 cm-1 corresponding to the OH stretching vibration due to the interlayer water molecules and hydroxyls groups in the brucite layer. The characteristic OH group band was at 3445 cm^{-1}. The band at 1636cm^{-1} was due to OH vibration of the water molecules [5]. A shoulder at 1600 to 1650 cm^{-1} corresponded to the bending motion of interlayer water. The weak band in the 1653 to 1638 cm^{-1} region was due to H_2O from the interlayer water [6]. 1385 to 1398 cm^{-1} band corresponded to the carbonate group. HT-2 and HT-3 exhibited strong band in the 450-650cm^{-1} region corresponding to MgO, Al_2O_3 and $Mg(OH)_2$. The band 600-800cm^{-1} for HT-2 and HT-3 was attributed to the brucite and pericalse phase.

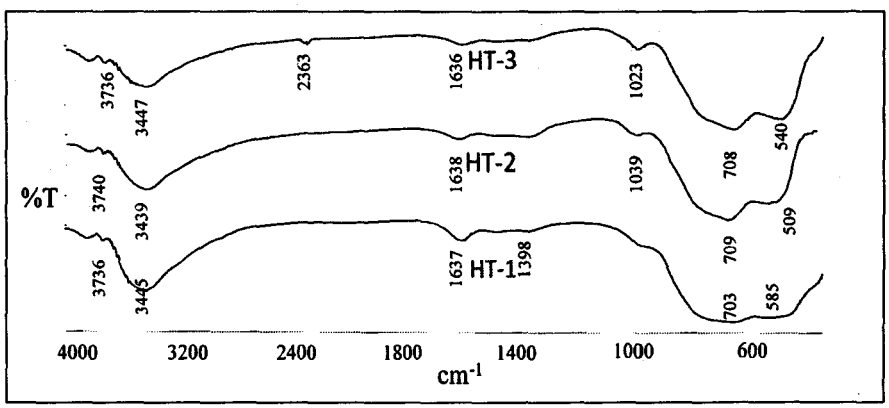

FIGURE 2. IR spectra for the calcined and uncalcined HTs

FIGURE 3 shows that the higher temperature treatment during solvothermal processing resulted in higher hydrotalcite enrichment thereby, promoting growth of the crystallites [8].

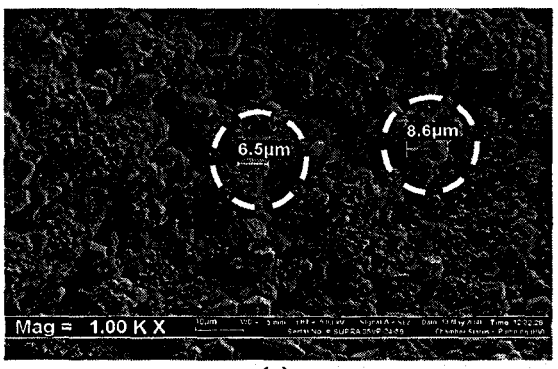

(a)

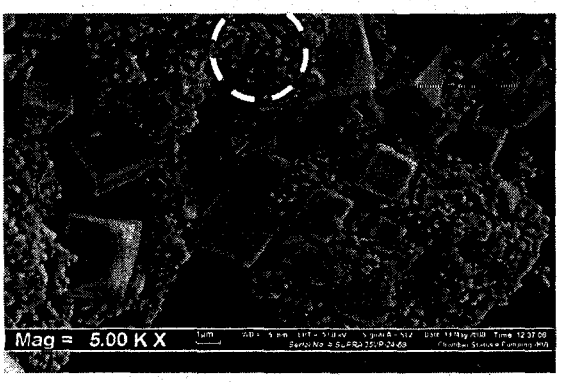

(b)

FIGURE 3. SEM images of HT samples undergoing solvothermal process at (a) 160°C, (b) 200°C.

CONCLUSION

The characteristics of solvothermal hydrotalcites synthesized under autogenous pressure at different temperatures from this study are discussed and presented. X-Ray diffraction analysis demonstrates that the solvothermal processing enriched the hydrotalcite content in the samples and promoted the hydrotalcite crystallinity without requiring further thermal treatment or calcination. XRD pattern of calcined HT-2 and HT-3 also shows that there existed crystallization of mixed oxide phase (periclase, alumina and brucite) while uncalcined HT-1 demonstrated pure rhombus hydrotalcite

phase. The difference in the crytallinity level and phase structures is due to the different crystallization conditions.

ACKNOWLEDGMENTS

Support from the RU Fund (research project No: 814050) is gratefully acknowledged.

REFERENCES

1. F. Cavani, F. Trifiro, A. Vaccari, Hydrotalcite-type anionic clays: preparation, properties and application. *Catal.* Today **11**, 173–301 (1991).
2. F. Leroux, JP. Besse, Polymer interleaved layered double hydroxide: a new emerging class of nanocomposites. *Chem. Mater.* **13**, 3507–3515 (2001).
3. Masashi Inoue, in: Chemical Processing of Ceramics, Second Edition Taylor & Francis Group, LLC. 22-56 (2005).
4. W. Meilan, P. Yanfei, L. Guoqun, H. Tao, Z. Zhicai, Z. Tao and Z. Ruiming. A novel solvothermal route to benzene ring-capped oxide nanocrystals. *Material Letters.* **61**, 4807–4810 (2007).
5. Lopez, T., Bosch, P., Ramos, E.,Asomoza, M. and Gomez, R. DTA, TGA and FTIR spectroscopies of sol-gel hydrotalcites; aluminium source effect on physicochemical properties. *Material Letters.* **31**, 311-316 (1997).
6. dos Reis, M.J., Silvero, F., tronto, J. and Valim, J.b. Effects of pH, temperature and ionic strength on adsorption of sodium dodecylbenzenesulfonate into Mg-Al-CO_3 layered double hydroxides. *Journal of Physics and Chemistry of Solids.* **65**, 487-492 (2004).
7. Aramendia, M.A., Borau, V., Jimenez, C., Marinas, J.M Luque, J.M., Ruiz, J.R. and Urbano, F.J. Synthesis and characterization of a novel Mg/In hydrotalcite-like compound. *Material Letters.* **43(3)**, 118-121 (2000).
8. Y. Aiguo, X. Liu, Q. Guanzhou, Z. Ning, S. Rongrong, Y. Ran, T. Motang and C. Renchao. A simple solvothermal synthesis and characterization of round-biscuit-like Fe_3O_4 nanoparticles with adjustable sizes. *Solid State Communications.* **144**, 315–318 (2007).
9. S. Lowell and J.E Shield, in: Powder Surface Area and Porosity. New York: Chapman & Hall Ltd. (1991).
10. F. Prinetto, G. Ghiotti, P. Griffin and D. Tichit. Synthesis and characterization of sol-gel Mg/Al and Ni/Al layered double hydroxide and comparison with co-precipitated samples. *Microporous and Mesoporous Materials.* **39**, 229-247 (2000).
11. K. Frantis, K. David, C. Zuzana and H. Va'clav.Crystallization of synthetic hydrotalcite under hydrothermal conditions. *Applied Clay Science*, **28**, 101– 109 (2005).
12. Carja, G., Nakamura, R., Aida, T. and Niiyama, H. Textural properties of layered double hydroxides: effect of magnesium substitution by copper or iron. *Microporous and Mesoporous Materials.* **47**, 275-284 (2001).
13. Mulder, M. in: Basic Principle of Membrane Technology. Netherlands: Kluwer Academic Publishers (1996).
14. Prinetto, F., Ghiotti, G., Graffin, P. and Tichit, D. Synthesis and characterization of sol gel Mg/Al and Ni/Al layered double hydroxides and comparison with co-precipitated samples. *Microporous and Mesoporous Materials.* **39**, 229-247 (2000).
15. Heish, H.P. in: Inorganic Membranes for Separation and Reaction. Membrane Science and Technology series 3. Amsterdam: Elsevier Science (1996).

Applied Organometallic Chemistry

Received: 26 May 2009 Accepted: 22 June 2009 Published online in Wiley Interscience: 5 August 2009

(www.interscience.com) DOI 10.1002/aoc.1532

The conversion of an organometallic compound into an intercalated thin-layer amorphous structure

M. R. Othman[a]*, W. J. N. Fernando[a] and J. Kim[b]

A thin alumina-hydrotalcite (Al-HT) film was fabricated from the synthesized boehmite and HT sol samples. The sols were a Newtonian fluid within 12 h of the sol synthesis and pseudo-plastic flow thereon. Co-precipitated HT demonstrated poorly crystallized periclase and spinel structures and apparent doublet peak of hydrotalcite at $2\theta = 39-44°$, indicative of a disordered structure. The heated Al-HT sample demonstrated highly amorphous structure with single hydrotalcite peak but barely observed γ-alumina and γ-boehmite phases. The exfoliation of the spinel, gibbsite and periclase in the Al-HT was caused by the intercalation of boehmite into the HT layers that impeded the formation of the oxides phases. Copyright © 2009 John Wiley & Sons, Ltd.

Keywords: coagulation; films; gels; non-Newtonian fluids; rheology

Introduction

The use of alumina (Al) in catalytic reaction has been well received. Al has been used as a catalyst support for many reactions such as in a steam-reforming of methane, removal of dyes and pigments from effluents, desulfurization of fuel or dechlorination, because Al demonstrates excellent durability and reliability, is economically advantageous, its porosity is well defined, and the surface area is sufficiently high to effect the desired reaction. Al contains active sites, it mediates direct coupling of reactants and it is able to influence the strength of surface basic sites that are favorable for a reaction process. It is used in many catalytic processes in the petrochemical industry, such as isomerization, alkylation, catalytic cracking and hydroforming. Al is usually prepared by the dehydration of aluminum hydroxide or from the hydrolysis of sodium aluminate in the Bayer process.[1]

Hydrotalcite (HT) or $Mg_6Al_2(OH)_2$ has been used as a catalyst in dehydrochlorination and recovery of hydrochloric acid[2,3] and decomposition of urea.[4] HT has already found use in pharmaceutical industries as a drug carrier because of its bio-compatibility and the swelling properties. The swelling of HT nanocomposite hydrogels has been known to cause uncharged drug solute released through the gel easily.[5] HT has also been used in the removal of arsenic from drinking water,[6] as CO_2 adsorbents[7,8] and for sequestration of CO_2 to reduce the greenhouse emission from industries[9–11] owing to its interesting ion exchange capacities and the structural negative charge that is balanced by the interlayer cations. Because of the interesting properties, HT has attracted researchers to study and modify its functionality such as the strength of basicity or carbonate phobicity level by exchanging the intercalated anions with different ones,[12] changing the Mg/Al compositions[13] or addition of a metal ion such as Ni[14] in order to fully exploit its potentials for use as adsorbents and in catalytic reactions.

In sequestering CO_2 from combustion gases at medium and high temperatures (400–527 °C), HT was typically pelletized to prepare particles with an average diameter of 1.4 mm before they were packed inside a tubular reactor for adsorption[15] or catalytic reaction experiment. Recently, there has been a requirement for HT to be formed into a membrane for gas separation application[16] in order to overcome the economic challenges,[17] because the current cryogenic separation and pressure/thermal swing adsorption technologies are energy-intensive. In industry, ranging from food and beverage processing, desalination of seawater, and gas separations, to medical devices, the use of polymeric membranes is on the rise,[18] but these membranes cannot be accommodated in an environment requiring chemical and thermal endurance. Thus, an inorganic membrane is a good alternative.

Normally, preparation of an inorganic membrane is achieved by impregnation, but the layer suffers defects associated with non-uniformity of pores, heterogeneity of particles, deformation and leaching of the active layer as reaction proceeds over time, leading to ineffective and unintended outcomes. Very often, HT is used in the form of particles or beads and fabrication of an HT membrane from co-precipitation can only be achieved by impregnation. In this work, sol precursors were prepared using sol–gel technique to develop an Al-HT or $(Al_2O_3)_{0.98}[Mg_6Al_2(OH)_2]_{0.02}$ membrane for separation and reaction applications. The rheological properties, bonding and functional group, hydrophobicity and the presence of multi-phases of the oxides as the samples progressively changed from sols, gels into heated solids are discussed.

* *Correspondence to: M. R. Othman, Sri Ampangan, Nibong Tebal 14300, Malaysia. E-mail: chroslee@eng.usm.my*

a *School of Chemical Engineering, Universiti Sains Malaysia, 14300 Nibong Tebal, Penang, Malaysia*

b *Department of Chemical Engineering, Kyung Hee University, Yongin, 449-701, Korea*

Material and Methods

The Al precursor for use as an active thin layer was prepared by hydrolization of aluminum alkoxide [$Al(OC_4H_9)_3$] with water. Peptization of the sol was achieved using molar composition of the alkoxide, acid and water at 1:0.07:100, equivalent to 12.8 ml of alkoxide, 0.1 ml of HCl and 90.3 ml of H_2O. In order to add strength to the final gel matrix, 2.1 ml of PVA was added to the mixture. The mixture was stirred rigorously and refluxed under continuous stirring for 24 h. The peptized sol was allowed to cool steadily to enable hydroxylation, alkoxilation or condensation to occur continuously. A small amount of the resulting aluminum monohydrate sol mixture (boehmite) was poured onto a polypropylene Petri dish and dried under ambient and highly humid conditions for 48 h to obtain a hardened, dried Al-boehmite gel for analysis. The gel was heated to 600 °C to analyze possible formation of ordered structures in the sample.

The HT sample was prepared by dissolving 9.4 g of aluminum nitrate nanohydrate [$Al(NO_3)_3 \cdot 9H_2O$] and 4.6 g magnesium nitrate hexahydrate [$Mg(NO_3)_2 \cdot 6H_2O$] in 32 ml of deionized water to achieve the Mg : Al atomic ratio of 3.0. The mixture was then added dropwise with 95 ml potassium carbonate (1 M) under vigorous stirring over a hot plate at 60 °C for 15 min. The pH was kept constant at 10 by adding 100 ml of 1 M NaOH. Half of the solution was kept as a stock solution (HT solution) under continuous stirring to add in the boehmite solution in the preparation of aluminum-hydrotalcite (Al-HT) sample. The remaining solution was allowed to precipitate; the precipitate was filtered and washed several times with warm deionized water to remove nitrate ions and excess Na^+.

In preparing Al-HT precursor, 6.37 ml HT solution (5 wt% loading) and 0.1 ml acid were added to 63.5 ml boehmite solution. The solution was stirred rigorously for about 24 h under reflux conditions. A similar procedure to obtain Al-HT dried gel, discussed earlier, was repeated. Initially, two types of acid namely HCl (12 M) and HNO_3 (15 M) were selected in the experiment because Cl^- and NO_3^- ions were thought would be important in modifying the acid base properties of the layered double hydroxide once the final sintered product was obtained.[19] However, we discovered that HNO_3 was not sufficiently strong to provide the necessary charge contribution in the sol to effect peptization, despite the fact that it was applied at higher molar concentration than HCl. Consequently, the use of HNO_3 in Al-HT precursor synthesis was terminated and HCl was applied instead, in order to achieve sufficient level of peptization in the sol samples.

The viscosity of the sol samples was determined using Brookfield Rheometer integrated with Rheocalc V2.1 software. The speed was set at 100 rpm in auto mode. The analysis was done at 30 °C and temperature was maintained using temperature bath. The X-ray diffraction pattern of the sample was obtained using Philips Analytical X-ray to determine the structure and composition of the material from monochromatized Cu–Kα radiation ($\lambda = 0.154056$). The X-ray diffractometer was taken over a 2θ range of 10–70°. The surface morphology of the hydrotalcite powder was analyzed by SEM from Germany, model Leo Supra 50 VP Field Emission. Samples were placed in the sample grid and coated with gold (20–30 nm thickness) for electron reflection and vacuumed (5–10 min) before analysis. The thermal gravimetric analyzer (TGA 7) supplied by Perkin Elmer was used to measure the weight loss of hydrotalcite sample as a function of temperature. An infrared (IR) spectrum of hydrotalcites was obtained using FTIR spectrophotometer (Perkin Elmer FTIR 2000, USA). Samples were prepared by mixing the powdered solids with potassium bromide, KBr (the blank) in a 15:85 ratio to get transparent pellet auto supported on the different solids at 8 ton pressure.

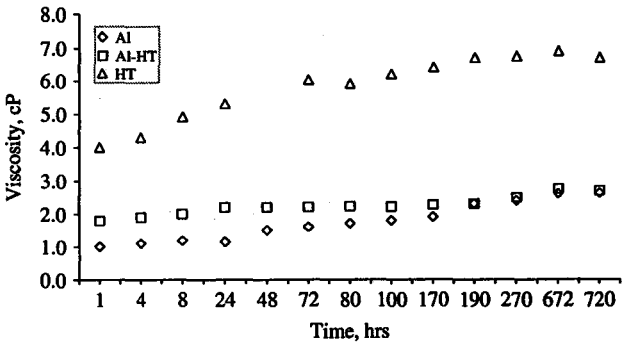

Figure 1. Viscosity of solution samples over time measured at 100 rpm.

Result and Discussion

The application of sol–gel in the development of inorganic membranes typically results in controllable, nano-scale structures unattainable by conventional practices. In sol–gel processing, a membrane with extremely fine pores would typically require peptization of its sol precursor to avoid significant particle aggregation by addition of some threshold amount of acid. The use of acid in particle segregation is accomplished due to similar electric charges as that of the particles and these charges cause the particles to repel each other to maintain a stable dispersion.

Figure 1 shows the rheology of all three sol samples. The viscosity or internal friction of the sol increased with time, demonstrating their rheopectic flow behavior as particles started to agglomerate. The viscosity was in the order of HT sol > Al-HT sol > Al (boehmite sol). The increase in viscosity was pronounced within 24 h of sol synthesis, especially evidenced by HT sol precursor sample, and then the viscosity increase was rather insignificant afterwards for all the samples. As the reaction proceeded, there was continued formation of polymer ligands and condensation growth of metal clusters between its own metal species and/or with different metal species that formed bigger clusters. The agglomeration of these clusters gave rise to higher viscosity of the sols. All three sol precursors demonstrated nearly constant values of viscosity after 168 h, provided that water was not allowed to liberate from the sol during the sol–gel transition.

All the sol samples behaved as a Newtonian fluid immediately after sol synthesis and within 12 h of the sol synthesis. The sol samples, initially, were well dispersed, stable and highly homogeneous. Afterwards, the sol suspensions exhibited a pseudo-plastic flow (or shear thinning) behavior, in that their viscosity decreased with increase in the shear rate due to the decrease in intermolecular forces as shear rate was increased (Fig. 2). This non-Newtonian characteristic was closely associated with extensive agglomeration of suspended particles, as the reaction proceeded with time, especially evidenced by the Al-HT sol suspension. The effect of temperature on the sol viscosity was observed to be similar to that of the shear rate, in that they both weakened the interaction between sol particles, causing the viscosity to decrease as temperature or shear rate was increased.

Figure 3 presents the FTIR spectral analysis of the gel samples after they were dried for 48 h. A broad band in the 3750–3000 cm^{-1}

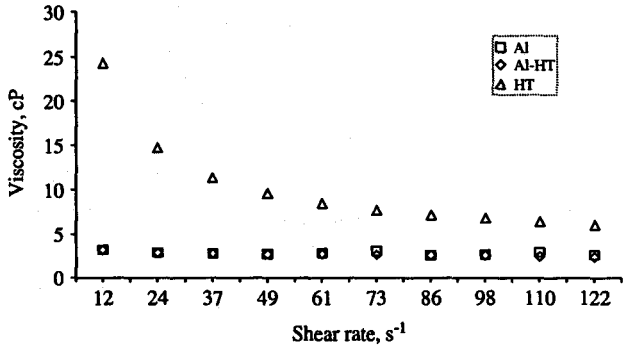

Figure 2. Viscosity of solution samples against shear rate. Data taken after 48 h of continuous s Stirring.

range for all the gel samples corresponded to the hydroxyl group (OH) or layers, indicative of O–H stretching due to transition metal-hydroxyl arising from Al–OH physical attachment and the residual interlayer water that remained trapped in the interstices of the dried gels. The overall intensity of the band decreased slightly for Al and Al-HT gels, indicating that the two samples were less hydroxylated and exhibited weaker Al-H_2O bonding than that of HT gel. This result was later verified from TGA analysis that showed less water removal from the HT and Al-HT samples as they were dried and heated at elevated temperatures (Fig. 4). The peak near the shoulder band corresponds to the hydrogen bonding between water and carbonate in the interlayer. The bending vibration of water was observed in all the gel samples, represented by the peaks in the 1700–1600 cm^{-1} spectrum. The peaks in the 1400–1070 cm^{-1} spectrum were assigned to carbonate anion. The absorption peak in lower frequency was assigned to metal–oxygen (M–O) and metal–hydroxyl (M–OH) groups in the lattice of Al gel arising from the inorganic metal (such as magnesium in the Al-HT sample) that were derived from $Mg(NO_3)_2 \cdot 6H_2O$ in the precursor solution.

Figure 4 shows results of the TGA for the dried gels. Further drying of the gels from 30 to 200°C caused all the samples to lose weight. The weight loss at this temperature region was primarily due to the removal of interstitial alcohol and interlayer water molecules and partial decomposition of hydroxyls from the pores of the boehmite gels, demonstrated by sharp endothermic peaks from DTA curves (not shown). The weight loss appeared substantial for Al sample due to the fact that the sample exhibited weaker water bonding than that of Al-HT and HT gels. Since the bonding was weak in the Al gel sample, most of the water was easily removed as the gels were heated. The OH–Al binding affinity in Al–HT and HT gel matrix within their interlocking hydroxyls layers, apparently, was stronger than that in Al sample. Only a small amount of water was liberated despite increase in temperature. The TGA curves may also be used to infer the syneresis and hydrophobicity level of the samples by correlating the amount of water removal from the gels. The syneresis effect as a result of water removal form the gel sample was experienced the most by Al, followed by HT and Al-HT. The hydrophobicity of the samples was in the order of Al-HT > HT > Al. Al-HT and HT were highly hydrophobic since they allowed the least interstitial water to occupy in their latticed structures. On heating there was not much water left to be evaporated from the hydrophobic samples, as shown in the figure. Samples with higher Al content typically exhibited higher resistance against decomposition, since Al^{2+} was capable of retaining hydroxyl groups even at elevated temperature. Al-HT and HT conspicuously displayed this characteristic since they were enriched with higher amounts of Al^{2+} than Al samples, as shown in Fig. 5.

From Energy Dispersive X-ray (EDX) analysis (Fig. 5), Al content was found to be the highest in Al-HT because the precursor to Al was derived from the two sources, Al-alkoxide and $Al(NO_3)_3 \cdot 9H_2O$. The Al gel sample contained the most H and O, rendering the Al content in the overall gel composition relatively lower that that in Al-HT and HT samples. This explains the reason for Al being the least hydrophobic (containing the most water) from the TGA results discussed earlier.

The process of HT conversion can be explained as follows. First, the resulting gel lost a fraction of its interlayer water as it was

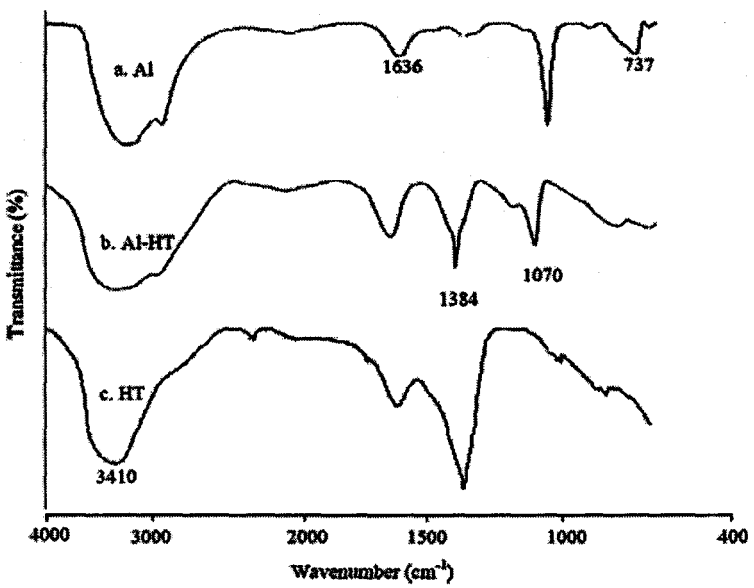

Figure 3. FTIR of dried solid samples: (a) Al; (b) Al-HT; (c) HT.

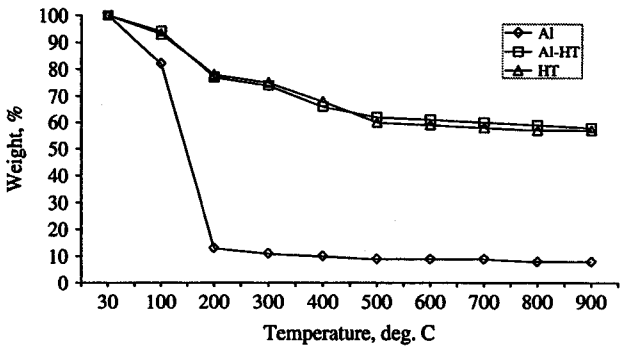

Figure 4. TGA of the dried solid samples.

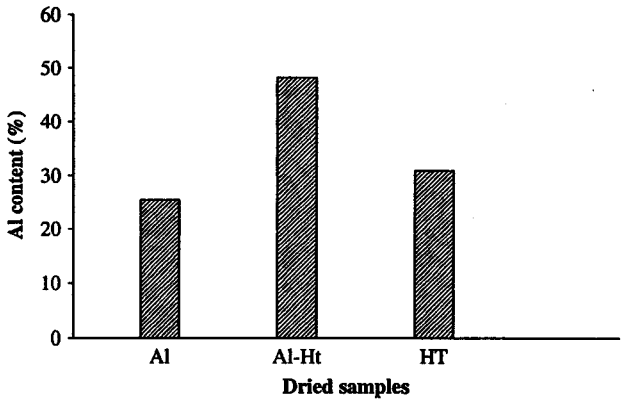

Figure 5. Percentage of Al in the dried solid samples. The sample was dried for 48 h.

heated from 25 to 200 °C.

$$Mg_6Al_2(OH)_{16}CO_3.4H_2O \longrightarrow Mg_6Al_2(OH)_{16}CO_3 + 4H2O \uparrow \quad (1)$$

At temperatures higher than 200–500 °C, the carbonate was eliminated and the resulting solids were partially dehydroxylated to form $Mg_6Al_2O_8(OH)_2$,

$$Mg_6Al_2(OH)_{16}CO_3 \longrightarrow Mg_6Al_2O_8(OH)_2 + 7H_2O \uparrow + CO_2 \uparrow \quad (2)$$

Further heating of $Mg_6Al_2(OH)_{16}CO_3$ at 500–600 °C would trigger secondary reaction to form layered double hydrotalcite, $Mg_6Al_2(OH)_2$, whereby water and carbonates were continuously released.

$$Mg_6Al_2(OH)_{16}CO_3 \longrightarrow Mg_6Al_2(OH)_2 + 14/2H_2O \uparrow + CO_3 \uparrow \quad (3)$$

$Mg_6Al_2O_8(OH)_2$ would be converted to MgO (periclase) and $MgAl_2O_4$ (spinel) if higher temperature than 600 °C was applied.

$$Mg_6Al_2O_8(OH)_2 \longrightarrow MgAl_2O_4 + 5MgO + H_2O \uparrow \quad (4)$$

The weight loss due to temperature increase from 200 to 600 °C was attributed to the following factors: (1) thermal decomposition of organic compounds from the alkoxy group; (2) further decomposition of other ligands that were used as solvents and additives (or binders); (3) elimination of residual H_2O from the interstices, pores and inter-particles that was difficult to remove at lower temperature; and (4) decomposition of the remaining nitrates from the Al-HT and HT. The decomposition of these compounds usually resulted in the development of a micro and meso pore network. As the polymer was burned off, it left pore and created a distinct pore network. Al-HT and HT samples appeared to have experienced rapid pore development (and syneresis) due to the relatively high differential weight loss it suffered in the 200–500 °C region. At temperature higher than 600 °C, all the organic compounds were completely removed, as evidenced from the TGA results. No further decrease in the samples' weight was observed, suggesting that there was virtually no more decomposition – an indication that the samples were structurally stable in this temperature regime. The exothermic peaks from DTA results (not shown) in the temperature between 500 and 700 °C indicated that the samples were in the prelude to a transition state between an amorphous (disordered) to a crystalline (ordered) γ-alumina phase. Formation of more stable crystallized phases of alumina or collapse of micro-pore to form meso- and macro-pore network in the oxide samples was expected at higher temperature. If the pores were collapsed altogether, a dense sample might be obtained but this would only materialize at excessively high temperature (and possibly if it were facilitated by high pressure).

The development of hydrotalcite phase was observed for samples heated at 600 °C as shown from the XRD result (Fig. 6) but undetectable in the TGA spectrum in this work due to the alumina phase transition that masked its presence. HT sample prepared from co-precipitation and heated at 600 °C demonstrated poorly crystallized mixed oxides phase (periclase and spinel structures) and the splitting (doublet) peak of hydrotalcite at $2\theta = 39–44°$ suggesting that the layer double hydroxide phase was not stable. The heated Al-HT sample from Fig. 6(b) demonstrated highly amorphous structure with a single hydrotalcite peak but barely observed presence of γ-alumina and γ-boehmite phases. The exfoliation of the spinel, gibbsite and periclase phases was apparent. The exfoliation was possibly caused by the intercalation of boehmite into the HT layer that promoted the anion-exchange process in the interlayer galleries of the Al-HT structure, causing the formation of the oxides phases to impede. This process also caused the distinguishable γ-alumina pattern in the Al sample [Fig. 6(c)] in the higher angle to disappear, and the γ-alumina phase in the lower angle to broaden and the splitting of γ-boehmite to converge to form a single, broader spectrum. The γ-alumina phase in Al sample was clearly visible from the spectrum [Fig. 6(c)]. The γ-boehmite appeared to remain in the sample (as observed from the spectrum in the higher angle) even after the sample was heated to 600 °C. HT and Al-HT may exhibit some form of intercalated structures as shown by the blunt peaks at 2θ of less than 20°,[19] whereas the existence of lamellar structures in Al was barely visible.

The surface fractal dimension (D), was used to infer the surface irregularities and space filling ability of the gel samples in this work. The fractal value varies from 2 to 3. A low value of surface fractal inferred high level of smoothness of a surface, while the higher surface fractal dimension inferred decreased space filling ability and increased irregularity. The fractal dimension was determined in this work using the Frenkel-Halsey-Hill (FHH) method from a

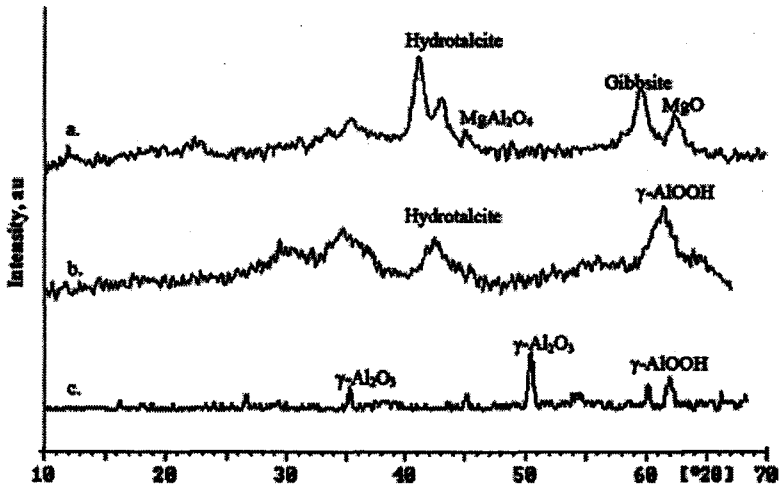

Figure 6. XRD of the heated samples at 600 °C: (a) HT from co-precipitation; (b) Al-HT from sol–gel; (c) Al from Boehmite sol.

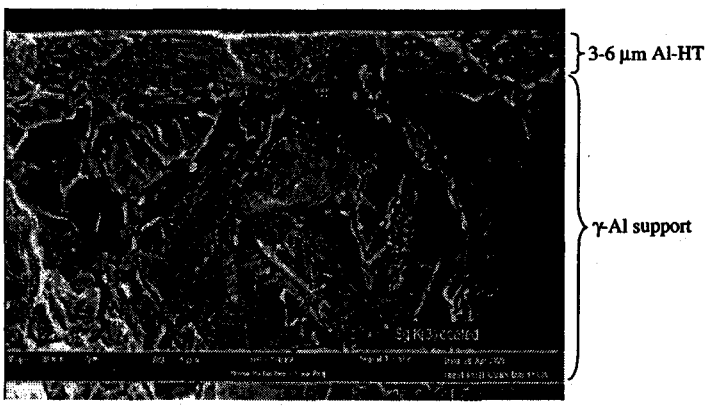

Figure 7. SEM image at magnification ×3000 of a cross sectional view of Al-HT layer deposited on the porous alumina support.

multilayer adsorption, employing the equation:

$$\ln\left(\frac{N}{N_m}\right) = (D-3)\ln\left[\ln\left(\frac{P_o}{P}\right)\right] \quad (5)$$

where N represents the number of adsorbed moles of nitrogen at a given relative pressure, and N_m corresponds to the number of adsorbed moles in a monolayer. D was computed based on a regressed plot of $\ln N/N_m$ against $\ln[\ln(P_o/P)]$. The values of fractal dimension and the space filling ability of the dried gel samples were in the order of HT (2.44) > Al-HT (2.37) > Al (2.35). Pore surface irregularity of HT was highest, possibly induced by a restructuring phenomenon caused by the formation of randomly combined Mg coarse clusters that protruded from the surfaces of the ligatures. Al-HT and Al pore surfaces were smoother and more pristine to enable accessibility of the gas adsorbate (N_2) to fill up the available pore spaces. The surface smoothness was possibly caused by the lustre of the coordinatively saturated metallic components and higher interaction between (better proximity of) the respective metallic constituents in the clusters. The lower surface fractal might also be caused by the smooth polymer material surface that covered the coordinatively unsaturated metallic components from being exposed to the outer surface, precluding contact with the nitrogen gas during the multilayer adsorption test. For the HT sample heated at 600 °C, the pore size distribution from nitrogen adsorption analysis from the previous effort[20] revealed a bimodal pattern, displaying peaks at 4.7 and 7.8 nm, respectively and Brunauer-Emmett-Teller (BET) surface area of 51 m^2/g. For Al-HT sample heated at 600 °C, the pore size distribution from nitrogen adsorption analysis gave a narrow peak at 5.2 nm and BET surface area of 268 m^2/g. For Al sample heated at 600 °C, the pore size distribution from nitrogen adsorption analysis gave a single peak at 2.75 nm and BET surface area of 439 m^2/g. The highly disordered Al-HT with narrow pore size distribution gave rise to higher CO_2 adsorption capacity (27.9 mg/g) than that demonstrated by HT (6.9 mg/g),[10] commercial activated carbon (11 mg/g)[21] and natural zeolites (2.70 mg/g).[22]

Figure 7 shows a SEM image of a thin $(Al_2O_3)_{0.98}[Mg_6Al_2(OH)_2]_{0.02}$ layer deposited by dip coating on a porous alumina (200 nm) that was used as a support material. The Al-HT layer with thickness of 3–6 μm displays distinguishingly denser, smoother surfaces and more closely packed microstructure than its support material. Initially, the Al-HT sol overlying on the coarse support filled up the support pores instead of forming the desirable layer on the support. After the porous alumina support was pre-treated with poly-(vinyl alcohol) as a pore filling substance, the polymer appeared to have reduced the support surface roughness and successfully prevented the Al-HT solution from infiltrating into the support pores. The pore filling substance was later removed by thermal decomposition during heat treatment.

Conclusion

The application of sol–gel technique to prepare sol precursors for development of Al-HT membranes was explored and reported in this work. Our findings from the sol analysis demonstrated that all the sol samples were rheopectic fluids, displaying pseudo-plastic flow behavior. The viscosity was in the order of HT > Al-HT > Al, and that the samples were favorable for dip and spray coating application to produce a thin layer since their viscosity value increased insignificantly, provided that the sols ceased further evaporation of water. From the analysis of gel samples, the hydrophobicity of the samples was found to be in the order of Al-HT > HT > Al, which was influenced considerably by the Al content and Al-H_2O bonding. The rate of porosity development was in the order of HT ≈ Al-HT > Al. The samples were structurally stable in 600–900 °C because of the transformation into more ordered, crystalline oxide phases. The pore surface irregularity was in the order of HT (2.44) > Al-HT (2.37) > Al (2.35) and pore size was in the order of HT (4.7, 7.8 nm) > Al-HT (5.2 nm) > Al (2.75 nm). The meso-porous Al-HT was found to successfully develop on the top surface of macro-porous alumina support.

Acknowledgment

The authors would like to acknowledge the support from the Universiti Sains Malaysia and Ministry of Science, Technology and Innovation of Malaysia. Contributions from N. M. Rasid and M. H. A. M. Ahmad from the Industrial Technology Division, Malaysia Nuclear Agency are also acknowledged.

References

[1] G. K. Chuah, S. Jaenicke, T. H. Xu, *Micro. Meso. Mat.* **2000**, *37*, 345.
[2] T. Kameda, T. Yoshioka, K. Watanabe, M. Uchida, A. Okuwaki, *App. Clay Sci.* **2007**, *37*, 215.
[3] G. Carja, G. Delahay, *Appl. Catal. B: Environ.* **2004**, *47*, 59.
[4] S. Vial, V. Prevot, C. Forano, *J. Phy. Chem. Sol.* **2006**, *67*, 1048.
[5] W. F. Lee, Y. C. Chen, *Eur. Polym. J.* **2006**, *42*, 1634.
[6] G.P. Gillman, *Sci. Tot. Environ.* **2006**, *366*, 926.
[7] H. Tagaya, K. Tsunaki, M. Hasegawa, M. Karasu, K. Chiba, *Bul. Yam. Univ. (Eng.)* **1992**, *22*, 21.
[8] M. R. Othman, J. Kim, *J. Korean Phys. Soc.* **2008**, *52*, 1231.
[9] T. Horiuchi, H. Hidaka, T. Fukui, Y. Kubo, M. Horio, K. Suzuki, T. Mori, *Appl. Catal. A: Gen.* **1998**, *167*, 195.
[10] M. R. Othman, N. M. Rasid, W. J. N. Fernando, *Chem. Eng. Sci.* **2006**, *61*, 1555.
[11] Z. Yong, V. Mata, A. E. Rodrigues, *Ind. Engr. Chem. Res.* **2001**, *40*, 204.
[12] A. Sampieri, G. Fetter, H. Pfeiffer, P. Bosch, *Sol. Stat. Sci.* **2007**, *9*, 394–403.
[13] J. I. D. Cosimo, V. K. Díez, M. Xu, E. Iglesia, C.R. Apesteguía, *J. Catal.* **1998**, *178*, 499.
[14] J. A. Rivera, G. Fetter, Y. Jiménez, M. M. Xochipa, P. Bosch, *Appl. Catal. A: Gen.* **2007**, *316*, 207.
[15] B. Ficicilar, T. Dogu, *Catal. Today* **2006**, *115*, 274.
[16] M. R. Othman, *Chem. Eng. Sci.* **2009**, *64*, 925.
[17] Z. Yong, V. Mata, A. E. Rodrigues, *Sep. Pur. Tech.* **2002**, *26*, 195.
[18] S. S. Kulkarni, E. W. Funk, N. N. Li, *AIChE Symp.* **1986**, *82*, 78.
[19] M. R. Othman, J. Kim, *J. Sol–Gel Sci. Technol.* **2008**, *47*, 274.
[20] M. R. Othman, N. M. Rasid, W. J. N. Fernando, *Micro. Meso. Mat.* **2006**, *93*, 23.
[21] R. V. Siriwardane, M. S. Shen, E. P. Fisher, J. A. Poston, *Energ. Fuel.* **2001**, *15*, 279.
[22] R. V. Siriwardane, M. S. Shen, E. P. Fisher, *Energ. Fuel.* **2003**, *17*, 571.

Applied Catalysis A: General 363 (2009) 1–10

Contents lists available at ScienceDirect

Applied Catalysis A: General

journal homepage: www.elsevier.com/locate/apcata

Review

Solid heterogeneous catalysts for transesterification of triglycerides with methanol: A review

Z. Helwani [a,b], M.R. Othman [b,*], N. Aziz [b], J. Kim [c,**], W.J.N. Fernando [b]

[a] Department of Chemical Engineering, Riau University, Pekanbaru 28293, Indonesia
[b] School of Chemical Engineering, Universiti Sains Malaysia, 14300 Nibong Tebal, Penang, Malaysia
[c] Department of Chemical Engineering, Kyung Hee University, Yongin 446-701, Republic of Korea

ARTICLE INFO

Article history:
Received 14 November 2008
Received in revised form 4 May 2009
Accepted 11 May 2009
Available online 19 May 2009

Keywords:
Biodiesel
Transesterification
Hydrotalcites
Alkaline solid catalysts
Metal hydroxides

ABSTRACT

Increasing number of researches focusing on the use of solid heterogeneous catalysts for the production of biodiesel provides evidence that these catalysts continue to evolve as viable alternatives. While liquid alkaline metal alkoxides remain to be appealing in the industries, it is expected that solid base catalyst will soon become more attractive due to the economics and environmental concern. Limited researches have shown that the conversion by solid base catalysts was comparable to that of the existing alkoxide system. This paper reviews various types of heterogeneous solid acids and bases in the production of biodiesel from transesterification of triglycerides. Unconventional enzymatic and non-catalytic supercritical methanol transesterification are also presented. The yields and conversion from various catalytic systems are compared, and the advantages and disadvantages of the systems discussed.

Contents

1. Introduction

Biodiesel is a liquid fuel similar to petroleum diesel in combustion properties, but essentially free of sulphur, making it a cleaner burning fuel than petroleum diesel [1]. Biodiesel is derived from renewable energy sources, such as vegetable oils and animal fats. It has similar physical and chemical properties with petro-diesel fuel. However, biodiesel properties can sometimes be

* Corresponding author. Tel.: +60 45996426; fax: +60 45941013.
** Corresponding author. Tel.: +82 031 201 2492; fax: +82 031 202 1946.
E-mail addresses: chroslee@eng.usm.my (M.R. Othman), jkim21@khu.ac.kr (J. Kim).

0926-860X/$ – see front matter © 2009 Elsevier B.V. All rights reserved.
doi:10.1016/j.apcata.2009.05.021

Table 1
Comparison of the standards for diesel and biodiesel based on American Society for Testing and Materials (ASTM) [2].

Property	Diesel	Biodiesel
Standard Number	ASTM D975	ASTM D6751
Composition	Hydrocarbon (C_{10}–C_{21})	Fatty acid methyl ester (C_{12}–C_{22})
Specific gravity (g/ml)	0.85	0.88
Flash point (K)	333–353	373–443
Cloud point (K)	258–278	270–285
Pour point (K)	243–258	258–289
Water (vol%)	0.05	0.05
Carbon (wt%)	87	77
Hydrogen (wt%)	13	12
Oxygen (wt%)	0	11
Sulphur (wt%)	0.05	0.05
Cetane number	40–55	48–60

superior than that of petro-diesel fuel because the former has higher flash point, ultra-low sulphur concentration, better lubricating efficiency, and better cetane number. The standards for biodiesel and petroleum based diesel [2] are provided in Table 1 for the comparison.

Conventionally, the biodiesel production is performed by transesterification of vegetable oils with methanol in the presence of homogeneous basic catalysts, such as sodium or potassium hydroxides, carbonates or alkoxides [3–6]. These catalytic systems suffer problems such as difficulty in removing the basic catalysts after the reaction, production of large amount of wastewater and emulsification. The latter problem is associated with the soaps that are known to emulsify the biodiesel with glycerin, especially if ethanol is used. Furthermore, the growing concern about the environment prompts the chemical industry to develop less polluting and more selective chemical processes. In this context, solid catalysts appear promising to replace the liquid homogeneous catalysts because they are less corrosive, easier to handle and separate, reusable and generating less amount of toxic wastes. The use of heterogeneous catalysis in transesterification reactions prevents the undesirable saponification, allows process simplification and offers reduction in the processing costs by eliminating the additional steps required by the liquid homogeneous catalysts [3,4,7].

2. Biodiesel production from vegetable oils

Biodiesel in another definition is a non-petroleum based fuel consisting of alkyl esters derived from transesterification of triglycerides (TG) or by the esterification of free fatty acids (FFA) with low molecular weight alcohols. The fuel properties of the esters produced from the transesterification can vary depending on the types of vegetable oils used. Table 2 enlists fuel properties of methyl esters derived from different vegetable oils [8].

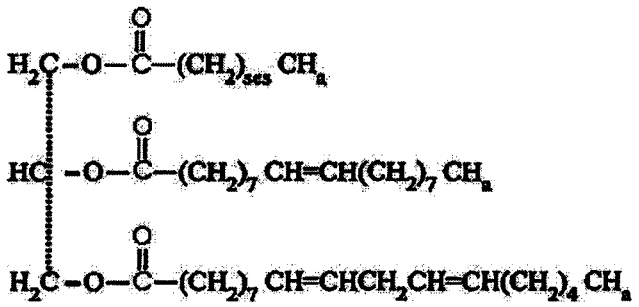

Fig. 1. Chemical structure of triglyceride.

Biodiesel production has become an area in which many researchers have increasing interest. This is due to its potential as an alternative fuel that offers a complementary strategy for sustainability [9]. The most common approach of biodiesel production is by transesterification of vegetable oils and animal fats. This is a well established process introduced since 1853. Varieties of vegetable oils have been exploited in the past and present for biodiesel production with varying but promising results. The oils used include cotton seed [10–13], soybean [14,15], waste cooking [5], rapeseed [16–18], sunflower seed [19–21], winter rape [22], frying [23,24], jojoba [25] and *Jatropha curcas* [26]. The choices of alcohols used are mainly methanol [27], ethanol [28] and butanol [29]. The catalysts used in the transesterification include sodium hydroxide [28,30], potassium hydroxide [25,28], sulphuric acid [31], supercritical fluids or enzymes such as lipases [14,32,33].

2.1. Vegetable oils as diesel fuels

Vegetable oils, also known as triglycerides, have the chemical structure given in Fig. 1. They comprise of 98% triglycerides and small amounts of mono- and diglycerides [34]. Triglycerides are esters of three fatty acids and one glycerol containing substantial amounts of oxygen in its structure [35]. The fatty acids vary in their carbon chain length and in the number of double bonds [36]. Different types of vegetable oils have different types of fatty acids. Table 3 shows the empirical formula and structure of various fatty acids present in vegetable oils [37].

The use of vegetable oils offers some advantages. First, they are available in almost every part of the world. Second, they are renewable since the vegetables from which oil seeds are obtained can be planted and harvested continuously throughout the year. Third, they appear to be a potentially "greener" fuel, because the fuel derived from the oils contains no or the least sulphur element [37,38]. Fourth, the plants help in CO_2 fixation during photosynthesis. The main drawbacks with vegetable oils for use as a diesel fuel are that, the viscosity of the biodiesel is high, the volatility and reactivity of the unsaturated hydrocarbon chains are

Table 2
Fuel properties of methyl esters of vegetable oils [8].

Methyl ester of vegetables oil	Cetane number	Cloud point (°C)	Pour point (°C)	Flash point (°C)	Density (kg/l)	Iodine value
Ground nut	54	5	–	176	0.883	80–106
Cotton seed	51	–	−4	110	–	–
Soybean	45	1	−7	178	0.885	117–143
Rapeseed	54	−2	−9	84	–	–
Babassu	63	4	–	127	0.875	10–16
Palm	62	13	–	164	0.880	35–61
Sunflower	49	1	–	183	0.860	110–145
Tallow	–	12	9	96	–	35–48
B20 (blend)	51	–	−16	128	0.859	–
Diesel	50	–	−16	76	0.885	–

Table 3
Chemical structure of common fatty acids [37].

Name of fatty acid	Chemical name of fatty acid	Structure (x:y)	Formula
Lauric	Dodecanoic	12:0	$C_{12}H_{24}O_2$
Myristic	Tetradecanoic	14:0	$C_{14}H_{28}O_2$
Palmitic	Hexadecanoic	16:0	$C_{16}H_{32}O_2$
Steatic	Octadecanoic	18:0	$C_{18}H_{36}O_2$
Arachidic	Eicosanoic	20:0	$C_{20}H_{40}O_2$
Behemic	Docosanoic	22:0	$C_{22}H_{44}O_2$
Lignoceric	Tetracosanoic	24:0	$C_{24}H_{48}O_2$
Oleic	cis-9-Octadecanoic	18:1	$C_{18}H_{34}O_2$
Linoleic	cis-9,cis-12-Octadecadienoic	18:2	$C_{18}H_{32}O_2$
Linolenic	cis-9,cis-12,cis-15-Octadecatrienoic	18:3	$C_{18}H_{30}O_2$
Erucic	cis-13-Docosenoic	22:1	$C_{22}H_{42}O_2$

low [39]. Growing the plants, as many claimed, requires greater area of land and huge amount of fertilizers, leaving some carbon footprint along the process and resulting in dramatic increase in the price of some food items due to food-biodiesel demand competition.

2.2. Transesterification

Transesterification is the reaction of vegetable oil or animal fat with an alcohol to form esters and glycerol. A catalyst is used to improve the reaction rate and yield. Since the reaction is reversible, excess alcohol is used to shift the equilibrium to the products side [40]. Fig. 2 shows the overall scheme for the transesterification of triglycerides.

Alcohols are the primary and secondary monohydric aliphatic compounds having 1–8 carbon atoms. Methanol and ethanol are used most frequently in the transesterification process. Methanol is preferred because of its lower cost and its physical and chemical advantages (polar and shortest chain alcohol) over ethanol. The former reacts immediately with TG and dissolves easily in NaOH. In order to complete a transesterification stoichiometrically, a 3:1 molar ratio of the alcohol to triglycerides is needed. In practice, the ratio needs to be higher to drive the equilibrium to a maximum ester yield [8,34,41].

3. Catalytic transesterification

The catalytic transesterification of vegetable oils with methanol to produce biodiesel is an important industrial process. Also known as methanolysis, this process is well studied and established. The process makes use of acids or bases, such as sulphuric acids or sodium hydroxides as catalysts to facilitate the reaction. Other types of catalysts have also been used. In general, all the catalysts for the transesterification of vegetable oils can be fitted into three classifications known as homogeneous, enzyme or heterogeneous catalysts. Enzyme can fall into either homogeneous or heterogeneous categories depending on its mobility.

Homogeneous base catalysts are an alkaline liquid such as sodium hydroxide, sodium methoxide, potassium hydroxide, or potassium methoxide. Homogeneous acid catalysts are an acidic liquid such as sulphuric acid, hydrochloric acid or sulphonic acid. Whereas, heterogeneous catalysts are acid or base solids that include immobilized enzymes, titanium-silicates, alkaline-earth metal compounds, anion exchange resins or guanadines heterogenized on organic polymers [21]. While the application of heterogeneous catalysts appears promising and growing, the use of homogeneous catalysts such as sodium or potassium hydroxide, sodium or potassium methoxide is still common in industries because the latter are relatively cheap and quite active for this reaction [42,43].

3.1. Homogeneous base-catalyzed transesterification

In homogeneous base-catalyzed transesterification, the process that was reportedly catalyzed by alkaline metal alkoxides [44,45], hydroxides [42,46–48], or sodium or potassium carbonates [49] demonstrated high catalytic activity and resulted in the production of high quality biodiesel. The methanol used in the process was recoverable and the glycerin by-product was safe and suitable for use in pharmaceutical and other applications. However, the glycerin needed to be separated and removed completely from the biodiesel as it would form formaldehyde or acetaldehyde on combustion.

A known drawback with homogeneous base-catalyzed transesterification is that the oil that contained significant amounts of free fatty acids could not be converted into biodiesels completely but remained as soap in huge quantity [50]. These free fatty acids reacted with base catalyst to produce soaps that inhibited the separation of biodiesel, glycerin and wash water [51]. While triglycerides were readily transesterified at atmospheric pressure and temperature of 60–70 °C with an excess of methanol, it took long time (at least several hours) to ensure that the alkali catalyzed the transesterification completely [52,53]. Removal of these catalysts appears to be technically challenging and it surely brings additional cost to the final product.

Alkaline metal alkoxides (such as CH_3ONa for the methanolysis) are one of the most active homogeneous catalysts being tested in laboratories and industries. They can give very high yields (>98%) in short reaction times (30 min) even if they are applied at low molar concentrations (0.5 mol%). Alkaline metal hydroxides (KOH and NaOH) are alternative sources to base catalysts, cheaper than

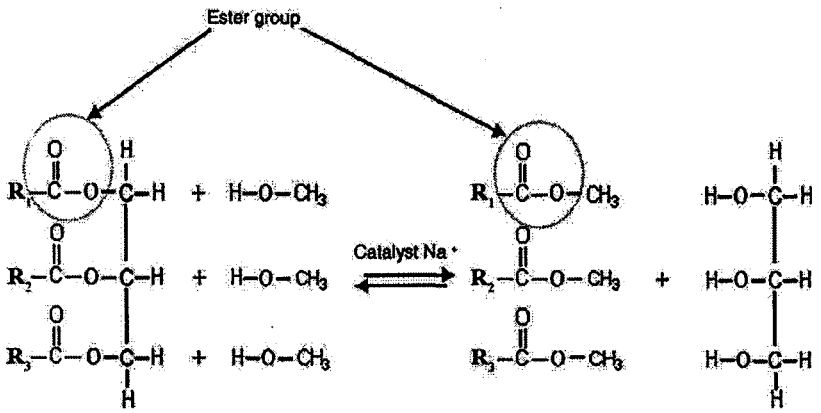

Fig. 2. Overall scheme of the triglycerides transesterification.

Table 4
The advantages and disadvantages of base catalyzed transesterification reaction [26,54].

Advantages	Disadvantages
1. Approximately 4000 times faster than acid catalyzed transesterification	1. Glycerides and alcohol must be substantially anhydrous, otherwise it leads to saponification which reduces the catalytic efficiency, forms gels and causes difficulty in separation of glycerol
2. The free fatty acid content of the oil should be as low as possible	2. The molar ratio of methanol to oil has to be 6:1 or higher instead of the stoichiometric 3:1 ratio
3. Methoxides are more effective than hydroxides	

metal alkoxides, but less active. Nevertheless, they can give sufficiently high conversions of vegetable oils to biodiesel by increasing the catalyst concentration to 1 or 2 mol% [54]. Table 4 summarizes the advantages and disadvantages of base catalyzed transesterification.

3.2. Homogeneous acid catalyzed transesterification

In catalytic transesterification using homogeneous acid catalyst, the reaction is catalyzed by sulphuric [55–57], hydrochloric [55,58] or sulphonic acids [59]. In general, acid catalyzed reactions are performed at high alcohol to oil molar ratios, low to moderate temperatures and pressures and high acid catalyst concentrations. Acid-catalyzed reactions require the use of high alcohol to oil molar ratios in order to obtain good product yields within reasonable reaction time. However, ester yields do not proportionally increase with molar ratio. For instance, in soybean methanolysis using sulphuric acid, ester formation was sharply improved from 77% using a methanol to oil ratio of 3.3:1 to 87.8% with a ratio of 6:1. Higher molar ratio demonstrated only moderate improvement to a maximum of 98.4% (at 30:1) [60]. Despite its insensitiveness to free fatty acids in the feedstock that makes the catalysts attractive, acid-catalyzed transesterification has been largely ignored mainly because of its relatively slow reaction rate [5]. However, homogeneous acid catalyst is still applicable for specific applications and provides options to the operators. The considerations for choices of homogeneous acid catalysis for transesterification are given in Table 5.

3.3. Reaction mechanism in homogeneous acid and base catalyzed transesterification

The mechanistic behavior in homogeneous acid-catalyzed transesterification can be described as follows. First, the TG carbonyl group is protonated by the acid catalyst. The activated carbonyl group then undergoes nucleophilic attack from an alcohol molecule, forming a tetrahedral intermediate. Solvent assisted proton migration gives rise to a leaving group, promoting the cleavage of the hemiacetal species (tetrahedral intermediate) and yielding a protonated alkyl monoester and a diglyceride molecule. The transfer of proton then regenerates the acid catalyst. This sequence is repeated twice to ultimately yield 3 alkyl monoesters and glycerol as products [60].

In transesterification using a base catalyst such as alkaline alkoxide, the catalyst reacts with alcohol to produce catalytically active species, RO^- (where, R is an alkyl or hydrogen deficient alkane and O is oxygen). A tetrahedral intermediate is formed by nucleophilic attack on a carbonyl carbon in the TG. The tetrahedral intermediate breaks down into a fatty acid ester and a diglyceride anion. Then, proton transferred to the diglyceride ion regenerates the RO^- catalytically active species. This sequence is then repeated twice to yield first a monoglyceride intermediate and finally the glycerol product and biodiesel [60].

The important factor that promotes the catalytic effect in the two reactions above is the protonation of the carbonyl group in the TG. The catalyst–reactants interaction increases the electrophilicity of the adjacent carbonyl carbon atom, making it more susceptible to nucleophilic attack. Comparing electrophilic species (in acid-catalysis) to the stronger nucleophile (in base-catalysis), the base catalyst appears to take on a more direct route to activate the reaction of RO^- catalytically active species, resulting in faster catalytic activity.

In the kinetics study of the alkali catalyzed transesterification of soybean oil with methanol and n-butanol [45], 3 regimes categorized the overall reaction process with the rate-limiting reaction step changing over time according to the observed reaction rate. Initially, the reaction was mass transfer limited because of the low miscibility of reagents; i.e., the non-polar oil phase was immiscible with the polar alcohol-catalyst phase; thereby, slowing down the reaction. As ester products were formed, these species acted as an emulsifying agent that gave rise to a second rate regime that was kinetically controlled and characterized by a sudden surge in product formation. Finally, in the last stages of reaction, a third regime was reached characterized again by a slower reaction rate.

3.4. Enzyme catalyzed transesterification

The transesterification is typically catalyzed by lipases such as *Candida antartica* [10,14,33,61], *Candida rugasa* [62], *Pseudomonas cepacia* [63,64], immobilized lipase (Lipozyme RMIM) [65,66], *Pseudomonas* spp. [67] or *Rhizomucar miehei* [67,68]. The yield of biodiesel from this process can vary depending on the type of enzyme used. For example, in the enzymatic alcoholysis of soybean oil with methanol and ethanol using a commercially available *immobilized lipase* (*Lipozyme RMIM*) [66], a 60% yield was obtained after optimum conditions were reached in a solvent-free system using ethanol/oil molar ratio of 3.0, temperature of 50 °C and enzyme concentration of 7.0% (w/w). In another study [64], yield of as high as 98% was obtained using *P. cepacia lipase* immobilized on celite at 50 °C in the presence of 4–5% (w/w) water for 8 h.

The enzyme-catalyzed system normally requires a much longer reaction time than the base catalyzed systems. Though base catalyzed transesterification reaction is fast, the disadvantages are mainly due to the energy intensiveness and difficulty in separating the glycerol from methyl esters. In addition to alkaline waste water

Table 5
Favorable and disadvantageous factors for homogeneous acid catalyzed transesterification [5,8].

Favorable factors	Disadvantageous factors
1. Transesterification can be carried out at high fatty acid content and more water	The transesterification reaction is slower than that of catalysis by base
2. Acid catalysis is preferred when oil component is low grade material like sulphur olive oil	
3. The extraction and transesterification proceed simultaneously. This avoids the use of pre-extracted seed oil	

Table 6
Comparison of base-catalyzed and lipase catalyzed transesterification reactions for biodiesel formation [74].

Parameter	Base catalyzed transesterification	Lipase catalyzed transesterification
Reaction temperature	333–343 K	303–313 K
Free fatty acids in raw materials	Saponified product	Methyl esters
Water content in raw materials	Interfere with reaction	No influence
Yield of methyl esters	Normal	Higher
Recovery of glycerol	Difficult	Easy
Purification of methyl esters	Repeated washing	None
Cost of catalysts	Cheap	Expensive. Enzyme denatures in the presence of methanol and may require additional solvents like THF

that requires further treatment, the free fatty acid and water inhibit the transesterification reaction. Both extracellular and intracellular lipases are favorable in that they are able to effectively catalyze the transesterification of triglycerides in either aqueous or non-aqueous systems [69,70]. As shown in Table 6, enzymatic transesterification methods can overcome the problems described above.

While enzyme reactions are highly specific and chemically clean, the main problem of the lipase-catalyzed process is the high cost of the lipases [10]. Most lipases are also inhibitory to alcohol. In order to overcome this issue, a typical strategy is to feed the alcohol into the reactor in three steps of 1:1 mole ratio each. The reactions are very slow in nature, with a three step sequence requiring from 4 to 40 h or more to complete. The reaction conditions become modest as temperature is raised, for example, from 35 to 45 °C [71].

3.5. Non-catalytic supercritical methanol transesterification

The transesterification of triglycerides by supercritical methanol (SCM), ethanol, propanol and butanol was claimed to be another promising process [27]. A catalyst-free method for biodiesel fuel production by employing supercritical methanol was reported previously [72,73] in which, supercritical treatment at 350 °C, 43 MPa and 240 s with a molar ratio of 42 in methanol was found to be optimum for the transesterification of rapeseed oil into biodiesel fuel. In another work [52], It was discovered that by increasing the reaction temperature, especially supercritical temperatures, the ester conversion was increased favorably.

The non-catalyst options are designed to overcome the reaction initiation lag time caused by the extremely low solubility of the alcohol in the TG phase. One approach that is nearing commercialization is the use of a co-solvent, tetrahydrofuran (THF), to solubilize the methanol. The result was a fast reaction, in the order of 5–10 min and no catalyst residues in either the ester or the glycerol phase was observed. The THF co-solvent was chosen, in part, because it has a boiling point very close to that of methanol. This system requires a rather low operating temperature of 30 °C. Another non-catalytic attempt was made using high (42:1) alcohol to oil ratio, under supercritical conditions (350–400 °C and >80 atm or 1200 psi). The reaction completed in about 4 min [71].

Reaction by supercritical methanol offers some advantages. First, glycerides and free fatty acids are reacted with equivalent rates. Second, the homogeneous phase eliminates diffusion problems. Third, the process tolerates great percentages of water in the feedstock catalytic process that otherwise would require the periodical removal of water in the feedstock or in intermediate stage to prevent catalyst deactivation. Fourth, the catalyst removal step is eliminated. And fifth, if high methanol:oil ratios are used, total conversion of the oil can be achieved in a few minutes [72–74]. The disadvantages of the one-stage supercritical methods are clear. First, it operates at very high pressures (25–40 MPa). Second, the high temperatures bring along proportionally high heating and cooling costs. Third, high methanol:oil ratios (usually set at 42) involve high costs for the evaporation of the unreacted methanol. Fourth, the process as reported to date does not explain how to reduce free glycerol to less than 0.02% as established in the ASTM D6584 or other equivalent international standards [70].

3.6. Heterogeneous catalysts

It is appropriate to begin the discussion on heterogeneously catalyzed transesterification with a comparison of factors in relation to the corresponding homogeneously catalyzed reaction. Such a comparison is summarized exclusively in Table 7.

In heterogeneous catalysis, a number of operating parameters such as temperature, extent of catalyst loading, mode of mixing, alcohol/oil molar ratio, presence/absence of impurities in the feed stock and the time of reaction are important. In a similar manner, transesterification reaction can also be carried out under supercritical conditions and this method may also evolve as a viable alternative to catalytic routes.

3.6.1. Solid acid catalysts

Solid acid catalysts have the potential to replace strong liquid acids to eliminate the corrosion problems and consequent environmental hazards posed by the liquid acids. However, the efforts at exploiting solid acid catalysts for transesterification are limited due to the pessimistic expectations on the possibility of low reaction rates and adverse side reaction. As a result, the factors governing the reactivity of solid catalysts have not been fully understood. For example, simple correlations between acid strength and activity of the catalyst have not been clearly formulated. Second, due to diffusional restrictions the catalyst must have a porous system with interconnecting pores, so that the entire surface of the solid is available for promoting the transesterification reaction. Even though, it is possible to generate these features in the solids, it is not yet routinely possible to obtain uniform pore architecture with absolute control over the size or radius or geometry of the pores as well as the stability of the solid in the system.

Zeolites, due to their uniform pore structure, appear to have definite advantages for this application. In order to be favorable, the surface should be made hydrophobic in order to promote preferential adsorption of oily hydrophobic species on the catalyst surface and to avoid deactivation of catalytic sites by strong adsorption of polar by products like glycerol or water. It is essential

Table 7
Comparison of homogeneous and heterogeneously catalyzed transesterification [4].

Factors	Homogeneously catalysts	Heterogeneously catalysis
Reaction rate	Fast and high conversion	Moderate conversion
After treatment	Catalyst cannot be recovered. must be neutralized leading to waste chemical production	Can be recovered
Processing methodology	Limited used of continuous methodology	Continuous fix bed operation possible
Presence of water/ free fatty acids	Sensitive	Not sensitive
Catalyst reuse	Not possible	Possible
Cost	Comparatively costly	Potentially cheaper

that a reliable quantitative measure of the hydrophobicity of solids is evolved so that one can appropriately correlate this function with the observed activity.

3.6.1.1. Zeolites. Zeolites can be synthesized with extensive variation of acidic and textural properties. They can be synthesized to overcome the diffusional limitations so that optimum biodiesel production can be achieved. Zeolites can also be modulated to exhibit hydrophobic characteristic without compromising its functionalized acidic sites. This can be done by incorporating certain organic species like heteropoly acids into their pore structures. In spite of this, the predictive capability for the zeolites and the necessary functionalization to alter their hydrophobicity is still in the stage of trial and error. Once an estimated hydrophobicity scale is established, it is possible that some predictive capacity of heteropoly acids for the adsorption of benzene/water will emerge [75].

3.6.1.2. Heteropoly acids. In the search for water tolerant acid catalysts, heteropoly acids appear to be the appropriate choice. Most of these systems have acidity in the range of super acids with the possibility of tailoring the porous architecture as well as solubility in water (such as the Cs salt). $Cs_{2.5}PW$ catalyst was reportedly chosen [76] on the basis of high activity, water tolerance, reusability and environmentally benign nature of this material for biodiesel production. The solid acid catalyst was so efficient that it produced 99% yield of biodiesel at the expense of only low catalyst concentration (1.85×10^{-3}:1 weight ratio of catalyst-to-oil), low methanol-to-oil ratio (5.3:1), low temperature (338 K), and relatively short reaction time (45 min). The process was environmentally benign and economical since the activity of the $Cs_{2.5}PW$ was not much affected by the free fatty acid and moisture content that were present in the vegetable oil. The catalyst could be separated easily from the product mixture and reused number of times.

Although it appears attractive, it is necessary that the activity of this class of catalysts is evaluated and compared with the other hydrophobic solid catalysts from the point of important variables and operating parameters such as methanol to oil molar ratio, reaction temperature and the extent of reusability [77]. These data, whenever available, will place the system in a proper perspective.

3.6.1.3. Functionalized zirconia and silica. The use of sulphated zirconia catalysts and organo sulphonic acids functionalized silica for the transesterification was reported previously [78,79]. The idea of utilizing sulphated zirconia catalyst in the esterification arose from the difficulty of recuperating sulphuric acid from the system. The main drawback with these systems was that the sulphate ions leached out from the porous support as a result of hydrolysis. As alternatives to sulphated zirconia, sulphated tin oxide and tungstated zirconia–alumina were also experimented [80–82]. The results demonstrated that the phase composition of zirconia contributed considerably in the reaction. The tetragonal zirconia that was formed from low calcinations temperature (500 °C) produced significantly higher yield than the monoclinic zirconia that was formed from higher calcinations temperature (900 °C). This comparison can be observed from Table 8. While it was found that the co-existence of amorphous WO_3 and tetragonal ZrO_2 was necessary in order to achieve high activity in biodiesel production, the presence of monoclinic phase of zirconia and crystalline WO_3, however small, carried detrimental effects on the esterification reaction. It was thought that the active sites that fostered notably large catalytic activity were located only at the interface between tetragonal zirconia and amorphous WO_3. The nature of these active sites and their strength (if they possess some characteristic) need to be evaluated and specified. It is expected that such data base will be generated in the near future.

3.6.1.4. Other solid acid catalysts. The other types of solid acid catalysts that were exploited for use in esterification and transesterification reaction studies in the past include tungsten oxides [50,57,83,84], sulphonated zirconia (SZ) [57,85–89], Amberlyst115 [57,86,90], Lewatit GF 101, sulphonated saccharides [91–94], Nafion1 resins [57,83,86,90,95–97], and organosulphonic functionalized mesoporous silicas [98–101]. Even though solid acid catalysts have been applied effectively in the esterification of carboxylic acids, the use of these catalysts to obtain high conversion of triglycerides to biodiesel necessitates much higher reaction temperatures than base catalysts because of their lower activity for transesterification [102]. Some resins, such as Amberlyst115, may be considered an exception as these catalysts catalyze appreciably both esterification and transesterification reactions under mild reaction conditions due to their high concentrations of acid sites [57,90]. However, thermal stability becomes an issue when resin-type catalysts are used at higher temperatures [103] in order to achieve higher reaction rates in an application such as reactive distillation. The other issue is associated with catalyst regeneration.

3.6.2. Solid base catalysts

3.6.2.1. Basic zeolites. The base strength of the alkali ion exchanged zeolite increases with increasing electropositive nature of the exchanged cation. The occlusion of alkali metal oxide clusters in zeolite cages through the decomposition of impregnated alkali metal salts results in an increase in the basicity of these materials [104]. These exchanges can affect the water tolerant behavior of the basic zeolite system. Systems like ETS-10, a microporous inorganic lithium containing zeolite has been shown to be a new generation solid base catalyst for transesterification. Most of these catalysts contain the basic sites (cation) generated by thermal decomposition of the supported salt. It has been shown that the conversion to methyl ester over NaX faujasite zeolite that was ion exchanged with more electropositive cations was higher than that of the parent zeolite. Fig. 3 illustrates the point where the intermediate electronegativity of the solid is correlated with the yield of the methyl ester [14]. This type of correlation has become one of the preferred methods for catalyst selection. Although some guidelines on these aspects are available, a general concept has yet to be developed to facilitate the catalyst selection for transesterification.

3.6.2.2. Hydrotalcites. Hydrotalcites (HT) are a class of anionic and basic clays known as layered double hydroxides (LDH) with the formula $Mg_6Al_2(OH)_{16}CO_3.4H_2O$. It presents a positively charged brucite-like layers ($Mg(OH)_2$) in which some of Mg^{2+} are replaced

Table 8
Correlation between preparation method of the catalysts and structural effect for esterification of palmitic acid on 5 wt% WO_3/ZrO_2 catalysts [50].

Calcination temperature (°C)	Impregnation		Co-precipitation	
	Conversion (%)	XRD phase	Conversion (%)	XRD phase
500	98	Tetragonal ZrO_2	95	Tetragonal ZrO_2
900	8	Monoclinic ZrO_2/WO_3	17	Monoclinic ZrO_2/WO_3

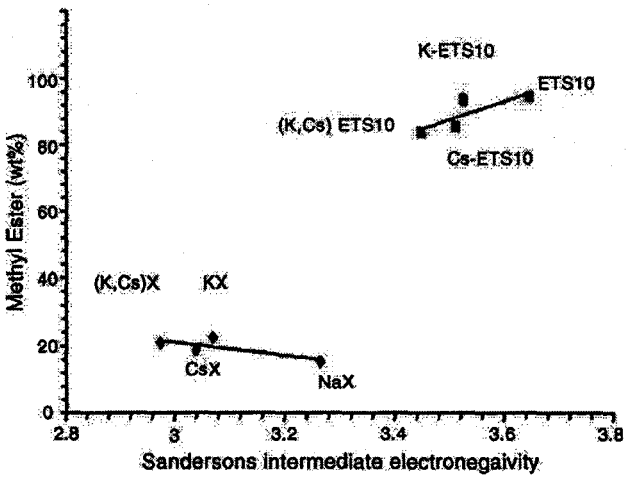

Fig. 3. Methyl ester (wt%) at 393 K as a function of intermediate electronegativity calculated from Sanderson intermediate rule. Sixty percent ion exchange is assumed for cesium to calculate electronegativity. Ninety-five percent ion exchange is assumed for potassium to calculate electronegativity.

by Al^{3+} in the octahedral sites of hydroxide sheets. Interstitial layers formed by CO_3^{2-} anions and water molecules compensate the positive charge resulting from this substitution [105]. A wide range of compositions containing various combinations of M(II), M(III) and different anions A^{n-} can also be synthesized [106].

Conventionally, HT is synthesized by coprecipitation, wherein metal nitrates and precipitants are added slowly and simultaneously at a fixed pH under stirring, followed by a long (about 1 day) ageing time and/or hydrothermal treatment in order to improve the crystallinity. A particular chemical composition and the method of synthesis, i.e., temperature, solution pH, and ageing time of the gels, have a strong influence on the final basicity of the mixed oxides [107,108]. Decomposition of Mg–Al HT yields a high surface area Mg–Al mixed oxide, which presumably exposes strong Lewis base sites [109]. The basic properties of these sites depend on the Mg–Al ratio in the precursor hydrotalcite [110]. The reconstruction of decomposed Mg–Al HT by rehydration at room temperature reportedly enhanced the catalytic activity [111]. During the rehydration, the brucite-like layers were reformed and the charge-compensating carbonate anions were replaced by hydroxyl anions, thus forming Brønsted base sites. The decomposed–rehydrated Mg–Al HT with Brønsted base sites exhibited higher catalytic activity than the decomposed Mg–Al HT with Lewis base sites for the transesterification of oleic acid methyl ester with glycerol [109]. A hypothetically simplified model for the reaction is given in Fig. 4.

In the methanolysis experiment using Mg–Al HT catalysts prepared by coprecipitaion, the best ester conversions from soybean oil and glyceryl tributyrate were below 80% [1,112–114]. In another work [115], transesterification of rapeseed oil with methanol using Mg–Al HT prepared using Mg/Al molar ratio of 3.0, aged for 12 h and calcined at 773 K converted the methanol ester to about 90.5% yield.

Although relatively lower yield was observed, HT can still provide large opportunity for improvement in the biodiesel production. This is especially true if the specific surface area of the solid pore is improved, its homogeneity is enhanced and the

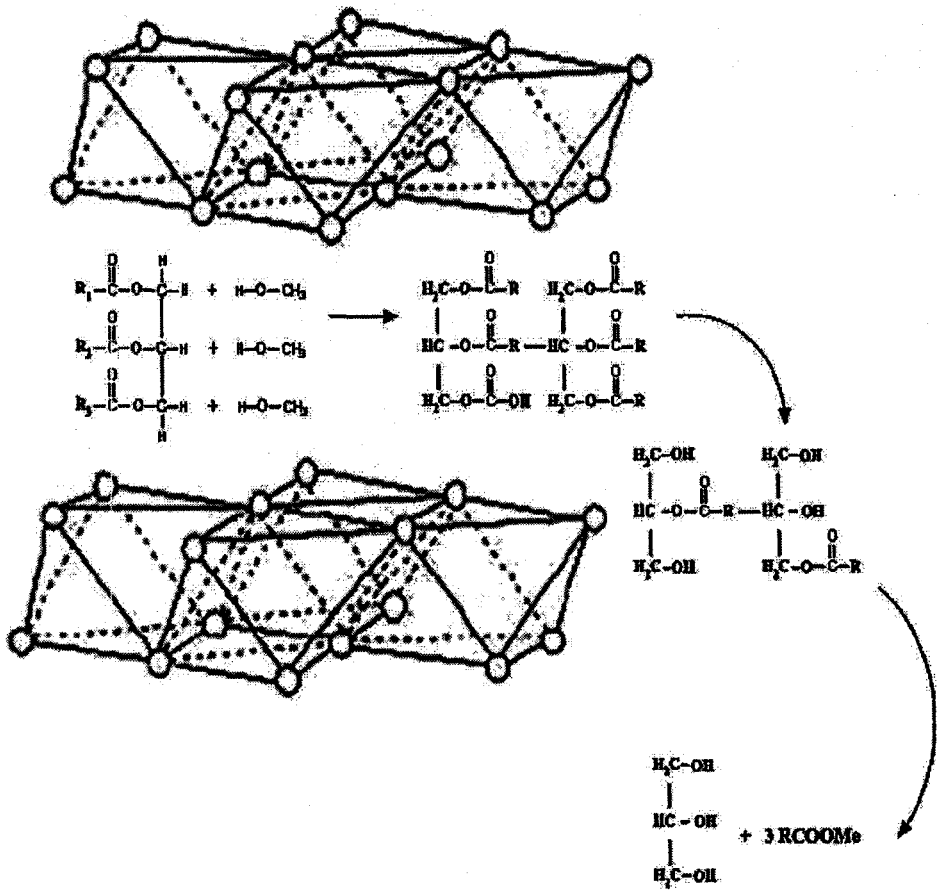

Fig. 4. A simplified model of hydrotalcite catalyzed transesterification.

Table 9
Different heterogeneous catalysts used for transesterification of vegetable oils.

Vegetable oil	Catalysts	Ratio MeOH/Oil	Reaction time, h	Temperature, °C	Conversion, %	References
Blended vegetable oil	Mesoporous silica loaded with MgO	8	5	220	96	[129]
Soybean oil	WO_3/ZrO_2, Zirconia-alumina and sulphated tin oxide	40	20	200–300	90	[50]
Soybean oil	La/Zeolite beta	14.5	4	160	48.9	[130]
Palm oil	Mg–Al–CO_3 (Hydrotalcite)	30	6	100	86.6	[112,131]
Rapeseed oil	$CaTiO_3$, $CaMnO_3$, $Ca_2Fe_2O_5$, $CaZrO_3$, $CaO–CeO_2$	6	10	60	90	[132]
Soybean oil	$MgO·MgAl_2O_4$	3	10	65	57	[133]
Sunflower oil	CaO/SBA-15	12	5	160	95	[134]
Soybean oil	MgO–ZnO–Al_2O_3	55	7	70, 100, 130	82	[7]
Soybean oil	Cu and Co	5	3	70		[38]
Soybean oil	CaO, $Ca(OH)_2$, $CaCO_3$		2	65	99	[135]
Jatropha curcas oil	CaO	9	2.5	70	93	[136]
VO	Cs-heteropoly acid, SO_4^{2-}/ZrO_2, SO_4^{2-}/Al_2O_3, SO_4^{2-}/SiO_2, WO_3/ZrO_2	19.4	1	75	70	[137]
Rapeseed oil	Mg–Al HT	6	4	65	90.5	[115]
Soybean oil	CaO, SrO	12	0.5–3	65	95	[138,139]
Soybean oil	ETS-10	6	24	120	94.6	[15]
Cotton seed oil	Mg–Al–CO_3 HT	6	12	180–210	87	[114]

particle size is greatly reduced. A way to achieve these desirable characteristics is by employing a sol–gel method during HT synthesis. By way of the sol–gel technique, core-shell nano-particle HT and thin films can be prepared [116–118]. In addition, sol–gel coatings can be applied at room temperature [119] and pressure by different but very simple arrangements [120]. It was transpired that the specific surface area of HT obtained from the sol–gel method was up to three times greater than that achieved by coprecipitation [121–125].

3.6.2.3. Alkaline earth oxide base catalysts. Alkaline earth oxides are potential base catalysts for use in triglyceride transesterification. The origin of basic sites in alkaline earth oxides has been the subject of review, and it is generally believed that they are generated by the presence of M^{2+}–O^{2-} ion pairs in different coordination environments. The basic strength of the group II oxides and hydroxides increased in the order Mg > Ca > Sr > Ba. Of these, Ca-derived bases are the most promising as they are inexpensive, the least toxic and they exhibit low methanol solubility [16]. CaO exhibited poor activity in transesterification, with only 2.5% conversion being observed after 25 min reaction. In contrast, catalyst with as little as 0.23 and 1.23 wt% Li loadings showed greatly enhanced performances with 83 and 100% conversion, respectively after the same reaction time. Further increase in Li content proved detrimental to catalyst activity with the 4 wt% Li sample giving only 37% conversion. Negligible leaching of $LiNO_3$ occurred during reaction. An optimum Li content of 1.23 wt% was found to give maximum activity for methyl butanoate formation. Lithium incorporation was also known to increase the base strength of CaO. XPS and DRIFTS measurements showed that the optimum loading correlated with the formation of an electron deficient Li^+ species and the evolution of –OH species at defect sites on the support [126,127].

3.6.2.4. Alkaline metal salt on porous support. Table 9 summarizes different types of heterogeneous catalysts supported on porous substrates and their conversion rate at different operating parameters reported previously [7,15,38,50,112,114,115,129–139]. The non-loaded alumina support did not yield methyl oleate or glycerol within 1 h, and yielded only 7% methyl oleate over 12 h at 423 K. Alumina loaded with K_2CO_3, KF, $LiNO_3$ and NaOH, on the other hand, produced glycerol and higher yield of methyl oleate over 1 h at 333K. This provides evidence that porous supports can be functionalized effectively by loading alkaline metal salts, with the exception of KOH/Al_2O_3 that reportedly exhibited low catalytic activity [128].

KF loaded on ZnO is an active and promising heterogeneous catalyst for the production of biodiesel from soybean oil. The active KF species is formed by the reaction of KF and ZnO and the surface hydroxyls provide strong basic sites in the catalyst. The 15 wt% KF loaded on ZnO after being calcined at 873 K for 5 h was found to exhibit the highest basicity and the best catalytic activity for the transesterification reaction. Heterogeneous solid oxide catalysts of the type $(Al_2O_3)_4(SnO)$ and $(Al_2O_3)_4(ZnO)$ for the transesterification of vegetable oil using different chain length alcohols reportedly produced the highest yield of 84% [129].

4. Conclusions

This review suggests that the interest in heterogeneous catalysis for biodiesel production has been growing. From the commercial point of view, solid base catalysts are seen more effective than acid catalysts and enzymes. However, more researches on solid base catalysis are needed to substantiate this because the favorable results from previously reported works were at the expense of high temperatures and high pressures. From the economic standpoint, it would be ideal if solid base catalysts could work efficiently at temperatures below 150 °C and low pressure. On the other hand, solid acid catalysts, enzymes and non-catalytic supercritical transesterification have been largely ignored in biodiesel research due to pessimistic expectations in terms of reaction rates, undesirable side reactions and high costs. However, these methods should continue to have a place in biodiesel synthesis so that more alternatives can be made available. Issues concerning their constraints should also be addressed continuously so that the limitations can be overcome and they evolve as viable alternatives in the near future.

Acknowledgement

Support from Ministry of Science Technology and Innovation of Malaysia and the Universiti Sains Malaysia is gratefully acknowledged.

References

[1] D.G. Cantrell, L.J. Gillie, A.F. Lee, K. Wilson, Appl. Catal. A: Gen. 287 (2005) 183–190.
[2] R.M. Joshi, M.J. Pegg, Fuel 86 (2007) 143–151.

[3] Y. Liu, E. Lotero, J.G. Goodwin Jr., X. Mo, Appl. Catal. A: Gen. 331 (2007) 138–148.
[4] E. Lotero, Y. Liu, D.E. Lopez, K. Suwannakarn, D.A. Bruce, J.G. Goodwin Jr., Ind. Eng. Chem. Res. 44 (2005) 5353.
[5] Y. Zhang, M.A. Dube, D.D. McLean, M. Kates, Bioresour. Technol. 90 (2003) 229–240.
[6] E. Leclereq, A. Finiels, C. Moreau, J. Am. Oil Chem. Soc. 78 (2001) 1161.
[7] W.M. Antune, C.O. Veloso, C.A. Henriques, Catal. Today 133–135 (2008) 548–554.
[8] A. Srivastava, R. Prasad, Renew. Sust. Energy Rev. 4 (2000) 111–133.
[9] J.M. Marchetti, V.U. Miguel, A.F. Errazu, Renew Sust. Energy Rev. 11 (2005) 1300–1311.
[10] D. Royon, M. Daz, G. Ellenrieder, S. Locatelli, Bioresour. Technol. 98 (2007) 648–653.
[11] F.A. Zaher, Energy Sour. 25 (2003) 819–826.
[12] A.S. Huzayyin, A.H. Bawady, M.A. Rady, A. Dawood, Energy Conv. Manage. 45 (2004) 2093–2112.
[13] H. Chen, J.-F. Wang, Stud. Surf. Sci. Catal. 159 (2006) 153–156.
[14] Y. Watanabe, Y. Shimada, A. Sugihara, T. Tominaga, J. Mol. Catal. B: Enzym. 17 (2002) 151–155.
[15] G.J. Suppes, M.A. Dasari, E.J. Doskocil, P.J. Mankidy, M.J. Goff, Appl. Catal. A: Gen. 257 (2004) 213–223.
[16] D. Kusdiana, S. Saka, Fuel 80 (2001) 693–698.
[17] S. Gryglewicz, Bioresour. Technol. 70 (1999) 249–253.
[18] C.D. Rakopoulos, K.A. Antonopoulos, D.C. Rakopoulos, E.C. Kakaras, E.G. Pariotis, Int. J. Vehicle Des. 45 (2007) 200–221.
[19] G. Labeckas, S. Slavinskas, Renew. Energy 31 (2006) 849–863.
[20] K.G. Georgogianni, M.G. Kontominas, P.J. Pomonis, D. Avlonitas, V. Gergis, Fuel Process. Technol. 89 (2008) 503–509.
[21] G. Vicente, M. Martınez, J. Aracil, Bioresour. Technol. 92 (2004) 297–305.
[22] C.L. Peterson, M. Feldman, R. Korus, D.L. Auld, Appl. Eng. Agric. 7 (2001) 711–716.
[23] N. Saifuddin, K.H. Chua, Malay. J. Chem. 6 (2004) 77–82.
[24] R. Alcantara, J. Amores, L. Canoira, E. Fidalgo, M.J. Franco, A. Navarro, Biomass. Bioenergy 18 (2000) 515–527.
[25] A. Bouaid, Y. Diaz, M. Martinez, J. Aracil, Catal. Today 106 (2005) 193–196.
[26] K. Pramanik, Renew. Energy 28 (2003) 239–248.
[27] A. Demirbas, Energy Conv. Manage. 48 (2006) 937–941.
[28] J.M. Encinar, J.F. Gonzalez, J.J. Rodriguez, A. Tejedor, Energy Fuel 16 (2002) 443–450.
[29] Y. Warabi, D. Kusdiana, S. Saka, Bioresour. Technol. 91 (2004) 283–287.
[30] H.J. Kim, B.S. Kang, M.J. Kim, Y.M. Park, et al. Catal. Today 93 (2004) 315–320.
[31] M.I. Al-Widyan, A.O. Al-Shyoukh, Bioresour. Technol. 85 (2005) 253–256.
[32] R.D. Abigor, P.O. Uadia, T.A. Foglia, M.J. Haas, K.C. Jones, E. Okpefa, et al. Biochem. Soc. Trans. 28 (2000) 979–981.
[33] Y. Watanabe, Y. Shimada, A. Sugihara, J. Am. Oil Chem. Soc. 77 (2000) 355–360.
[34] A. Demirbas, H. Kara, Energy Sour. 28 (2006) 619–626.
[35] M. Balat, Energy Sour. A 29 (2007) 895–913.
[36] N. Tippayawong, T. Wongsiriamnuay, W. Jompakdee, Asian J. Energy Environ. 3 (2002) 139–158.
[37] B.K. Barnwal, H.P. Sharma, Renew. Sustain. Energy Rev. 9 (2005) 363–378.
[38] Y.D. Wang, T. Al-Shemmeri, P. Eames, J. McMullan, N. Hewitt, Y. Huang, et al. Appl. Thermal Eng. 26 (2006) 1684–1691.
[39] R.B. da Silva, A.F.L. Neto, L.C.S. dos Santos, J.R. de oliviera, M.H. Chaves, et al. Biosour. Technol 99 (2008) 6793–6798.
[40] A. Demirbas, Energy Conv. Manage. 47 (2006) 2271–2282.
[41] G. Knothe, R.O. Dunn, M.O. Bagby, ACS Symposium Series no. 666: Fuels And Chemicals From Biomass, Washington, DC, USA, (1997), pp. 172–208.
[42] L.C. Meher, D.V. Sagar, S.N. Naik, Renew. Sust. Energy Rev. 10 (2006) 248–268.
[43] C.C.S. Macedo, F.R. Abreu, A.P. Tavares, M.P. Alves, L.F. Zara, J.C. Rubim, et al. J. Braz. Chem. Soc. 17 (2006) 1291–1296.
[44] A.W. Schwab, M.O. Bagby, B. Freedman, Fuel 66 (1987) 1372–1378.
[45] B. Freedman, R.O. Butterfield, E.H. Pryde, J. Am. Oil Chem. Soc. 63 (1986) 1375–1380.
[46] C. Stavarache, M. Vinatoru, R. Nishimura, Y. Maed, Ultrason. Sonochem. 12 (2005) 367–372.
[47] A. Ohi, H. Aoyama, H. Ohuchi, A. Kato, M. Yamaoka, Nenryo Kyokaishi 62 (1983) 24–31.
[48] H.A. Aksoy, I. Becerik, F. Karaosmanoglu, H.C. Yamaz, H. Civelekoglu, Fuel 69 (1990) 600–603.
[49] V. Varghaa, P. Truterb, Eur. Polym. J. 41 (2005) 715–726.
[50] S. Furuta, H. Matsuhasbi, K. Arata, Catal. Commun. 5 (2004) 721–723.
[51] M. Canakci, J. van gerpen, Trans. ASAE 46 (2003) 945–955.
[52] A. Demirbas, Energy Conv. Manage. 43 (2002) 2349–2356.
[53] A. Demirbas, Energy Conv. Manage. 44 (2003) 2093–2109.
[54] U. Schuchardta, R. Serchelia, R.M. Vargas, J. Braz. Chem. Soc. 9 (1998) 199–210.
[55] M.J. Goff, N.S. Bauer, S. Lopes, W.R. Sutterlin, G.J. Suppes, J. Am. Oil Chem. Soc. 81 (2004) 415–420.
[56] Y. Liu, E. Lotero, J.G. Goodwin Jr., J. Mol. Catal. A: Chem. 245 (2006) 132–140.
[57] D.E. Lopez, J.G. Goodwin Jr., D.A. Bruce, E. Lotero, App.l Catal. A: Gen. 295 (2005) 97–105.
[58] Y. Lee, S.H. Park, I.T. Lim, K. Han, S.Y. Lee, Enzyme Microb. Technol. 27 (2000) 33–36.
[59] R. Stern, G. Hillion. Purification of esters. Eur. Patent Appl. EP 356317. (Cl. C07C67/56). [cf. Chem. Abstr. 113 (1990) 58504k].
[60] E. Lotero, J.G. Goodwin, D.A. Bruce, K. Suwannakarn, Y. Liu, D.E. Lopez, Catalysis 19 (2006) 41–83.
[61] D. Reyes-Duarte, N. Lopez-Cortes, M.J. Ferrer, F. Plou, A. Ballesteros, Biocatal. Biotrans. 23 (2005) 19–27.
[62] Y.Y. Linko, M. Lamsa, X. Wu, W. Uosukainen, J. Sappala, P. Linko, J. Biotechnol. 66 (1998) 41–50.
[63] A. Ghanem, Org. Biomol. Chem. 1 (2003) 1282–1291.
[64] S. Shah, M.N. Gupta, Process Biochem. 42 (2007) 409–414.
[65] A. De, A.P. Vieira, M.A.P. Da Silva, M.A.P. Langone, Lat. Am. Appl. Res. 36 (2006) 283–288.
[66] O.L. Bernardes, J.V. Bevilaqua, M.C.M.R. Leal, D.M.G. Freire, M.A.P. Langone, Appl. Biochem. Biotechnol. 137–140 (2007) 105–114.
[67] O.M. Lai, H.M. Ghazali, C.L. Chong, Food Chem. 64 (1999) 83–88.
[68] P. Skagerlind, M. Jansson, B. Bergenstahl, K. Hult, Colloids Surf. B: Bioint. 4 (1995) 129–135.
[69] O.S. Stamenkovi, M.L. Lazic, V.B. Veljkovic, D.U. Skala, Hemijska Ind. 59 (2005) 49–59.
[70] J. Van Gerpen, B. Shanks, R. Pruszko, D. Clements, G. Knothe, August 2002–January 2004, National Renewable Energy Laboratory (NREL), Colorado, July 2004 [NREL/SR-510-36240].
[71] S. Saka, D. Kusdiana, Fuel 80 (2001) 225–231.
[72] D. Kusdiana, S. Saka, Bioresour. Technol. 91 (2004) 289–295.
[73] H. He, T. Wang, S. Zhu, Fuel 86 (2007) 442–447.
[74] M. Balat, H. Balat, Energy Conv. Manage. 49 (10) (2008) 2727–2741.
[75] I.K. Mbaraka, B.H. Shanks, J. Catal. 229 (2005) 365–373.
[76] F. Chai, F. Cao, F. Zhai, Y. Chen, X. Wang, Zhongmuisu, Adv. Synth. Catal. 349 (2007) 1057–1065.
[77] P. Morin, B. Hamad, G. Sapaly, M.G. Carneiro Rocha, P.G. Pries de Oliviera, et al. Appl. Catal. A: Gen. 330 (2007) 69–76.
[78] F. Omota, A.C. demian, A. Bliek, Chem. Eng. Sci. 58 (2003) 3175–3185.
[79] G.D. Yadav, A.D. Murkute, J. Catal. 224 (2004) 218–223.
[80] S. Furuta, H. Matsuhashi, K. Arata, Appl. Catal. A 269 (2004) 187–191.
[81] H. Matsuhashi, H. Miyazaki, Y. Kawamura, H. Nakamura, K. Arata, Chem. Mater. 13 (2001) 3038–3042.
[82] V.V. Brei, S.V. Prudius, O.S. Melezhyk, Appl. Catal. 239 (2003) 11–19.
[83] D.E. Lo'pez, K. Suwannakarn, J.G. Goodwin Jr., D.A. Bruce, J. Catal. 247 (2007) 43.
[84] K.N. Rao, A. Sridhar, A.F. Lee, S.J. Tavener, N.A. Young, K. Wilson, Green Chem. 8 (2006) 790.
[85] J. Jitputti, B. Kitiyanan, P. Rangsunvigit, K. Bunyakiat, L. Attanatho, P. Jenvanitpanjakul, Chem. Eng. J. 116 (2006) 61.
[86] A.A. Kiss, A.C. Dimian, G. Rothenberg, Adv. Synth. Catal. 348 (2005) 75.
[87] A.A. Kiss, F. Omota, A.C. Dimian, G. Rothenberg, Topics Catal. 40 (2006) 141.
[88] A.H. West, D. Posarac, D.N. Ellis, Int. J. Chem. React. Eng. 5 (2007).
[89] J. Ni, F.C. Meunier, Appl. Catal. A: Gen. 333 (2007) 122.
[90] S.C.M. dos Reis, E.R. Lachter, R.S.V. Nascimento, J.A.J. Rodriguez, M. Garcia Reid, J. Am. Oil Chem. Soc. 82 (2005) 661.
[91] M. Toda, A. Takagaki, M. Okamura, J.N. Kondo, S. Hayshi, K. Domen, K.M. Hara, Green Chem. 438 (2005) 178.
[92] A. Takagaki, M. Toda, M. Okamura, J.N. Kondo, S. Hayashi, K. Domen, M. Hara, Catal. Today 116 (2006) 157.
[93] M.-H. Zong, Z.-Q. Duan, W.-Y. Lou, T.J. Smith, H. Wu, Green Chem. 5 (2007) 434.
[94] X. Mo, D.E. Lo'pez, K. Suwannakarn, Y. Liu, E. Lotero, J.G. Goodwin Jr., C. Lu, J. Catal. 254 (2008) 332.
[95] Y. Liu, E. Lotero, J.G. Goodwin Jr., J. Catal. 243 (2006) 221.
[96] Y. Liu, E. Lotero, J.G. Goodwin Jr., J. Catal. 242 (2006) 278.
[97] T.A. Nijhuis, A.W. Beers, F. Kapteijn, J.A. Moulijn, Chem. Eng. Sci. 57 (2002) 1627.
[98] I.K. Mbaraka, D.R. Radu, V.S.Y. Lin, B.H. Shanks, J. Catal. 219 (2003) 329.
[99] I.K. Mbaraka, B.H. Shanks, J. Am. Oil Chem. Soc. 83 (2006) 79.
[100] I.K. Mbaraka, K.J. McGuire, B.H. Shanks, Ind. Eng. Chem. Res. 45 (2006) 3022.
[101] M.A. Jackson, I.K. Mbaraka, B.H. Shanks, Appl. Catal. A: Gen. 310 (2006) 48.
[102] D.E. Lopez, J.G. Goodwin Jr., D.A. Bruce, S. Furuta, Appl. Catal. A: Gen. 339 (2008) 76–83.
[103] S. Furuta, H. Matsuhashi, F. Arata, Biomass Bioenergy 30 (2006) 870.
[104] A. Philippou, M.W. Anderson, J. Catal. 189 (2000) 395–400.
[105] M.R. Othman, J. Kim, J. Sol–Gel Sci. Technol. 47 (2008) 274–282.
[106] G. Carja, R. Nakamura, T. Aida, H. Niiyama, Micropor. Mesopor. Mater. 47 (2001) 275–284.
[107] K. Schulze, W. Makowski, R. Chyzy, R. Dziembaj, G. Geismar, Appl. Clay Sci. 18 (2001) 59–69.
[108] A. Morato, C. Alonso, B. Coq, F. Medina, Y. Cesteros, J.E. Sueiras, P. Salagre, D. Tichit, Appl. Catal. 32 (2001) 167–179.
[109] A. Corma, S. Abd Hamid, S. Iborra, A. Velty, J. Catal. 234 (2005) 340–347.
[110] J.I. Di Cosimo, J.v. Díez, M. Xu, E. Iglesia, C.R. Apesteguía, J. Catal. 178 (1998) 499–510.
[111] K.K. Rao, M. Gravelle, J. Valente, F. Figueras, J. Catal. 173 (1998) 115.
[112] W.L. Xie, H. Peng, L.G. Chen, J. Mol. Catal. A: Chem. 246 (2006) 24–32.
[113] N. Barakos, S. Pasias, N. Papayannakos, Biosour. Technol. 99 (2008) 5037–5042.
[114] J.L. Shumaker, C. Crofcheck, S.A. Tackett, E. Santillan-Jimenez, T. Morgan, Y. Ji, M. Crocker, T.J. Toops, Appl. Catal. B: Environ. 82 (2008) 120–130.
[115] H.-Y. Zeng, Z. Feng, X. Deng, Y.-Q. Li, Fuel 87 (13–14) (2008) 3071–3076.
[116] M.R. Othman, N.M. Rasid, W.J.N. Fernando, Chem. Eng. Sci. 61 (2006) 1555–1560.
[117] M.R. Othman, Chem. Eng. Sci. 64 (2009) 925–929.
[118] B. Roy, J.D. Perkins, T. Kaydanova, D.L. Young, Thin Solid Film 516 (2008) 4093–4101.
[119] Q. Fu, C.-B. Cao, H.-S. Zhu, Thin Solid Film 348 (2008) 99–102.
[120] M. Garcia-Heras, A. Jimenez-Morales, B. Casal, J.C. Galvan, S. Radzki, M.A. Villegas, J. Alloys Compd. 380 (2004) 219–224.
[121] M.A. Aramendia, V. Borau, C. Jimenez, J.M. Marinas, J.R. Ruiz, F.J. Urbano, J. Solid-State Chem. 168 (2002) 156–161.

[122] M. Jitianu, M. Zaharescu, M. Balasoiu, A. Ivanov, A. Jitianu, J. Sol-Gel Sci. Technol. 19 (2000) 453–457.
[123] M. Bolognini, F. Cavani, D. Scagliarini, C. Flego, C. Perego, M. Saba, Micropor. Mesopor. Mater. 66 (2003) 77–89.
[124] M.R. Othman, N.M. Rasid, W.J.N. Fernando, Micropor. Mesopor. Mater. 93 (2006) 23–28.
[125] F. Prinetto, G. Ghiotti, P. Graffin, D. Tichit, Micropor. Mesopor. Mater. 39 (2000) 229.
[126] A.A. Davydov, M.L. Shepotko, A.A. Budneva, Catal. Today 43 (1995) 25–230.
[127] C.S. Macleod, A.P. Harvey, A.F. Lee, K. Wilson, Chem. Eng. J. 135 (2008) 63–70.
[128] T. Ebiura, T. Echizen, A. Ishikawa, K. Murai, T. Baba, Appl. Catal. A: Gen. 283 (2005) 111–116.
[129] W. Xie, X. Huang, Catal. Lett. 107 (2005) 53–57.
[130] E. Li, V. Rudolph, Energy Fuels 22 (2008) 143–149.
[131] W. Trakarnpruk, S. Porntangjitlikit, Renew. Energy 33 (2008) 1558–1563.
[132] Q. Shu, B. Yang, H. Yuan, S. Qing, G. Zhu, Catal. Commun. 8 (2007) 2159–2165.
[133] Y. Wang, F. Zhang, S. Yu, L. Yang, D. Li, D.G. Evans, X. Duan, Chem. Eng. Sci. 63 (17) (2008) 4306–4312.
[134] G. Arzamendi, I. Campo, E. Arguinarena, M. Sanchez, M. Montes, L.M. Gandia, Chem. Eng. J. 134 (2007) 123–130.
[135] M.C.G. Albuquerque, I. Jimenez-Urbistondo, J. Santamaria-Gonzalez, J.M. Merida-Robles, et al. Appl. Catal. A: Gen. 334 (2008) 35–43.
[136] Z. Huaping, W. Zongbin, C. Yuanxiao, Z. Ping, D. Shije, L. Xiaohua, M. Zongqiang, Chin. J. Catal. 27 (5) (2006) 391–396.
[137] Y.-M. Park, D.-W. Lee, D.-K. Kim, J.-S. Lee, K.-Y. Lee, Catal. Today 131 (2008) 238–243.
[138] X. Liu, H. He, Y. Wang, S. Zhu, X. Piao, Fuel 87 (2008) 216–221.
[139] X. Liu, H. He, Y. Wang, S. Zhu, X. Piao, Catal. Commun. 8 (2007) 1107–1111.

Review

Applied Organometallic Chemistry

Received: 20 April 2009 Accepted: 12 May 2009 Published online in Wiley Interscience: 7 July 2009

(www.interscience.com) DOI 10.1002/aoc.1517

Synthetic hydrotalcites from different routes and their application as catalysts and gas adsorbents: a review

M. R. Othman[a*], Z. Helwani[a,b], Martunus[a,b] and W. J. N. Fernando[a]

In this paper, widely accepted methods of hydrotalcite preparation such as co-precipitation, urea hydrolysis, hydrothermal, sol–gel, microwave irradiation, steam activation and solvothermal have been selected and reviewed. Our review indicates that the nature of the divalent cations, the synthesis method, the calcination temperature and the nature of the interlayer species are determinant factors in shaping the surface properties of the layered double hydoxides. The basic strength of the surface base site and structural changes produced in the mixed oxides can be adjusted conveniently by varying the Al content during the synthesis. The combination of sol–gel with microwave irradiation during the gelling and crystallization steps has also been found to increase the surface area of the hydrotalcite-like compound.

Keywords: hydrotalcite; co-precipitation; sol–gel method; microwave irradiation; catalyts; adsorbent

Introduction

Layered double hydoxides (LDHs), also known as anionic clays or hydrotalcite (HT)-like materials, have anionic exchanged capacity. The ability to capture and exchange organic and inorganic anions makes the compounds almost unique as inorganic materials. Hydrotalcites have been used in large number of practical applications such as neutralizers (antacids), anion exchangers, polymer stabilizers, anion scavengers, catalysts and catalyst supports, adsorbents, filtration, electroactive, photoactive materials and pharmaceutics.[1–7] HTs are usually chosen over other compounds due to the versatility, simplicity, easily tailored properties and low cost of the materials.

HTs consist of a brucite-like $[Mg(OH)_2]$ network wherein an isomorphous substitution of Mg^{2+} ion by a trivalent cation M^{3+} occurs and the excess positive charge is compensated by gallery anions which are located in the interlayer along with water molecules.[8–10] Figure 1 shows the structure of the compounds with interlayer carbonate anions. Mg^{2+} may be accommodated in the octahedral sites of the close-packed hydroxide ions in the brucite-like layers to form LDH structures.[11] Cations which are too small, such as Be^{2+}, or too large, such as Cd^{2+}, give rise to other types of compounds.[12]

Hydrotalcites can be synthesized by various techniques depending on the specific requirement and properties of the compounds. The widely acceptable methods to prepare hydrotalcites include: salt-oxide method,[13] hydrolysis reaction,[2–4,14] deposition/precipitation reactions, structure reconstruction,[15] hydrothermal synthesis, anion exchange,[16] two-powder synthesis, electrochemical methods, precipitation at constant pH (also called co-precipitation to indicate that all cations precipitate simultaneously), precipitation at variable pH, precipitation at different levels of supersaturation,[3] combustion, sol–gel,[17,18] microwave irradiation, steam activation and solvothermal method.

Considering the current preferences by researchers to opt for hydrotalcites in their research work, as reported in the literature, LDHs synthesized in the laboratory from different routes are reviewed in this paper. The physico-chemical properties of the materials (such as phase purity, crystallinity and surface area) influenced largely by the synthesis method will be highlighted. The applications of these materials as catalysts and CO_2 adsorbents will also be addressed.

Hydrotalcite-Like Compounds and Their Synthesis Techniques

Coprecipitation Synthesis

LDHs are commonly prepared by co-precipitation of inorganic salts in alkaline media either at constant or at increasing pH. The morphology and particle size distribution depend on the supersaturation of the synthesis solution. Usually supersaturation is achieved by physical (evaporation) or chemical (variation of pH) methods. For the preparation of HTs, the method of pH variation is frequently used. The pH value must be chosen carefully. If the pH is too low, not all the different metal ions will precipitate. On the other hand, if the pH is too high, the dissolution of one or more metal ions may occur. Another point to take note of is that the pH value needed for the precipitation of HTs is not necessarily equal to the pH of the precipitation of the most soluble metal hydroxide.[2–4]

Generally, a basic pH is required for the preparation of hydrotalcites. However, the optimal pH depends on the types

* *Correspondence to: M. R. Othman, School of Chemical Engineering, Universiti Sains Malaysia, 14300 Nibong Tebal, Penang, Malaysia. E-mail: chroslee@eng.usm.my*

a *School of Chemical Engineering, Universiti Sains Malaysia, 14300 Nibong Tebal, Penang, Malaysia*

b *Department of Chemical Engineering, Riau University, Pekanbaru 28293, Indonesia*

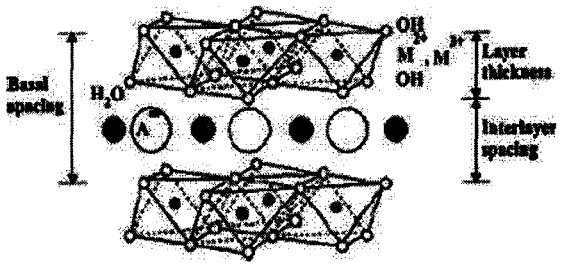

Figure 1. Schematic representation of the hydrotalcite-type anionic clay structure.

of cations used and where their hydroxide precipitation curves cross.[19,20] The pH at which the precipitation occurs leads to different natures and properties of the finally sintered products.[2,4,21] For single hydroxides, a pH range of 8–10 can be used to prepare most anionic clays.[2–4] At lower pH, the synthesis proceeds by a more complex pathway and may not be complete, as indicated by the differences between the chemical composition of the phases obtained and that of the starting solutions.[2]

Co-precipitation may be carried out at low or high supersaturation.[2–4,21] Precipitation at low supersaturation is performed by slow addition of mixed solutions of divalent and trivalent metal salts with appropriate ratio into a reactor containing an aqueous solution of the desired interlayer anion. A second solution of an alkali is added into the reactor simultaneously at a fixed pH to promote co-precipitation of the two metallic salts.[12] An obvious advantage of this method is that it allows control of the charge density (M^{2+}/M^{3+} ratio) of the hydroxide layers of the resulting LDH by simply regulating the solution pH. The products obtained by co-precipitation at low supersaturation are usually more crystalline in comparison with those prepared at high supersaturation conditions.[22] Anionic clays with anions other than carbonate may be prepared by precipitation under nitrogen using alkali hydroxides. However, small amounts of carbonates are always present.[23]

Co-precipitation at high supersaturation gives rise to less crystalline materials, owing to the high number of crystallization nuclei.[22,24] The precipitation may be carried out using the same devices as reported above by increasing the concentrations of the solutions and/or the addition rate, or by putting a solution of the salts of the elements into a solution containing a small excess of alkali bicarbonates or bicarbonate/carbonate mixtures, previously heated at 333 K. This method is simple and does not require a specific experimental apparatus. The only requirement is prolonged washing to reduce the amount of residual alkali because of the low solubility of the alkali bicarbonates. The classical co-precipitation route yields highly crystalline materials, giving rise (after calcinations) to mixed oxides of low specific surface areas and of very low basic strength.[25–27] After precipitation at low and high supersaturation, a thermal treatment process is performed to increase the yields and crystallinity of the materials. This is followed by an aging process conducted for a period ranging from a few hours to several days.[2,12] In order to ensure the purity of the synthesized LDHs, the use of the decarbonated ultrapure water and the application of vigorous stirring in combination with nitrogen purging in the synthesis process are necessary.

Factors that are considered important in the precipitation of HT compounds include the nature of the cations, their ratio, the nature of anions, pH, temperature, aging and the precipitation method. Although anionic clay particles are generally larger than the cationic counterparts, the former can yield homogeneous mixed oxide structures with higher specific surface areas and narrower pore size distributions. High surface areas and narrow pore size distribution are known to enhance the catalytic properties of the LDHs and these desirable properties can be achieved simply by thermal decomposition.[17,26,28,29]

Thermal decomposition of co-precipitated LDHs up to 700 °C is well-documented in the literature. Their morphology and particle size distribution depend on the supersaturation of the synthesis solutions. Below 200 °C, the compounds lose the interlayer water. At 450–500 °C, the LDHs experience dehydroxylation and decomposition of all carbonate into carbon dioxide and the corresponding metal oxides. Characterization of the LDHs after thermal decomposition generally reveals mesoporous structures with slit shape pores. At 660–700 °C DTA–TG analysis indicates that LDHs completely decomposes and FTIR analysis reveals a band of Mg–O and Al–O attributed to the spinel and periclase phase.[17,29–42]

Urea Hydrolysis

Urea hydrolysis utilizes urea as its precipitating agent. Although NaOH can be used to replace urea, the use of urea is better since it progresses slowly, which leads to a low degree of super saturation during precipitation. Urea is a very weak Bronsted base ($pK_b = 13.8$). It is highly soluble in water and its controlled hydrolysis in aqueous solutions can yield ammonium cyanate (or its ionic form: NH_4^+, NCO^-). Prolonged hydrolysis results in either CO_2 in acidic medium or to CO_3^{2-} in basic medium as shown below:[43–45]

$$H_2N{-}CO{-}NH_2 \longrightarrow NH_4^+ + NCO^- \quad (1)$$

$$NCO^- + 2H_2O \longrightarrow NH_4^+ + CO_3^{2-} \quad (2)$$

$$NCO^- + 2H^+ + 2H_2O \longrightarrow NH_4^+ + H_2CO_3 \quad (3)$$

A homogeneous solution containing urea, Mg and Al nitrates during the hydrothermal reaction can lead to the following reactions, resulting in the formation of hydrotalcite compounds. The relevant reaction scheme is:

$$Mg(H_2O)_n^{2+} + H_2O \longrightarrow Mg(OH)(H_2O)^+_{n-1} + H_3O^+ \quad (4)$$

$$Al(H_2O)_n^{3+} + H_2O \longrightarrow Al(OH)(H_2O)^{2+}_{n-1} + H_3O^+ \quad (5)$$

$$Mg(OH)(H_2O)^+_{n-1} + Al(OH)(H_2O)^+_{n-1} + OH^- + CO_3^{2-} \longrightarrow MgAl(OH)_3CO_3H_2O \quad (6)$$

The precipitate from urea hydrolysis can be washed easily, unlike the co-precipitated samples where repeated washings are required to get them free of the alkali metal ions and devoid of these cations.

In a thermally induced urea hydrolysis[46–48] where the effects of varying the temperature, total metal cation concentration, molar fraction of urea to metal cations in the solution and the crystallinity of the samples were investigated, the optimum conditions to prepare LDHs with good crystallinity in a relatively short time were found to involve the application of a urea/metal ion molar ratio of 3.3. In another work,[44] hexagonal plates of monodispersed hydrotalcite particles were obtained by urea hydrolysis at 120 °C. It was found that the LDHs resulted in better crystallinity as the aging time was prolonged, the total metal concentration decreased and the reaction temperature controlled. Control of the reaction temperature is important because it not only affects

the crystalinity level but also the uniformity and size of the particles. At lower temperatures, particle sizes are larger due to the lower nucleation rate while at high temperatures, particle sizes are smaller and more uniform.[45] Although hydrolysis occurs at elevated temperature, relatively larger particle size was obtained using the urea method than by other techniques because of the low degree of supersaturation during precipitation.

Obtaining pure HT single phase is possible using urea hydrolysis where it may be otherwise impossible using other techniques. A pure HT single phase was obtained in the previous research attempts[29,43] for Mg:Al ratios of 1:1 and Ni:Al = 2:1 and 3:1, respectively. The urea hydrolysis method also allows the preparation of HT compounds with a high charge density not easily obtainable using other procedures. This is supported by the results of the structural and charge density model reported previously[49] and from another work that utilized hexamethylenetetramine (HMTA) to produce highly crystallized LDHs.[50]

Hydrothermal Treatment and Synthesis

In preparing LDHs from hydrolysis or a co-precipitation process, optimization of experimental conditions is usually required. However, this may not be sufficient to yield a well-crystallized hydrotalcite-like phase as intended. Improved crystallined structures can be achieved by hydrothermal treatment in the presence of water vapor at temperatures not exceeding the decomposition temperature of the hydrotalcite-like compound. Besides crystallinity, hydrothermal treatment can also be used to help maintain or compensate forthe required residual water that is lost in the previous stages of LDHs development. When co-precipitated LDHs fails, a combined co-precipitated and hydrothermal synthesis can be proposed to improve crystallization. The hydrothermal crystallization is usually carried out at temperatures up to *ca* 200 °C under autogenous pressure for a time ranging from hours to days.[28,51,52]

While heating the reactants in a pressurized aqueous media improves the crystallinity of the resultant LDHs, hydrothermal synthesis may require additional effort and time. This method can also result in the increase of particle size. In a direct hydrothermal synthesis of MgAl–LDH and MgCr–LDH compounds,[44,53] the particle size of the final products was increased in relation with the hydrothermal aging. The growth occurred on the edges, resulting in the formation of hexagonal plate shaped hydrotalcite crystals. The effect of a hydrothermal treatment on the crystallite size and strain of synthetic Mg–Al hydrotalcite-like compounds with various Mg:Al molar ratios was studied previously.[54] Maximum crystallite size was achieved after 24 h of hydrothermal treatment between 180 and 200 °C, with molar ratio Al:(Al + Mg) ranging from 0.337 to 0.429. Other aspects of the hydrothermal treatment of hydrotalcite-like compounds at elevated temperatures were also reported to improve the crystallinity of Ni–Al and Ni–Cr,[24] and Ni–Al–Cr and Ni–Al–Fe prepared initially by co-precipitation at 60 °C, followed by hydrothermal treatment at 150 °C and with different cation precursors.[54–61]

Combustion Synthesis

The preparation of LDHs by combustion can save energy and time[62,63] because it involves a very rapid chemical process. The method is based on the explosive decomposition of some organic fuels such as urea or glycine, among others.[64] The fuels serve as the source of C and H, which on combustion form CO_2 and H_2O to produce complexes with the metal ions.[62] The reaction is initiated and then promoted by the continuous heat energy supplied to the precursor materials. The advantages of the combustion technique are that it requires no solvents and therefore produces no wash water. The technique also requires a much shorter time for the materials to crystallize (within minutes) into hydrotalcites, vis-à-vis the conventional co-precipitation technique, which normally requires long crystallization time (several hours, days or weeks), high amounts of solvents and repeated heating. The combustion method is interesting in that it requires a heating time of only a few minutes and the fuels can be converted readily into hydrotalcites.

In the synthesis of HTs from aluminum and magnesium nitrates and sodium carbonate where sugar (saccharose) was used as fuel, HTs were obtained and their characteristics were claimed to be similar to those obtained from co-precipitation when analyzed with FTIR and XRD.[65] The obtained hydrotalcites were then calcined and recrystallized in the presence of a carbonate aqueous solution to produce mixed oxides. This cycle (memory effect) was sequentially reproduced three times. The 27Al MAS NMR results show that the success of the synthesis procedures was largely influenced by the temperature and the level of aluminum diffusion into the oxide network.

Sol–gel Method

Sol–gel method is known for its cost effectiveness and purity. In addition, the homogeneity and structural properties of the finished solids are controllable at the synthesis level by simply varying the composition of the precursors, temperature, aging time and removal/addition of reactant species. Recently, there have been emerging applications in bio-technology that require the use of high-purity materials. For example, high-purity hydrotalcite synthesized from sol–gel method has been considered as an alternative drug carrier.[66] HTs in the form of thin films are also in high demand in catalytic membrane reactions and separation applications. The films can be formed on a substrate by spin-coating, dip-coating, spraying, electrophoresis, inkjet printing or roll coating of a colloidal liquid system called sol that later turns into a semi-rigid solid phase called gel. The sol can also be cast into a mold, dried and sintered to form HT solids that exhibit interesting and unusual features.

During the sol–gel processing, the desired metal precursors such as inorganic salts or metal organic compounds are hydrolyzed in water, aqueous solution or liquid-organic solvent in room conditions to produce a polymeric or particulate sol. Insoluble salts may be hydrolyzed either by supplying heat to the sol mixture or using an appropriate solvent. An appropriate amount of acid or base can be added into the sol mixture during hydrolysis to facilitate peptization of the solution so that highly dispersed metals in the solution can be obtained. The development of HT compound from a sol–gel method was reported previously.[66] The hydrolysis was initiated with the addition of $Al(OC_4H_9)_3$, highly purified water and HCl at a predetermined ratio, followed by the addition of the equivalent amount of $Mg(OCH_3)_2$ and Na_2CO_3 into the boehmite solution. PVA solution was added into the mixture to add strength during the gelation and to avoid ruptures, cracks or delaminations of film. Fully hydrated sol mixture at pH of 9.6 was dried under ambient and highly humid conditions. XRD analysis indicated that pure and highly crystallined HT solids (without calcination) were obtained following this procedure.[67]

Modification of the textural properties of sol–gel LDHs is possible in convenient and useful ways with various and interesting possibilities.[68,69] For example, decreasing the reaction

temperature or the aging time could increase the specific area or particle size of LDHs. Increasing acid–boehmite molar ratio would decrease the pore size and porosity of the sintered LDHs. Changing the cation and anion species would change the physical and chemical properties of the LDHs. The sol–gel hydrotalcites are also known to exhibit thermal stability up to 550 °C depending on the aluminum precursor in the following sequence: aluminum chloride > aluminum nitrate > aluminum sulfate.[70,71] Another feature that makes these sol–gel materials distinguishable from and more attractive than the naturally occurring hydrotalcites or those produced from other synthetic methods is their high specific surface area of *ca* 150 m^2/g or higher.[26,68,71,72] The specific surface area of the hydrotalcites was 10–25% greater than that achieved by co-precipitation,[17,29,42,68–90] but with controversial results regarding the basicity and the M^{II}/M^{III} ratios.[26,51,52]

Microwave Irradiation

Microwave irradiation can be aplied directly to the sol mixtures obtained from the previously discussed topics or in sequential order during the aging process. Microwaves are non-ionizing electromagnetic radiations; upon interacting with liquid or solid materials, they produce dipole reorientation in dielectric materials and ionic conduction if there are ions which can be drifted under the field. In this way, it is possible to achieve a uniform bulk heating of the materials, reducing thermal gradients originated in conventional heating where energy is transferred by conduction, convection or radiation from the surface of the vessel. The fast heating of the suspension or solution within the autoclave leads to significant advantages compared with high-pressure steel autoclaves used in conventional hydrothermal heating processes,[91,92] thus improving the procedure significantly.

The applications of microwave–hydrothermal technique have been increasing since its use in 1992 to synthesize several oxides.[93] It has been used widely to produce zeolites,[94] hydroxylated phases[95] and hydrotalcite-like compounds.[25,76,96–99] In the production of nickel hydroxide for applications in rechargeable Ni–base alkaline batteries where microwave-assisted hydrothermal method was used, a hexagonal layered structure with two materials with an interlayer spacing of 7.0 Å was obtained. Uniform 3D nanosized flower-like α-nickel hydroxides composed of aggregates of flakes built from nanocrystals were successfully developed. These intercalated materials were found to exhibit enhanced electrochemical activity for the reduction of O_2 to OH^-.[100] Microwave irradiation was also harnessed in the preparation of homogeneous materials based on the competitive diffusion determined by charge, weight and ion size. The reaction that occurred depended on the intensity of the irradiation. It took place at the contact surface between the solid and the solution without involving the crystallized bulk. In the synthesis of Zn–Mg/Al hydrotalcites, an aluminum enriched core was first formed and, then, magnesium was driven into the structure. Finally, zinc remained on the hydrotalcite surface in agreement with the weight and size of the elements. At lower irradiation intensity, magnesium remained in the outer layers of the hydrotalcite inhibiting the Zn diffusion which, subsequently, formed zinc oxide. At higher intensity, a more homogeneous hydrotalcite structure was obtained than that at lower irradiation intensity.[101]

Microwave irradiation has been applied for rapid synthesis of inorganic solids and organic synthetic reaction[41,75,76,96,101–104] to reduce the long time period of aging and tedious washing. The use of microwave radiation as a source of heating not only reduces the aging time considerably but also enhances the kinetics of crystallization.[76,91] A well-crystallized material was reportedly obtained in 12 min, in comparison with 1530 min for a conventionally synthesized samples.[60] The extent of the crystallization rate upon irradiation was influenced largely by the nature of the trivalent cation present in the HT-like network and the orientation of water molecules in the interlayer spaces. Because of the bipolar nature of these materials, microwave interaction was promoted that eventually enhanced the rate of crystallization. The irradiation method was also claimed to increase the specific surface area and improve the basic properties[25,105] of hydrotalcites.

Hydrotalcites obtained from microwave irradiation coupled with ultrasound treatment during the aging step was claimed to produce smaller particle sizes and higher specific surface areas than those samples obtained from conventional approaches.[105] A surface area of 288 m^2/g was reportedly achieved by means of microwave irradiation.[106] Despite the advantages, an irradiation approach could also contribute to erosion of the hydrotalcite layers and render surface-defective sites with an increase in both basic and acid sites in the resulting LDHs when the solution precursor was aged by microwave irradiation.[25,96,107]

Steam Activation

High-temperature steam treatment has been widely used to treat catalysts and catalyst supports and to extract trivalent framework atoms (often Al but also Fe and/or Ga) from zeolites so that higher catalytic activity and improved (hydro) thermal stability can be achieved.[108–110] A classical example is the steam treatment of Y zeolite for fluid catalytic cracking.[111] High-temperature steam activation of alumina led to improved thermal stability of the resulting product.[112] Steam activation can also be applied during the preparation of HT to improve its properties. Similar to hydrothermal treatment, steam activation at temperatures not exceeding the decomposition temperature of the hydrotalcite-like compound may improve crystalline structures and maintain the required residual water that is lost in the previous stages of LDHs development.

Steam activation may also deteriorate the quality of HT in the following ways. In a separate work,[113] steam activation was found to eliminate small mesopores (<4 nm) that contribute to the total surface area and pore volume of the material. While the decomposition behavior in the presence of steam remained similar to dry decomposition, a noticeable drop in surface area and pore volume was observed from N_2 isotherms. This drop was largely due to the dehydration and condensation of M–OH bonds between adjacent layers and/or platelets.

Solvothermal Method

Hydrothermal synthesis involves use of water as a solvent at elevated temperatures and pressures in a closed system, often in the vicinity of its critical point. A more general term, 'solvothermal', refers to a similar reaction in which a different solvent (organic or inorganic) is used. Under hydro(solvo) thermal conditions, certain properties of the solvent, such as density, viscosity and diffusion coefficient change dramatically and the solvent behaves very differently from what is expected at ambient conditions. Consequently, the solubility, the diffusion process and the chemical reactivity of the reactants (usually solids) are greatly changed or enhanced. This enables the reaction to take place at a much lower temperature. The method has been widely applied

and well adopted for crystal growth of many inorganic materials, such as zeolites, quartz, metal carbonates, phosphates and other oxides and halides.[114]

The solvothermal pathway is a newly developed route which may require low temperatures to run. Various kinds of nanocrystalline materials have been obtained using the solvothermal process at a relatively low temperature.[115] The solvothermal procedure may combine hydrothermal synthesis and reverse micelle solution to synthesize HT. Generally, the solvothermal and hydrothermal synthesis involves two steps: the first is the nucleation process at room temperature; the second is the growth of HT under higher temperature and pressure. The products of solvothermal and hydrothemal reactions are usually crystalline and do not require post-annealing treatments. At the same time, the morphologies of the products can be controlled by the reverse micelles. Most of the solvothermal products are nano- or microparticles with well-defined morphologies and improved hydrotalcite crystallinity as reported in the previous work.[116,117]

Hydrotalcites as Catalysts and Adsorbents

Since these materials have a well-defined layered structure with nanometer (0.3–3 nm) interlayer distances and contain important functional groups, they are widely used as adsorbents for liquid ions[118–120] and gas molecules.[121,122] They also find use as catalysts for oxidation,[123–125] reduction[126] and other catalytic reactions.[127,128] LDH compounds are used in novel membrane CO_2 separation[129,130] and reactive separation applications, wherein the conversion of catalytic reactions can be increased by directly removing one of the products from the reactor.[131,132] This process is possible due to the permanent anion-exchange and adsorption capacity, the mobility of the interlayer anions and water molecules, the large surface areas and the stability and homogeneity of the HT materials.[133]

The ability of HT to adsorb inorganic as well as organic anions makes these materials very attractive for many applications. HT has been used in the plastics industry,[134,135] as an antacid substance and as a carrier for drugs.[136–138] HT-based metal oxides also have the potential to be used as new bifunctional catalysts with a unique combination of acid–base and redox properties.[139] The great interest for the LDH materials is related to the fact that the acid–base properties of LDH-based catalysts, as well as the redox properties, may be easily tailored by isomorphous substitution of Mg and Al cations with various other di- and trivalent cations. The effects of isomorphous substitution on the surface and catalytic properties have been investigated by various methods, namely FTIR, XPS and TPR, TPD and microcalorimetry in many test reactions, such as cyclohexanol conversion,[138,140,141] 2-octanol conversion,[142] Knoevenagel condensation and aldol condensation[105,143] and the isomerisation of bisophorone to a-isophorone.[144]

HTs as Base Catalysts

Hydrotalcites are commercially available and cheap solid bases. Calcined HTs are highly active and selective, and they can play an important role in many base-catalyzed reactions. Their reactive surface base sites were actively researched and characterized using temperature programmed desorption (TPD),[145,146] FTIR spectroscopy[29,147] and gas-phase microcalorimetry.[141,148] Their basicity is mainly related to the amount and nature of divalent cations present. Controlled thermal decomposition of hydrotalcites gives high surface area of mixed oxides that have the potentials in numerous catalytic applications such as the removal of SO_x and NO_x, aldol condensations, phenol alkylations, epoxidation of olefines, and partial oxidation, hydrodehalogenation or hydrogenation reactions.[104,149–158]

HTs show a memory effect, a property by which they can recover the original lamellar structure if they come into contact with water vapor or are immersed in liquid water. These rehydrated materials have been applied to a number of base-catalyzed reactions on account of their Brønsted basic character.[156,158,159] In addition, acid sites or acid–base pairs on these materials may also influence the catalytic performance. Acid–base sites can be active sites for many reactions including Meerwein–Ponndorf–Verley reactions,[160,161] cyclo additions of carbon dioxide to epoxides,[162] and aldol condensations to form 2-nonenal.[163] The acid–base properties of Mg–Al mixed oxides are governed by the Mg:Al molar ratio,[29,146,147] calcination temperature[164] and preparation conditions.[29,38,105,145]

The mixed oxides derived from thermal treatment of Mg–Al HT are among the solids that have the potential to complement homogeneous catalysts with considerable success since they are inexpensive and non-toxic and their basic properties can be tailored to the process of interest. They can be easily separated and recycled, while pollutant salts and by-products are not formed in the processes.[165] The catalytic applications of Mg–Al mixed oxides obtained from hydrotalcites were tested in base-catalyzed reactions such as aldol condensation of aldehydes and ketones and condensation of the carbonyl group with compounds presenting methylene activated groups (for example, Knoevenagel and Claisen-Schmidt reactions),[105,148,163,166–169] and selective reduction of unsaturated ketones/aldehydes by hydrogen transfer from alcohols.[160] The catalytic performance was found to depend largely on the surface basic properties and chemical composition of the parent hydrotalcite. The basic site density and strength required to activate the reactants of the reaction under study were found to be influenced by the optimum Mg:Al ratio.[146,166,170–172] Other researchers[105,173–179] reported that Mg–Al mixed oxides in the absence of CO_2 enhance their activity in base-catalyzed reactions such as aldol, Knoevenagel and Claisen–Schmidt condensations (Fig. 2) and Michael additions in liquid phase under mild conditions upon rehydration. The rehydration of the Mg–Al mixed oxides gives rise to a meixnerite-like Mg–Al hydroxide in which the original layered structure was restored by compensating the lost anions.

Knoevenagel Condensation

Knoevenagel condensations are the reactions between a ketone and active methylene compounds. They proceed over a variety of basic solid catalysts, including alkali-ion-exchanged zeolites, alkali-ion-exchanged sepiolite, oxynitrides and hydrotalcite-related catalysts. Rehydrated hydrotalcite that gave quantitative yields for a variety of Knoevenagel condensations, as shown in Fig. 3, at room temperature using toluene or DMF as solvent in liquid phase was reported previously.[180] Knoevenagel condensations of malononitrile with cyclohexanone, benzophenone and *p*-amino acetophenone produced alkenes containing electron-withdrawing nitrile groups, which facilitate additions to the double band. These alkenes are useful in anionic polymerization reactions leading to plastics, synthetic fibers or the production of liquid

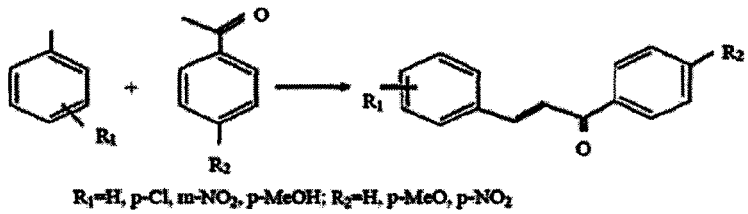

Figure 2. Claisen–Schmidt condensations to produce chalcones.

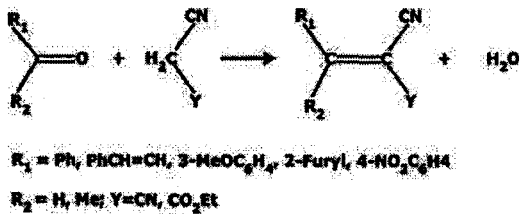

Figure 3. Rehydrated hydrotalcite catalyzed synthesis of Knoevenagel condensation.

crystals. They can be synthesized using ion-exchanged zeolite X, sepionlite and hydrotalcite as catalysts.[181]

Higher specific activity for Knoevenagel and aldol condensations was reportedly obtained using calcined HT in homogeneous and heterogeneous phases.[107] The high activity was attributed to the increased surface area of HT and increase in the total number of accessible Brønsted basic sites exposed to the reactants. The active basic sites correspond to O^{2-} located in the corners of the HT crystals. It was discovered that the smaller the crystal size, the larger the fraction of the above sites, and the larger the total number of the exposed sites. The regenerated HT that exhibited this quality enabled achievement of pseudoionone yields of 96% with 99% selectivity, in 15 min reaction time working at a very low acetone : citral molar ratio.

Aldol Condensation

Aldol condensation is an important reaction for carbonyl compound (aldehyde or ketone) coupling via C–C bond formation. Aldol self-condensation of acetone to diacetone alcohol is catalyzed by a variety of solid bases, such as alkaline earth oxides, La_2O_3 and ZrO_2, and $Ba(OH)_2$.[182] Alkaline earth oxides are active for the reaction in the following order: BaO > SrO > CaO > MgO[183] and the active sites are suggested to be surface OH groups. This reaction can also be catalyzed by meixnerite-like hydrotalcite-based catalysts with high selectivity towards the desired product.

Aldol condensation of acetone at 273 K in liquid phase using Mg–Al LDH with Cl^- and/or CO_3^{2-} as compensating anions was reported.[184] The products of the reaction were mainly diacetone alcohol and mesityl oxide. The catalytic activities increased with the Al content of the LDH and a conversion around 20% was reached when the carbonated compounds were calcined at 723 K and the catalysts constituted mixed oxides of the Mg(Al)O type. It was found that the nature and the amount of the compensating anion in the LDH, particularly trace amounts of Cl^-, influenced the catalytic activity to a greater extent. Mesityl oxide resulting from the dehydration of diacetone alcohol on acid sites was found to strongly inhibit the reaction. The addition of H_2O in controlled amounts in acetone enhanced the conversion into diacetone alcohol with a higher selectivity, while allowing HT catalyst to recover its lamellar structure. An excessively high amount of H_2O, however, was found to inhibit the reaction. The effect of rehydration of HT in vapor or in liquid phases of the mixed oxides on the yield of the reaction was also investigated. The rehydrated HT showed that the catalyst demonstrated meixnerite-like structure and the conversion reached thermodynamic equilibrium (23%) in less than 1 h.

In another effort,[176] activated hydrotalcite was employed in the condensation of citral (a mixture of geranial and neral with a proportion of 25 and 75 wt%, respectively) and acetone into pseudoionone (shown in Fig. 4), which is an intermediate in the commercial production of vitamin A. Results from the study show that conversion of 65% and a selectivity of 90% were obtained when the reaction was performed at room temperature. Since calcined and rehydrated HT can be used at elevated reaction temperature, higher conversions and selectivities can be expected at this condition.[173] In fact, encouraging results have been reported in the condensation of aromatic aldehydes such as benzaldehyde or substituted benzaldehydes and acetone using rehydrated hydrotalcites.[180]

In an aldol condensation between a ketone and an aldehyde (Claisen–Schmidt condensation), vesidryl, which is of pharmacological interest owing to its diuretic and choleretic properties, was produced from substituted acetephenone and substituted benyaldehyde (shown in Fig. 5). By using calcined hydrotalcite as a catalyst (5 wt%), 85% yield of vesidryl was obtained at 170 °C after 20 h.[166] A strongly basic catalyst, which was obtained by impregnation of natural phosphate with a solution of sodium nitrate, followed by calcination at 900 °C, could also catalyze the Claisen–Schmidt condensations to produce chalcones

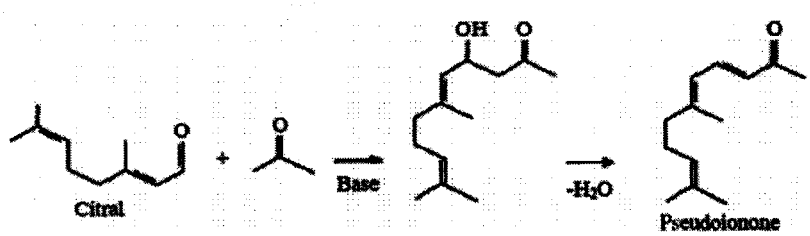

Figure 4. Activated hydrotalcite in condensation of citral and acetone into pseudoionone.

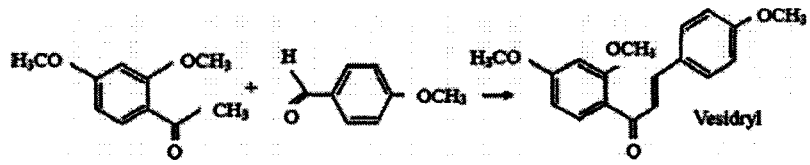

Figure 5. Aldol condensation between a ketone and an aldehyde (Claisen–Schmidt condensation).

with high yields.[185] The catalyst could be easily recovered and efficiently reused. Among aldol condensations, nitroaldol condensation (Henry reaction) is the reaction of a nitro compound with a carbonyl compound to form a nitroalcohol under basic conditions. The products, nitroalcohols, can be converted by hydrogenation to β-aminoalcohols, which are then converted to pharmacologically important chemicals, or proceed further to produce nitroalkene.

The nitroaldol condensation of propionaldehyde and nitromethane to produce 1-nitro-2-hydroxybutane, in the presence of different solid bases at 313 K was reported previously.[186] Among the solid bases studied, MgO was found to be the most active. The activity was not strongly dependent on the pretreatment temperature and was scarcely retarded by exposure to air. In the reaction of benzaldehyde and chlorobenzene with nitromethane, CsNaX catalyst was known to produce nitroalkenes at 80% yield at 413 K.[187] In another study, Mg–Al mixed oxides prepared by calcination of hydrotalcite were used to catalyze the nitroaldol condensation to nitroalcohols at 95% yield.[188]

Michael Addition

Michael addition is widely used as a C–C bond coupling reaction in the production of pharmaceuticals and fine chemicals. The reaction is conventionally catalyzed with soluble bases, such as KOH or amines. Normally, it involves nucleophilic addition of a carbon ion, formed by abstraction of a proton from a C–H bond of the organic donor molecule by a base, to α,β-unsaturated carbonyl compounds.[178,189–192] Environmental and economical concerns are driving forces in the replacement of soluble bases by suitable solid catalysts. The latter are easy to separate, recover, and thus, reuse. So far, several solid base catalyst systems, such as $Ba(OH)_2$, MgO, $KF-Al_2O_3$, $Na-NaOH-Al_2O_3$, and modified Mg–Al hydrotalcite have been used in Michael additions. The efficient catalyst varies with the type of reactant. Some transition metal complexes such as heterogeneous Lewis acid catalysts instead of conventional strong bases, like montmorillonite-enwrapped scandium, nickel (II) and cobalt (II) complexes were also applied in Michael additions. The factors to be considered for an efficient catalyst are basic strength of the site, acidity of reactant and charge on the carbon atom at β-position to the carbonyl group.[193,194]

An efficient and very selective catalyst for Michael additions was reportedly found by rehydrating Mg–Al hydrotalcite (Mg : Al ratio of 2.5) at room temperature under a flow of dry nitrogen gas saturated with water vapor. A yield of 88% was obtained in 2 h. The high yield was ascribed to the presence of Brønsted base sites in the rehydrated catalyst.[178] The high catalytic activity also was found to be correlated well with the amount of the base sites determined by benzoic acid microcalorimetry, which was dependent on the Mg : Al molar ratio.

Transesterification of Triglycerides

Transesterification is the reaction of vegetable oil or animal fat with an alcohol to form esters (biodiesel) and glycerol. A catalyst is usually used to improve the reaction rate and yield. Because the reaction is reversible, excess alcohol is used to shift the equilibrium to the products side.[195] The catalytic transesterification of vegetable oils with methanol is an important industrial method used in biodiesel synthesis. Also known as methanolysis, this reaction has been well studied and established using acids or alkalis, such as sulfuric acids or sodium hydroxide as catalysts. However, these catalytic systems are less active or completely inactive for long-chain alcohols. Usually, industries use sodium or potassium hydroxide or sodium or potassium methoxide as a homogeneous catalyst, since they are relatively cheap and quite active for this reaction.[196]

While the use of homogeneous liquid base catalyst is kinetically fast and economically viable, the removal of the catalyst or recycling it can sometimes be difficult and brings extra cost to the final product. The need to use heterogeneous solid catalyst in this reaction is increasingly felt and attempts to improve the process have been ongoing for decades. In the previous work,[197] it was reported that calcined Li–Al and Mg–Al LDHs were used as heterogeneous catalysts to convert fatty acid methyl esters to monoglycerides (the reverse of biodiesel synthesis). An uncalcined Li–Al LDH, $[Al_2Li(OH)_6]OH^{\bullet}nH_2O$, was also reportedly active in the transesterification of 5-carboxyfluorescein diacetate with 1-butanol. In a separate study[198] Li–Al catalyst, corresponding to calcined $[Al_2Li(OH)_6](-CO_3)^{\bullet}_{0.5}nH_2O$, was reported to be more active than the Mg–Al material (or MgO) due to its higher Lewis basicity.

A report on the catalytic properties of calcined $[Al_2Li(OH)_6](CO_3)^{\bullet}_{0.5}nH_2O$ for biodiesel production from soybean oil revealed that near-quantitative conversion of the soybean oil was achieved at low catalyst loadings (2–3 wt%) and short reaction times (~2 h).[199] The catalyst maintained a high level of activity over repeated use, although the study indicated that a small amount of lithium was leached from the catalyst. The calcined samples were also found to show similar catalytic properties in the methanolysis of glyceryl tributyrate and soybean oil. XPS and XRD data indicated that an amorphous Li–Al mixed oxide was the catalytically active phase.

Wenlei *et al.* reportedly used calcined Mg–Al hydrotalcites as solid base catalysts for methanolysis of soybean oil to methyl-esters. The reaction was carried out at reflux of methanol, with a molar ratio of soybean oil to methanol of 15 : 1 and a catalyst amount of 7.5%. After 9 h, 67% conversion was achieved.[200] The same type of catalyst was studied in the work of Cantrell *et al.* for the liquid phase transesterification of glyceryl tributyrate with methanol for biodiesel production at 60 °C with encouraging results[201–203] that showed higher conversion at higher reaction temperature. In the transesterification of rape oil with methanol in the presence of calcined Mg–Al hydrotalcite (CHTs) prepared by co-precipitation method, conversion of 90.5% was achieved at optimized conditions.[204] It was reported that CHTs exhibited strong surface basicity, much like the pure oxides, but potentially containing more surface defects owing to the Al^{3+} cations

Table 1. Comparison of adsorption capacities for various high temperature CO_2 sorbents

Sorbent	CO_2 capacity, mmol/g (@ 100 kPa)	Temperature (K)	Comments	Preparation of HT	Reference
HTlc with K-promoted	0.77	450	Pretreated at 500 °C	Co-precipitation at low and high super-saturation	[214]
HTlc, $Ca_{0.75}Al_{0.25}(OH)_2(CO_3)_{0.125}$	1.79	603	Pre-treated at 673 K; static measurement	Co-precipitation	[219]
HTlc, $Ca_{0.75}Al_{0.25}(OH)_2(ClO_4)_{0.25}$	3.55	603	Pre-treated at 673 K; static measurement	Co-precipitation	[219]
HTlc, $Mg_{0.75}Al_{0.25}(OH)_2(CO_3)_{0.125}$	2.29	603	Pre-treated at 673 K; static measurement	Co-precipitation	[210, 219]
HTlc, $Mg_{0.75}Al_{0.25}(OH)_2(CO_3)_{0.125}$	0.60	573	Pre-treated at 673 K; gravimetric measurement	Co-precipitation	[219]
Lithium silicate, Li_4SiO_4	6.80	873	Gravimetric measurement		[234]
HTlc, $Mg_{0.75}Al_{0.25}(OH)_2(CO_3)_{0.125}$	0.486	473	Pre-treated at 673 K; static measurement	Co-precipitation	[222]
HTlc, $Mg_{0.75}Al_{0.25}(OH)_2(CO_3)_{0.125}$	0.249	573	Pre-treated at 673 K; static measurement	Co-precipitation	[222]
Perovskite-type metal oxides, $La_{0.1}Sr_{0.9}Fe_{0.5}O_{2.6}$	2.95	1073	Sintered at 1173 K; gravimetric measurement		[235]
HTlc	0.0272	600	Pre-treated at 600 K	Co-precipitation	[233]
HTlc	0.635	600	Pre-treated at 600 K	Sol-gel	[233]
Calcium oxide, CaO	2.95	873	Gravimetric measurement		[236]
Cs-doped CaO	11.36	873	Gravimetric measurement		[236]
Lithium zirconate, Li_2ZrO_3	4.55	773	Gravimetric measurement		[225]
HTlc, $Mg_{0.7}Al_{0.3}(OH)_2(CO_3)_{0.15}$	0.50	573	Pre-treated at 573 K; gravimetric measurement	Synthetic HT	[209]

incorporated in the MgO lattice.[205] In addition, these materials showed high surface areas and pore volumes developed during the thermal decomposition of the parent hydrotalcites. Being an inorganic base, CHTs have high thermal stability, thus affording the potential for easy regeneration by re-calcination. Furthermore, as shown by previous studies,[200,205] the surface chemistry of these materials could be tuned by careful control of compositional and pretreatment parameters, such as carbonate content, Mg : Al ratio, and activation temperature. CHTs have been applied in a variety of base-catalyzed organic transformations with success.[100,175] They are considered as attractive candidates for biodiesel synthesis and some preliminary studies are already accessible in the literature.[200–202]

HT as Adsorbent of Carbon Dioxide

The removal and recovery of carbon dioxide from gas streams are increasingly significant in the field of energy production, in natural gas treatment,[206] in the production of hydrogen gas[207] and in the aerospace industry.[208] Several options are available to reduce carbon dioxide emissions, including substitution of fossil fuels with sustainable and renewable energy resources, reduction of fossil fuel consumption, increased efficiency of fossil plants, improved energy efficiency and capturing the carbon dioxide prior to emission into the environment.[122,209,210] These options provide opportunities for abatement and mitigation of CO_2 emissions.[211,212] While all of these techniques have the attractive feature of limiting the amount of carbon dioxide emitted into the atmosphere, each has economic, technical or societal challenges.[213,214]

A large-scale separation of carbon dioxide by absorption is a commercial operation used throughout the world. Other technologies to separate CO_2 include cryogenic separation, membrane separation and adsorption processes. Adsorption has been applied in a wide variety of gas separations[215] and has been proposed for CO_2 separation and capture from fossil-fueled power plants and other sources.[215,216,217] Adsoprtion can be operated at elevated temperatures to remove most of the carbon dioxide.[218] In order to effect better separation of gas, the adsorbent must have (1) high selectively and adsorption capacity for carbon dioxide at high temperature, (2) adequate adsorption/desorption kinetics for carbon dioxide under operating conditions, (3) stable adsorption capacity for carbon dioxide after repeated adsorption/desorption cycles[214,219] and (4) adequate mechanical strength of adsorbent particles after cyclic exposure to high-pressure, high-temperature streams.[220,221]

Inorganic materials such as activated carbons and zeolites (13X, LSX and type A) can address some of these requirements, though for low-temperature (<100 °C) CO_2 separation application. However, zeolites are only effective for CO_2 separation from gas mixtures containing species that are less polar than CO_2. Activated carbons exhibit high adsorption capacity,[222,223] but only at low temperatures. Other potential adsorbents that exhibit high adsorption capacity even at elevated temperature

have been reported to include CaO,[224] lithium zirconate[225] and hydrotalcite-like compounds.[210] Thermally activated HT for adsorbing carbon dioxide were experimented with promising results.[207,209,226]

Most adsorbents for CO_2 at high temperatures are composed of alkali metal oxides that utilize their basic properties for adsorbing acidic CO_2.[209,226–229] Alkaline metal oxides (Na_2O, K_2O), alkaline earth oxides (CaO, MgO, and Al_2O_3) and alumina are basic and thus suitable for adsorbing CO_2. Alumina as an adsorbent was found to enhance the CO_2 adsorption at elevated temperatures.[230] Several different oxides as modifiers such as oxides of rare earth metals (La, Ce, Nd, Pr), alkaline earth metals (Mg, Ca, Sr, Ba), and alkaline metals (Na, K, Rb, Cs) were also tried. In a separate work, Mg–Al HT that was used as adsorbent was able to adsorb CO_2 at temperatures between 400 and 500 °C from CO_2-steam gas stream operated at 10 and 0.3 atmospheric partial pressures.[226,231,232] The adsorption was considerably enhanced by impregnating HT with K_2CO_3. The level of adsorption depended on the amount of K_2CO_3 used during HT preparation[213]. HT with 20 wt% K_2CO_3 impregnation was found to yield the highest CO_2 adsorption of 0.77 mmol/g at 450 °C and 800 mmHg. At 600 °C, co-precipated and sol–gel HT adsorbed 0.635 and 0.0272 mmol/g, respectively.[233] Table 1 compares the capacity of various HT adsorbents from previous studies.

Conclusion

Preparation of LDHs from the sol–gel route naturally leads to the development of HT and mixed oxides with increased number of active sites. In addition to active sites, high surface area and narrow pore size distribution are requisites for a good catalyst and adsorbent because they can effect high catalytic activity and adsorption capacity. The desired properties of HTs can be achieved by using a single method or combination of approaches during the HT synthesis as discussed in this paper. Because of its acceptance in many applications and the fact that its synthesis methods are simple and cost-effective, hydrotalcite prepared from different routes is expected to offer flexibility for further improvement and use in a wider scope of application.

Acknowledgment

The authors acknowledge financial supports from the Ministry of Science Technology and Innovation and the Universiti Sains Malaysia.

References

[1] H. H. Kung, E. I. Ko, *Chem. Eng. J.* **1996**, *64*, 203.
[2] F. Cavani, F. Trifiro, A. Vaccari, *Catal. Today* **1991**, *11*, 173.
[3] A. de Roy, C. Forano, K. El Malki, J. P. Besse, *Synthesis of Microporous Materials* (Ed.: M. L. Occelli, H. Robson), Van Nostrand-Reinhold: New York, **1992**, pp. 108–169.
[4] F. Trifiro, A. Vaccari, *Comprehensive Supramolecular Chemistry, Solid State Supramolecular Chemistry: Two and Three-dimensional Inorganic Networks*, Vol. 7, Pergamon: Oxford, **1996**, pp. 251–291.
[5] A. Vaccari, *Catal. Today* **1998**, *41*, 53.
[6] V. Rives, M. A. Ulibarri, *Coord. Chem. Rev.* **1999**, *181*, 61.
[7] W. Kagunya, Z. Hassan, W. Jones, *Inorg. Chem.* **1996**, *35*, 5970.
[8] V. Rives (Ed.), *Layered Double Hydroxides: Present and Future*, Nova Science: New York, **2001**, pp. 251–411.
[9] S. M. Auerbach, K. A. Carrado, P. K. Dutta, *Handbook of Layered Materials*, Marcel Dekker: New York, **2004**.
[10] X. Duan, D. G. Evans (Ed.), *Layered Double Hydroxides, Structure and Bonding Series*, Vol. 119, Springer: Berlin, **2006**.
[11] A. De Roy, C. Forano, J. P. Besse, *Layered Double Hydroxides: Present and Future* (Ed.: V. Rives), Nova Science: New York, **2001**, pp. 1–37.
[12] J. He, M. Wei, Y. Kang, B. Li, D. G. Evans, X. Duan, *Struct Bond* **2006**, *119*, 89.
[13] H. P. Boehm, J. Steinle, C. Vieweger, *Angew. Chem. Int. Ed. Engl.* **1977**, *16*, 265.
[14] R. M. Taylor, *Clay Mineral* **1984**, *19*, 591.
[15] M. A. Dredzon, *Inorg. Chem.* **1988**, *27*, 4628.
[16] H. Nijs, A. Clearfield, E. F. Vansant, *Microp. Mesop. Mater.* **1998**, *23*, 97.
[17] M. A. Aramendia, V. Borau, C. Jimenez, J. M. Marinas, J. R. Ruiz, F. J. Urbano, *J. Solid State Chemistry* **2002**, *168*, 156.
[18] Y. Zhao, F. Li, R. Zhang, D. G. Evans, X. Duan, *Chem. Mater.* **2002**, *14*, 4286.
[19] J. T. Kloprogge, L. Hickey, R. L. Frost, *J. Solid State Chem.* **2004**, *17*, 4047.
[20] A. Seron, F. Delorme, *J. Phys. Chem. Solids* **2008**, *69*(5–6), 1088.
[21] F. Trifirò, A. Vaccari, G. Del Piero, *Characterisation of Porous Solids* (Ed.: K. K. Unger, J. Roquerol, K. S. W. Sing and H. Kral), Elsevier: Amsterdam, **1988**, pp. 571–580.
[22] W. H. Zhang, G. J. He, Z. Y. Qian, *J. Eur. Ceramic Soc.* **2008**, *28*(8), 1623.
[23] M. A. Ulibarri, I. Pavlovic, C. Barriga, M. C. Hermosín, J. Cornejo, *Appl. Clay Sci.* **2001**, *18*, 17.
[24] O. Clause, M. Gazzano, F. Trifiro, A. Vaccari, L. Zatoski, *Appl. Catal.* **1991**, *73*, 217.
[25] D. Tichit, A. Rolland, F. Prinetto, G. Fetter, M. J. Martinez-Ortiz, M. A. Valenzuela, P. Bosch, *Mater. Chem.* **2002**, *12*, 3832.
[26] D. Tichit, O. Lorret, B. Coq, F. Prinetto, G. Ghiotti, *Micropor. Mesopor. Mater.* **2005**, *80*, 213.
[27] O. W. Perez-Lopez, A. Senger, N. R. Marcilio, M. A. Lansarin, *Appl. Catal. A: Gen.* **2006**, *303*, 234.
[28] F. Kovanda, T. Grygar, V. Dornicak, T. Rojka, P. Bezdicka, K. Jiratova, *Appl. Clay Sci.* **2005**, *28*, 121.
[29] F. Prinetto, G. Ghiotti, P. Graffin, D. Tichit, *Micropor. Mesopor. Mater.* **2000**, *39*, 229.
[30] G. Carja, R. Nakamura, T. Aida, H. Niiyama, *Micropor. Mesopor. Mater.* **2001**, *47*, 275.
[31] F. Kovanda, K. Jiratova, J. Rymes, D. Kolousek, *Appl. Clay Sci.* **2001**, *18*, 71.
[32] F. Kovanda, T. Grygar, V. Dornicak, *Solid State Sci.* **2003**, *5*, 1019.
[33] F. Kovanda, T. Rojka, J. Dobesova, V. Mackovic, P. Bezdicka, L. Obalova, K. Jiratova, T. Grygar, *Solid State Chem.* **2006**, *179*, 812.
[34] R. L. Frost, Z. Ding, *Thermochim. Acta* **2003**, *397*, 119.
[35] K. Yan, X. Xie, J. Li, X. Wang, Z. Wang, *J. Nat. Gas Chem.* **2007**, *16*, 371.
[36] F. Basile, G. Fornasari, M. Gazzano, A. Vaccari, *Appl. Clay Sci.* **2000**, *16*, 185.
[37] F. Basile, M. Campanati, E. Serwicka, A. Vaccari, *Appl. Clay Sci.* **2001**, *18*, 51.
[38] D. Tichit, M. H. Lhouty, A. Guida, B. H. Chinche, F. Figueras, A. Auroux, D. Bartalini, E. Garonne, *J. Catal.* **1995**, *151*, 50.
[39] E. Kanezaki, *Solid State Ionics* **1998**, *106*, 279.
[40] E. Lopez-Salinas, M. Garcia-Sanchez, M. A. Llanos-Serrano, J. Navarrete-Bolanoz, *J. Phys. Chem. B* **1997**, *101*, 5112.
[41] P. Benito, I. Guinea, F. M. Labajos, J. Rocha, V. Rives, *Micro. Meso. Mater.* **2008**, *110*(2), 292.
[42] M. Jitianu, M. Balasoiu, M. Zaharescu, A. Jitianu, A. Ivanov, *J. Sol–Gel Sci. Technol.* **2000**, *19*, 453.
[43] M. M. Rao, B. R. Reddy, M. Jayalaksmi, V. S. Jaya, B. Sridhar, *Mater. Res. Bull.* **2005**, *40*, 347.
[44] J.-M. Oh, S.-H. Hwang, C.-H. Choy, *Solid State Ionics* **2002**, *15*, 285.
[45] M. Ogawa, H. Kaiho, *Langmuir* **2002**, *18*, 4240.
[46] U. Costantino, F. Marmottini, M. Nocchetti, R. Viviani, *Eur. J. Inorg. Chem.* **1998**, *10*, 1439.
[47] U. Constantino, N. Coletti, M. Noccheti, G. G. Aloisi, F. Elisei, L. Latterini, *Langmuir* **2000**, *16*, 10351.
[48] U. Costantino, M. Curini, F. Montanari, M. Nocchetti, O. Rosati, *J. Mol. Catal. A: Chem.* **2003**, *195*, 245.
[49] J. J. Bravo-Suarez, E. A. Paez-Mozo, S. T. Oyama, *Micro. Meso. Mater.* **2004**, *67*, 1.
[50] N. Iyi, T. Matsumoto, Y. Kaneko, K. Kitamura, *Chem. Lett.* **2004**, *33*, 1122.

[51] U. Olsbye, D. Akporiaye, E. Rytter, M. Ronnekleiv, E. Tangstad, *Appl. Catal. A: General* **2002**, *224*, 39.
[52] Z. Yang, H. Zhou, J. Zhang, W. Cao, *Acta Phys.-chim. Sin.* **2007**, *23*(6), 795.
[53] P. B. On, S. Nadiv, *Thermochim. Acta* **1988**, *133*, 119.
[54] F. Kooli, V. Rives, M. A. Ulibarri, *Inorg. Chem.* **1995**, *34*, 5114.
[55] M. del Arco, P. Malet, R. Trujillano, V. Rives, *Chem. Mater.* **1999**, *11*, 624.
[56] A. S. Prakash, P. V. Kamath, M. S. Hegde, *Mater. Res. Bull.* **2000**, *35*, 2189.
[57] V. Rives, F. M. Labajos, *Inorg. Chem.* **1993**, *32*, 5000.
[58] F. M. Labajos, V. Rives, P. Malet, M. A. Centeno, M. A. Ulibarri, *Inorg. Chem.* **1996**, *35*, 1154.
[59] C. Barriga, W. Jones, P. Malet, V. Rives, M. A. Ulibarri, *Inorg. Chem.* **1998**, *37*, 1812.
[60] S. Kannan, R. V. Jasra, *J. Mater. Chem.* **2000**, *10*, 2311.
[61] L. Hickey, J. T. Kloprogge, R. L. Frost, *J. Mater. Sci.* **2000**, *35*, 4347.
[62] K. C. Patil, S. T. Aruna, T. Mimani, *Curr. Opin. Solid State Mater. Sci.* **2002**, *6*, 507.
[63] D. Cruz, S. Bulbulian, *J. Nucl. Mater.* **2003**, *312*, 262.
[64] K. C. Patil, S. T. Aruna, S. Ekambaram, *Curr. Opin. Solid State Mater. Sci.* **1997**, *2*, 158.
[65] V. Davila, E. Lima, S. Bulbulian, P. Bosch, *Micro. Mesop. Mater.* **2008**, *107*, 240.
[66] W. F. Lee, Y. C. Chen, *Eur. Polym. J.* **2006**, *42*, 1634.
[67] M. R. Othman, J. Kim, *J. Sol–Gel Sci. Technol.* **2008**, *47*, 274.
[68] M. Jitianu, M. Zaharescu, M. Balasoiu, A. Jitianu, *J. Sol–Gel Sci. Technol.* **2003**, *26*, 217.
[69] O. Lorret, S. Morandi, F. Prinetto, G. Ghiotti, D. Tichit, R. Durand, B. Coq, *Micro. Meso. Mater.* **2007**, *103*, 48.
[70] T. Lopez, P. Boch, E. Ramos, R. Gomez, O. Novarro, D. Acosta, F. Figueras, *Langmuir* **1996**, *12*, 189.
[71] E. Lopez-Salinas, M. Garcia-Sanchez, M. A. L. Ramon-Garcia, I. Schifter, *J. Porous Mater.* **1996**, *3*, 169.
[72] E. Lopez-Salinas, E. Torres-Garcia, M. Garcia-Sanchez, *J. Phys. Chem. Solids* **1997**, *58*, 919.
[73] E. Ramos, T. Lopez, P. Bosch, M. Asomoza, R. Gomez, *J. Sol–Gel Sci. Technol.* **1997**, *8*, 437.
[74] M. Bolognini, F. Cavani, D. Scagliarini, C. Flego, C. Perego, M. Saba, *Micro. Meso. Mater.* **2003**, *66*, 77.
[75] P. Benito, F. M. Labajos, J. Rocha, V. Rives, *Micro. Meso. Mater.* **2006**, *94*, 148.
[76] G. Fetter, F. Hernandez, A. M. Maubert, V. H. Lara, P. Bosch, *Porous Mater.* **1997**, *4*, 27.
[77] D. Tichit, S. Ribet, B. Coq, *Eur. J. Inorg. Chem.* **2001**, *2*, 539.
[78] T. Sato, H. Fujita, T. Endo, M. Shimada, *React. Solid* **1988**, *5*, 219.
[79] S. Miyata, *Clays Clay Miner.* **1975**, *23*, 369.
[80] G. S. Thomas, M. Rajamathi, P. V. Kamath, *Clays Clay Miner.* **2004**, *52*, 693.
[81] Y. Seida, T. Nakano, *Chem. Eng. Jpn.* **2001**, *34*(7), 906.
[82] Y. Seida, T. Nakano, Y. Nakamura, *Clays Clay Miner.* **2002**, *50*, 525.
[83] D. Kishore, D. Kannan, *Appl. Catal. A: Gen.* **2004**, *270*, 227.
[84] F. Malherbe, C. Forano, J. P. Besse, *Micro. Mater.* **1997**, *10*, 67.
[85] G. Del Piero, M. Di Cona, D. Triffiro, A. Vaccari, *Reactivity of Solids* (Ed.: P. Barret, L. C. Dufour), Vol. 1029, Elsevier: Amsterdam, **1985**.
[86] S. K. Yun, T. J. Pinnavaia, *Chem. Mater.* **1995**, *7*, 348.
[87] S. Kannan, C. S. Swamy, *J. Mater. Sci.* **1997**, *32*, 1623.
[88] F. M. Labajos, V. Rives, M. A. Ulibarri, *J. Mater. Sci.* **1992**, *27*, 1546.
[89] V. R. Choudhary, D. K. Dumbre, B. S. Uphade, V. S. Narkhede, *J. Mol. Catal. A: Chem.* **2004**, *215*, 129.
[90] J. J. Bravo-Suárez, E. A. Paez-Mozo, S. T. Oyama, *Micro. Meso. Mater.* **2003**, *67*, 1.
[91] S. Komarneni, Q. H. Li, R. Roy, *J. Mater. Res.* **1996**, *11*, 1866.
[92] H. Katsuki, S. Furuta, S. Komarneni, *J. Am. Ceram. Soc.* **1999**, *82*, 2257.
[93] S. Komarneni, R. Roy, Q. H. Li, *Mater. Res. Bull.* **1992**, *27*, 1393.
[94] A. Arafat, J. C. Jansen, A. R. Ebaid, H. van Bekkum, *Zeolites* **1993**, *13*, 162.
[95] A. Vaidhyanathan, K. J. Rao, *Bull. Mater. Sci.* **1996**, *19*, 1163.
[96] G. Fetter, A. Botello, V. H. Lara, P. Bosch, *J. Porous Mater.* **2001**, *8*, 227.
[97] J. Olanrewaju, B. I. Newalkar, C. Mancino, S. Komarneni, *Mater. Lett.* **2000**, *45*, 307.
[98] B. Zapata, P. Bosch, G. Fetter, M. A. Valenzuela, J. Navarrete, V. H. Lara, *Int. J. Inorg. Mater.* **2001**, *3*, 23.
[99] B. Zapata, P. Bosch, M. A. Valenzuela, G. Fetter, S. O. Flores, I. R. Cordova, *Mater. Lett.* **2002**, *57*, 679.
[100] L. Xu, Y.-S. Ding, C.-H. Chen, L. Zhao, C. Rimkus, R. Joesten, S. L. Suib, *Chem. Mater.* **2007**, *20*, 308.
[101] J. A. Rivera, G. Fetter, P. Bosch, *Micro. Meso. Mater.* **2006**, *89*, 306.
[102] P. Benito, I. Guinea, F. M. Labajos, V. Rives, *J. Solid State Chem.* **2008**, *181*(5), 987.
[103] P. Benito, F. M. Labajos, V. Rives, *J. Solid State Chem.* **2006**, *179*, 3784.
[104] O. Bergada, I. Vicente, P. Salagre, Y. Cesteros, F. Medina, J. E. Sueras, *Micro. Meso. Mater.* **2007**, *101*, 363.
[105] M. J. Climent, A. Corma, S. Iborra, A. Velty, *J. Catal.* **2004**, *221*, 316.
[106] S. P. Paredes, G. Fetter, P. Bosch, S. Bulbulian, *J. Mater. Sci.* **2006**, *41*, 3377.
[107] S. Mohmel, I. Kurzawski, D. Uecker, D. Müller, W. Gebner, *Cryst. Res. Technol.* **2002**, *37*, 359.
[108] J. Perez-Ramırez, F. Kapteijn, J. C. Groen, A. Domenech, G. Mul, J. A. Moulijn, *J. Catal.* **2003**, *214*, 33.
[109] M. L. Occelli, M. Kalwei, A. Wolker, H. Eckert, A. Auroux, S. A. C. Gould, *J. Catal.* **2000**, *196*, 134.
[110] J. A. van Bokhoven, D. C. Koningsberger, P. Kunkeler, H. Van Bekkum, *J. Catal.* **2002**, *211*, 540.
[111] P. B. Venuto, E. T. Habib Jr, *Fluid Catalytic Cracking with Zeolite Catalysts*. Marcel Dekker: New York, **1979**.
[112] H. Arai, M. Machida, *Appl. Catal. A: Gen.* **1996**, *138*, 161.
[113] S. Abello, J. Perez-Ramirez, *Micro. Meso. Mater.* **2006**, *96*, 102.
[114] J. Li, Z. Chen, R.-J. Wang, D. M. Proserpio, *Coord. Chem. Rev.* **1999**, *190–192*, 707.
[115] Y. Xie, Y. T. Qian, W. Z. Wang, *Science* **1996**, *272*, 1926.
[116] Y. Xie, Y. T. Qian, W. Z. Wang, *Appl. Physic Lett.* **1996**, *69*, 334.
[117] M. K. Hafiz, M. R. Othman, N. Aziz, *International Conference on Nanoscience and Nanotechnology*, UITM, 18–21 November **2008**, pp. 151–156.
[118] R. L. Goswamee, P. Sengupta, K. G. Bhattacharyya, D. K. Dutta, *Appl. Clay Sci.* **1998**, *13*(1), 21.
[119] P. C. Pavan, G. A. Gomes, J. B. Valim, *Micro. Meso. Mater.* **1998**, *21*(4–6), 659.
[120] H. S. Shin, M. J. Kim, S. Y. Nam, H. C. Moon, *Water Sci. and Technology* **1996**, *34*(1–2), 161.
[121] Y. Ding, E. Alpay, *Chem. Eng. Sci.* **2000**, *55*, 3461.
[122] Z. Yong, V. Mata, A. E. Rodrigues, *Ind. Eng. Chem. Res.* **2001**, *40*, 204.
[123] A. Alejandre, F. Medina, X. Rodriguez, P. Salagre, Y. Cesteros, J. E. Sueiras, *Appl. Catal. B: Environ.* **2001**, *30*(1–2), 195.
[124] K. Bahranowski, G. Bueno, V. C. Corberan, F. Kooli, E. M. Serwicka, R. X. Valenzuela, K. Wcislo, *Appl. Catal. A: Gen.* **1999**, *185*(1), 65.
[125] E. Gardner, T. J. Pinnavaia, *Appl. Catal. A: Gen.* **1998**, *167*(1), 65.
[126] S. M. Auer, J. D. Grunwaldt, R. A. Koppel, A. Baiker, *J. Mol. Catal. A: Chem.* **1999**, *139*(2–3), 305.
[127] F. Malherbe, C. Depege, C. Forano, J. P. Besse, M. P. Atkins, B. Sharma, S. R. Wade, *Appl. Clay Sci.* **1998**, *13*(5–6), 451.
[128] J. Santhanalakshmi, T. Raja, *Appl. Catal. A: Gen.* **1996**, *147*, 69.
[129] K. T. Liu Paul, *Gas Separation Using Membrane Organic*. Media and Process Technology Inc.: **2002**.
[130] W. J. Onstot, T. T. Tsotsis, R. G. Minot, *Ind. Eng. Chem. Res.* **2001**, *40*, 242.
[131] Y. Ding, E. Alpay, *Chem. Eng. Sci.* **2000**, *55*, 3929.
[132] S. Sircar, M. B. Rao, *AIChE J.* **1999**, *45*, 2326.
[133] J. W. Wang, A. G. Kalinichev, R. J. Kirkpatrick, X. Q. Hou, *Chem. Mater.* **2001**, *13*(1), 145.
[134] X. D. Wang, Q. Zhang, *Polym. Int.* **2004**, *53*, 698.
[135] G. Camino, A. Maffezzoli, M. Braglia, M. D. Lazzaro, M. Zammarano, *Polym. Degrad. Stab.* **2001**, *74*, 457.
[136] A. Ookubo, K. Ooi, H. Hayashi, *J. Pharm. Sci.* **1992**, *81*(11), 1139.
[137] M. Del Arco, E. Cebadera, S. Gutiérrez, C. Martín, M. J. Montero, V. Rives, J. Rocha, M. A. Se villa, *J. Pharm. Sci.* **2004**, *93*(6), 1649.
[138] D. Meloni, R. Monaci, V. Solinas, A. Auroux, E. Dumitriu, *Appl. Catal A: Gen.* **2008**, *350*, 86.
[139] A. Vaccari, *Appl. Clay Sci.* **1999**, *14*, 161.
[140] S. Casenave, H. Martinez, C. Guimon, A. Auroux, V. Hulea, E. Dumitriu, *J. Therm. Anal. Cal.* **2003**, *72*, 191.
[141] B. M. Nagaraja, V. Siva Kumar, V. Shashikala, A. H. Padmasri, S. S. Reddy, B. D. Raju, K. S. R. Rao, *J. Mol. Catal. A: Chem.* **2004**, *223*(1/2), 339.
[142] M. Crivello, C. Perez, E. Herrero, E. Ghione, S. Casuscelli, E. Rodriguez-Castellon, *Catal. Today* **2005**, *107*, 215.

[143] M. J. Climent, A. Corma, S. Iborra, A. Velty, *J. Mol. Catal. A: Chem.* **2002**, *182/183*, 327.
[144] J. Sanchez Valente, F. Figueras, M. Gravelle, P. Kumbhar, J. Lopez, J. P. Besse, *J. Catal.* **2000**, *189*, 370.
[145] A. L. McKenzie, C. T. Fishel, R. J. Davis, *J. Catal.* **1992**, *138*, 547.
[146] J. I. Di Cosimo, V. K. Diez, M. Xu, E. Iglesia, C. R. Apesteguıa, *J. Catal.* **1998**, *178*, 499.
[147] V. K. Díez, C. R. Apesteguía, J. I. Di Cosimo, *J. Catal.* **2003**, *215*, 220.
[148] S. Casenave, H. Martinez, C. Guimon, A. Auroux, V. Hulea, A. Cordoneanu, E. Dumitriu, *Thermochim. Acta* **2001**, *379*, 85.
[149] C. N. Perez, C. A. Perez, C. A. Henriques, J. L. F. Monteiro, *Appl. Catal. A: Gen.* **2004**, *272*, 229.
[150] I. Kirm, F. Medina, X. Rodrıguez, Y. Cesteros, P. Salagre, J. Suieras, *Appl. Catal. A: Gen.* **2004**, *272*, 175.
[151] S. Velu, C. S. Swamy, Alkylation of phenol with 1-propanol and 2-propanol over catalysts derived from hydrotalcite-like anionic clays. *Catal. Lett.* **1996**, *40*, 265.
[152] F. Basile, G. Fornasari, V. Rosetti, F. Trifirò, A. Vaccari, *Catal. Today* **2004**, *91–92*, 293.
[153] K. M. Lee, W. Y. Lee, *Catal. Lett.* **2002**, *83*, 65.
[154] Y. Cesteros, P. Salagre, F. Medina, J. E. Sueiras, D. Tichit, B. Coq, *Appl. Catal. B: Environ.* **2001**, *32*, 25.
[155] A. Chen, H. Xu, Y. Yue, W. Shen, W. Hua, Z. Gao, *Appl. Catal. A: Gen.* **2004**, *274*, 101.
[156] S. Abelló, F. Medina, D. Tichit, J. Perez-Ramırez, X. Rodrıguez, J. E. Sueiras, P. Salagre, Y. Cesteros, *Appl. Catal. A: Gen.* **2005**, *281*, 191.
[157] A. Morato, C. Alonso, F. Medina, J. E. Sueiras, D. Tichit, B. Coq, *Appl. Catal. B: Environ.* **2001**, *32*, 167.
[158] S. Abello, F. Medina, D. Tichit, J. Perez-Ramırez, Y. Cesteros, P. Salagre, J. E. Sueiras, *Chem. Commun.* **2005**, 1453.
[159] S. Abello, F. Medina, D. Tichit, J. Perez-Ramırez, J. C. Groen, J. E. Sueiras, P. Salagre, Y. Cesteros, *Chem. Eur. J.* **2005**, *11*, 728.
[160] P. Kumbhar, J. Sanches Valente, J. Lopes, F. Figueras, *J. Chem. Soc. Chem. Commun.* **1998**, 535.
[161] M. A. Aramendia, V. Borau, C. Jimenez, J. M. Marinas, J. R. Ruiz, F. J. Urbano, *Appl. Catal. A: Gen.* **2001**, *206*, 95.
[162] K. Yamaguchi, K. Ebitami, K. Kaneda, *J. Org. Chem.* **1999**, *64*, 2966.
[163] D. Tichit, B. Coq, *Cattech* **2003**, *7*(6), 206.
[164] J. Shen, M. Tu, C. Hu, *J. Solid State Chem.* **1998**, *137*, 295.
[165] C. O. Veloso, C. N. Perez, B. M. de Souza, E. C. Lima, A. G. Dias, A. J. F. Monteiro, C. A. Henriques, *Micro Meso. Mater.* **2008**, *107*, 23.
[166] M. J. Climent, A. Corma, S. Iborra, J. Primo, *J. Catal.* **1995**, *151*, 60.
[167] C. Veloso, C. Henriques, A. Dias, J. L. Monteiro, *Catal. Today* **2005**, *107–108*, 294.
[168] A. Corma, V. Fornes, R. M. Martin-Aranda, F. Rey, *J. Catal.* **1992**, *134*, 58.
[169] A. Guida, M. Lhouty, D. Tichit, F. Figueras, P. Geneste, *Appl. Catal. A: Gen.* **1997**, *164*, 251.
[170] H. Sharper, J. J. Berg-Slot, W. J. H. Stork, *Appl. Catal. A: Gen.* **1989**, *54*, 79.
[171] A. Corma, V. Fornés, F. Rey, *J. Catal.* **1994**, *148*, 205.
[172] S. Velu, C. S. Swamy, *Appl. Catal. A: Gen.* **1994**, *119*, 241.
[173] M. J. Climent, A. Corma, S. Iborra, A. Velty, *Green Chem.* **2002**, *4*, 474.
[174] M. J. Climent, A. Corma, S. Iborra, A. Velty, *Catal. Lett.* **2002**, *79*, 157.
[175] M. J. Climent, A. Corma, S. Iborra, A. Velty, *J. Catal.* **2004**, *225*, 316.
[176] J. C. A. A. Roelofs, D. J. Lensveld, A. J. van Dillen, K. P. de Jong, *J. Catal.* **2001**, *203*, 184.
[177] J. C. A. A. Roelofs, A. J. Van Dillen, K. P. de Jong, *Catal. Today* **2000**, *60*, 297.
[178] A. Choudary, M. L. Kantam, C. Reddy, K. Rao, F. Figueras, *J. Mol. Catal. A: Chem.* **1999**, *146*, 279.
[179] K. K. Rao, M. Gravelle, J. Sanchez Valente, F. Figueras, *J. Catal.* **1998**, *173*, 115.
[180] M. L. Kantam, B. M. Choudhary, C. V. Reddy, K. K. Rao, F. Figueras, *Chem. Commun.* **1998**, 1033.
[181] A. Corma, R. A. Martin-Aranda, *Appl. Catal. A: Gen.* **1993**, *105*, 271.
[182] K. Kabashima, H. Hattori, *Appl. Catal. A: Gen.* **1997**, *161*, L33.
[183] G. Zhang, H. Hattori, *Appl. Catal.* **1988**, *40*, 183.
[184] D. Tichit, M. Naciri Bennani, F. Figueras, J. R. Ruiz, *Langmuir* **1998**, *14*, 2086.
[185] S. Sebti, A. Solhy, R. Tahir, S. Abdelatif, S. Boulaajaj, J. A. Mayoral, J. I. García, J. M. Fraile, A. Kossir, H. Oumimoun, *J. Catal.* **2003**, *213*, 1.
[186] K. Akutu, H. Kabashima, T. Seki, H. Hattori, *Appl. Catal. A: Gen.* **2003**, *247*, 65.
[187] R. Ballini, F. Bigi, R. Maggi, G. Sartori, *J. Catal.* **2000**, *191*, 348.
[188] V. J. Bulbule, V. H. Deshpande, S. Velu, A. Sudalai, S. Sivasanker, V. T. Sathe, *Tetrahedron* **1999**, *55*, 9325.
[189] H. Kabashima, H. Tsuji, T. Shibuya, H. Hattori, *J. Mol. Catal. A: Chem.* **2000**, *155*, 23.
[190] A. Corma, S. Iborra, I. Rodriguez, M. Iglesias, F. Sanchez, *Catal. Lett.* **2002**, *82*, 237.
[191] M. Sasidharan, R. Kumar, *J. Catal.* **2003**, *220*, 326.
[192] I. Rodriguez, S. Iborra, F. Rey, A. Corma, *Appl. Catal. A: Gen.* **2000**, *194–195*, 241.
[193] J. Yamawaki, T. Kawate, T. Ando, T. Hanafusa, *Bull. Chem. Soc. Jpn* **1983**, *56*, 1885.
[194] K. Kabashima, H. Tsuji, H. Hattori, *Appl. A: Gen.* **1997**, *165*, 319.
[195] A. Demirbas, *Energy Conv. Mgmt* **2006**, *47*, 2271.
[196] C. C. S. Macedo, F. R. Abreu, A. P. Tavares, M. P. Alves, L. F. Zara, J. C. Rubim, *et al. J Braz Chem. Soc.* **2006**, *17*, 1291.
[197] A. Corma, S. B. A. Hamid, S. Iborra, A. Velty, *J. Catal.* **2005**, *234*, 340.
[198] M. B. J. Roeffaers, B. F. Sels, H. Uji-i, F. C. De Schryver, P. A. Jacobs, D. E. De Vos, Hofkens, *J. Nature* **2006**, *439*, 572.
[199] J. L. Shumaker, C. Crofcheck, S. A. Tackett, E. Santillan-Jimenez, M. Crocker, *Catal. Lett.* **2007**, *115*, 56.
[200] X. Wenlei, H. Peng, L. Chen, *J. Mol. Catal. A: Chem.* **2006**, *246*, 24.
[201] D. G. Cantrell, L. J. Gillie, A. F. Lee, K. Wilson, *Appl. Catal. A: Gen.* **2005**, *287*, 183.
[202] M. Di Serio, M. Ledda, M. Cozzolino, G. Minutillo, R. Tesser, E. Santacesaria, *In. Eng. Chem. Res.* **2006**, *45*, 3009.
[203] M. D. Siano, E. Nastasi, E. Santacesaria, M. Di Serio, R. Tesser, G. Minutillo, M. Ledda and T. Tenore, International Patent Application no. WO 2006/050925, **2006**.
[204] H.-Y. Zeng, Z. Feng, X. Deng, Y.-Q. Li, *Fuel* **2008**, *87*(13–14), 3071.
[205] G. Fetter, M. T. Olguin, S. Bulbulian, P. Bosch, *J. Porous Mater.* **2000**, *7*, 469.
[206] T. D. Burchell, *Carbon* **1997**, *35*(9), 1279.
[207] J. Hufton, S. Mayorga, S. Nataraj, S. Sircar, *AIChE J.* **1999**, *45*(2), 248.
[208] M. Lila, J. E. Finn, *Carbon Dioxide Adsorption on 5A-Zeolite Designed for CO_2 Removal in Spacecraft Cabins.* Report NASA/TM-1998-208752. National Aeronautics and Space Administration: Washington, DC, **1998**.
[209] Z. Yong, V. Mata, A. E. Rodrigues, *Adsorption* **2001**, *7*, 41.
[210] N. D. Hutson, *Chem. Mater.* **2004**, *16*, 4135.
[211] T. Suzuki, A. Sakoda, M. Suzuki, J. Izumi, *J. Chem. Eng. Jpn* **1997**, *30*(5), 954.
[212] T. Suzuki, A. Sakoda, M. Suzuki, J. Izumi, *J. Chem. Eng. Jpn* **1997**, *30*, 1026.
[213] T. D. Burchell, R. R. Judkins, *Energy Convers. Mgmt* **1996**, *37*(6–8), 947.
[214] J.-I. Yang, J.-N. Kim, *Korean J. Chem. Eng.* **2006**, *23*(1), 77.
[215] R. T. Yang, *Gas Separation by Adsorption Processes*, Imperial College Press: Singapore, **1997**, pp. 4–124.
[216] A. S. Kikkinides, R. T. Yang, S. H. Cho, *Ind. Eng. Chem. Res.* **1993**, *32*, 2714.
[217] V. G. Gomes, K. W. K. Yee, *Sep. Purif. Technol.* **2002**, *28*, 161.
[218] T. R. Gaffney, T. C. Golden, S. G. Mayorga, J. R. Brzozowski, F. W. Talyer, US Patent 5917136, **1999**.
[219] N. D. Hutson, B. C. Attwood, *Adsorption* **2008**, *14*, 781.
[220] R. Dave, *et al.* US Department of Energy Report, **1999**, http://www.fe.doe.gov/coal_power/sequestration/index_rpt.html.
[221] J. Hufton, S. Mayorga, T. Gaffney, S. Nataraj, S. Sircar, *Proceedings of the 1997 US DOE Hydrogen Program Review* **1997**, *1*, 179.
[222] M. K. Ram Reddy, Z. P. Xu, G. Q. Lu, J. C. Diniz da Costa, *Ind. Eng. Chem. Res.* **2006**, *45*, 7504.
[223] M. K. Ram Reddy, Z. P. Xu, G. Q. Lu, J. C. Diniz da Costa, *Ind. Eng. Chem. Res.* **2008**, *47*, 2630.
[224] H. Lu, E. P. Reddy, P. G. Smirniotis, *Ind. Eng. Chem. Res.* **2006**, *45*, 3944.
[225] J. Ida, Y. S. Lin, *Environ. Sci. Technol.* **2003**, *37*, 1999.
[226] J. Hufton, S. Mayorga, T. Gaffney, S. Nataraj, M. Rao, S. Sircar, *Proceedings of the 1998 USDOE Hydrogen Program Review*, **1998**, *2*, 693.

[227] J. L. Soares, R. F. P. M. Moreira, H. J. Jose, C. A. Grande, A. E. Rodrigues, *Sep. Sci. Technol.* **2004**, *39*, 1989.
[228] R. F. P. M. Moreira, J. L. Soares, G. L. Casarin, A. E. Rodrigues, *Sep. Sci. Technol.* **2006**, *41*, 341.
[229] S. P. Reynolds, A. D. Ebner, J. A. Ritter, *Ind. Eng. Chem. Res.* **2006**, *45*, 4278.
[230] T. Horiuchi, H. Hidaka, T. Fukui, Y. Kubo, M. Horio, K. Suzuki, T. Mori, *Appl. Catal. A: Gen.* **1998**, *167*, 195.
[231] K. B. Lee, A. Verdooren, H. S. Caram, S. Sircar, *J. Colloid Interface Sci.* **2007**, *308*, 30.
[232] H. T. J. Reijers, S. E. A. Valster-Schiermeier, P. D. Cobden, R. W. Van den Brink, *Ind. Eng. Chem. Res.* **2006**, *45*, 2522.
[233] M. R. Othman, N. M. Rasid, W. J. N. Fernando, *Chem. Eng. Sci.* **2006**, *61*, 1555.
[234] M. J. Venegas, F. Fregoso-Israel, R. Escamilla, H. Pfeiffer, *Ind. Eng. Chem. Res.* **2007**, *46*, 2407.
[235] Q. Yang, Y. S. Lin, *Ind. Eng. Chem. Res.* **2006**, *45*, 6302.
[236] E. P. Reddy, P. G. Smirniotis, *J. Phys. Chem. B* **2004**, *108*, 7794.

Catalytic activity of sol-gel hydrotalcite like-compound in methanolysis of jatropha oil

Z. Helwani[1,2], N. Aziz[1] and M.R. Othman[1,*]

[1]*School of Chemical Engineering, Universiti Sains Malaysia, 14300 Nibong Tebal, Penang, Malaysia.*
[2]*Department of Chemical Engineering, Riau University, Pekanbaru, 28293, Indonesia*
**Email: chroslee@ eng.usm.my.*

Abstract

This paper reports experimental work on the use of a novel heterogeneous solid basic catalyst for transesterification of jatropha oil into biodiesel. The catalyst use was Mg/Al hydrotalcite produced by sol-gel method, calcined at high temperature. The process variables studied were reaction temperature, reaction time, molar ratio methanol to oil and amount of catalyst. Results from this study reveal that individual as well as interaction between variables affected the conversion of free fatty acid methyl ester significantly. The most suitable catalyst system studied was hydrotalcite with Mg:Al ratio of 3:1, calcined at 500 °C, methanol:oil molar ratio of 9:1 at reaction temperature of 65 °C, catalyst loading of 3wt.% and 6 h of reaction time to yield the optimum conversion of 91.2 wt.%.

Keywords: *heterogeneous catalyst, hydrotalcite, sol-gel, jatropha oil, biodiesel*

1. Introduction

Different methods of biodiesel production were reviewed [1]. The most preferred and viable method is the catalytic transesterification of vegetable oils with a short-chain alcohol such as methanol. This process is also known as *methanolysis*, in which, alkaline metal alkoxides and hydroxides, as well as sodium or potassium carbonates are used as *homogeneous catalysts*. Despite its preference, this homogeneous system has some technological problems associated with corrosion of equipment, emulsification, difficulties of separating the catalyst, decomposition and polymerization. These problems can be prevented if *heterogeneous catalyst* is used. The use of heterogeneous catalyst makes separation of the products easier and without corrosion or emulsion [2]. Among the heterogeneous basic catalysts for transesterification, hydrotalcite (HT) appears to have a great potential to be developed further as the catalyst of choice for biodiesel production.

HTs are usually obtained by *co-precipitation* method at constant pH using appropriate metallic salts [3]. The solids obtained by this method are crystalline, having surface areas between 10 and 120 m^2/g [4]. HTs can also obtained by the sol–gel method. HTs obtained in this manner exhibit higher thermal stability than those obtained by the coprecipitation method [5]. Sol-gel method allows better control of the textural, thermal and structural properties of HTs [6]. The specific

surface area of the solids obtained with the sol-gel method was higher by three fold than that achieved by co-precipitation [7-11].

In the present work, calcined Mg–Al HT derived form the sol-gel was applied for the first time in methanolysis of jatropha oil into methanol. The characteristics of Mg–Al HT and Free Fatty Acid Methyl Ester (FAME) conversion are reported in this paper.

2. Methods

2.1 HT preparation

An appropriate ratio of aluminium tri-sec-butoxide and magnesium methoxide were mixed with hot ethanol, respectively. The Mg/Al atomic ratio of 3:1 was selected. Hydrolysis of alkoxides was done separately for approximately 30 minutes under vigorous stirring at 70-90°C to form sol. 9.5ml 1M K_2CO_3 was added to the mixture, followed by peptization of the sol using molar composition of the alkoxide, acid and water at 1:0.07:100, with continuous stirring until homogeneity. Polyvinyl alcohol (PVA) was added to add strength and promote peptization. The peptized sol was allowed to cool steadily to allow further hydroxylation, alkoxilation or condensation. The solution was refluxed at 353 K up to 16 hours until gellation and filtered. The filtrate was dried in an oven at 90°C for 4 hours and then calcined in programmable carbolite furnace from 400-850°C for 15 hours to obtain mixed oxides of HT.

2.2 Biodiesel production

Jatropha *curcas* oil and an appropriate volume of methanol with HT catalysts were placed into a 500 ml three-angel necked flask equipped with reflux condenser and Teflon stirrer. The reaction mixture was blended for a period of time and at 55-75 °C temperature under atmospheric pressure. Molar ratio of methanol to oil was varied at 3-15:1. After reaction, the methanol was recovered by a rotary evaporator in vacuum at 45 °C. Subsequently, the catalyst was separated by filtration and the ester layer was separated from the glycerol layer in a separating funnel. The upper layer of the sample was separated from the bottom layer and immediately quenched with *n*-hexane (dilution) prior to analysis of FAME content. Methyl heptadecanoate was used as Internal Standard.

3. Result and discussion

3.1 Catalyst Characterization

Table 1 shows the physical-chemical properties of HT prepared at different calcination temperatures. All samples exhibited the basic strength in the range of 7.2-11.0. The main basic sites with H_ were in the range of 7.2-9.8 and the other sites with H_ were in the range of 9.8-11.0. This suggests that the calcined hydrotalcites contained wide basic site distribution and different types of surface basic sites. According to Di Cosimo et al., and Xie et al., while pure MgO possesses strong basic sites consisting predominantly of O^{2-}, calcined

hydrotalcites contain surface basic sites of low (OH- groups), medium (Mg-O pairs) and strong (O^{2-}) basic strength [12,13]. Our results conform to this viewpoint. H_ values ranging from 7.2 to 11.0 were mainly ascribed to Bronsted hydroxyl groups and coordinatively unsaturated oxide anions of the Lewis type.

Table 1. Physico-chemical properties of hydrotalcite at different calcination temperature

Sample	Surface area[a] (m^2/g)	Pore volume (cm^3/g)	Pore diameter[b] (nm)	Base strength (pK_{BH+})
SG-400	111.44	0.27	3.4	≤7.2
SG-500	285.20	0.35	8.1	7.2-11.0
SG-550	230.17	0.24	7.4	7.2-11.0

[a]BET surface area
[b]BJH desorption average pore diameter

The X-ray diffraction patterns for the HT products are shown in Fig. 1. The diffraction pattern of uncalcined sample showed sharp and symmetric peaks giving clear indication that the samples were well crystallized. The peaks corresponding to (003), (006) and (009) planes were the characteristics of hydrotalcite type materials. The peaks at (110) and (113) planes were weak signals of the brucite-type phase. This result confirms that the sample exhibited a double layered structure.

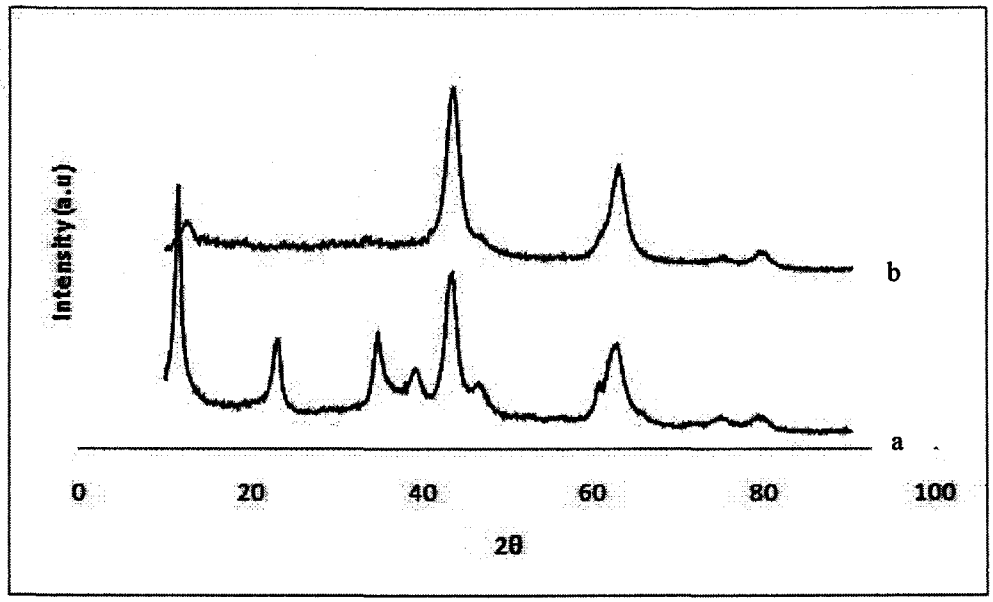

Figure 1. X-ray diffraction pattern of: a) uncalcined sample, b) calcined sample at 500 °C

Mg-Al oxides phases developed after the sample was calcined at 500°C as shown by the XRD pattern. The characteristic reflections were observed clearly at $2\theta \approx 43$ and 62° corresponding to MgO-like phase (periclase) or rather magnesia-alumina solid solution. The peaks of Al_2O_3 phase were very small, indicating that Al^{3+} cations were dispersed in the structure of MgO [13]. Sample calcined at

500°C exhibited clean peaks, indicating the presence of well crystallized Mg-O in this sample.

SEM micrograph of sample calcined at 500 °C is shown in Fig. 2. The micrograph shows the presence of platelets and more grained, many of which are hexagonal in form.

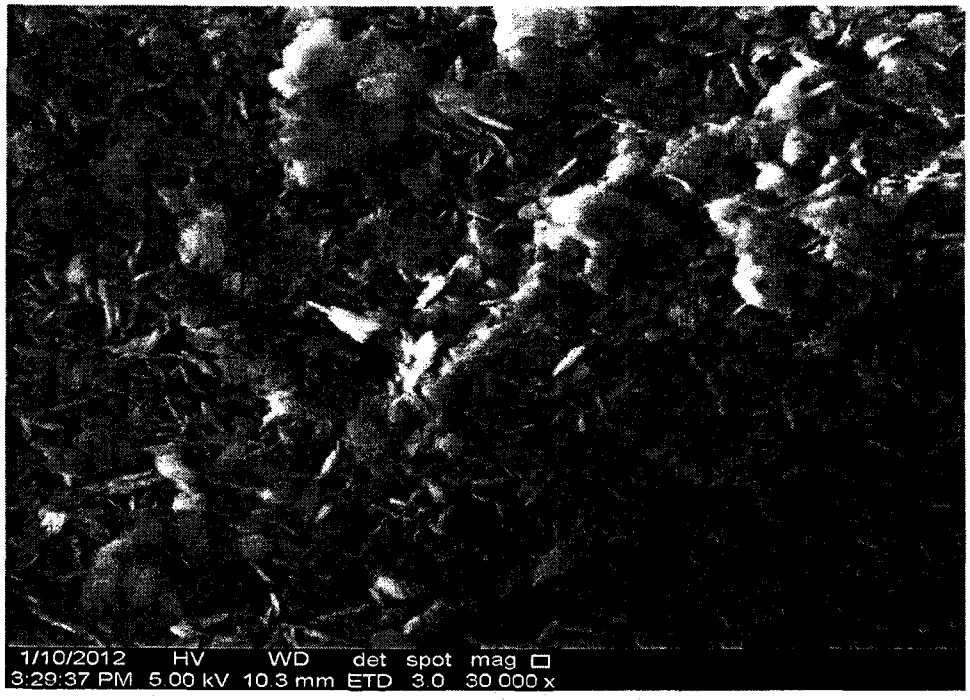

Figure 2. SEM image of sample calcined at 500 °C (magnification x 30.000)

This morphology is typical of well-crystallized hydrotalcite-type compounds. The fact that the platelets packed to form a rather open network helps to explain the higher surface area and porosity (Table 1) of sample calcined at 500 °C.

3.2 Transesterification reaction

The effect of calcination temperature on the catalytic activity was investigated and found to be higly influential. With increasing calcination temperature to 500°C, the ester conversion increased gradually and reached the maximum of 91.2% (450°C: 43.3%). However, when the temperature was higher than 500°C, the conversion dropped considerably (550°C: 76.9%, 650°C: 62.4% and 850°C: 24.2). Temperature 500 °C was the optimum calcination temperature for the sample.

The *ideal* stoichiometric molar ratio of methanol to oil of 3.0 normally generates low ester conversion. An excess molar ratio is needed to drive the equilibrium to the right-hand side and increase the conversion in shorter time. In our experiments, the ester conversions increased considerably from methanol/oil

molar ratio of 3.0 to reach 40.5%, to 9.0 to reach maximum of 91.3% conversion. Higher molar ratio than 9.0 decreased the conversion.

Higher concentration of catalyst also drives the reaction equilibrium to the product side and increases the conversion [14]. But, the amount of the catalyst should be balanced between the reactivity and viscosity of the reaction system [15]. Increasing catalyst amount may not increase production yield, because the fluid becomes heavily viscous at some point, giving rise to a problem of mixing and a demand of higher power consumption for adequate stirring. On the other hand, when the catalyst amount is not sufficient, maximum conversion cannot be reached [1, 16].

In most cases, sodium hydroxide or potassium hydroxide was used in alkaline methanolysis, both in concentrations ranging from 0.5% to 1.5% w/w of oil [16]. In our work, the ester conversion increased with the increase of catalyst loading from 1 to 3% (1.0% w/w of oil:55.0%, 2.0:68.0%, 3.0:91.2%). However, the conversion decreased with further increase of the catalyst loading from 4.0 (72.7%) to 5.0 (72.1%), which was possibly due to mixing problem of reactants, products and solid catalyst [13]. The maximum ester conversion was 91.2% when 3.0% catalyst was added.

The rate of methanolysis is also strongly influenced by the reaction temperature. Increasing reaction temperature not only leads to better reaction kinetics, but also improves phase miscibility. Phase miscibility is important in a potentially diffusion-limited process. Faster kinetic process and shorter residence times can be achieved by increasing reaction temperature. However, the use of higher temperatures requires not only greater energy consumption, but also higher system pressure to keep methanol in the liquid phase, which leads to increased reactor cost [17]. Commonly, the methanolysis is conducted close to boiling point of methanol at atmospheric pressure. The effect of reaction temperature on the ester conversion was studied with the catalyst at five temperature, i.e. 55, 60, 65, 70, 75 °C.

The results indicate was merely 56.2% in a 6 h reaction at 55 °C. Lower temperatures resulted in a drop of the ester conversion because only a small amount of molecules was able to get over the required energy barrier [18]. The ester conversion increased with the increase of reaction temperature up to 91.3% in 6 h reaction at 65 °C. But the conversion fell to about 67% in the temperature range of 70-75 °C. The primary advantage of higher temperature is a shorter reaction time. However, if the reaction temperature exceeds the boiling point, the methanol vaporizes and forms bubbles, inhibiting the reaction on the three-phase interface. Therefore, the optimum temperature for the preparation of the ester was 65 °C, which is near the boiling point of anhydrous methanol.

4. Conclusion

HT with Mg/Al ratio of 3 was synthesized by sol-gel method. The calcined HT gel exhibited mixed oxide with a small amount of brucite-phase. The conversion

of the FAME was optimum at 91.2% when the following conditions were applied: Mg:Al ratio of 3:1, calcined at 500 °C, 6h reaction time at 65 °C reaction temperature, methanol to oil molar ratio at 9:1 and 3wt.% catalyst loading.

Acknowlegdements

The authors gradefully acknowlegde the University Sains Malaysia for providing the Research University Grant and Postgraduate Research Grant Scheme (USM-RU-PRGS).

References

[1]. Vicente, G., Martınez, M., and Aracil, J. 2008. Integrated biodiesel production: a comparison of different homogeneous catalysts systems. *Bioresource Technology* 92: 297–305.

[2]. Hak, J.K., Bo, S.K., Min, J.K., Young, M.P. 2004. Transesterification of vegetable oil to biodiesel using heterogeneous base catalysts. *Catalysis Today* 93: 315–320.

[3]. He, J., Wei, M., Li, B., Kang, Y., Evans, D.G., and Duan, X., 2006. Preparation of layered double hydroxides. *Structure Bonding* 119: 89-111.

[4]. Lazaridis, N.K., Pandi, T.A., Matis, K.A., 2004. Chromium (VI) removal from aqueous solutions by Mg–Al–CO_3 hydrotalcite: sorption–desorption kinetic and equilibrium studies. Industrial & Engineering Chemistry Research 43, 2209–2215.

[5]. Fetter, G., Ramos, E., Olguin, M.T., Bosch, P., Bulbulian, S., 1997. Sorption of 131I− by hydrotalcites. *Journal of Radioanalysis Nuclear Chemistry* 6: 221–223.

[6]. Ramos, E., Lopez, T., Bosch, P., Asomoza, M., and Gomez, R., 1997. Thermal stability of sol–gel hydrotalcites. *Journal of Sol–Gel Science and Technology* 8: 437–442.

[7]. Aramendia, M.A., Borau, V., Jimenez, C., Marinas, J.M., Ruiz, J.R., and Urbano F.J., 2002. Comparative study of Mg/M (III) (M=Al, Ga, In) layered double hydroxides obtained by coprecipitation and the sol-gel method. *Journal of Solid State Chemistry* 168: 156-161.

[8]. Bolognini, M., Cavani, F., Scagliarini, D., Flego, C., Perego, C., and Saba, M., 2003. Mg/Al mixed oxides prepared by coprecipitation and sol-gel routes: a comparison of their physico-chemical features and performances in m-cresol methylation. *Journal of Microporous and Mesoporous Materials* 66: 77-89.

[9]. Jitianu, M., Zaharescu, M., Balasoiu, M., Ivanov, A., and Jitianu, A., 2000. Comparative study of sol-gel and coprecipitated Ni-Al hydrotalcites. *Journal of Sol-gel Science and Technology* 19: 453-457.

[10]. Prinetto. F., Ghiotti, G., Graffin, P., and Tichit, D., 2000. Synthesis and characterization of sol-gel Mg/Al and Ni/Al layered double hydroxides and comparison with co-precipitated samples. *Microporous and Mesoporous Materials* 39: 229-247.

[11]. Othman, M.R., Rasid, N.M., Fernando, and W.J.N., 2006. Effect of thermal treatment on the micro-structures of co-precipitated and sol-gel

synthesized Mg-Al hydrotalcites. *Microporous and Mesoporous Materials* 93: 23-28.

[12]. Di Cosimo, J.I., Díez, J.V., Xu, M., Iglesia, E., and Apesteguía, C.R., 1998. Structure and surface and catalytic properties of Mg-Al basic oxides. *Journal of Catalysis* 178: 499–510.

[13]. Xie, W.L., Peng, H., and Chen, L.G., 2006. Calcined Mg–Al hydrotalcites as solid base catalysts for methanolysis of soybean oil. *Journal of Molecular Catalysis A: Chemical* 246: 24–32.

[14]. Antolin, G., Tinaut, F.V., Bricerio, Y., Castano, V., Perez, C., and Ramirez, A.I. 2002. Optimization of biodiesel production by sunflower oil transesterification. *Bioresource Technology* 83(2): 111-114.

[15]. Lee, D.W., Park, Y.M., and Lee, K.Y. 2009. Heterogeneous base catalysts for transesterification in biodiesel synthesis. *Catalysis Surveys from Asia* 13: 63-77.

[16]. Tomasevic, A.V., and Siler-Marinkovic, S.S. 2003. Methanolysis of used frying oil. *Fuel Processing Technology* 81: 1–6.

[17]. Huaping, Z., Zongbin, W., Yuanxiao, C., Ping, Z., Shije, D., Xiaohua, L., Zongqiang, M. 2006. Preparation of biodiesel catalyzed by solid Super base of calcium oxide and its refining process. *Chinese Journal Catalysis*, 27: 391-396.

[18]. Zeng, H.Y., Feng, Z., Deng, X., and Li, Y.Q., 2008. Activation of Mg-Al hydrotalcite catalysts for transesterification of rape oil. *Fuel* 87: 3071-3076.

Mg/Al layered double hydroxides from combustion procedure

Martunus, Z. Helwani, A.D. Wiheeb, M.R. Othman

Abstract—**Layered double hydroxides (LDHs) was synthesized by combustion method using powdered aluminum and magnesium nitrates and sodium carbonate. Different types of fuel were used to facilitate the reaction. The synthesis temperatures were systematically varied to understand the role of temperature on the resulting crystallites. The resulting samples were characterized by X-ray diffraction (XRD) and Fourier transform infrared (FTIR). The surface morphology and chemical composition were characterized by scanning electron microscope (SEM) and energy dispersive X-ray (EDX). The LDHs structures demonstrated higher degree of crystallinity when thermally treated at 650° C.**

Keywords—**Hydrotalcite, intercataled material, characterization, synthesis, LDH**

I. Introduction

AMONG the compounds having layered structures, lamellar double hydroxides (LDHs) or hydrotalcites (HTs) represent one of the most important materials having numerous potential applications as adsorbents, catalysts, anion exchangers, hosts of electro-active, flame retardant in polymers and many more [1]. The compounds consist of positively charged brucite like hydroxyl sheets separate by layers of intercalated anions and additional water molecules, and can be represented by the general formula:$[(M^{2+}_{(1-x)}M^{3+}_{x}(OH)_2)^{x+}.(A^{n-}_{x/n}\ nH_2O)^{x-}]$ where M^{2+} is a di-valent cation (Mg^{+}, Ca^{2+}, Zn^{2+}, Cu^{2+}, Co^{2+}, Ni^{2+} or Mn^{2+}), M^{3+} is a three-valent cation (Al^{3+}, Fe^{3+} or Cr^{3+}). The layer are positive charged as M^{3+} cations substitute M^{2+} cations. This charge balanced by A anions with charge n-, for instance OH^{-}, C NO_3^{-}, CO_3^{2-} or SO_4^{2-}, among others and x is normally betwe 0.17 and 0.33. Carbonates (CO_3^{2-}) are generally the preferr anion [2]-[3] and they have been widely described in t literature [3]-[4].

LDHs are commonly prepared by co-precipitation inorganic salts in alkaline media either at constant or increasing pH. The morphology and particle size distributi of the resulting compounds depend on the supersaturation the synthesis solutions [5] if the precursors are in the form liquid, suspension or colloid. Generally, a sol-gel method produce LDHs is used. It starts from alkoxides and/ acetylacetonate precursors [5]. Other methods of LD production include decomposition-recrystallization, ur method and microwave irradiation. These procedures a highly successful but they may consume time and require hi amounts of water [6].

Another method to produce LDHs in shorter period of ti using solid precursors is through combustion. This is t method selected in this presentation. The method is based explosive decomposition of some organic fuels, initiated heat [1]. LDHs were successfully synthesized from this wo and they were characterized using XRD, SEM, EDX a FTIR.

II. Materials and Method

A. Combustion Method

To prepare the Mg-Al-O mixed oxides; the precursors LDHs; a solid mixture was prepared from magnesium nitr hexahydrate, aluminum nitrate nonahydrate and potassi carbonate. The amount of Al and Mg nitrates was maintain constant (Mg/Al ratio of 3) and the amount of sodi carbonate was fixed to 0.20 g per gram of mixture. T hundred milligrams of fuel were added and the mixture w suspended in water. The suspension was stirred rigorou while heated at temperature ranging from 75 to 80° C u water evaporated. The resulting paste was transferred into a ml crucible before calcination took place in a furnace at 4 850° C. The combustion process was over in 5 min produci mainly a mixture of oxides. The mixed oxides were placed

Martunus was with the School of Chemical Engineering, Universiti Sains Malaysia, 14300 Nibong Tebal, Penang, Malaysia and Department of Chemical Engineering, Riau University, Pekanbaru 28293, Indonesia (e-mail: martunusche@yahoo.co.id).

Z. Helwani is with the School of Chemical Engineering, Universiti Sains Malaysia, 14300 Nibong Tebal, Penang, Malaysia and Department of Chemical Engineering, Riau University, Pekanbaru 28293, Indonesia (e-mail: zuchrahelwani@yahoo.com).

A.D. Wiheeb is with the School of Chemical Engineering, Universiti Sains Malaysia, 14300 Nibong Tebal, Penang, Malaysia and Department of Chemical Engineering, College of Engineering, University of Tikrit, Salah ad Din, Iraq (e-mail: aboabody13@yahoo.co.uk).

M. R. Othman is with the School of Chemical Engineering, Universiti Sains Malaysia, 14300 Nibong Tebal, Penang, Malaysia (corresponding author's phone number: (60)-459964261; fax: (60)-45941013; e-mail: chroslee@ eng.usm.my).

contact with 60 ml 1 M of Na_2CO_3 solution at room temperature. The obtained products were stirred for 5 min and the solid was separated by centrifugation, washed with deionized water and dried at 100° C.

B. Characterization

The crystallization phases were studied using XRD. The analysis was carried out using Philips Goniometer PW 1820 diffractometer, PW 1710 diffraction controller and X-ray generator PW 1729. The diffractometer was used with monochromatized CuK_α radiation and taken in the range of 10-70° (2θ). The X-ray tube was operated at 40 kV and 120 mA.

The surface morphology of the LDHs powder was analyzed by SEM from Germany, model Leo Supra 50 VP Field Emission. Samples were placed in the sample grid for electron reflection and vacuumed (5 min) before analysis. SEM equipped with Oxford INCA 400 EDX microanalysis system with an operating voltage in the range of 0.1-30 kV was used in the present work. EDX was used to determine elemental composition of LDHs by analyzing the microscopic image under EDX instrument. The EDX analysis used MnK_α as the energy source operated at 15 kV of accelerating voltage, 155 eV resolution 22.4° takeoff angle.

An infrared (IR) spectrum of LDHs was obtained using FTIR spectrophotometer (Perkin Elmer FTIR 2000, USA). Samples were prepared by mixing the powdered solids with potassium bromide, KBr (the blank) in a 15:85 ratio to get transparent pellet auto supported on the different solids at 8 ton pressure. The infrared spectra were recorded both over the wave number range from 400 to 2000 cm^{-1}.

III. Results

Figure 1 shows XRD patterns of the samples using different types of fuel heated at 650 °C. All the samples exhibited the attribute of HTs as described in JCPDS file (220700). The $d_{(003)}$ spacing values obtained are 7.88, 7.89, 7.89, 7.91 and 7.91 Å for the sample prepared using saccharose, fructose, glucose, urea and glycine as fuel, respectively. These values appear to be in good agreement with the previously reported literature [2]. The $d_{(003)}$ spacing value represents the distance between LDHs layers, and changes in this value indicate the effect of anions on the LDHs structure.

The intensity counts (Fig.1) follows the order of saccharose > fructose = glucose > urea > glycine. The highest intensity counts by saccharose was possibly due to the higher content of C and H in order to form complexes with the metal ions [3]. Saccharose is a disaccharide molecule containing the highest energy to fuel the combustion. It is derived from glucose ($C_6H_{12}O_6$) and fructose ($C_6H_{12}O_6$) with molecular formula of $C_{12}H_{22}O_{11}$. The energy (entalphy) of combustion at 25° C for saccharose is -5,646.7 kJ/mol, fructose is -2,826.7 kJ/mol, glucose is -2,815.8 kJ/mol, urea is -632.2kJ/mol and glycine is -528 kJ/mol.

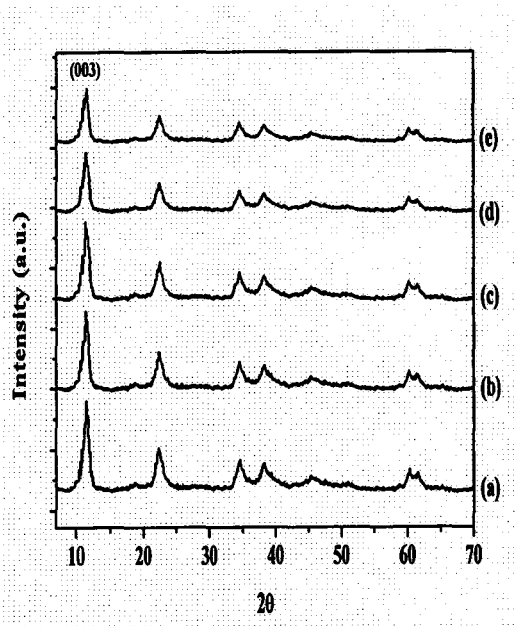

Figure 1. XRD pattern of LDHs with fuel type varied at 650° C: (a) saccharose, (b) fructose, (c) glucose, (d) urea and (e) glycine.

Table 1 shows the elemental composition of the sampl synthesized using the five different type of fuels. The Mg/ ratio for sample fueled by saccharose, fructose, glucose, ur and glycine as shown in the table was 2.90, 2.80, 2.79, 2.(and 2.64, respectively. The highest Mg/Al ratio by saccharo was possibly due to the higher content of C and H in order complete the combustion or calcination. This is consistent wi the XRD results discussed earlier. The order of the Mg and content may also be influenced by the partial hydrolysis a condensation during contact with the carbonate solution a later syneresis on drying [7].

TABLE I
CHEMICAL COMPOSITION OF LDHS SAMPLES WITH FUELVARIED FROM EDX ANALYSIS

LDHs by Fuel	Chemical Composition, %wt				
	Mg	Al	O	C	Na
Saccharose	28.83	9.94	51.19	5.02	5.02
Fructose	27.69	9.89	52.80	4.81	4.81
Glucose	27.45	9.84	53.19	4.76	4.76
Urea	26.05	9.73	55.18	4.52	4.52
Glycine	25.65	9.70	55.75	4.45	4.45

Figure 2 compares the FTIR spectra of samples synthesiz by the 5 different fuels. No significant differences w observed from the spectra. The band as observed in the 16 1655 cm^{-1} region was due to the H_2O from the interla water. The peak appeared weaker for sample that was trea at high temperature, indicating that water molecule still exis in the interstices of the mixed oxide sample in order to h the LDHs structure. The 1385 cm^{-1} peak corresponded to stretching vibrations of carbonate anions. The peaks at 10

1020 and 854-874 cm^{-1} corresponded to covalent carbonate [8]. Bands at around 598-630 cm^{-1} corresponded to the characteristic vibration of the metal oxides (Mg-O and Al-O) [1], [8].

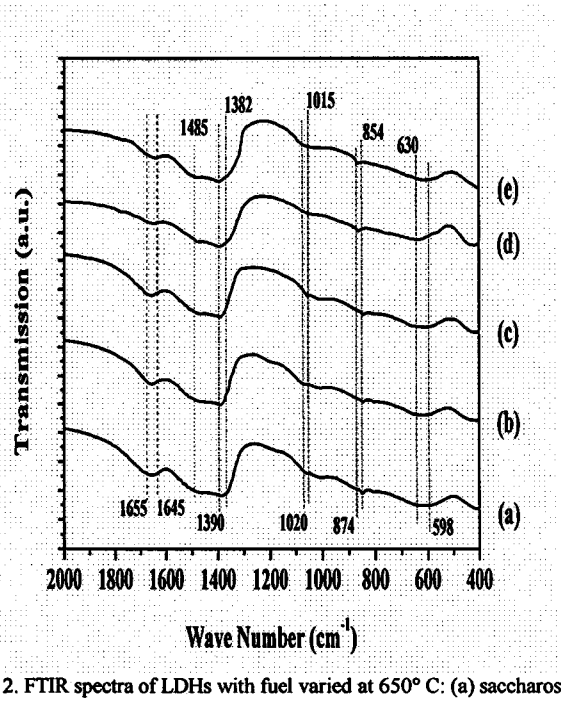

Figure 2. FTIR spectra of LDHs with fuel varied at 650° C: (a) saccharose, (b) fructose, (c) glucose, (d) urea and (e) glycine.

Figure 3 shows XRD pattern of samples before and after contact with carbonate solution. The samples were fueled by fructose. Figure 3 (a) shows combusted product at 450 °C without making contact with carbonate solution that appeared broad and the least crystalline. Figure 3 (b-d) shows combusted products at 450, 650 and 850 °C, respectively followed by contact with carbonate solution. The samples exhibited sharper peaks and more crystalline in nature. The presence of magnesium oxide is shown by the X-ray diffraction peaks at 42.5 and 63 degrees (2θ) [1] for sample thermally treated at 850 °C. The other peaks corresponded to LDHs were 11.6, 23.1, 34.8, 39, 46.5, 60.5, and 61.4 based on the JCPDS file.

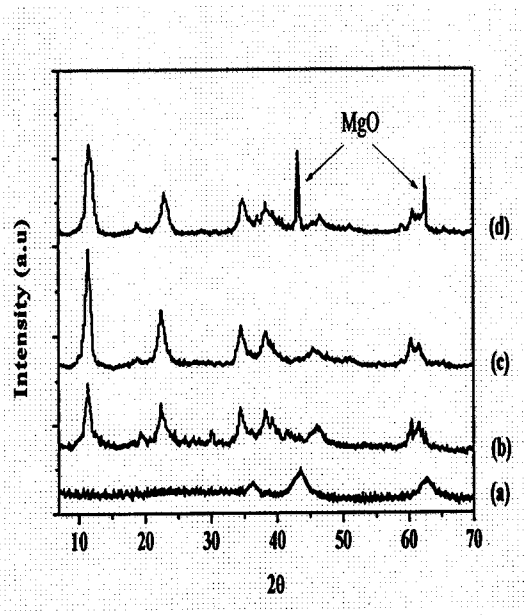

Figure 3. XRD pattern of (a) mixed oxide of LDHs at 450° C, (b) LDHs 450° C (c)LDHs at 650° C and (d) LDHs at 850° C using fructose as fuel.

Samples thermally treated at 650 °C was the mo crystalline (based on the highest intensity counts) becaus aluminum was progressively incorporated into the Mg network. As temperature was increased, more aluminum wa included. In contrast, at low synthesis temperature, aluminu diffused slowly and did not reach the crystallite core [1].

Figure 4 shows SEM images taken at 5.00 K magnification for sample directly obtained after combustion 650 °C and after it was reacted with the carbonate solutio The sample after making contact with Na_2CO_3 solution sho more homogeneous microstructure possibly due agglomeration of particles and reduction of metal oxi elements during the contact.

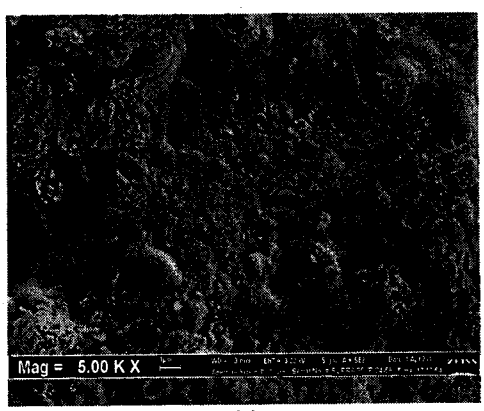

(a)

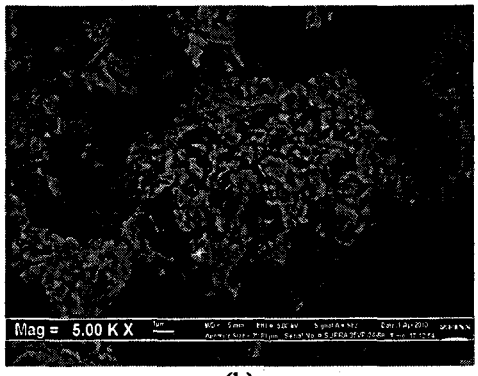

(b)

Figure 4. SEM images of combusted product heated at 650°C using fructose as fuel (a) before contacting carbonate solution, (b) after contacting carbonate solution.

IV. CONCLUSION

Mg/Al LDHs were prepared successfully by combustion procedure using all the five different fuel types tested in the experiment. Products directly obtained from combustion exhibited the attribute of hydrotalcites, but lamella was established only after the combusted product made contact with carbonate solution. The crystallinity of LDHs increased as the combustion temperature was increased. The crystallinity level was in the order of saccharose > fructose = glucose > urea > glycine

ACKNOWLEDGMENT

The authors gratefully acknowledge the Universiti Sains Malaysia for providing research grants for this project.

REFERENCES

[1] V. Dávila, E. Lima, S. Bulbulian and P. Bosch,"Mixed Mg(Al)O oxides synthesized by the combustion method and their recrystallization to hydrotalcites," *Micro. Meso. Mater.*, vol. 107, pp. 240-246, 2008.

[2] S. J. Palmer, L. R. Frost and T. Nguyen, "Thermal decomposition of hydrotalcite with molybdate and vanadate anions in the interlayer," *J. Thermal Analysis and Calorimetry*, vol. 92, No. 3, pp. 879-886, 2008.

[3] M. R. Othman, Z. Helwani, Martunus and W. J. N. Fernando,"Synthetic hydrotalcites from different routes and their application as catalysts and gas adsorbents: a review," *App. Organometallic Chem.*, vol. 23, no. 9, pp. 235-246, 2009.

[4] F. Cavani, F. Trifirò and F. Vaccari, "Hydrotalcite-type anionic clays: preparation, properties and applications", *Catal. Today*, vol. 11, pp. 173-301, 1991.

[5] M. R. Othman, N. M. Rasid and W. J. N. Fernando," Effects of thermal treatment on the micro-structures of co-precipitated and sol-gel synthesized (mg-Al) hydrotalcites," *Micro. Meso. Mater.*, Vol. 93, pp. 23-28, 2006.

[6] J. He, M. Wei, B. Li, Y. Kang, D. G. Evans and X. Duan,"Preparation of layered double hydroxides," *Struc. Bond.* Vol. 119, pp. 89-11, 2006.

[7] T.S. Stanimirova, G. Kirov and E. Donolova," Mechanism of hydrotalcite regeneration," *J. Mater. Sci. Lett.* Vol. 20, pp. 453-455, 2001.

[8] M. R. Othman, N. M. Rasid and W. J. N. Fernando," Mg-Al hydrotalcite coating on zeolites for improved carbon dioxide adsorption," *Chem. Eng. Sci.*, Vol. 61, pp. 1555-1560, 2006.

Martunus, received his BSc. from Diponegoro University, Ace Indonesia in 1996. In 2000 he received his master in Chemic Engineering from Gadjah Mada University (UGM), Indonesia.

Z. Helwani received her BSc. from Syiah Kuala University, Ace Indonesia in 1994. In 1999 she received her master in Chemic Engineering from Institute Technology of Bandung (ITB), Indones Zuchra is currently a PhD student at University Sains Malaysia (USM Malaysia.

A.D. Wiheeb received his BSc. and MSc. in Chemical Engineering fr University of Baghdad, Iraq in 1999 and 2002, respectively. He currently a PhD student at USM.

M.R. Othman received his BSc. and MSc. in Petroleum Engineeri from the Missouri University of Science and Technology, USA in 19 and 1997, respectively. In 2002, he received his Doctorate in Chemic Engineering from the Universiti Sains Malaysia (USM).

WETTING AND SPREADING OF LIQUID DROPLETS ON SOLID SUBSTRATES

[1,2]Z. Helwani, [1]N. Aziz, [3]J. Kim, [*,1]M.R. Othman

[1]School of Chemical Engineering, Universiti Sains Malaysia
14300 Nibong Tebal, Penang, Malaysia.
[2]Department of Chemical Engineering, Riau University
Pekanbaru 28293, Indonesia.
[3]Department of Chemical Engineering and Green Energy Center, Kyung Hee University, Seocheon-dong Giheung-gu, Yongin, Gyeonggi-do 446-701, Korea

*Email: chroslee@eng.usm.my
Tel: (60)-45996426
Fax: (60)-45941013

ABSTRACT

Wetting phenomena plays a crucial role in a wide range of technological applications. Spreading of liquids on solids involving phase change is encountered in many areas ranging from biological systems to industrial applications such as coatings, printing, painting and spraying. The fundamental study on wetting of membrane precursors namely hydrotalcite sols on a solid surface with different types of precursor material was successfully carried out. Relationship between the contact angle and the Marangoni effect was also investigated.

The presence of PVA in hydrotalcite sols was found to influence the rheological properties of the sols significantly. The degree of hydrotalcite's philicity on a solid surface was improved by the addition of PVA and presence of silica layer. The spreading of the liquid droplet on the solid surface was controlled by a surface tension gradient, due to Marangoni effect. Marangoni Number was found to be proportionally related to the surface tension of the sols but inversely proportional to the contact angles. Marangoni forces that decreased the contact angle, promoted spreading of hydrotalcite droplets.

Keywords: *contact angle, hydrotalcite, marangoni effect, wetting, spreading*

Introduction

Inorganic membranes have been extensively studied for decades and used in many applications due to their stability at high-temperature and high-pressure. They exhibit good chemical stability, high-mechanical resistance, long life, good defouling properties, high surface area and porosity to enable high flux.

Sol-gel method is considered to be one of the most practical methods for fabrication of porous ceramic membranes. Membrane synthesis by sol-gel method enables production of uniform pore size, high purity membranes at ambient conditions. Successful development of a uniform film requires that a liquid precursor be wetted and spread effectively on a solid substrate. Poor precursor spreading on the substrate surface usually results in defective films that suffer peelings of flakes, delamination, craters and pinholes. In many cases, surfactants are used to reduce defects and enhance the spreading since they are known to have the ability to reduce the surface tension of a particular liquid and induce a surface tension gradient. In the previous work to prepare inorganic membranes, polyvinyl alcohol (PVA), polyvinyl butyral (PVB) or polymethyl metacrylate (PMMA) were used as surfactants to

enhance spreading of the liquid membrane precursor in order to successfully produce a thin film on a porous alumina substrate [1-3]. Although surfactants could help in reducing cracks, they could also render the membrane to curl and warp as the membrane dries and ages possibly due to the phobicity of the precursor material and other unidentified causes. The phenomena of membrane warping was observed in mesoporous Al_2O_3 and Pd- Al_2O_3 asymmetric composites during preparation of pd-alumina membrane [4].

The phenomena of spreading and warping in membrane preparation could be governed by the Marangoni effect [5]. The Marangoni effect (sometimes also called the Gibbs-Marangoni effect) is the mass transfer on, or in, a liquid layer due to surface tension differences. The spreading is controlled by a surface tension gradient, which forms when a drop of surfactant solution is placed on a solid surface. The proposed model suggests that, as the spreading front stretches, the surface tension increases (concentration of surfactant becomes lower) at the front relative to the top of droplet, thereby establishing a dynamic surface tension gradient. The driving force for spreading is due to Marangoni effect; the higher the gradient, the faster the spreading. Few reports addressed the Marangoni effect of trisiloxane ethoxylates on polystyrene surface [6] inorder to increase wettability of herbicide on leaf surfaces and spreading behaviour of a volatile drop on a hot surface [7,8].

The phenomena of spreading governed by Marangoni effect are not well understood. The presence of Marangoni effect in membrane synthesis and development has not been reported so far, nor the explanation of the phenomena of wetting of sol precursors on a porous solid substrate. Therefore, in this paper the fundamental study on a liquid spreading of a liquid precursor droplet with different sizes and different types of precursor material is performed. This is to be able to describe the phenomena of spreading of a sol precursor droplet and warping of membrane.

Materials and method

Aluminum secondary butoxide (alkoxide) and ethanol were added and stirred with hot deionized water and heated at 90 °C for 1 h. The mole ratio of the alkoxide with water used was Al^{3+}: H_2O, 1:100 following the documented work in [3]. The solution with hydrotalcite 2 wt.% from the total sol volume was blended vigorously. The solution was stirred at 90 °C for 30 min. Hydrochloric acid at mole ratio of the acid to the alkoxide of 0.07:1 was added and the solution was stirred for about 30 min. The mixture was subsequently heated at 90 °C for about 16 h under reflux conditions to form sol. The sol was dried in fume cupboard overnight to form dried gel. 10 ml of the sol was poured into petri dish and was dried at ambient temperature for 48 hours. The sol dried up and formed dried gel. The dried gel was calcined in programmable carbolite furnace for 24 hours. The same procedures were repeated for the next samples but this time, with addition of PVA solution to prepare hydrotalcite sol with PVA binder. The obtained sols were designated as $HT_{sg\text{-}PVA}$ and HT_{sg} to represent Mg-Al hydrotalcite prepared by sol-gel technique in the presence of PVA and absence of PVA, respectively. Silica was used as membrane support in this work. 8.4 ml of tetraethyl orthosilicate, $Si(OC_2H_5)4$ and 75.7 ml of ethanol were added into 18 ml of deionized water and 97.9 ml of ammonia solution. The sol mixture was stirred rigorously for 2 to 4 hours until precipitates formed. The precipitates were washed with ethanol and dried at 100°C for 24 hours. An impermeable substrate was dipped into the silica sol for about 10 seconds for both surfaces. The coated support was dried at ambient temperature until the dried membrane layer was obtained. Then the dried coated silica membrane was calcined at 500°C.

The addition of PVA was to promote better spreading of liquid membrane precursor and reduce cracks formation on a thin film. However, high viscosity of the sol as a result of excessive PVA addition can enhance the risk of cracks and lower adhesion of coating due to formation of aggregates at higher viscosity, which led to the formation of easily detachable particles on the surface. Therefore, it was proposed that for dip coating technique, the sol must not exceed the value of viscosity at approximately 50cP to prevent the absence of fluidity [9].The viscosity reading was taken at 30°C and

spindle speed of 150rpm with shear rate of 183.45s^{-1}using Brookfield rheometer. The viscosity of HT_{sg} sol was 30.292cP and $HT_{sg\text{-}PVA}$ was 47.88cP.

Results and discussion

Wetting is the ability of a sol or liquid to maintain contact with a solid surface, resulting from intermolecular interactions when the two are brought together. The degree of wetting is determined by a force balance between adhesive and cohesive forces. It is important in the bonding or adherence of two materials. Adhesive forces between a liquid and solid cause a liquid drop to spread across the surface whereas, cohesive forces within the liquid cause the drop to ball up and avoid contact with the surface.The contact angle, θ, is an important parameter to quantify the wettability of solid surfaces. It is defined as the angle made by the intersection of the liquid/solid interface and the liquid/air interface. It can be alternately described as the angle between solid sample's surface and the tangent of the droplet's ovate shape at the edge of the droplet. A high contact angle indicates a low solid surface energy or chemical affinity. This is also referred to as a low degree of wetting. A low contact angle indicates a high solid surface energy or chemical affinity, which leads to a high or sometimes complete degree of wetting.

Three different liquids/sols namely; HTsg, HTsg-PVA, and water, were dropped onto different hydrotalcite substrates with/out PVA and coated with silica layer. Differences in the contact angles for all sols on the substrates were observed and recorded. All sols were dropped carefully on to the respective substrate and contact angles were measured using an optical contact angle meter at ambient conditions. It was found that hydrophilicity of hydrotalcite pellet was improved after the addition of PVA solution in the substrate. Introduction of acid and PVA was known to not only peptize and strengthen the sol but also reduce the surface tension of the sol, by inducing a surface tension gradient facilitated by what is termed as a *Marangoni* mechanism. Marangoni defines that a sessile drop that has low surface tension tends to move to another drop that has relatively higher surface tension, thereby reducing the contact angle of the latter [10]. In this work, the Marangoni's effect is shown by the reduction of the contact angle of water on the substrate from 10.1° to 1.5° such as shown in Table 1. When highly diluted solution with low viscosity was used to a substrate, a homogeneous, crack-free and continuous films were produced [11]. Reduction in contact angle as a result of diluted sols on a particular substrate is expected to enhance spreading or wettability of the sols on the substrate. The similarity of materials might as well contribute to better spreading and coating as observed in the previous work, in which, multi-step TiO_2 shell deposition was applied on a silica core [12].

In this experiment, it was observed that when sol and substrate shared the same materials (PVA), it results in better ability of the sol to wet the substrate's surface. This is evident from the contact angle measurement made between HT_{sg} sol and $HT_{sg\text{-}PVA}$ on the respective substrates (Table 1). The addition of PVA effectively reduced the contact angle and hence increased the wetting ability.

Table 1. Contact angle of hydrotalcite sol on hydrotalcite pellet

Sols	Contact angle, θ			
	HT substrate without PVA	HT substrate with PVA	Impermeable substrate	Silica coated impermeable substrate
HT_{sg}	6.9	0.1	40.9	0
$HT_{sg\text{-}PVA}$	0.9	0.6	35.4	0
Water	10.1	1.5	59.3	15.2

The effect of silica coating on the wettability of different sols was also investigated in this experiment. An impermeable material was used as the substrate onto which, silica layer was coated. Table 1 shows the measured contact angles. It is found that silica coating improved the wetting ability of all the three sols.

A solid substrate exposed to the environment is almost invariably covered by a layer of fluid material. A drop, placed on a substrate which it wets, spreads out to form a film. A particularly important effect on the spreading kinetics of liquid is due to Marangoni forces induced by surface tension gradients. Marangoni forces drive spreading of liquid droplet on substrate and promote wetting ability of the droplet as discussed earlier. The Marangoni forces can be represented by the Marangoni Number, Ma, calculated using the following equation:

$$M_a = \frac{\Delta\sigma.h}{\mu.D_{AB}} \quad (1)$$

Where :
$\Delta\sigma$ = surface tension of sols (kg.m/m.s^2)
h = height of pellet (m) = 0.002 m
μ = viscosity of sols (kg/m.s)
D_{AB} = diffusivity of sols in substrate (m^2/s)

M_a was found to be proportionally related with the surface tension of the sols on HT substrate such as shown in Table 2. As surface tension of sols was increased, M_a also increased. This is acceptable since Marangoni effect was induced by surface tension gradient. Higher surface tension would result in higher value of M_a.

Table 2. Marangoni Number on HT substrate

Sols	Surface Tension, σ (N/m)		Marangoni Number, M_a	
	HT_{sg}substrate	$HT_{sg\text{-}PVA}$ substrate	HT_{sg} substrate	$HT_{sg\text{-}PVA}$ substrate
HT_{sg}	1521.23	106.22	$5.55x10^{13}$	$3.91x10^{12}$
$HT_{sg\text{-}PVA}$	492.44	954.41	$1.83x10^{13}$	$3.64x10^{13}$
Water	3.88	3.75	$1.18x10^{11}$	$1.14x10^{11}$

Conclusion

Wettability of the sols on the substrate can be enhanced by reducing the contact angle of the sol on a substrate. In this work, it was found that adding an appropriate amount of PVA and the presence of silica layer would enhance wettability of hydrotalcite sols. A complete wetting of hydrotalcite sol was observed on silica-coated hydrotalcite substrates. Spreading of a liquid droplet was controlled by a surface tension gradient, which was formed when a drop of sol was placed on a solid surface or substrate. The presence of surface tension gradient induced the Marangoni effect eventually drove better spreading of the liquid droplet. Better wetting of liquid on a particular substrate was observed with larger surface tension gradient and higher Marangoni Number (M_a).

Acknowledgment

The supports from the Universiti Sains Malaysia Research Fund through FGRS and the Ministry of Science Technology and Innovation of Malaysia are gratefully acknowledged. The help from P.L. Kiew is also appreciated.

References

[1]. Othman, M. R. and Kim, J., *The effect of synthesis method and content of Mg/Al ratio on the adsorption of CO2 by HT*, Journal of Ecotechnology Research,13 (3), 1881-9982, 2007.

[2]. Othman, M.R. and Kim, J., *Simulated adsorption and diffusion of CO_2 gas across a mesoporous material using convective flow materials*, 4th Conference of the Asian Consortium on Computational Material Science, Seoul, Korea, 2007.

[3]. Othman, M. R., Rasid, N. M. and Fernando, W. J. N., *Effect of thermal treatment on the microstructures of co-precipitated and sol-gel synthesized Mg-Al hydrotalcites,* Journal of Mircoporous and Mesoporous Materials, 93, 23-28, 2006.

[4]. Othman, M. R. and Kim, J., *Permeation characteristics of H_2, N_2 and CO_2 in a binary mixture across mesoporous Al_2O_3 and Pd-Al_2O_3 asymmetric composites.*, Journal of Microporous and Mesoporous Material, 112, 403-410, 2008.

[5]. Ganesan, N. and Zebin, W., *Effect of interfacial mobility on rupture of thin stagnant films on a solid surface due to random mechanical pertubations,* Journal of Colloid and Interface Science, 298, 491-496, 2006.

[6]. Nikolov, A. D., Wasan, D. T., Chengara, A., Koczo, K., Policello G. A. and Kolossvary, I., *Superspreading driven by Marangoni effect,* Journal of Colloid and Interface Science, 96, 325-338, 2002.

[7]. Sefiane, K., *The coupling between evaporation and adsorbed surfactant accumulation and its effect on the wetting and spreading behaviour of volatile drops on a hot spot,* Journal of Petroleum Science and Engineering,51, 238-252, 2006.

[8]. Tseng, Y. T, Tseng, F. G., Chen, Y. F. and Chieng, C. C., *Fundamental studies on micro-droplet movement by Marangoni and capillary effect,* Journal of Sensors and Actuators, 114, 292-301, 2004.

[9]. Haas- Santo, K., Fichtner, M. and Schubert, K., *Preparation of microstructure compatible porous supports by sol-gel synthesis for catalyst coatings*, Appl. Cat. A: General, 220, 79-92, 2001.

[10]. Othman, M.R. and Kim, J., *The study of the conversion of intercalated compounds synthesized from a sol-gel procedure*. Journal of Sol-Gel Science and Technology. 47: 274–282, 2008

[11]. Celik, E., Yildiz, A.Y., AkAzem., N.F., Tanoglu, M., Toparli, M., Emrullahoglu, O.F., Ozdemir, I., *Preparation and characterization of Fe_2O_3-TiO_2 thin films on glass substrate for photocatalytic applications*, Materials Science and Engineering B, 129, 193-199, 2006.

[12]. Lee, J.W., Othman, M.R., Eom, Y., Lee, T.G., Kim, W.S., Kim, J., *The effects of sonification and TiO_2 deposition on the micro-characteristics of the thermally treated SiO_2/TiO_2 spherical core–shell particles for photo-catalysis of methyl orange*. Microporous and Mesoporous Materials. 116, 561–568, 2008

Hydrotalcite from Modified Combustion Method

M. R. Othman, Martunus, and W. J. N. Fernando

Abstract—Hydrotalcite-like compounds were successfully synthesized using the modified combustion method from aluminum and magnesium nitrates and potassium carbonate. Glucose was used as fuel. The synthesis temperatures were systematically varied. The resulting hydrotalcites were calcined until lattice destruction and recrystallization in the presence of a carbonate aqueous solution was achieved. The structural modifications were evaluated using X-ray diffraction, SEM, EDX and FTIR.

Keywords: hydrotalcite, combustion modified, Mg , Al, K_2CO_3

I. Introduction

HYDROTALCITE (HT) is a natural occurring anionic clay. The most common formula Hydrotalcite-like compounds or layered double hydroxides is $[(M^{2+}_{(1-x)}M^{3+}_{x}(OH)_2)^{x+}.(A^{n-}_{x/n}\ nH_2O)^{x-}]$ where M^{2+} is a di-valent cation (Mg^{+}, Ca^{2+}, Zn^{2+}, Cu^{2+}, Co^{2+}, Ni^{2+} or Mn^{2+}), M^{3+} is a three-valent cation (Al^{3+}, Fe^{3+} or Cr^{3+}). The layer are positively charged as M^{3+} cations substitute M^{2+} cations. This charge is balanced by A anions with charge n-, for instance OH^{-}, Cl^{-}, NO_3^{-}, CO_3^{2-} or SO_4^{2-}, among others and x is normally between 0.17 and 0.33. Carbonates (CO_3^{2-}) are generally the preferred anion [1-2] and they have been widely described in the literature [2-3]. Hydrotalcite-like compounds are used as adsorbents, catalysts, anion exchangers, hosts of electro-active and flame retardant in polymers [4].

The layered double hydroxides that occur naturally are scarcely found. They are usually synthesized. Two common methods of synthesis are: co-precipitation and sol-gel. Other methods such as decomposition-recrystallization, urea method and microwave irradiation may also be used but the are time consuming and require high amounts of water [5 [6].

A relatively new method to produce HT in shorter perio of time is through combustion. This method is based on th explosive decomposition of some organic fuels such as ure or glycine among others, initiated with heat [4]. In this wor HT from combustion method with modification from th previous method [4] was successfully synthesized an characterized using XRD, SEM, EDX and FTIR.

II. Materials and Method

II.1. Modified Combustion Method

To prepare the Mg-Al-O mixed oxides; the precursors layered double hydroxides; a solid mixture was prepare from magnesium nitrate hexahydrate, aluminum nitra nonahydrate and potassium carbonate. The amount of Al an Mg nitrates was maintained constant (Mg/Al ratio of 3) an the amount of potassium carbonate of 8 g (20% g/g mixture) was used. 4 g of glucose (as fuel) was added an the mixture was heated at 80°C and stirred for 5 minutes. ml of hot water at 90°C was added, until the mixture forme a solution at 80°C for 10 minutes under continuous stirrin Two drops of 4% wt Poly-Vinyl Alcohol (PVA) were adde until water evaporated for 10-15 minutes. The resulti paste was transferred into a crucible before calcination to place in a furnace at 450-850° C. The combustion proce was over in 5 min producing mainly a mixture of oxides.

The mixed oxides were placed in contact with 50 ml 1 of K_2CO_3 solution at room temperature. The obtain products were stirred for 5 min and the solid was separat by filtration, washed with deionized water and dried at 12 C for 20 minutes for recrystallization.

II.2. Characterization

The crystallization phases were studied using XRD. T analysis was carried out using Philips Goniometer PW 18 diffractometer, PW 1710 diffraction controller and X-r generator PW 1729. The diffractometer was used wi monochromatized CuK_α radiation and taken in the range 10-70° (2θ). The X-ray tube was operated at 40 kV and 1 mA.

The surface morphology of the hydrotalcite powder w analyzed by SEM from Germany, model Leo Supra 50 Field Emission. Samples were placed in the sample grid electron reflection and vacuumed (5 min) before analys

This work was supported by Research University Grant, Universiti Sains Malaysia (No. 814046).

M. R. Othman is with the School of Chemical Engineering, Universiti Sains Malaysia, 14300 Nibong Tebal, Penang, Malaysia (corresponding author to provide phone: (60)-459964261; fax: (60)-45941013; e-mail: chroslee@ eng.usm.my).

Martunus is with the School of Chemical Engineering, Universiti Sains Malaysia, 14300 Nibong Tebal, Penang, Malaysia and Department of Chemical Engineering, Riau University, Pekanbaru 28293, Indonesia (e-mail: martunusche@yahoo.co.id).

was used in the present work. EDX was used to determine elemental composition of hydrotalcite by analyzing the microscopic image under EDX instrument. The EDX analysis used MnK_{α} as the energy source operated at 15 kV of accelerating voltage, 155 eV resolution 22.4° takeoff angle.

An infrared (IR) spectrum of hydrotalcites was obtained using FTIR spectrophotometer (Perkin Elmer FTIR 2000, USA). Samples were prepared by mixing the powdered solids with potassium bromide, KBr (the blank) in a 15:85 ratio to get transparent pellet auto supported on the different solids at 8 ton pressure. The infrared spectra were recorded both over the wave number range from 400 to 4000 cm^{-1}.

III. Results

'Figure 1' shows XRD pattern of a mixed oxide of hydrotalcite at 450° C (a) and the XRD patterns of hydrotalcite at 450 to 850 ° C (b) to (d). The samples of a mixed oxide of hydrotalcite and the hydrotalcite at the highest temperature (d) contains amount of magnesium oxide shown by the X-ray diffraction peaks at 42 and 62.5 degrees (2θ) [4]. All other peaks correspond to hydrotalcite =11.4, 22.9, 34.6, 38.9, 45.9, 60.2, and 61.7, the result is in good agreement with that reported previously [3].

Hydrotalcite at 650° C was more crystalline than the others because aluminum was progressively incorporated into the MgO network. As temperature was increased, more aluminum was included. In contrast, at low synthesis temperature, aluminum diffused slowly and did not reach the crystallite core [4].

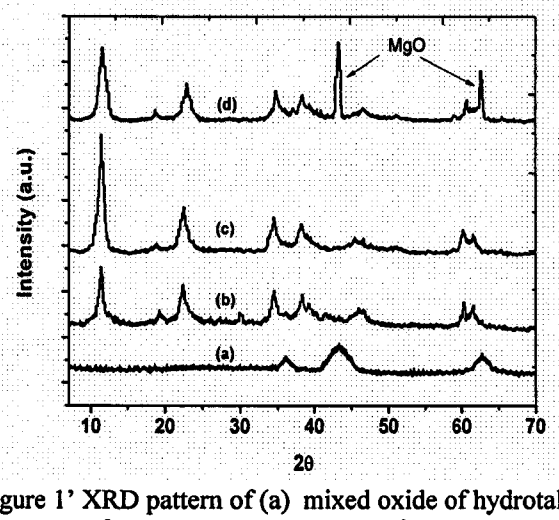

'Figure 1' XRD pattern of (a) mixed oxide of hydrotalcite at 450°C, (b) hydrotalcite at 450 °C (c) hydrotalcite at 650°C and (d) hydrotalcite at 850 °C.

'Figure 2' shows SEM images taken at 500 magnification for mixed oxide hydrotalcite and hydrotalcite samples at 650° C. 'Figure 2b' shows more closely packed microstructure than 'Figure 2a'. Hydrotalcite sample after recrystlalization shown in 'Figure 2b' became more compact due to particles that reduced oxide elements and agglomerated after contact with K_2CO_3 solution and

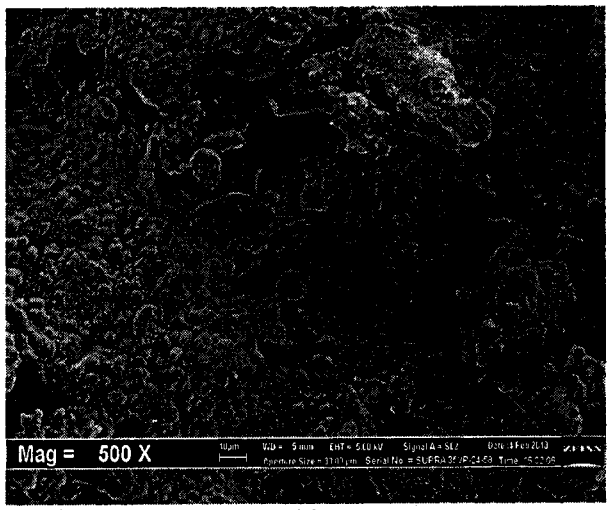

(a)

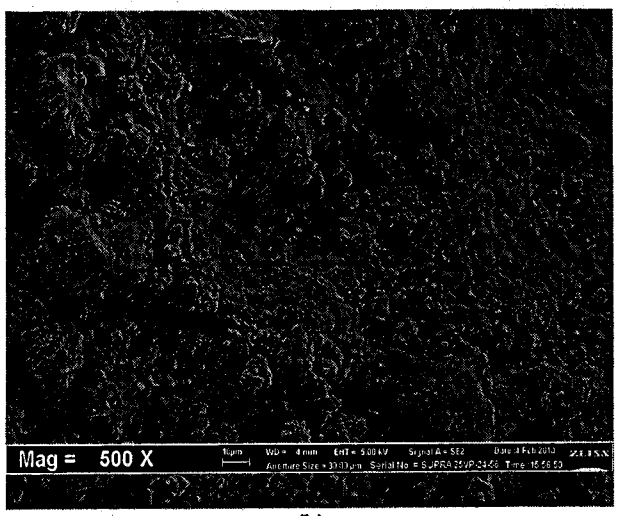

(b)

'Figure 2' SEM images of (a) mixed oxide of hydrotalcite (b) hydrotalcite at 650° C.

'Figure 3' shows the typical EDX analysis of hydrotalcit at 650° C. The EDX shows that the 32 g hydotalcite sampl was constituted of Mg (27.32%), Al (9.52%), C (5.85%), (51.46%) and K (5.85%).

The EDX shows that the sample contained Mg/Al at rati of 2.87 and K_2CO_3/mixture at 5.85%. The high oxyge content in the sample was probably attributed to th presence of magnesium nitrate hexahydrate, aluminu nitrate nonahydrate and potassium carbonate.

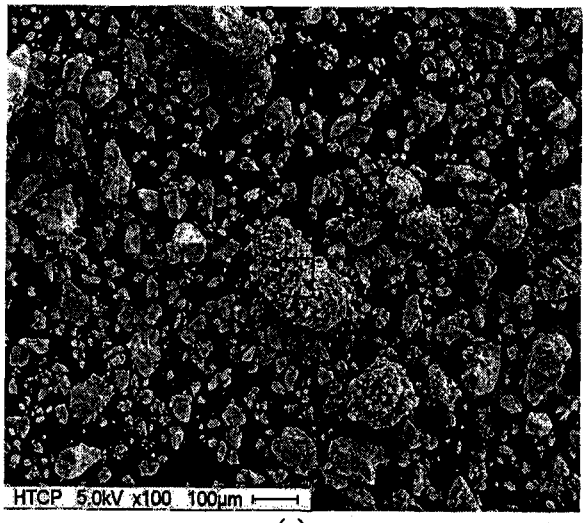

(a)

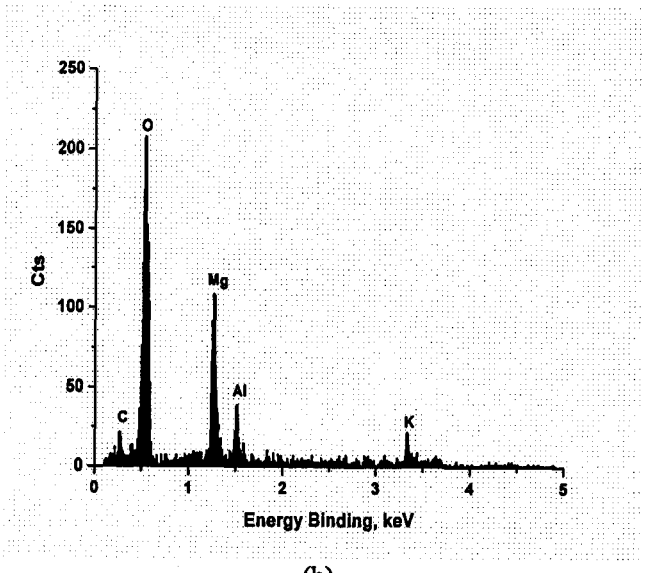

(b)

'Figure 3'(a) SEM of the hydrotalcite at 650° C sample at 100x magnification; (b) EDX analysis to the area: box

The FTIR spectra of mixed oxide hidrotalcite and the hydrotalcite samples is shown in 'Figure 4'. The first band at 3450-3485 cm^{-1} corresponds to the OH mode, caused by the interlayer water molecules and hydroxyls groups in the brucite-like layers [6]. The weak band as observed in the 1640-1660 cm^{-1} region was due to the H_2O from the interlayer water. The 1375-1387 cm^{-1} peak corresponds to stretching vibrations of carbonate anions. The peaks at 1015-1020 and 877-867 cm^{-1} correspond to covalent carbonate. Bands at around 575-630 cm^{-1} corresponds to the characteristic vibration of the metal oxides (Mg-O and Al-O) [4].

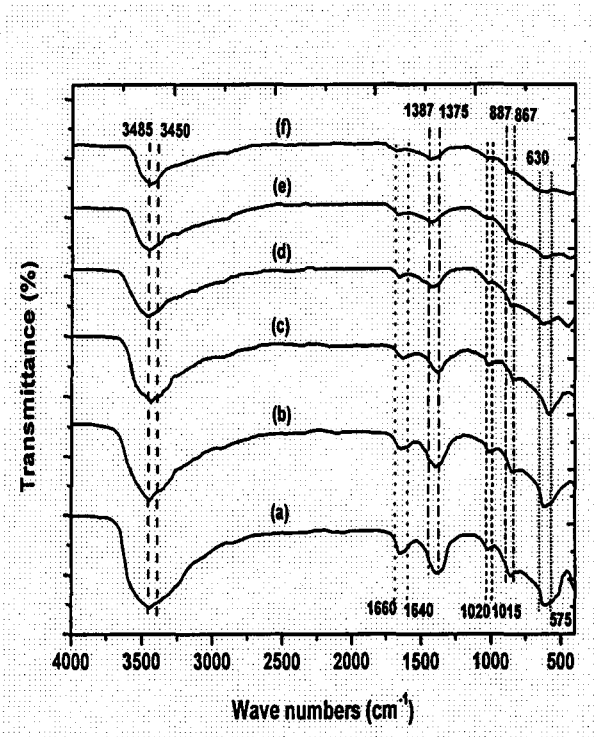

'Figure 4' FTIR spectra of (a-c) hydrotalcite: (a) at 450° C (b) at 650° C, (c) at 850° C and (d-f) mixed oxide of hydrotalcite: (d) at 450° C, (e) at 650° C, (f) at 850° C.

ACKNOWLEDGEMENT

The authors acknowledge the support from Research University of Universiti Sains Malaysia Fund.

REFERENCES

[1] S. J. Palmer, L. R. Frost and T. Nguyen, "Thermal decomposition of hydrotalcite with molybdate and vanadate anions in the interlayer" *J. Thermal Analysis and Calorimetry* , Vol. 92, No. 3, pp. 879-88 2008.

[2] M. R. Othman, Z. Helwani, Martunus and W. J. N Fernando,"Synthetic hydrotalcites from different routes and the application as catalysts and gas adsorbents: a review", *Ap Organometallic Chem.* Available: http://www.interscience.com (DO 10.1002/aoc.1517)

[3] F. Cavani, F. Trifirò and F. Vaccari, "Hydrotalcite-type anionic clay preparation, properties and applications", *Catal. Today*, Vo. 11, p 173-301, 1991.

[4] V. Dávila, E. Lima, S. Bulbulian and P. Bosch,"Mixed Mg(Al)O oxides synthesized by the combustion method and their recrystallization to hydrotalcites", *Micro. Meso. Mater.*, Vol. 107, p 240-246, 2008.

[5] J. He, M. Wei, B. Li, Y. Kang, D. G. Evans and X Duan,"Preparation of layered double hydroxides", *Struc. Bond.* Vo 119, pp. 89-11, 2006.

[6] M. R. Othman, N. M. Rasid and W. J. N. Fernando," Effects thermal treatment on the micro-structures of co-precipitated and so gel synthesized (mg-Al) hydrotalcites", Micro. Meso. Mater., Vol. 9 pp. 23-28, 2006.

Production of Layered Hydrotalcite Using Tapai as Fuel

MR Othman[1,a], MR Anuar[1,b] and WJN Fernando[1,c]

[1]School of Chemical Engineering, Universiti Sains Malaysia, 14300 Nibong Tebal, Penang, Malaysia.

[a]chroslee@eng.usm.my, [b]sotong_keras@yahoo.com.my, [c]chnoel@eng.usm.my

Keywords: Hydrotalcite, combustion method, LDH, catalyst, adsorbent, tapai, urea

Abstract. Lamellar hydrotalcite (HT) was synthesized in the laboratory following combustion method. Tapai fueled HT was found to exhibit more orderly packed microstructure and was more crystalline in nature than its urea fueled counterpart, particularly at higher combustion temperature. The pore structure of tapai fueled HT resembled that of bottle neck with possibility of tapered with open-end that might also be present. The crystal size of tapai fueled HT was larger than urea fueled HT but greater size reduction was experienced by the former material, suggesting that more energy might have been supplied to the sample to disintegrate the particles, since tapai has higher and cleaner carbohydrate source than urea.

Introduction

Hydrotalcite (HT) has been used largely in applications such as neutralizers (antacids), anion exchangers, polymer stabilizers, anion scavengers, catalysts and catalyst supports, adsorbents, filtration, electroactive, photoactive materials and pharmaceutics [1].

HT can be synthesized or found naturally. Natural HT mostly occurs as anionic clay. But, intercalated HT consisting of layered double hydroxide is the one that attracts numerous researches [1] due to its ability to shuffle and exchange anions. The most common formula to denote layered double hydroxides is $[(M^{2+}_{(1-x)}M^{3+}_{x}(OH)_2)^{x+}.(A^{n-}_{x/n}\ nH_2O)^{x-}]$ where M^{2+} is a di-valent cation (Mg^{+}, Ca^{2+}, Zn^{2+}, Cu^{2+}, Co^{2+}, Ni^{2+} or Mn^{2+}), M^{3+} is a three-valent cation (Al^{3+}, Fe^{3+} or Cr^{3+}). The layers can be positively charged such as M^{3+} cations or substituted with M^{2+} cations. Sandwiched within these positive charges are A anions with charge n- such as OH^{-}, Cl^{-}, NO_3^{-}, CO_3^{2-} or SO_4^{2-}. Carbonates (CO_3^{2-}) are generally the preferred anion [1-3] and HT containing this anion has been described in the literature for potential use as adsorbents, catalysts, anion exchangers, hosts of electro-active and flame retardant in polymers [4-7].

The layered double HT compounds that occur naturally are scarcely found. They are usually synthesized in the laboratory or artificially massed produced. Two common methods of synthesis are: co-precipitation and sol-gel. Other methods such as decomposition-recrystallization, urea method, microwave irradiation and solvothermal [8] may also be employed. In this work, we propose preparation of the compounds via combustion method using organic fuels. This method has reportedly saved energy and time [1], since the combustion synthesis is very rapid. The method is based on the explosive decomposition of precursor materials, initiated and promoted by continuous heat energy supplied by an organic fuel. One of the advantages using combustion technique is that it requires no solvents and therefore, no production of wash water. The technique also involves much shorter time for crystallization (within minutes) into HT, vis-à-vis the conventional co-precipitation and sol gel techniques that normally require long crystallization time (several hours, days or weeks).

In this study, tapai was selected as the organic fuel to facilitate the combustion. Tapai, which is

comparison because its application was widely documented [1]. These fuels serve as a source of C and H in order to form complexes with the metal ions in the precursor.

Method

Mg–Al–O mixed oxides were first prepared using solid mixture of magnesium nitrate, aluminum nitrate and sodium carbonate. The amount of Al and Mg nitrates was maintained constant (Mg/Al ratio of 3) and the amount of sodium carbonate was fixed at 0.20 g per gram of mixture. 200 mg of fuels were added and the mixture was suspended in water. The suspension was stirred rigorously while heated at the temperature ranging from 70 to 80 °C until most water evaporated. The resulting paste was heated at 450, 650 and 850°C, respectively. The combustion was over within 5 min producing mainly mixture of oxides. The mixed oxides was contacted with 60 ml of 1N Na_2CO_3 solution at room temperature and the solid was later separated by centrifugation. The solid was washed with de-ionized water to remove impurities and later dried. Sample heated at 450°C using tapai and urea as fuel was designated as HT-tapai-450 and HT-urea-450, respectively.

Result and discussion

The samples emerging from the combustion before treating with carbonate solution consisted of Mg(Al)O mixed oxides with a periclase-like structure with broad asymmetric peaks (not shown) indicating that the materials were in disordered state. Figure 1 shows the XRD patterns after these oxides (obtained using urea fuel) were contacted with carbonate solution. With the exception of heated sample at 650°C which was mostly brucite, the other two samples demonstrate the attribute of HT.

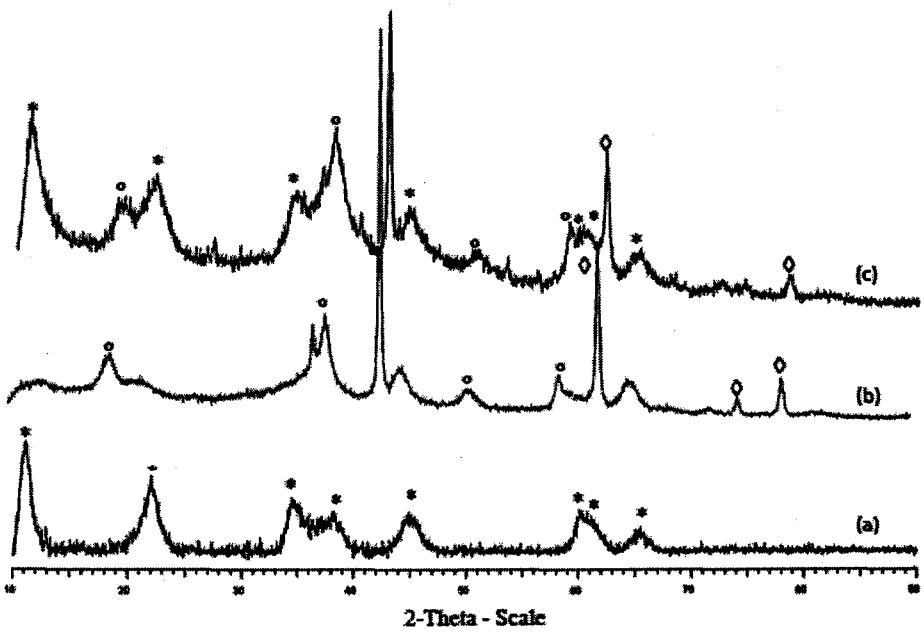

Figure 1. XRD pattern for (a) HT-urea-450 (b) HT-urea-650 (c) HT-urea-850 (*) hydrotalcite, (°) brucite, (◊) periclase

Figure 2 shows the XRD patterns of samples obtained using tapai fuel during the combustion. The samples were contacted with carbonate solution. The XRD spectra at higher combustion temperature demonstrate more ordered state and better defined than those of HT obtained using urea fuel. The urea-fueled HT suffered agglomeration of micro-particles in less orderly manner, while the

Figure 2 display the attribute of a layered material described by the highly distinguished peak at 2θ of less than 20° [7].

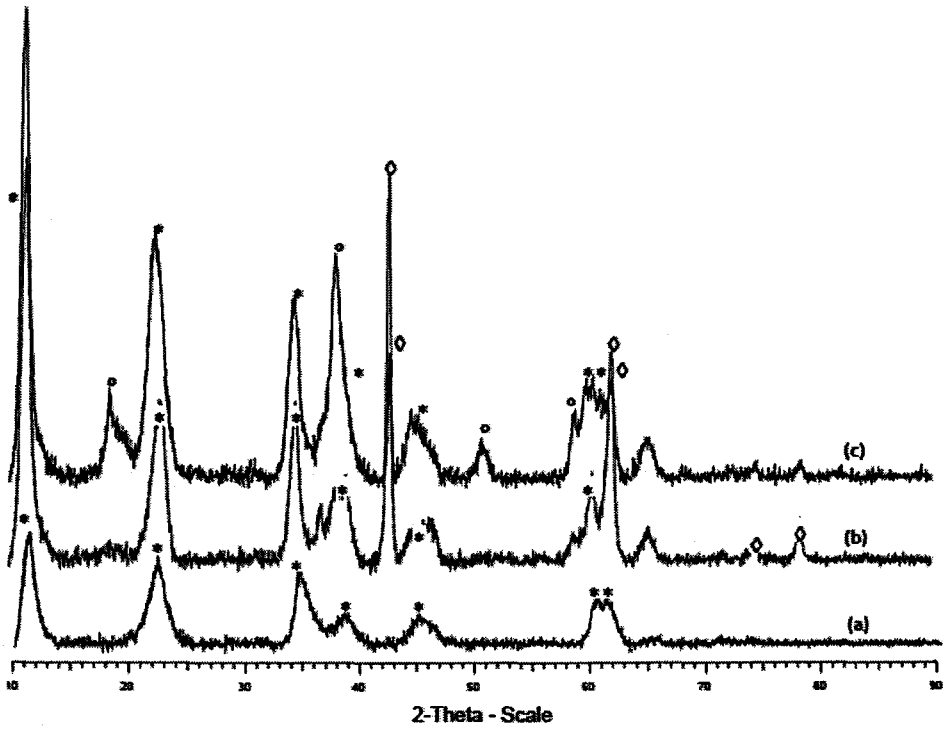

Figure 2. XRD pattern for (a) HT-tapai-450 (b) HT-tapai-650 (c) HT-tapai-850 (*) hydrotalcite, (°) brucite, (◊) periclase

All the 6 samples (using urea and tapai fuel) demonstrate almost similar hysteresis loop of Type E (Figure 3), indicating that the majority of pores resemble 'bottle neck' structure. The presence of tapered or wedge shaped pore with open-end may also be interpreted to intermix with the bottle neck structure. The particle size of the HT crystal using urea and tapai fuel was reduced at higher temperature from 55Å (450°C) to 50Å (850°C) and 90Å (450°C) to 75Å (850°C), respectively. Greater size reduction was experienced by HT from tapai fuel, suggesting that more energy might have been supplied to the sample to disintegrate the particles, since tapai has higher and cleaner carbohydrate source than urea. Tapai contained higher energy than urea to fuel the combustion. Tapai is derived from glucose ($C_6H_{12}O_6$) and fructose ($C_6H_{12}O_6$) with molecular formula of $C_{12}H_{22}O_{11}$. Urea, on the other hand, has molecular formula of $(NH_2)_2CO$.

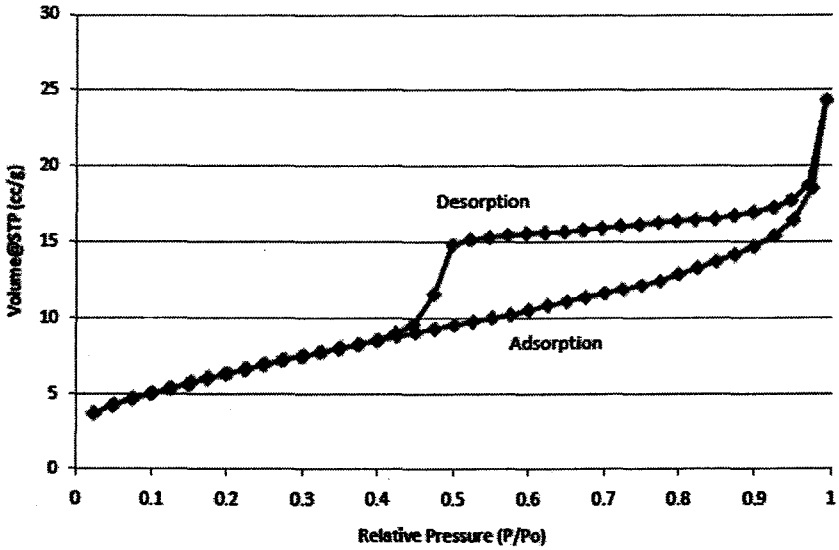

Figure 3. Hysteresis pattern of synthetic HT

Summary

HT with intercalated structure was successfully synthesized following combustion method using tapai as its organic fuel. Tapai fueled HT exhibited greater average crystal size than urea fueled HT at all the combustion temperatures tested in the experiment. Although greater in size, tapai fueled HT was more crystalline in nature, especially when higher combustion temperature was used.

References

[1] M.R. Othman, Z. Helwani, Martunus and W. J. N. Fernando. Appl Organometal. Chem. 23 (2009) 335.
[2] M.R. Othman, M.N. Rasid, W.J.N. Fernando, Chem. Eng. Sci. 61 (2006) 1555.
[3] M.R. Othman, N.M. Rasid, W.J.N. Fernando, Micro. Meso. Mater. 93 (2008) 23.
[4] Z. Helwani, M.R. Othman, N. Aziz, Applied Catalysis A: General 363 (2009) 1.
[5] M.R. Othman, J. Kim, J. Ecotechnol. Res. 13(3) (2007) 160.
[6] T.S. Stanimirova, G. Kirov, E. Donolova, J. Mater. Sci. Lett. 20 (2001) 453.
[7] M.R. Othman and J. Kim. J. Sol-Gel Sci. Techn. 47 (2008) 274.
[8] M.K. Hafiz, M.R. Othman, N. Aziz. AIP Conf. Proc. 1136 (2009) 454

K-Na Impregnated Hydrotalcite: The Effects of Washing on High Temperature CO_2 Adsorption

Martunus[a,b], M.R. Othman[a], W.J.N. Fernando[a]
[a]School of Chemical Engineering, Universiti Sains Malaysia
14300 Nibong Tebal, Penang, Malaysia
[b]Department of Chemical Engineering, Riau University
Pekanbaru 28293, Indonesia

Abstract- **Mg-Al hydrotalcite-like compounds (HT) impregnated with K and Na were synthesized following combustion method using saccharose (sucrose) as fuel. HT prepared from 20 wt% sucrose containing increased Na loading caused the adsorption of CO_2 to increase up to 1.5%, beyond which, the adsorption started to fluctuate. Results from the CO_2 adsorption measurement at 300, 400 and 500 °C reveal that washing of HT samples reduced the adsorption performance rather significantly due to the removal of considerable amount of the metal elements from the sample that were necessary for adsorption.**

I. INTRODUCTION

The removal and recovery of carbon dioxide from hot gas streams is becoming increasingly significant in the field of energy production. The urgency is much felt after realizing the fact that billions tons of CO_2 was released from fossil-fueled power plants in order to generate electricity [1].

Several solid adsorbents have been utilized to remove carbon dioxide by capturing it and then storing it permanently or converting/fixing it into carbonated products. Many adsorbents for CO_2 have been explored [2-10], among the preferred choices include zeolite [3-6] and activated carbon [6-10]. While these materials are excellent for CO_2 adsorption, they may suffer low adsorption capacity at elevated temperatures and are thus limited to operation at lower temperature (<100 °C). For example, ASRT-5A zeolites demonstrated very high CO_2 adsorption equivalent to 15.8% by weight at 25 °C, but subsequently decreased to 1.43% at 250 °C [6]. In addition, zeolites are effective for CO_2 separation from the gas mixtures containing species that are less polar than CO_2 but less effective in the presence of water and SO_2.

For an application operating at high temperature such as removing CO_2 from flue gases of coal fired power plant, the potential CO_2 adsorbents are reportedly metal oxides (e.g. CaO, MgO, etc.), lithium metal oxides (e.g. Li_2ZrO_3, Li_4SiO_4, etc.), hydrotalcites and double salts [2]. Of these materials, HT was proposed due to the stability of the material at elevated temperature and improved adsorption [11] as a result of the acid base interaction between acidic CO_2 and the basic sites of HT.

The CO_2 adsorption capacity of HT can be improved when its structure is modified. For example, when commercially acquired HT was doped with cesium, the adsorption capacity was improved from ca. 0.10 to 0.35-0.44 mol/kg. Incorporation of potassium into its micro-structural network also increased the adsorption capacity of up to 0.76 mol/kg [12]. For these materials, their preparation normally inv washing and drying prior to use.

In this paper, HT prepared from a relatively new appr is introduced and its structure modified by incorpora potassium and sodium in order to improve its adsorp capacity at elevated temperature. The effect of washing on adsorption performance will also be investigated.

II. MATERIAL AND METHOD

A. K-Na impregnated HT

The preparation of HT from combustion method described previously [13] using magnesium nit hexahydrate, aluminum nitrate nonahydrate, potass carbonate solid precursors and sucrose as fuel. impregnation ensued after calcination of the combu product at 650 °C for 4 hrs followed by contact with 112 m a solution containing 31.9 to 33.8 g of potassium carbo and sodium carbonate of 0.19 to 2.8 g to achieve total K Na loading of 20%. After 1 h of contact, the remaining li (<2 ml) was separated by filtration. They were, then, was with de-ionized water or left unwashed prior to being drie 120°C for 12 hrs.

B. CO_2 adsorption measurement

The CO_2 adsorption was measured using Ther Gravimetric Analysis (TGA) by placing 60 mg of HT sar on the sample holder inside the TGA. The temperature increased from room temperature at a rate of 5°C/min in a atmosphere (flow rate of 30 ml/min) to the preset point (300, 400 and 500 °C) at 1.34 bar, and kept at this tempera until the sample weight became constant, typically for 2 min. Upon reaching the desired temperature, the feed switched to mixed N_2/CO_2 (20 ml/min, N_2 of 70%) maintained for 3 hrs. Then the sample was evacuated for switched back to binary mixed gas for 3 hrs, until the sa weight became constant.

III. RESULTS

Table 1 shows that the CO_2 adsorption capacity at 4(increased steadily at increasing sodium loading of up to 1. beyond which, the adsorption became erratic and unusual (not shown). The adsorption was clearly impr

rather substantially when compared with those obtained in the previous literature utilizing potassium and cesium as reinforced metals [12]. The maximum adsorption was 1.029 mmol/g using HT impregnated with 18.5% K and 1.5% Na. The adsorption capacity dropped for washed sample for every percentage of metal loadings tested in the experiment. Nevertheless, the capacity is still higher than those previously reported in the literature.

TABLE I
CO_2 ADSORPTION CAPACITY OF HTI SAMPLES AT 400 ° C AND 1.34 BAR

Sample	K Loading (%)	Na Loading (%)	CO_2 Adsorption Capacity (mmol/g)
Unwashed	20	0	0.822
	19.5	0.5	0.887
	19	1	0.958
	18.5	1.5	1.029
Washed	20	0	0.684
	19.5	0.5	0.738
	19	1	0.825
	18.5	1.5	0.861

The reason for the drop in the adsorption capacity as seen earlier has been identified. It is attributed to the partial removal of the metals contained in the sample after washing such as shown in Table 2 obtained from the EDX data depicted in Figure 1. The loss of the metals due to leachate after washing was in the order of 25.3% by weight. The actual Mg/Al ratio (not shown in the table) for the sample was also reduced from 2.84 and 2.14 from the analysis. This reveals a rather significant finding, considering that washing of HT is a normal procedure that accords as standard in laboratory or industrial setting. While it is necessary to wash in order to obtain clean and pure HT, washing also degrades the adsorption performance. Therefore, washing of HT is not advisable in this application.

TABLE II
CHEMICAL COMPOSITION OF OF HT –POTASSIUM 18.5%, SODIUM 1.5% SAMPLES FROM EDX ANALYSIS

Sample	Chemical Composition (%wt)	
	K	Na
Unwashed	18.50	1.50
Washed	13.04	1.35

wt = weight

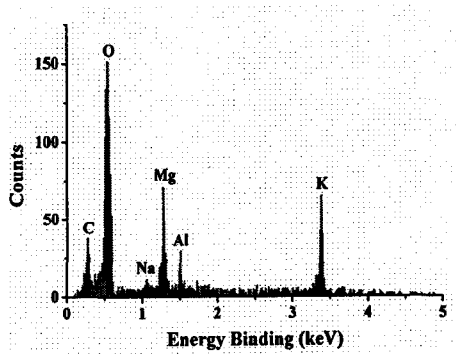

(a)

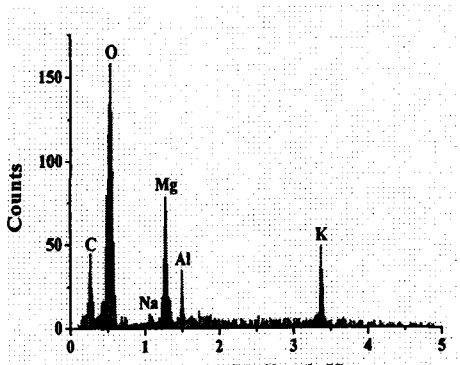

(b)

Figure 1. EDX analysis on magnification 500 X of (a) unwashed , (b) washed HT containing 18.5% K, 1.5% N

Table 3 shows the adsorption of carbon dioxide m with nitrogen (at 30% CO_2, 70% N_2) at different opera temperatures. Despite the decrease in the adsorption capa as temperature was increased, the adsorption was stable after 5th cycle of adsorption and desorption. This cle demonstrates the remarkable improvement over the materials reported previously.

TABLE III
CO_2 ADSORPTION CAPACITY OF HT (POTASSIUM 18.5%, SODIUM 1.5% 1.34 BAR

Sample / CO_2 Adsorption	300 °C (mmol/g)	400 °C (mmol/g)	500 °C (mmol/g)
Unwashed	1.210	1.029	0.861
Washed	0.969	0.861	0.591

IV. CONCLUSIONS

The highest CO_2 adsorption was achieved at 1.210 mm by unwashed HT containing 18.5 wt% K, 1.5 wt% Na l loading when it was measured at 300 °C 1.34 bar (or 0.4 CO_2 partial pressure). Washing of HT is not recommende

this type of application because it leaches considerable amount of metals necessary for the adsorption.

ACKNOWLEDGMENT

The work was supported by the Universiti Sains Malaysia research grants.

REFERENCES

[1] M.R. Othman, Martunus, R. Zakaria, and W.J.N. Fernando, "Strategic planning on carbon capture from coal fired plants in Malaysia and Indonesia: A review," *Energy Policy*, vol. 37, pp. 1718-1735, 2009.

[2] M.R. Othman, Z. Helwani, Martunus, and W.J.N. Fernando, "Synthetic hydrotalcites from different routes and their application as catalysts and gas adsorbents: a review," *Appl. Organometal. Chem.*, vol. 23, pp. 335-346, 2009.

[3] T. Yamazaki, M. Katoh, S. Ozawa, and Y. Ogino, "Adsorption of CO_2 over univalent cation-exchanged ZSM-5 zeolites," *Molecular Physics*, vol. 80, pp. 313-324, 1993.

[4] P. Li, and F.H. Tezel, "Adsorption separation of N_2, O_2, CO_2 and CH_4 gases by β-zeolite," *Micro. Meso. Mater.*, vol. 98, pp. 94-101, 2007.

[5] E.G. Pérez, J.B. Parra, C.O. Ania, A.G. Sánchez, J.M. van Baten, R. Krishna, D. Dubbeldam, and S. Calero, "A computational study of CO_2, N_2, and CH_4 adsorption in zeolites," *Adsorption*, vol. 13, pp. 469-476, 2007.

[6] Z. Yong, V.G. Mata, and A.E. Rodrigues, "Adsorption of carbon dioxide on chemically modified high surface area carbon-based adsorbents at high temperatures." *Adsorption*, vol. 7, pp. 41-50, 2001.

[7] M.M. Sabio, M.A. Munecas, F.R. Reinoso, and B. McEnaney, "Adsorption of CO_2 and SO_2 on activated carbons with a wide range of micropore size distribution," *Carbon*, vol. 13(12), pp. 1777-1782, 1995.

[8] R.C. Sarkar, and A. Bose, "Role of activated carbon pellets in carbon dioxide removal," *Energy Convers. Mgmt.*, vol. 38, pp. 105-110, 1997.

[9] M.G. Plaza, C. Pevida, A. Arenillas, F. Rubiera, and J.J. Pis, "CO_2 Capture by adsorption with nitrogen enriched carbon," *Fuel*, vol. 86, pp. 2204-2212, 2007.

[10] M.K. Aroua, W.M.A.W. Daud, C.Y. Yin, and D. Adinata, "Adsorption capacities of carbon dioxide, oxygen, nitrogen and methane on carbon molecular basket derived from polyethyleneimine impregnation on microporous palm shell activated carbon," *Sep. Pur. Technol.*, vol. 62, pp. 609-613, 2008.

[11] M.R. Othman, M.N. Rasid, and W.J.N. Fernando, "Mg-Al hydrotalcite coating on zeolites for improved carbon dioxide adsorption," *Chem. Eng. Sci.*, vol. 61, pp. 1555-1560, 2006.

[12] E.L.G Oliviera, C.A. Grande, and A.E. Rodrigues, "CO_2 sorption on hydrotalcite and alkali-modified (K and Cs) hydrotalcites at high temperatures." *Sep. Pur. Technol.*, vol. 62, pp. 137-147, 2008.

[13] M.R. Othman, Martunus, and W.J.N. Fernando, "Hydrotalcite from modified combustion method," In proceeding of International Conference on X-ray & Related Techniques in Research & Industry (ICXRI), pp. 290-292, June 9-10, 2010.

Hydrotalcite via a Combustion Method

I.K. Shamsudin*, M.R. Othman*

Pusat Pengajian Kejuruteraan Kimia

Kampus Kejuruteraan, Universiti Sains Malaysia, Malaysia.

ilykhairunnisa@yahoo.com, ch_roslee@eng.usm.my

ABSTRACT. Hydrotalcite has become a new emerging catalytic material in fine chemical industry. Its appealing characteristic includes of diminishing pollutions and catalyst re-use, made it a worthy candidate. This study entailed hydrotalcite like compound synthesized by combustion method from aluminum and magnesium nitrates and sodium carbonate with glycine as fuel. The fuel amount, carbonate amount and synthesis temperature were accordingly varied. Mg-Al hydrotalcites with Mg:Al molar ratio 3:1 were prepared and the resulting structural modifications were evaluated by X-ray diffraction(XRD) and Fourier-transform infra red spectra(FTIR) analysis.

INTRODUCTION

Hydrotalcite-like compounds are double-layered hydroxides with general formula, $(M^{2+}_{1-x}M^{3+}_{x}(OH)_2)^{x+}(A^{m-}_{x/m}).nH_2O$. The exact formula of hydrotalcite(HT) was first found halfway the nineteenth century in Snarum, Sweden and the exact formula primarily presented by Manasse in 1915 [1]. It was acknowledged that hydrotalcite structure used to be assumed to exist of consecutive layers of brucite, $Mg(OH)_2$ and gibbsite, $Al(OH)_3$ [2]. During the end of 1960's, the idea was rebutted by publications of Almann and Taylor [3] pointed out that both constituted of localized cations. Hydrotalcite is an alternating layered structure with positively charged brucite-like layers where M^{2+} cations are substituted by M^{3+} cations and interlayers containing the charge balancing anions and water molecules. Thermal treatment responsible for structural modifications (activation of HT) whilst inducing dehydration, dehydroxylation and loss of charge compensating anions, resulting mixed oxides, consequently transpired to a useful precursor for preparation of a catalytically active oxides with basic properties. The consequential oxides have small particle in size, large surface area and basic properties thus potentially useful as adsorbents also as heterogeneous base catalysts and catalytic supports. In which would intensify their existence as catalyst in industry in substitutes of chemical such as alkali bases from liquid phase aldol-condensations reactions in mission to produce less polluting processes. This substitution is vital to eradicate the problems faced by using homogeneous catalyst [4, 5]. Hydrotalcite is rarely found naturally but conventionally synthesized via co-precipitation and sol gel route, spending high volume of solvents and low temperature heating for a long time. Furthermore, being an inorganic solid base, hydrotalcite have high thermal stability which in a way could afford easy re-generation by calcinations.

Combustion method is preferred prior due to the short period of heating required whilst saves significant amount of energy and time [6]. This highly exothermic process involves glycine as fuel. The reaction is initiated with heat. The mixed oxides produced is Mg(Al)O with periclase like structure. The recrystallization process is done by contacting the mixed oxides with carbonate aqueous solution. Its catalytic performance is mainly dependent on pretreatment and operating conditions. This motivates the urge in finding the optimum calcinations temperature in the way to obtain the highest possible catalytic activity. Also, the influence of structural parameters on the hydratalcite manufactured by combustion is yet to be explored. The present work is dedicated to the synthesis and characterization of hydrotalcite produced. X-ray diffraction and FT-IR spectroscopy were method used to analyze the structural transformation. The effects of calcinations and recrystallization of the synthesized Mg-Al hydrotalcite by combustion are discussed.

TABLE 1. Sample label, synthesis temperature and content amount of sodium carbonate.

Sample	Synthesis temperature(^{0}C)	Amount of Na_2CO_3 per gram of mixture	Amount of fuel (glycine) per gram of mixture
HT 450 (10A/10B)	450	0.10	0.10
HT 450 (10A/10B)	450	0.20	0.10
HT 650 (10A/10B)	650	0.10	0.10
HT 650 (10A/20B)	650	0.20	0.10
HT 850 (10A/10B)	850	0.10	0.10
HT 850 (10A/20B)	850	0.20	0.10
HT comm 450	450	-	-
HT comm 650	650	-	-
HT comm 850	850	-	-

EXPERIMENTAL

Materials

All analytical grade reagents were purchased from Merck and used directly with the exception of further purification process.

Appropriate ratios of magnesium nitrate and aluminum nitrate were mixed with deionized water respectively. The Mg/Al atomic ratio in the solution chosen was 3:1. It would be wise to hydrolyze the nitrates separately for approximately 30 minutes to optimize the hydrolyzation process of the solution, under vigorous stirring at 70°C. Then, the amounts of sodium carbonate (Na2CO3) were varied from 0.10 to 0.20 per gram of solid mixture. 10% of fuel (glycine) per gram of mixture were added and the mixture was allowed to be suspended in water. The solution was heated at 80°C until water evaporated. For binder addition, 5ml of polyvinyl alcohol (PVA) (4g PVA/100ml H_2O) was added. The resulting paste was later placed into Carbolite furnace and heated from 450 °C, 650 °C and 850°C for 5 min. The combustion process producing mainly mixed oxide were put in contact with 60 mL of 0.1N of sodium carbonate solution at room temperature and then the solid was separated using centrifugation. After being washed with deionized water, the paste was dried in the oven at 100°C to allow crystallization (HT). **TABLE 1** reviews the details of samples examined.

Characterization

X-ray diffraction analysis was used upon the samples to identify the various crystalline form known as 'phases', of compounds present in powdered and solid samples. The powder XRD patterns were recorded using XRay Bruker/D8 Advance instrument.

The FTIR spectra were ontained at room temperature using Perkin Elmer Spectrum One FTIR Spectrometer by preparing the samples with the standard KBr pellet method.

Results

Samples withdrawn from heat treatment showed mixed oxides with periclase structure. Hydrotalcites were formed as soon as in contact with carbonate solution through recrystallization process. As known, mixed oxides were formed with varying sizes depending on calcinations temperature. The calcined samples showed similar pattern particularly for crystallization of mixed oxides structure (hydrotalcite, brucite, periclase and spinel structure (**FIGURE 1**)). HT were identified at 2θ = 11°, 23°, 34°, 38°, 39°, 45°, 46°, 51°, 60°, 62°, 65°, 72°, 75° and 82°, and brucite were identified at 2θ = 19°, 33°, 38°, 51°, 58°, 68°, 72° and 82°. Spinel were identified at 2θ = 19°, 31°, 37°, 45°, 56°, 65°, 75° and 80°. Hence periclase were identified at 2θ = 37°, 43°, 62°, 65°, 75°, 78°, 82° and 89°.

The comparison is made to distinguish the effects upon variations on sodium carbonate content, fuel content and decomposition temperature.

C450 contained better crystalline strucuture of hydrotalcite content followed by B450, A450 and D450(**FIGURE 2**). Sample C450 was observed to have more intensive line and less broad peaks, to which most likely owing to the increased particle size and improved crystallinity or to both. Both A450 and B450 showed slightly similar pattern of crystallinity but have significantly much lower amount of other type of undesired crystal. However, for sample being applied temperature as high as 450°C, the higher amount of sodium carbonate being introduced to sample mixture, the more define crystallinity of periclase with intense peaks were exhibited. For group of sample being calcined at 600°C, B600 showed much narrower peaks followed by A600, C600 and D600. Sample C600 identified as having the intense peaks showing potent form of periclase structure. Sample D600 nonetheless showed broader peaks and shrinkage of periclase structure. For calcinations at 850°C, B850 showed much narrower and intense peaks followed by D850, C850 and A850. Obviously, all samples showed same pattern, except for sample C850, additionally showed deterred periclase peaks. The inconsistency of diffractograms pattern in facilitating different amount of sodium carbonate added in the reaction was proven to be independently correlated.

Among the entire sample with 0.05 g Na_2CO_3 per g of mixture, sample A600 showed most adequate crystal structure of hydrotalcite and not so well define structure of periclase (**FIGURE 3**). Sample A850 showed well define hydrotalcite but too much intense were deposited on periclase peaks. This could only means that crytallinity of substance were improved by calcinations temperature and with that, 450°C was tend to provide optimum decomposition temperature in installing better hydrotalcite content. In case of sample with 0.10 g Na_2CO_3 per g of mixture, higher applied temperature gave better crystallinity with much sharper peaks. However, the structure for undesired phase became more defined and better peaks than desired ones. In this group of same amount sodium carbonate compound, B600 produced well crystalline hydrotalcite and mediate crystallinity of other product. This pattern of diffractograms was the same for group sample C and D. All 3 calcination temperatures illustrated the same pattern with more intense peaks as the decomposition temperature applied rises. And, as the temperature rises, the slight shrinkage of hydrotalcite phase could be due to removal of interlayer water and carbonate which altering the structure of the phases. Thus, the calcinations temperature has to be low enough to minimize the formation of unwanted phase while maximizing the production of hydrotalcite.

FIGURE 4 described the infrared spectroscopic analysis of hydrotalcite. There is a good agreement amongst the spectras with only slight variations in band positions of all calcined samples. Calcination at an approximately high temperature induced dehydration, dehydroxylation and decarbonation that would lead to the formation of mixed oxide. The broad and centered band around 3500 cm^{-1} corresponded to the hydroxyl group which the OH mode of interlayer water molecules and hydroxyl groups in the brucite layer. This signifies that water still existed in the samples even after being calcined at 800°C. At 1680-1636 cm^{-1} referred to characteristics of vibrations in water molecules. A most likely intensive peak around 1384cm^{-1} attributed to carbonate or nitrate. Although sodium nitrate should be in a separate phase from hydrotalcite, the effect of high pH condition could lead to incorporation of nitrate ions into the hydrotalcite interlayer region along with carbonate and water. The existence of carbonate was due to readsorption of gaseous carbon dioxide from the atmosphere onto the basic site of resulting oxides or partial decomposition of carbonate, which could explain the residing carbonates on hydrotalcite [7]. There was no band around 868-827cm^{-1} which means it could definitely be a non interlayer carbonate. The carbonate species presented in the interlayer region was assumed as free ion and not specifically involved in any bonds. As for the low energy range of the spectra (lower than 1000 cm^{-1}) the peaks could be defining MgO or AlO in the brucite layer. The band about 415 cm^{-1} was assigned to MgO, while at higher frequency of 553 cm^{-1} considered to be Al-O since Al has higher mass number. Figuratively, the pretreatment gamma samples had a weaker bands compared to the post treatment ones. X-ray diffractograms confirmed the present of spinel, periclase, gibbsite and MgO as

breakdown products. Heat treatment may hold the slight effect on the samples as the bands below 1000cm-1 became sharper caused a decrease in intensity and increase in bandwidth as the calcinations temperature applied was higher. Also, there was a significant decrease in the intensity of water and carbonate characteristics peaks that surely due to the evolution of water and carbon dioxide vapors. All in all, the spectra do not give away any effects on addition of sodium carbonate.

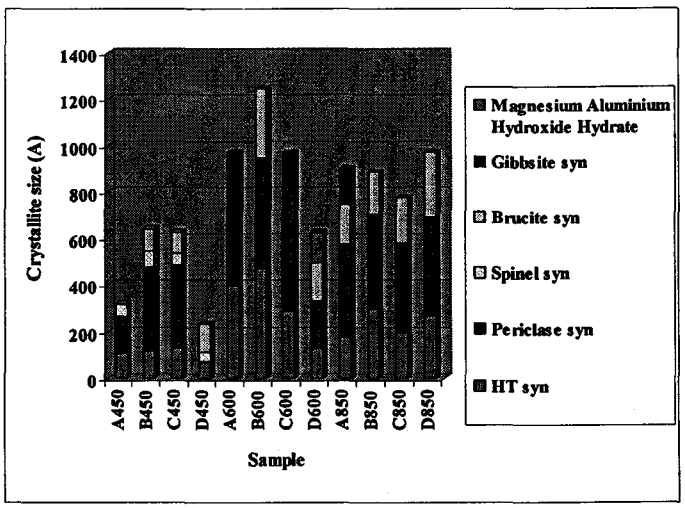

FIGURE 1. Sample crystalline phases.

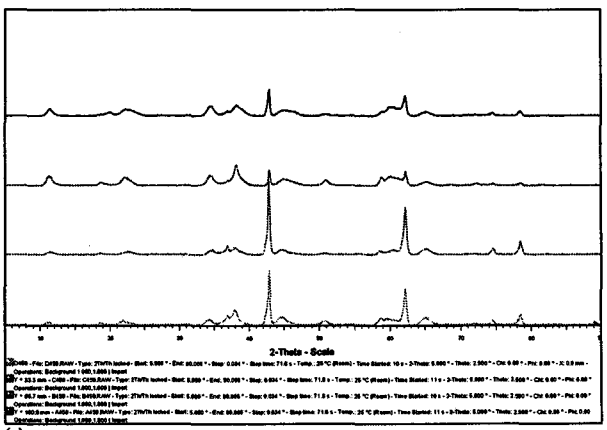

(a)

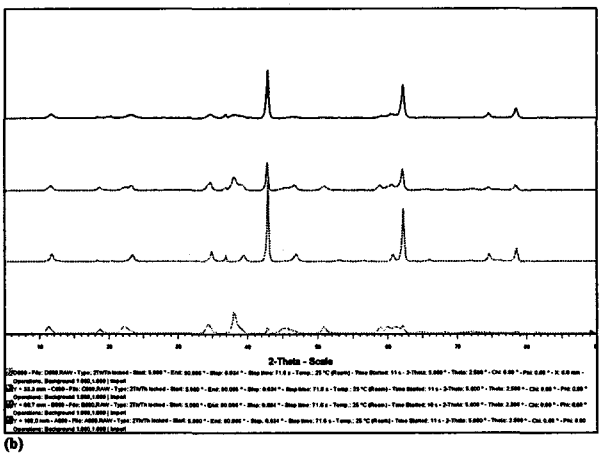

(b)

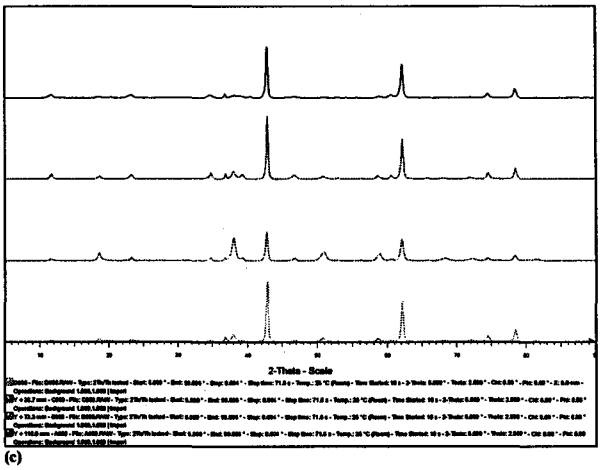

(c)

FIGURE 2. XRD patterns of mixed oxide by combustion method. Effect of different amount of sodium carbonate added and calcined (a) at 450°C (b) at 600°C and (c) at 850°C.

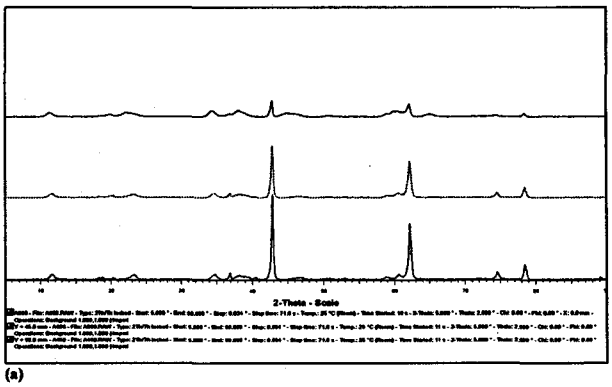

(a)

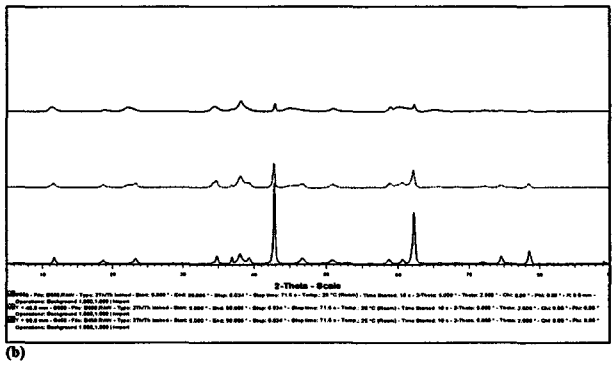

(b)

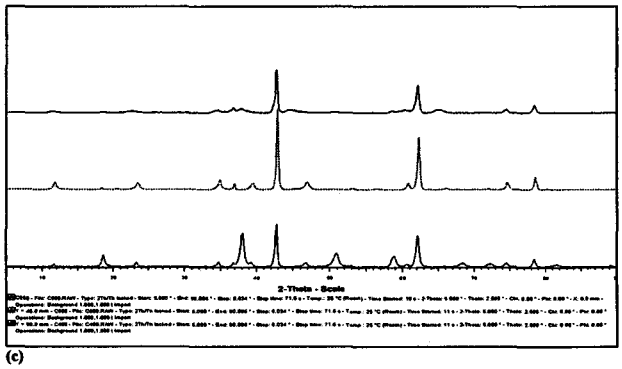

(c)

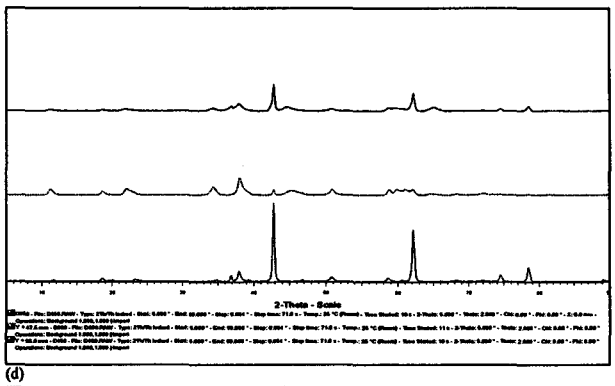

(d)

FIGURE 3. XRD patterns of mixed oxide by combustion method. Effect of different calcination temperatures on samples mixed with (a) 0.05g Na_2CO_3 (b) 0.10g Na_2CO_3 and (c) 0.15g Na_2CO_3 and (d) 0.20g Na_2CO_3.

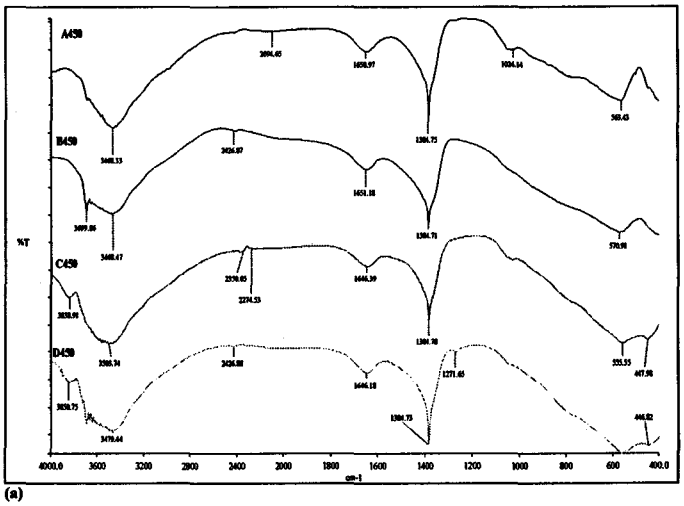

(a)

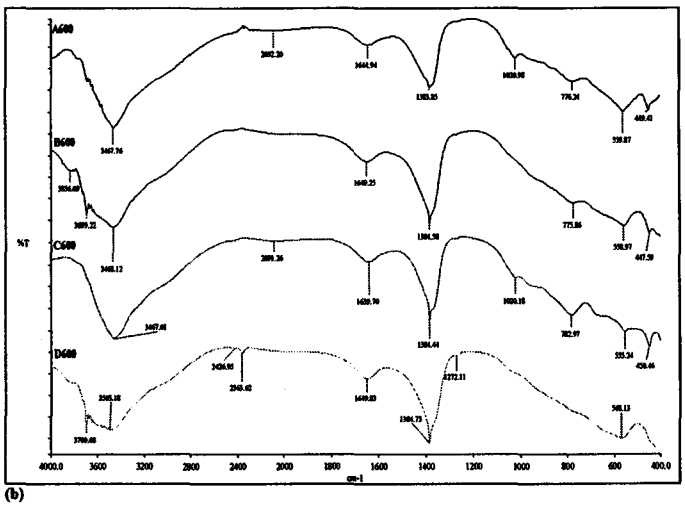

(b)

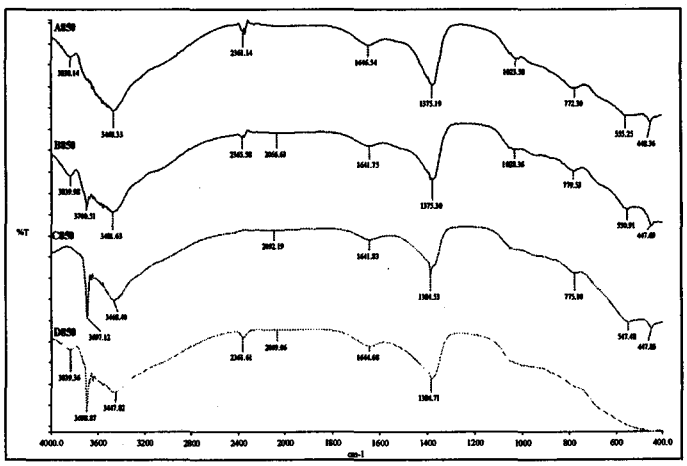

FIGURE 4. Spectras of mixed oxide by combustion method. Effect of different amount of sodium carbonate added and calcined (a) at 450°C (b) at 600°C and (c) at 850°C.

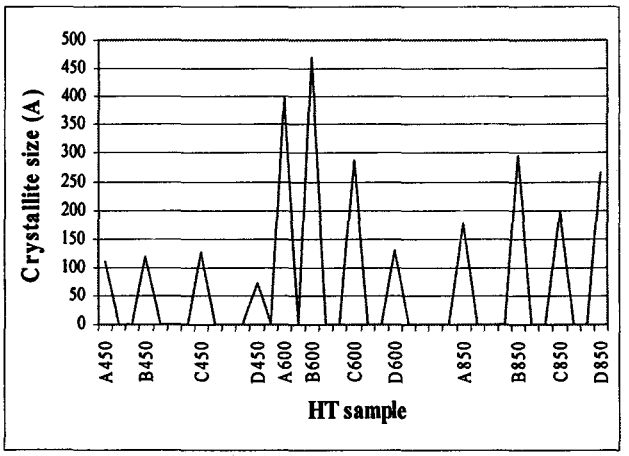

FIGURE 5. Comparison for crystallite size of hydrotalcites.

Generally, upon heating Mg-Al hydrotalcite, the process usually involves the released of water and carbon dioxide. From **Figure 5**, the crystallite size was larger for calcined sample were due to much defined crystal phase formation at higher temperature. Calcination at 600°C displayed much higher size compared to the others. The resulted oxide sides were dried and courser which would led to a larger amount of surface area. Thus, the effect of heat application could give a slight decreased of crystallite size as the crystalline structure possibly melted for samples calcined at 850°C.

Figure 6 illustrated that the resulting combustion samples have inconsistency pH values pattern. It was decided that pH values of catalysts were independent of amount of sodium carbonate and calcinations temperatures. The pH was estimated to be in range of 8-14.

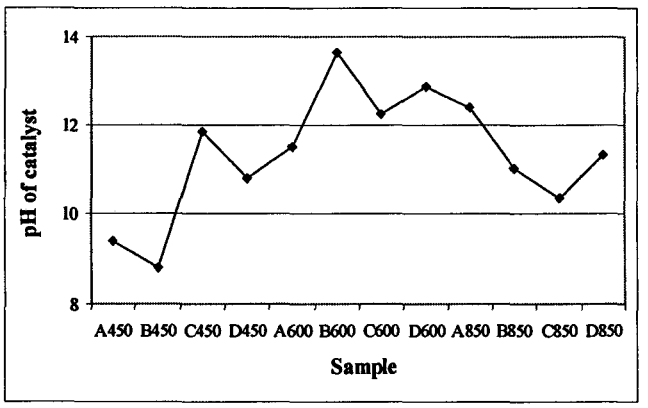

FIGURE 6. pH of hydrotalcite catalysts.

CONCLUSION

MgAl hydrotalcite-like compounds can be synthesized via combustion method using glycine as fuel. This highly base catalyst will be used in transesterification study to produce biodiesel.

REFERENCES

[1] E. Manasse. Atti.Soc.Toscana.Sc.Nat.Proc.Verb 24 (1915) 92.

[2] W. Feitknecht, Helv.Chim.Acta 25 (1942) 131 and 555.

[3] R. Almann, Acta Cryst. 24 (1968) 972.

[4] E. Lotero, J.G. Goodwin Jr., D.A. Bruce, K. Suwannakarn, Y. Liu, D. E. Lopez, in: J. Spivey (Ed.), The Catalysis of Biodiesel Synthesis in Catalysis, Royal Society of Chemistry London, 2006.

[5] E. Leclercq, A. Finiels, C. Moreau, J. Am. Oil Chem. Soc. 78 (2001) 1161.

[6] K.C. Patil. S. T. Aruna, S. Ekambaram, Curr. Opin. Solid State Mater. Sci. 6 (2006) 507.

[7] A. Varma, A.S. Rogachev, A.S. Mukasyan, S. Hwang, Adv. Chem. Eng. 24 (1998) 79.

[8] D.Cruz, S. Bulbulian, J. Nucl. Mater. 312 (2003) 262.

[9] P. Mustowski, L. Chmielarz, E. Bozek, M. Sawalha, F. Roessner, Mater. Res. Bull. 39 (2004) 2

The characteristics of intercalated compound precursor sol during hydrolysis, condensation and drying processes

M.R. Othman[1*] and J. Kim[2]
[1]School of Chemical Engineering, Universiti Sains Malaysia, 14300 Nibong Tebal, Penang, Malaysia
[2]College of Environment and Applied Chemistry, Kyung Hee University, Yongin, 449-701, South Korea
*Corresponding author. Phone: +604 5996425, Fax: +604 5941013
Email: chroslee@eng.usm.my

ABSTRACT
In this work, synthesis of two compounds for use as CO_2 adsorbents using sol-gel technique is presented. One compound contained carbonate ions, while the other is free from the ions. The former material demonstrated more rapid weight loss during the first falling rate period of drying than the material without the ions. The former material was also found to be unable to adsorb water, whereas the latter was not stable and tend to dissolve on hydration. Results from SEM analysis indicated that sample containing carbonate ions exhibited the characteristics of an intercalated compound. Upon heating at 600°C, the sample was transformed into a more ordered, semi-crystalline structure.

Keywords: Adsorbent, conversion energy, intercalated compounds, sol-gel.

1. INTRODUCTION
Malaysia is under Non-Annex I country that has no green house gas emission restrictions under Kyoto protocol. Although the per capita emission of the gas in Malaysia is relatively insignificant compared to that in the Annex I countries, the share of global emission originating in Malaysia will grow as it strives to be a developed nation in 2020. Malaysia must take a pre-emptive stand and participate in a greenhouse gas emission reduction project or Greenhouse Gas Project (GCP) in order to reap the benefits and champion the cause towards minimizing the global warming.

Several options exist to abate carbon dioxide emissions. These include increasing the efficiency of fossil fuel combustion component systems or replacing fossil fuels with renewable energy sources. Complete switching to other energy sources, however, appears implausible. Increasing fossil fuel combustion efficiency has approached near saturation. Another alternative would be through sequestration of the gas through carbon capture and storage (CCS). Various options of CCS processes for fossil fuel power plants have been recognized. These include the traditional absorption technology using MEA (monoethanolamines), adsorption technology by pressure/thermal swing adsorption (PTSA), vacuum swing adsorption (VSA), electrical swing adsorption (ESA), membrane adsorption technology, cryogenic technology and more recently chemical looping by using metal oxide as an oxygen carrier.

The cryogenic technology appears to have been matured and the least improvement can be realized from it. Chemical looping is relatively new to have an immediate impact in the commercial sectors. The absorption technology using MEA for CO_2 capture has been considered a feasible option. Nevertheless, recent studies indicate that the adsorption process can be highly attractive, competitive and economically advantageous over the MEA system if the adsorbent performance is improved. Intercalated adsorbents modified with basic metal oxides are known to exhibit high carbon dioxide adsorption capacity even at elevated temperature (Yong et al, 2001). In this work, an intercalated compound is developed from a sol precursor especially tailored for CO_2 adsorption for use in a flue gas stream. However, due to the constraint and requirement of the paper, and the fact that the discussion on the hydrolysis-condensation (HC) and drying of this compound is rare in the past and present literature, the three stages of the compound development in this work are highlighted in this paper.

2. MATERIALS AND METHODS

The synthesis started with the addition of 12.8 mL aluminum alkoxide into highly purified water by using molar composition of the alkoxide, HCl and water at 1:0.07:100. Acid was used to peptize the solution. This was followed by the addition of the equivalent amount of magnesium methoxide, 20 mL of 1M sodium carbonate into the boehmite solution and stirred until homogeneity. 2.1 mL PVA solution was added to add strength to avoid ruptures, cracks or delaminations of samples on drying. The peptized sol was cooled steadily to allow for continued hydroxylation, alkoxilation or condensation. A small amount of the resulting sol mixture was poured onto a polypropylene petri dish, dried under ambient and highly humid conditions for 48 hours to obtain a hardened, dried gel that solidified on continuous drying. The dried gel was then heated to 600°C. Table 1 shows the chemicals that were used during the synthesis of the materials. The material containing carbonate was designated HT, whereas the material that did not contain the ion was designated as AlMgOH.

Table 1

Chemicals used in the experiment

Chemicals	Molecular weight
Aluminum tri-sec-butoxide, $Al(OC_4H_9)_3$	246.33
Magnesium methoxide, $Mg(OCH_3)_2$	86.38
Sodium carbonate anhydrous, Na_2CO_3	105.99
Poly (vinyl-alcohol), PVA	88000
Hydrochloric acid, HCl	36.50
Highly purified water, H_2O	18.02

The dried gels were immersed in 10 mL H_2O at 25°C until swelling equilibrium was attained. The weight of wet sample was determined after removing the surface water by blotting with filter paper. Dry weight was determined after drying the gel overnights. The equilibrium-swelling ratios (Q) of the gels were calculated as:

$$Q = (\text{Wet gel-dried gel})/\text{dried gel} \quad (1)$$

3. RESULTS AND DISCUSSION

Synthesis of the material from the sol-gel process initially produced beohmite (AlOOH). The reaction scheme, where R=(C_4H_9), is as follows:

$$Al(OR)_3 + 2H_2O \rightarrow AlOOH + 3ROH \quad (2)$$
$$H_2O + 2AlOOH \rightarrow Al(OH)_3 + H^+ \quad (3)$$

The production of alumina from the boehmite might also be possible if water is evaporated completely,

$$AlOOH + AlOOH \rightarrow Al_2O_3 + H_2O \quad (4)$$

Magnesium methoxide [$Mg(OR')_2$], where R'= CH_3, was added into the boehmite sol to form hydroxyl of magnesium and butoxyl-oxygen-methyl ligands in the following way,

$$Mg(OR')_2 + 2ROH \rightarrow Mg(OH)_2 + 2ROR' \quad (5)$$

Sodium carbonate reacted with the remaining, residual water in the sol to yield,

$$2H_2O + Na_2CO_3 \rightarrow 2NaOH + H_2CO_3 \quad (6)$$

The resulting ligand, $[MgAl(OH)_5]\bullet CO_3$, designated as HT, was perceived to follow the generic formula for hydrotalcite like compound reported previously [(Wang et al., 2001); (Trave et al., 2002); (Yong et al., 2001)]. The relevant reaction is as follows,

$$Al(OH)_3 + Mg(OH)_2 + CO_3^{2-} \rightarrow [MgAl(OH)_5]\bullet CO_3 \quad (7)$$

The carbonate anions and water molecules were considered to be present in the interstitial positions, sandwiched in between the metal hydroxide sheets in order to compensate for the excess positive charge of the cations. The anions also served as a counter ion to increase the ionic strength in the liquid and facilitate coordination of aquo ligands to the metal centres. Figure 1 shows the weight reduction of the intercalated materials as they were aged and dried. A hydrolysis-condensation and the three stages of

drying; Constant Rate Period (CRP), First Falling Rate Period (FFRP) and Second Falling Rate Period (SFRP); are depicted in the figure.

During HC, the tension due to the chemical potential gradient caused the osmotic pressure to build up, leading to the expulsion of liquid from the solid-gel network. Inter-diffusion between liquids in the gel contributed to a preferential evaporation and concentration gradient, leading to further shrinkage of the gel. After HC, the gel samples underwent three stages of drying commencing with CRP and followed by FFRP and SFRP over a period between 1.6 and 261 hours.

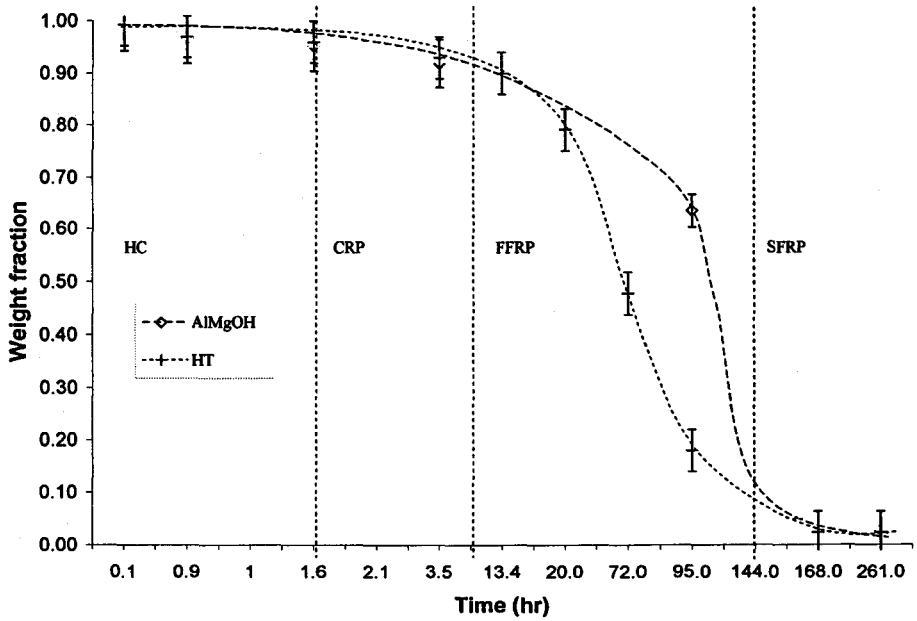

Figure 1 Temporal evolution of sol into gel

During CRP, the temperature drop caused by the evaporation at the interface led hotter air and liquid in the surrounding to exchange heat, promoting faster evaporation in the inner liquid layer and thus a prelude to a liquid loss from the gel underneath. The most substantial liquid loss was observed during FFRP following aggressive invasion of air deep into the gel pore structure. This was aided by the increase in the temperature drop and vapor pressure differences between the liquid and air. The gel shrank significantly as it lost much of the liquid. The two samples experienced the most rapid weight loss within 20-144 hours of drying during FFRP and HT sample appeared to show more rapid weight loss than AlMgOH. The reason for the higher rate of weight loss by HT was conceivably due to the better expulsion of water from the solid network as a result of HT that was thought to be more affinitive for the carbonate ions than water (refer to equation 7). The carbonate anions were linked closer to the metal hydroxide sheets than the water molecules in the interlayer structures. For AlMgOH, in contrast, the water molecules were placed closer to the metal centres of the structures, formed immediate links to the structures and therefore less readily liberated upon drying.

Beyond 144 hours of drying, the gel experienced SFRP where evaporation slowed down and the temperature of the gel approached to that of the ambient temperature. During this stage of drying, evaporation might still occur but was confined locally in the isolated pores of liquid and at solid interstices by the advancing vapor front that eventually revealed the solid structure. The rate of drying for both of the samples during this stage was almost comparable.

During an experiment to determine the swelling ratio of the two samples, it was observed that HT did not dilate after prolong immersion in water. The swelling ratio of AlMgOH was not able to be determined due to the partial dissolution of AlMgOH in the solvent. AlMgOH was found to be unstable on hydration and this effect was undesirable. As such, further analysis of AlMgOH was not attempted. This leads us to focus the remaining discussion only on the HT sample.

Figure 2 (a-d) shows images of HT sol sample, HT gel, SEM of the dried gel and heated HT samples, respectively. Although additional analyses might be required to ascertain a structure of an intercalated material, SEM analysis might be safely adequate to prove the presence of such a structure if it were substantiated by a previously similar analysis. Figure 2c shows SEM image to provide an evidence for the lamellar structure, which was in corroboration with the typical morphology of the intercalated hydrotalcite like materials described in the previous work (Greenwell et al., 2006). Figure 2d shows that the former structure was transformed into a blend of cubic, slit and cylindrical crystals after being heated at the elevated temperature.

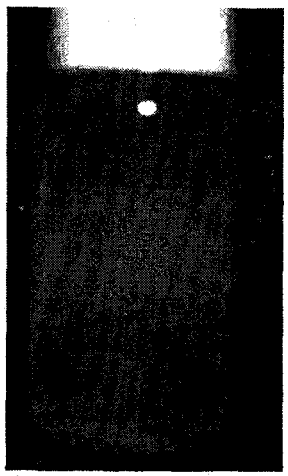

(a)

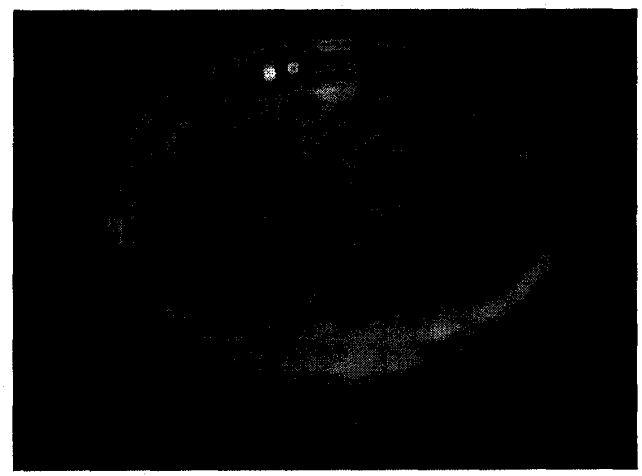

(b)

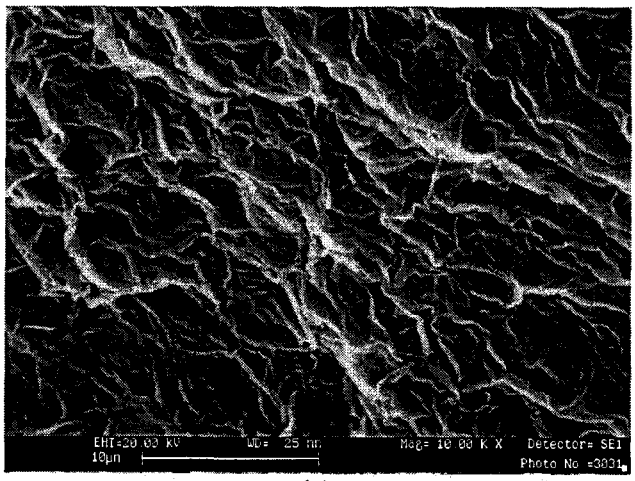

(c)

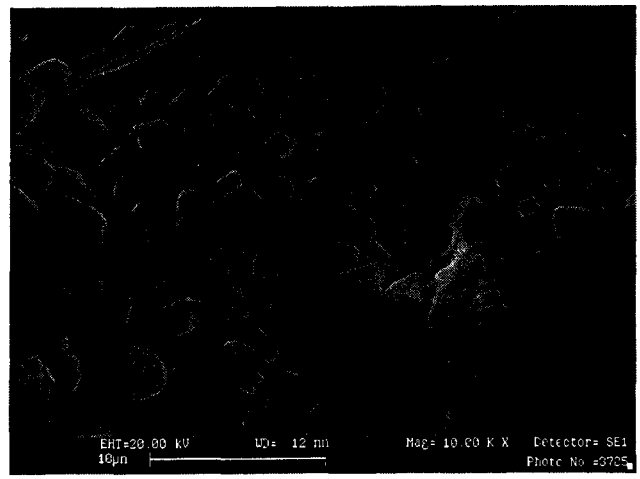

(d)

Figure 2: Images of (a) HT sol sample, (b) HT gel, (d) SEM of dried HT, (e) SEM of heated HT at 600°C

4. CONCLUSION

Two materials; one with carbonate ions, the other without the ions; were synthesized with the aim at understanding their characteristics (at sol and gel level) during HC and drying stage, which are scarcely a subject of the intercalated materials reported in the past and present literatures. The former demonstrated faster weight loss on drying possibly due to the loose bonding or better expulsion of water from the solid network, while water exhibited higher adherence to the latter compound. Swelling test indicated that HT gel did not dilate on hydration, whereas, the other gel simply dissolved partially and was not stable. SEM image of HT gel shows that the sample exhibited the characteristics of an intercalated compound.

ACKNOWLEDGEMENT

Support from the Ministry of Science, Technology and Innovation of Malaysia and Korea Science and Engineering Foundation is gratefully acknowledged. The SEM images provided by H.J. Choi are greatly appreciated.

REFERENCES

Greenwell, H.C; Holliman, P.J; Jones, W and Velasco, B.V. (2006). Studies of the effects of synthetic procedure on base catalysis using hydroxide-intercalated layer double hydroxides. *Catalysis Today*. 114, 397–402

Trave, A; Selloni, A; Goursot, A; Tichit, D and Weber, J. (2002). First Principles Study of the Structure and Chemistry of Mg-Based Hydrotalcite-Like Anionic Clays. *J. Phys. Chem. B*.106, 12291-12296.

Wang, J; Kalinichev, A.G; Kirkpatrick; R.J. and Hou, X. (2001). Molecular Modeling of the Structure and Energetics of Hydrotalcite Hydration. *Chemistry of Materials.* 13, 145-150

Yong, Z; Mata, V and Rodrigues, A.E., (2001). Adsorption of carbon dioxide onto Hydrotalcite – like compounds (HTIcs) at high temperature. *Ind. Eng. Chem. Res.* 40, 204 – 209.

Re-crystallized Mg-Al hydrotalcite for methanolysis of jatropha *curcas* oil into biodiesel

Z. Helwani[a,b], N. Aziz[a], M.R. Othman*[, a]

[a]School of Chemical Engineering, Universiti Sains Malaysia

14300 Nibong Tebal, Penang, Malaysia.

[b]Department of Chemical Engineering, Riau University

Pekanbaru 28293, Indonesia.

*Corresponding author

Email: chroslee@eng.usm.my

Tel: (60)-45996426

Fax: (60)-45941013

Abstract

Hydrotalcite (HT) was prepared to serve as a heterogeneous base catalyst during jatropha oil into *bio*-diesel conversion. During HT preparation, mixed oxide was produced from the combustion, in which, saccharose was used as fuel. The oxide was calcined and then recrystallized in carbonate aqueous solution to produce layered HT structure. The HT was then used during methanolysis of jatropha oil under different operating conditions. The highest conversion was 75.2% when reaction was carried out at 65 °C with a methanol:jatropha oil molar ratio of 12:1, a reaction time of 6 h and a catalyst loading of 4 wt.%. The conversion is higher than the previously reported experiment with 50% conversion, longer reaction time of 24 h.

Keywords: Combustion; recrystallization; hydrotalcite; biodiesel; jatropha oil

1. Introduction

The increasing demand for energy and environmental awareness has prompted many researchers to think of alternative fuels from renewable resources that are environmentally acceptable. Biodiesel is the preferred choice since it decreases the effect of acid rain and greenhouse by reducing the emission of CO_2, SO_x and unburned hydrocarbons during combustion.

Biodiesel production from edible vegetable oil is known to favor combustion in compression ignition (CI) engines. However, it incurs higher feedstock cost, inferior storage and oxidative stability, lower heating value, inferior low temperature operability and higher NO_x emissions compared to petrodiesel [1]. The problem of high feedstock cost can be mitigated by choosing inedible vegetable oil [2-3]. Development of low-value, non-edible feedstock alternative for biodiesel production is, therefore, an important field in the current and future research, because it accounts for about 60-80% of the total biodiesel production cost. The use of *non*-edible vegetable oils is important, in this case, mainly because edible oil is considered as necessary food item.

The low cost feedstocks are reportedly the inedible vegetable oils such as jatropha, karanja, castor, rubber seed and see mango [3]. Thirteen vegetable oils were compared in terms of fuel properties and their suitability to be used as alternative diesel fuel [4]. It was reported that biodiesels from jatropha, karanja, mahua, neem and castanhola oils met the current biodiesel standards, (i.e. European EN 14214 and US ASTM D 6751-02). Jatropha and karanja oils were reportedly more suitable to be used in cold weather.

Jatropha *curcas* is a multipurpose species with many attributes and considerable potential. The oil from the seeds is potentially the most valuable end product, with low acidity, good oxidation stability and, low viscosity. In addition, the viscosity, free fatty acids

and density of the oil and the biodiesel derived from it are stable within the period of storage [5].

Different methods for producing biodiesel were reported [6-8]. The most common method is via catalytic trans-esterification of vegetable oils with a short-chain alcohol, usually methanol. This reaction involves the use of soybean, sunflower and rapeseed oils, with homogeneous acids and alkalis as catalysts [7, 9-11]. However, these conventional catalytic systems pose technical problems, associated with corrosion due to acid and emulsification, separation difficulties and side reaction such as decomposition and polymerization when base was used. To eliminate these problems, heterogeneous solid catalysts were developed and introduced [12-14]. The use of heterogeneous catalysts makes separation of the product easier. It also produces neither corrosion nor emulsion. Biodiesel production costs were reportedly reduced when a heterogeneous catalyst was used during *trans*-esterification [15-16].

Hydrotalcite (HT), benign catalyst was used to catalyze the transesterification of vegetable oils with methanol [17]. HT is a naturally occurring anionic clay with the formula $[(M^{2+}_{(1-x)}M^{3+}_{x}(OH)_2)^{x+}.(A^{n-}_{x/n}\ nH_2O)^{x-}]$ where M^{2+} is a di-valent cation (Mg^{+}, Ca^{2+}, Zn^{2+}, Cu^{2+}, Co^{2+}, Ni^{2+} or Mn^{2+}), M^{3+} is a three-valent cation (Al^{3+}, Fe^{3+} or Cr^{3+}). The layers are positively charged as M^{3+} cations or substituted M^{2+} cations. This charge is balanced by A anions with charge n-, for instance OH^{-}, Cl^{-}, NO_3^{-}, CO_3^{2-} or SO_4^{2-}, among others x is normally between 0.17 and 0.33. Carbonates (CO_3^{2-}) are generally the preferred anion [18-20]. In addition to being used as a catalyst, hydrotalcite-like compounds were also used as adsorbents, anion exchangers and flame retardant in polymers [21].

Homogeneously interdispersed mixed Mg-Al oxides (CHTs) is needed as precursor to HT. CHTs have strong surface basicity, much like the pure oxides, in addition to high surface areas and pore volumes [22-23]. CHTs are easily converted into HT by contacting the solid

with an aqueous solution containing the desired interlayer anions, thus recovering the original structure (re-cyrstallization). The procedure to convert mixed oxides into lamellar HT was reported in the previous work [19, 21, 24, 25].

Hydrotalcites synthesized using an alkali-free co-precipitation method in the absence of calcinations reportedly provided no catalytic activity for transesterification reaction [23, 26]. However, when HT was calcined, it promoted the transesterification of glyceryl tributyrate with methanol with 74.5% conversion at 60 °C for 3 h. The reaction rate increased steadily with Mg content and the most active catalyst (with Al/(Mg+Al) ratio of 0.25) was an order of magnitude more active than MgO [27]. In another report [23] it was found that the most active calcined hydrotalcite had an atomic ratio Al/(Mg+Al) of 0.25 in soybean oil transesterification at 60 °C where 67% conversion was obtained in 9 h. The maximum activity obtained by calcinations at 500 °C was directly correlated with the highest basicity.

The importance of calcinations temperature in trans-esterification was also described elsewhere [28]. The report described the transesterification of rape oil with methanol from which, the catalyst with Mg/Al ratio of 3.0, aged for 12 h, calcined at 773 K possessed the best catalytic activity for the trans-esterification. The reaction conditions for the system were optimized to achieve the methanol ester conversion of about 90.5%. By using urea hydrolysis in the preparation of HT, they also found that the catalyst was able to achieve with about 94% oil conversion at 338 K for 3 h. The water content of the oil was kept below 2.0 wt.% and free fatty acid content of the oil was kept below 3.0 mg KOH.g[oil]$^{-1}$. This heterogeneous catalyst was comparably more tolerant to free fatty acid and water in rape oil than the current homogeneous basic-catalysts [29].

In the present work, HT prepared from combustion-recrystallization was selected as heterogeneous base catalyst for methanolysis of jatropha *curcas* oil into biodiesel or methyl ester. Saccharose was selected as organic fuel to facilitate the combustion into mixed oxides.

The oxides were then calcined and contacted with carbonate solution to form HT. Different amount of fuels and different synthesis temperature were used during HT synthesis. The effects of calcination temperature and recrystallization processes on the catalytic performance of these catalysts were also investigated.

2. Experimental

2.1 HT preparation

To prepare the CHT, the precursor of HT, 20 g of magnesium nitrate hexahydrate and 6.67 g of aluminium nitrate nonahydrate (Mg/Al mole ratio of 3) were placed into a 100 ml beaker followed by addition of 6.67 g of potassium carbonate and 1.67 to 8.34 g of fuel (saccharose). The mixture was stirred and heated to a temperature of 80 °C for 5 min. A 2 ml hot water at 90 °C was added and the mixture was maintained at 80 °C. The solution was stirred at a constant speed for 10 min. Two drops of 4wt.% of poly-vinyl alcohol was added. The resulting paste was transferred into a 50 ml crucible and calcined in a furnace at different temperatures (450-850 °C) for slightly over 5 min to produce a mixture of oxides. The resulting sample was designed as CHT-X, where X is the calcination temperature. The sample was ground into powder and placed into a 100 ml beaker, followed by addition of 50 ml 0.1 M K_2CO_3 solution. The solution containing the sample was stirred for 5 min and then filtered. The solid sample was washed with de-ionized water and dried at 120 °C for 20 min to produce re-crystallized HT sample. The re-crystallized HT was designated as HT-X.

2.2 Characterization

The crystallization phases were studied using XRD. The analysis was carried out using Philips Goniometer PW 1820 diffractometer, PW 1710 diffraction controller and X-ray

generator PW 1729. The diffractometer was used with monochromatized CuK_α radiation and taken in the range of 10-70° (2θ). The X-ray tube was operated at 40 kV and 120 mA.

The surface morphology of the hydrotalcite powder was analyzed by SEM from Germany, model Leo Supra 50 VP Field Emission. Samples were placed in the sample grid for electron reflection and vacuumed (5 min) before analysis. SEM equipped with Oxford INCA 400 EDX microanalysis system with an operating voltage in the range of 0.1-30 kV was used in the present work. EDX was used to determine elemental composition of hydrotalcite by analyzing the microscopic image under EDX instrument. The EDX analysis used MnK_α as the energy source operated at 15 kV of accelerating voltage, 155 eV resolution 22.4° takeoff angle.

An infrared (IR) spectrum of hydrotalcites was obtained using FTIR spectrophotometer (Perkin Elmer FTIR 2000, USA). Samples were prepared by mixing the powdered solids with potassium bromide, KBr (the blank) in a 15:85 ratio to get transparent pellet auto supported on the different solids at 8 ton pressure. The infrared spectra were recorded both over the wave number range from 500 to 4000 cm^{-1}.

2.3 Biodiesel production

Jatropha *curcas* oil was supplied by Indonesian Spice and Industrial Crops Research Institute (Sukabumi, Indonesia). Table 1 shows the measured physical and chemical properties of jatropha *curcas* oil. Jatropha *curcas* oil and an appropriate volume of methanol with calcined Mg-Al hydrotalcite catalysts were placed into a 500 ml three-angel necked flask equipped with reflux condenser and Teflon stirrer. The reaction mixture was blended for a period time at 55-75 °C temperature under atmospheric pressure. Molar ratio of methanol to oil was taken at 3-15:1. After reaction, the methanol was recovered by a rotary evaporator in vacuum at 45 °C. Subsequently, the hydrotalcite catalyst was separated by filtration and the

ester layer was separated from the glycerol layer in a separating funnel. The upper layer of the sample was separated from the bottom layer and immediately quenched with n-hexane (dilution) prior to analysis of FAME content.

2.4 Analysis

The analysis of jatropha *curcas* oil FAME in the samples was carried out using Gas Chromatography with Flame Ionization Detector (GC-FID) which was equipped with Nukol^{TM} column (15 mm x 0.53 mm, I.D. 0.5 μm film). Helium was used as the carrier gas. Oven temperature at 110 °C was initially hold for 0.5 min and then increased to 220 °C (hold 15 min) at a rate of 10 °C min^{-1}. The temperatures of the injector and detector were set at 220 °C and 250 °C, respectively. A quantity of 1 μl from each sample was injected into the column. Methyl heptadecanoate was used as internal standard. The yield of jatropha oil FAME from the transesterification processes was calculated in similar method reported previously [30].

3. Results and discussion

3.1 Catalyst characterization

Figure 1a shows XRD pattern of a mixed oxide of hydrotalcite at 450 °C (CHT-450). The samples emerging from the combustion process before treating with carbonate solution, exhibited the XRD pattern typical of Mg(Al)O mixed oxides with a periclase-like structure. The particles exhibited a single phase with broadened and shifted peak which might evolve from HT (009). The other peaks at 450 °C were major reflections of MgO with poor crystallinitiy or small particle size, or possibly both [28]. Previous work [31] demonstrated that these mixed oxides have a chemical composition following the formula $Mg_6Al_2O_{9-(x+y)}(OH)_{2x}(CO_3)$. They could recrystallize as hydrotalcite-like compound after contacting

with carbonate solution. After re-crystallization with carbonate solution, CHT-450 returned to the more ordered state into HT crystal such as shown in Figure 1b. The XRD pattern of HT-650 and HT-850 are shown in Figure 1(c-d). The recrystallized sample was layered double HT with at least a mono-molecular layer described by the distinguished peak at 2θ of less than 20° [32]. The existence of lamellar structures was barely detectable for the samples not contacted with the carbonate solution.

We found that HT calcined at 850 °C were more crystalline in nature, possibly due to aluminum that was progressively incorporated into the MgO network shown by the XRD peaks at 42° and 62.5° (2θ). These peaks can be used to describe the presence of well crystallized MgO-like phase or magnesia-alumina solid phase in this sample. As temperature was increased, more aluminum was included. The peaks of Al_2O_3 phase were small, indicating that Al3+ cations were dispersed in the structure of MgO without the formation of the spinel species [28]. The other peaks (11.4, 22.9, 34.6, 38.9, 45.9, 60.2 and 61.7) correspond to hydrotalcite structure that match with JCPDS file (220700) and previously reported literatures [20-21]. In contrast, at low synthesis temperature, aluminum diffused slowly and did not reach the crystallite core [21].

The peaks at 11.4 and 22.9° were assigned to the (0 0 3) and (0 0 6) reflection, respectively, and could be used to calculate the basal spacing between the layers, *d*. The $d_{(003)}$ spacing values represents the distance between hydrotalcite layers, and therefore changes in this value indicate the effect of anions on the hydrotalcite structure. The $d_{(003)}$ spacing values obtained for the synthetic hydrotalcite are 7.89, 7.85 and 7.92 Å for HT-K@450, HT-K@650 and HT-K@850 respectively. These values appear to be in good agreement with the previously reported literature [18].

Figure 2 shows SEM images taken at 5000 magnification for mixed oxide hydrotalcite and hydrotalcite samples calcined at 850 °C. Figure 2b shows closely packed flakes

resembling lamellar microstructure present in hydrotalcite. The hydrotalcite sample after recrystallization shown in Figure 2b was originated from the CHTs that agglomerated after contact with K_2CO_3 solution and washing.

The EDX result of mixed oxide and recrystallized hydrotalcite at 850 °C is given in Table 2. The 32 g hydotalcite sample that was used constituted Mg (27.32%), Al (9.52%), C (5.85%), O (51.46%) and K (5.85%). The result shows that the sample contained Mg/Al at ratio of 2.87 and K_2CO_3/mixture at 5.85%. The high oxygen content in the sample was possibly due to the presence of magnesium nitrate hexahydrate, aluminum nitrate nonahydrate and potassium carbonate. This was as a result of partial hydrolysis and condensation during contact with the carbonate solution and then syneresis on drying [25]. The elemental potassium showed the strongest energy binding in the hydrotalcite network despite its insignificant amount.

The FTIR spectra of mixed oxide and the hydrotalcite samples is shown in Figure 3. The first band at 3450-3485 cm^{-1} was attributed to brucite-like layers (OH^- streching vibration) corresponding to OH mode, caused by the interlayer water molecules and hydroxyls groups in the brucite-like layers [33]. The peak appears weaker as observed in the 1640-1660 cm^{-1} region due to the H_2O from the interlayer water. These values appear to be in good agreement with the previously reported literature for the sample that was treated at high temperature, indicating that water molecule still exists in the interstices of the mixed oxide sample in order to hold the hydrotalcite structure [33-34]. The broad band around 1375-1387 cm^{-1} peak corresponded to either carbonate or nitrate group or possibly both [35]. However, nitrate was absent from EDX analysis, thus the peak must correspond to carbonate. The peaks at 1015-1020 and 877-867 cm^{-1} correspond to covalent carbonate. Bands at around 575-630 cm^{-1} correspond to the characteristic vibration of the metal oxides (Mg-O and Al-O) [21].

3.2 *Catalytic activity measurements*

The calcination temperature influences transesterification by changing the surface basicity of the resulting Mg(Al)O hydrotalcite. This was proven from a variety of physico-chemical characterization of the hydrotalcite materials [22-23, 35]. To determine whether calcination temperature affects the catalytic activity of our sample, we run methanolysis of jatropha curcas oil, using HT calcined at different temperatures. The result is displayed in Figure 4. From the results it is shown that calcination temperature affected the catalytic activity rather significantly. The conversion of jatropha oil increased up to 72.5% when the calcination temperature reached 850 °C.

During combustion to prepare the CHT-X, the heat released per mole of burned sugar (saccharose) was 5635 kJ/mol. This energy was available to decompose the magnesium and nitratre salts and produce an oxide network. The enthalpy required to form Mg-O and Al-O bonds was 363.2 and 511 kJ/mol, respectively. CO_2 and H_2O were produced from the combustion of $C_{12}H_{22}O_{11}$. The released CO_2 and H_2O from the combustion formed the Mg, Al-oxide periclase like structure. In fact, CO_2 was considered as a probe molecule of oxide surfaces to enable various form of adsorption. This may explain why the layered structure could still be formed in the sample even without sodium carbonate [21].

The yield of methyl ester increased with increase in the amount of the fuel used (data did not shown). The yield of methyl ester increased almost logarithmically and the maximum conversion was obtained when 20wt.% of saccharose was used, beyond which, the conversion started to decline. The highest yield was possibly due to the higher content of C and H in order to form complexes with the metal ions [25].

From this information, we selected HT sample prepared using Mg/Al ratio of 3.0, 20wt.% of saccharose as fuel, calcined at 850 °C to be used in the next transesterification of jatropha oil with methanol.

3.3 Transesterification reaction

The molar ratio of methanol to vegetable oil is one of the most important variables affecting biodiesel formation because the conversion and the viscosity of the produced ester depends on it. When mass transfer is limited due to problems of mixing in which the mass transfer rate becomes slower than the reaction rate, the conversion can be elevated by introducing excess amount of methanol to shift the equilibrium to the right. Higher molar ratios result in greater ester conversions in a shorter time [28]. In this work, the initial stoichiometric molar ratio of methanol to oil of 3.0 was selected.

Figure 5a shows the effect of methanol/oil molar ratio on the conversion. As shown in this figure, by increasing the methanol amount, the conversion was increased considerably. The conversion reached the maximum value when the methanol to jatropha oil molar ratio was close to 12:1, beyond which the ester conversion dropped.

The rate of methanolysis reaction was also strongly influenced by the reaction temperature. Increasing reaction temperature not only increases reaction kinetics, but also improves phase miscibility. Phase miscibility is important in a potentially diffusion-limited process. Faster kinetic process and shorter residence times can be achieved by increasing reaction temperature. However, the use of higher temperatures requires not only greater energy consumption, but also higher system pressure to keep methanol in the liquid phase, which leads to increased reactor cost [36]. Commonly, the methanolysis is conducted close to boiling point of methanol at atmospheric pressure. In this work, the effect of reaction

temperature on the ester conversion was studied with the catalyst at five reaction temperatures, i.e. 55, 60, 65, 70, 75 °C.

In Figure 5b, the conversion versus reaction temperature is presented. The results indicate that the reaction rate was slow at low temperature, where the conversion was merely 48.5% in a 6 h reaction at 55 °C. Lower temperatures resulted in a drop of the ester conversion because only a small amount of molecules was able to get over the required energy barrier [28]. The ester conversion increased with the increase of reaction temperature up to 75.3% in 6 h reaction at 65 °C. But the conversion fell to about 67% in the temperature range of 70-75 °C. The primary advantage of higher temperature was a shorter reaction time. However, if the reaction temperature exceeded the boiling point, the methanol vaporized and formed a large number of bubbles, inhibiting the reaction on the three-phase interface. Therefore, the optimum temperature for the preparation of the ester was found to be 65 °C, which was near the boiling point of anhydrous methanol.

Generally, a higher concentration of catalyst drives the reaction equilibrium to the product side. It also increases the rate of reaction, thus resulting in higher productivity [9]. The amount of solid catalyst should be balanced between the reactivity and viscosity of the reaction system [37]. Increasing catalyst amount may not increase production yield, because the fluid becomes heavily viscous at some point, giving rise to a problem of mixing and a demand of higher power consumption for adequate stirring. On the other hand, when the catalyst amount is not sufficient, maximum conversion cannot be reached [6, 38].

The effect of the catalyst concentration on the jatropha oil conversion is shown in Figure 5c. As expected, the oil conversion increased with the catalyst concentration. Due to their intrinsic lower activity compared with the homogeneous catalysts, significantly higher concentrations of the heterogeneous transesterification catalysts are required [39], especially when using low-quality feedstocks such as used frying oil (10-12wt%) [40-41]. However, the

conversion decreased with further increase of catalyst amount, which was possibly due to mixing problem of reactants, products and solid catalyst discussed earlier. The maximum ester conversion was up to 75.2% when 4wt.% catalyst was used. This is higher than the previously reported experiment with 50% conversion, longer reaction time of 24 h at 60°C using MgO derived hydrotalcite [41].

4. Conclusion

Mg-Al hydrotalcite-like compounds were synthesized following combustion method using saccharose as fuel. The samples were mostly metal oxides on combustion. They returned to a more ordered hydrotalcite-like structure after contacting with carbonate solution. The re-crystallized hydrotalcite was used for the transesterification of jatropha oil with methanol. The catalytic performance was found to be significantly affected by pretreatment and operating conditions. The re-crystallized hydrotalcite gave the best catalytic activity for transesterification of jatropha oil when 20wt.% of saccharose was used as fuel to facilitate chemical reaction on combustion at 850 °C. Optimum reaction conditions were obtained with methanol/oil ratio of 12:1, 4wt.% catalyst for 6 h reaction at 65 °C to achieve methyl ester conversion of about 75.2%.

Acknowlegdements

The authors gradefully acknowlegde the University Sains Malaysia for providing the University Research grant for this project.

References

[1]. Moser BR. Biodiesel production, properties, and feedstocks. In Vitro Cell Dev Bio Plant. 2009;45;229-66.

[2]. Leung DCY, Wu X, Leung MKH. A review on biodiesel production using catalyzed transesterification. App Energy. 2010;87(4);1083-95.

[3]. Gui MM, Lee KT, Bathia S. Feasibility of edible oil vs. non-edible oil vs. waste edible oil as biodiesel feedstock. Energy. 2008;33;1646-53.

[4]. Pinzi S, Garcia IL, Lopez-Gimenez FJ, Luque de Castro MD, Dorado G, Dorado MP. The ideal vegetable oil-based biodiesel composition: a review of social, economical and technical implications. Energy Fuel. 2009;23;2325-41.

[5]. Om Tapanes NC, Gomes Aranda GA, de Mesquita Carneiro JW, Ceva Antunes OA. Transesterification of Jatropha *curcas* oil glycerides: Theoretical and experimental studies of biodiesel reaction. Fuel. 2008;87;2286-93.

[6]. Vicente G, Martınez M, Aracil J. Integrated biodiesel production: a comparison of different homogeneous catalysts systems. Bioresour. Technol. 2008;92;297–305.

[7]. Fukuda H, Konda A, Noda N. Biodiesel fuel production by transestirification of oils. J. Biosci. Bioeng. 2001;92;405–16.

[8]. Stavarache C, Vinatoru M, Nishimura R, Maed Y. Fatty acids methyl esters from vegetable oil by means of ultrasonic energy. Ultrasonic Sonochem. 2005;12;367–72.

[9]. Antolin G, Tinaut FV, Bricerio Y, Castano V, Perez C, Ramirez AI. Optimization of biodiesel production by sunflower oil transesterification. Bioresour. Technol. 2002;83(2);111-4.

[10]. Lang X, Dalai AK, Bakshi NN, Reaney MJ, Hertz PB. Preparation and characterization of bio-diesel from various bio-oils. Bioresour. Technol. 2001;80;53–62.

[11]. Al-Widyan MI, Al-Shyoukh AO, Experimental evaluation of the transesterification of waste palm oil into biodiesel. Bioresour. Technol. 2002;85;253–6.

[12]. Meher LC, Sagar DV, Naik SN. Technical aspects of biodiesel production by transesterification: a review. Renew. Sustain. Energy Rev. 2006;10;248–68.

[13]. Corma A, Abd Hamid S, Iborra S, Velty A. Lewis and bronsted basic sites on solid catalysts and their role in the synthesis of monoglycerides. J. Catal. 2005;234;340-7.

[14]. Hak JK, Bo SK, Min JK, Young MP. Transesterification of vegetable oil to biodiesel using heterogeneous base catalysts. Catal. Today. 2004;93;315–20.

[15]. Kiss AA, Omota F, Damian AC, Rothenberg G. The heterogeneous advantages biodiesel by catalytic reactive distillation. Topic. in Catal. 2006;40;141-50.

[16]. Kiss AA, Omota F, Damian AC, Rothenberg G. Biodiesel by catalytic reactive distillation powered by metal oxides. Energy & Fuel. 2008;22;598-604.

[17]. Helwani Z, Othman MR, Aziz N, Kim J, Fernando WJN. Solid heterogeneous catalysts for transesterification of triglycerides with methanol: A review. Appl. Catal. A: Gen. 2009;363(1-2);1-10.

[18]. Palmer SJ, Frost LR, Nguyen T. Thermal decomposition of hydrotalcite with molybdate and vanadate anions in the interlayer. J. Thermal Anal. Calorimetry. 2008;92(3);879-86.

[19]. Othman MR, Helwani Z, Martunus, Fernando WJN. Synthetic hydrotalcites from different routes and their application as catalysts and gas adsorbents: a review. Appl. Organometallic Chem. 2009;23;335-46.

[20]. Cavani F, Trifiro F, Vaccari A. Hydrotalcite-type anionic clays: preparation, properties and application. Catal. Today. 1991;11;173–301.

[21]. Davila V, Lima E, Bulbulian S, Bosch P. Mixed Mg(Al)O oxides synthesized by combustion method and their recrystallization to hydrotalcites. Micropor. Mesopor. Mater. 2008;107;240-6.

[22]. Di Cosimo JI, Díez JV, Xu M, Iglesia E, Apesteguía CR. Structure and surface and catalytic properties of Mg-Al basic oxides. J. Catal. 1998;178;499–510.

[23]. Xie WL, Peng H, Chen LG, Calcined Mg–Al hydrotalcites as solid base catalysts for methanolysis of soybean oil. J. Mol. Catal. A: Chem. 2006;246;24–32.

[24]. He J, Wei M, Li B, Kang Y, Evans DG, Duan X. Preparation of layered double hydroxides. Structure Bond. 2006;119;89-111.

[25]. Martunus, Othman MR, Fernando WJN. Elevated temperature carbon dioxide capture via reinforced metal hydrotalcite. Micropor. Mesopor. Mater. 2011;138;110-7.

[26]. Liu Y, Lotero E, Goodwin Jr J, Mo X. Transesterification of poultry fat with methanol using Mg-Al hydrotalcite derived catalysts. Appl. Catal. A: Gen. 2007;331;138-48.

[27]. Cantrell DG, Gillie LG, Lee AF, Wilson K. Structure-reactivity correlations in MgAl hydrotalcite catalysts for biodiesel synthesis. Appl. Catal. A: Gen. 2005;287;183-90.

[28]. Zeng HY, Feng Z, Deng X, Li YQ. Activation of Mg-Al hydrotalcite catalysts for transesterification of rape oil. Fuel. 2008;87(13-14);3071-6.

[29]. Zeng HY, Deng X, Wang YJ, Liao KB. Preparation of Mg-Al hydrotalcite by urea method and its catalytic activity for transesterification. AICHE, 2009;55(5);1229-35.

[30]. Jitputti J, Kitiyanan B, Rangsunvigit P, Bunyakiat K, Attanatho L, Jenvanitpanjakul P. Transesterification of crude palm kernel oil and crude coconut oil by different solid catalysts. Chem. Eng. J. 2006;116;61-6.

[31]. Martinez-Gallegos S, Martinez V, Bulbulian S. Chromium (IV) separation from tannery wastes utilizing hydrotalcites. Sep. Sci. Technol. 2004;39;667-81.

[32]. Othman MR, Kim J. The study of the conversion of intercalated compounds synthesized from a sol gel procedure. J. Sol-gel Sci. Technol. 2008;47;274-82.

[33]. Othman MR, Rasid NM, Fernando WJN. Effect of thermal treatment on the micro-structures of co-precipitated and sol-gel synthesized Mg-Al hydrotalcites. Micropor. Mesopor. Mater. 2006;93;23-8.

[34]. Jitianu M, Zaharescu M, Balasoiu M, Ivanov A, Jitianu A. Comparative study of sol-gel and coprecipitated Ni-Al hydrotalcites. J. Sol-gel Sci. Technol. 2000;19;453-7.

[35]. Prinetto F, Ghiotti G, Graffin P, Tichit D. Synthesis and characterization of sol-gel Mg/Al and Ni/Al layered double hydroxides and comparison with co-precipitated samples. Micropor. Mesopor. Mater. 2000;39;229-47.

[36]. Huaping Z, Zongbin W, Yuanxiao C, Ping Z, Shije D, Xiaohua L, Zongqiang M. Preparation of biodiesel catalyzed by solid Super base of calcium oxide and its refining process. Chinese J. Catal. 2006;27;391-6.

[37]. Lee DW, Park YM, Lee, KY. Heterogeneous base catalysts for transesterification in biodiesel synthesis. Catal. Survey Asia. 2009;13;63-77.

[38]. Tomasevic AV, Siler-Marinkovic SS. Methanolysis of used frying oil. Fuel Proc. Technol. 2003;81;1–6.

[39]. Arzamendi G, Campo I, Arguinarona E, Sanchez M, Montes M, Gandia LM, Synthesis of biodiesel with heterogeneous NaOH/alumina catalysts: Comparison with homogeneous NaOH. Chem. Eng. J. 2007;134;123-30.

[40]. Brito M, Borges ME, Gari M, Hernandez A. Biodiesel production from waste oil using Mg-Al layered double hydroxide catalysts. Energy Fuel. 2009;23;2952-8.

[41]. Georgogianni K, Katsoulidis AP, Pomonis PJ, Kontominas ME. Transesterification of soybean frying oil to biodiesel using heterogeneous catalysts. Fuel Proc. Technol. 2009;90;671-6.

List of figure

Table 1

The properties of Jatropha oil

Parameter	
Spesific gravity, g/mL	0.912 (15 °C)
Viscosity, mm2/s	8.72 (40 °C)
Acid number, mg KOH/g	6.4
Pour point (°C)	-2
Water content (wt.%)	0.135
Flash Point (°C)	125

Table 2

Chemical composition of mixed oxide of hydrotalcite and hydrotalcite at 850 °C from EDX analysis

Sample	Weight (g)	Mg/Al in analysis	Chemical composition, %wt				
			Mg	Al	O	C	K
HT oxide@850	28	2.87	27.32	9.52	51.46	5.85	5.85
HT@850	13	2.89	28.03	9.38	52.67	4.96	4.96

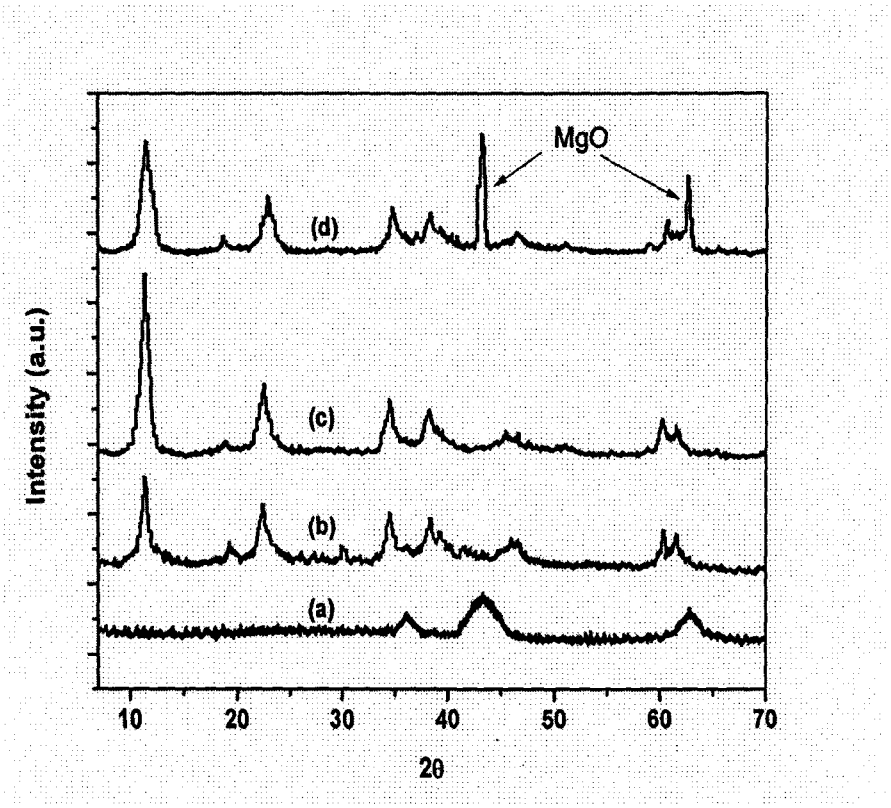

Figure 1. XRD pattern of (a) mixed oxide at 450 °C, (b) hydrotalcite at 450 °C (c) hydrotalcite at 650 °C and (d) hydrotalcite at 850 °C.

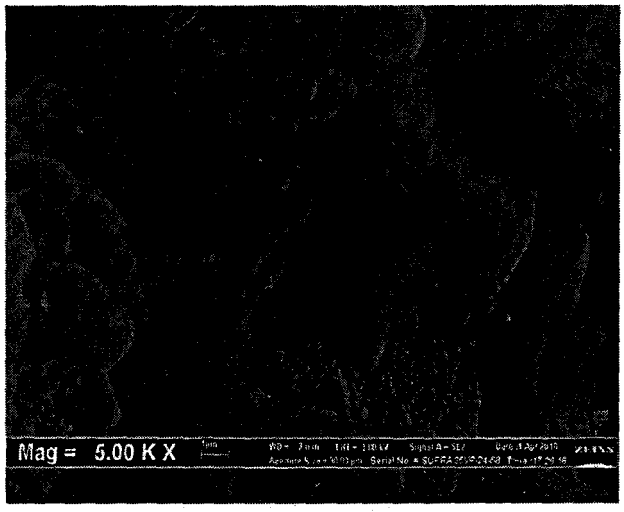

(a)

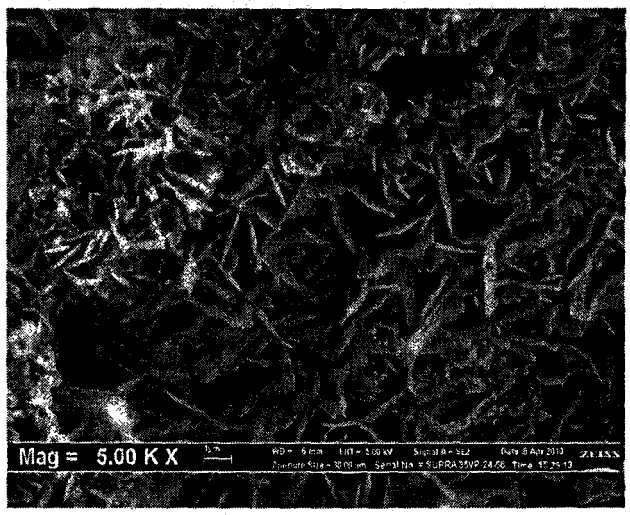

(b)

Figure 2. SEM images of (a) mixed oxide, (b) hydrotalcite at 850 ^{o} C.

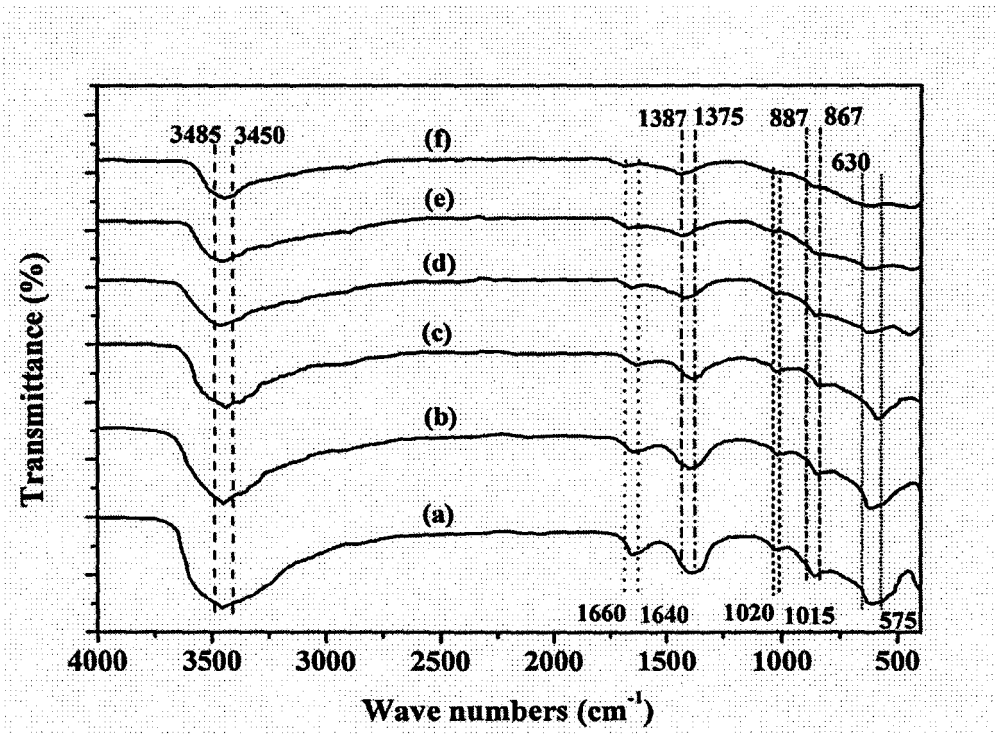

Figure 3. FTIR spectra of (a-c) hydrotalcite: (a) at 450 °C, (b) at 650 °C, (c) at 850 °C and (d-f) mixed oxide: (d) at 450 °C, (e) at 650 °C, (f) at 850 °C.

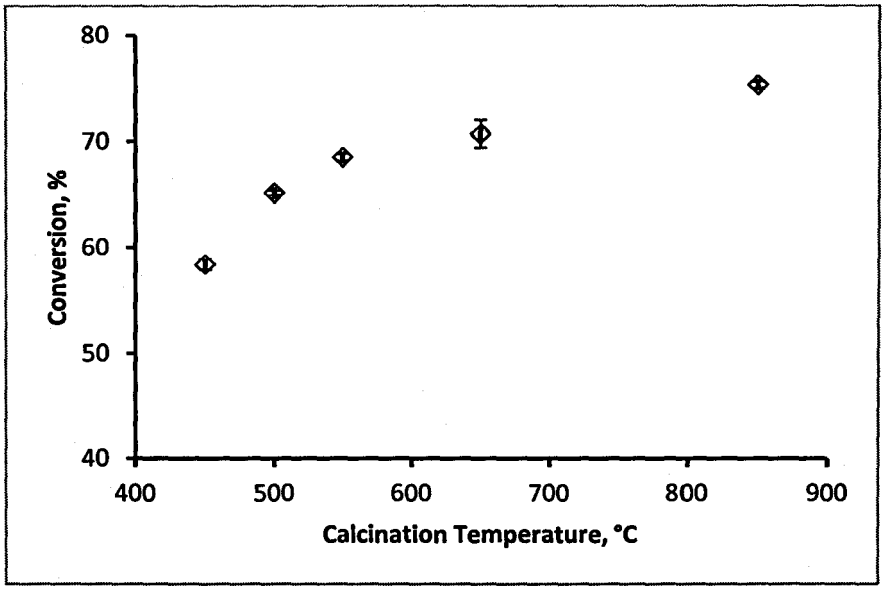

Figure 4. Effect of calcination temperature on the conversion. Reaction conditions : methanol to oil molar ratio 12:1, catalyst amount 4wt.%, reaction temperature 65 °C and reaction time 6h

a

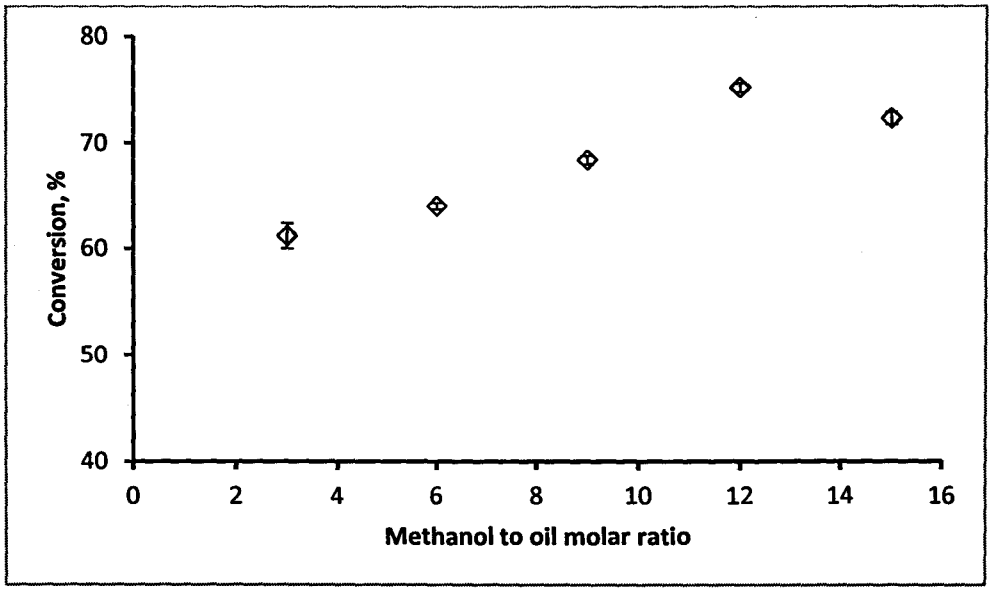
80
70
60
50
40
Conversion, %
0
2
4
6
8
10
12
14
16
Methanol to oil molar ratio

b

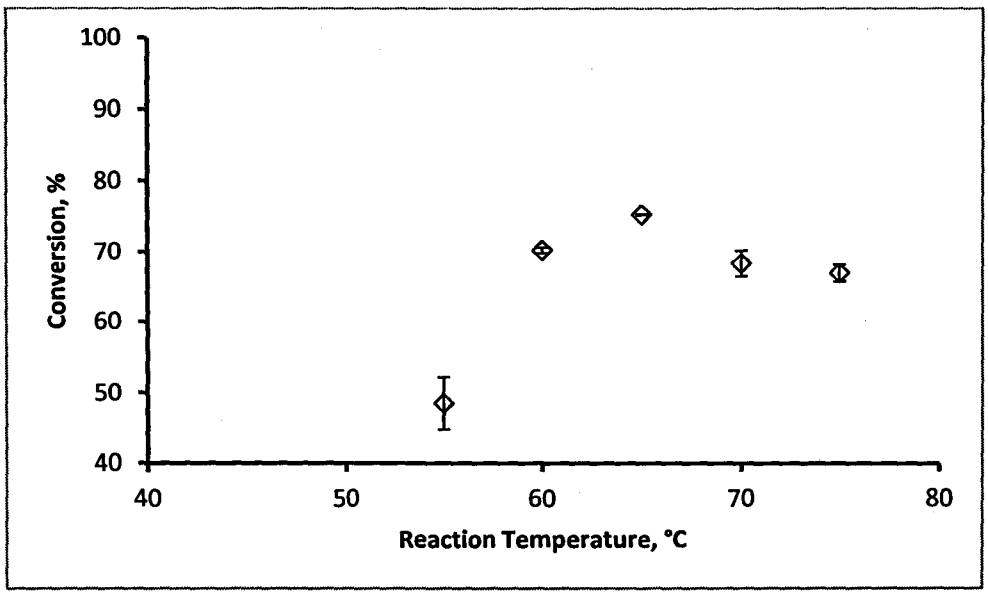
100
90
80
70
60
50
40
Conversion, %
40
50
60
70
80
Reaction Temperature, °C

c

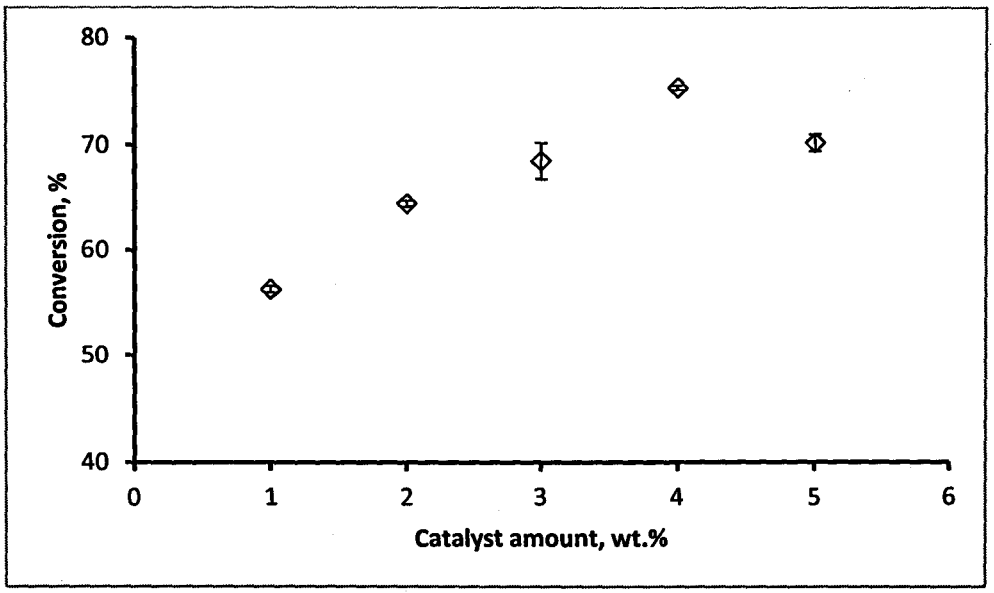

Figure 5. Effects of variables on biodiesel yield: a) methanol to oil molar ratio (Reaction temperature = 65 °C, catalyst amount = 4wt.%), b) temperature (Molar ratio methanol/oil = 12:1, catalyst amount = 4wt.%), and c) catalyst concentration (Reaction temperature = 65 °C, molar ratio methanol/oil = 12:1)

Study on the use of Mg/Al hydrotalcites synthesized by sol-gel method as solid heterogeneous catalysts for transesterification of Jatropha oil with methanol

Z. Helwani[a,b], N. Aziz [b], M.R. Othman*, [b]

[a]Department of Chemical Engineering, Riau University

Pekanbaru 28293, Indonesia.

[b]School of Chemical Engineering, Universiti Sains Malaysia

14300 Nibong Tebal, Penang, Malaysia.

*Corresponding author

Email: chroslee@eng.usm.my

Tel: (60)-45996426

Fax: (60)-45941013

Abstract

This paper reports experimental work on the use of new heterogeneous solid basic catalysts for transesterification of jatropha oil to biodiesel. The Mg/Al hydrotalcite produced by sol-gel method and calcined at high temperature was used in the study. The trans-esterification variables were reaction temperature, reaction time, molar ratio methanol to oil and catalyst loading. Results from this study reveal that individual as well as interaction between variables affected the conversion of FAME rather significantly. Mg/Al hydrotalcite calcined at 500 °C yielded FAME conversion of 91.3% at only 65°C of reaction temperature and ambient pressure. The molar ratio methanol:oil used was 9:1, catalyst loading of 3wt.% and 6 h of reaction time.

Keywords: solid heterogeneous catalyst, hydrotalcite, sol-gel, jatropha oil, biodiesel

Introduction

Biodiesel is defined as alkyl esters of fatty acids produced from vegetable oils and animal fats. There has been an increasing interest in biodiesel as a green and alternative fuel as a result of recent legislations that require a major reduction of vehicle emissions, as well as the soaring price of petroleum [C.C.C.M. Silva, 2010].

Biodiesel can be produced through transesterification of vegetable oils and fats with methanol in the presence of a suitable catalyst [Ma and Hanna, 1999]. The transesterification reaction can be carried out using both acidic and basic (homogeneous or heterogeneous) catalysts [Lopez, 2005]. Among these, base catalysts are more active for transesterification reaction. Homogeneous catalysts have its own demerits as it is considerably costly to separate it from the reaction mixture and is not environmentally benign [Lopez, 2005]. Tan et al. (2010) reported a catalyst-free biodiesel production method, using waste palm cooking oil as raw material and supercritical methanol. But the method has a high cost in reactor and operation (due to high pressures and high temperature), and high methanol consumption (e.g., high methanol/oil molar ratio of 40/1) [Tan et al., 2010].

In contrast, heterogeneous catalysts are easily removed from the reaction mixture, making the purification step easier and can provide green and recyclable catalytic systems. Biodiesel production costs could certainly be reduced by using a heterogeneous catalyst for transesterification reaction instead of a homogeneous catalyst [Cantrell, 2005].

Hydrotalcite (HT) is a natural occurring anionic clay. The most common formula hydrotalcite-like compounds or layered double hydroxides (LDHs) is $[(M^{2+}_{(1-x)}M^{3+}_{x}(OH)_2)^{x+}.(A^{n-}_{x/n}\ nH_2O)^{x-}]$ where M^{2+} is a di-valent cation (Mg^{+}, Ca^{2+}, Zn^{2+}, Cu^{2+}, Co^{2+}, Ni^{2+} or Mn^{2+}), M^{3+} is a three-valent cation (Al^{3+}, Fe^{3+} or Cr^{3+}). The layers are positively charged as M^{3+} cations substitute M^{2+} cations. This charge is balanced by A anions with charge n-, for instance OH^{-}, Cl^{-}, NO_3^{-}, CO_3^{2-} or SO_4^{2-}, among others and x is normally between 0.17 and 0.33. The anions have a remarkable mobility and are able to participate to anionic exchange. Carbonates (CO_3^{2-}) are generally the preferred anion [Othman, 2009] and they have been widely described in the literature [Othman, 2009; Cavani, 1991]. As classical solid base materials, calcined LDHs are widely used as catalyst in the production of biodiesel [Brito et al., 2009; Xie et al., 2006; Cantrell et al., 2005; Barakos et al., 2008; Shumaker et al., 2008; Deng et al; 2011; Zeng et al., 2008; 2009; Navajas, 2011].

HTs are usually obtained by the coprecipitation method at constant pH using appropriate metallic salts [He, 2006]. The solids obtained by this method are crystalline and exhibit surface areas between 10 and 120m^2/g [Lazaridis, 2004]. Although the HTs obtained by the sol–gel method are more expensive than those obtained from the coprecipitation method, the sol–gel method allows for the preparation of a more homogeneous and less crystalline HTs. Furthermore, HTs obtained by the sol–gel method exhibit higher thermal stability than those obtained by the coprecipitation method [Fetter, 1997]. HTs have also been synthesized by the sol–gel method in order to control and modify their

textural, thermal and structural properties [Ramos, 1997]. The sol–gel method involves the hydrolysis of metal alkoxides and has been used for the preparation of hydrotalcites containing different M(II) and M(III) metals such as Cr/Ni [Jitianu, 2003a], Zn/Al [Tichit, 2005], Co/Al [Wang, 2007], Mg/Cr [Jitianu, 2003b] and Al/Mg [Othman, 2006; Paredes, 2006]. The specific surface area of the solids obtained with the sol-gel method was higher by three fold than that achieved by co-precipitation [Aramendia et al., 2002; Jitianu et al., 2000; Bolognini et al., 2003; Prinetto et al., 2000; Othman et al., 2006].

Most of the studies were focused on the usage of pure vegetable oils for biodiesel production and very few studies have been reported on non-edible oils like used frying oil, grease, tallow and land [Alcantara, 2000]. Apart of these, there exit a number of other non-edible tree based oil seeds such as jatropha and karanja. The conversion of these non-edible oils into biodiesel has been studied using mostly homogeneous alkali solutions as catalyst [Tiwari, 2007], whereas reports on these transformations using heterogeneous solid base catalysts are scarce. Thus, the development of a solid basic heterogeneous catalyst to carry transesterification of oils proficiently under mild reaction conditions in short reaction times still remains an intriguing challenge.

The purpose of this work is to synthesize hydrotalcite by sol-gel method. The synthesized particles, after calcination were used as solid basic catalyst in the transesterification of jatropha oil with methanol to test their activities in batch reactor. Experiment under different reaction conditions, such as methanol/jatropha oil molar

ratio, catalyst amount, reaction time and reaction temperature, were performed in order to optimize fatty acid methyl esters (FAME) content.

Experimental

Materials and Chemicals

Jatropha *curcas* oil was supplied by *Indonesian Spice and Industrial Crops Research Institute* (Sukabumi, Indonesia). Methanol and *n*-hexana were purchased from R & M Marketing, Essex, UK and Merck, respectively. Pure methyl esters such as methyl palmitate, methyl stearate, methyl oleate and methyl linoleate were obtained from Fluka Chemie, Germany. The purities of all these esters were above 99.5% and they were used as reference standards for Gas Chromatography, GC analysis.

HT preparation

For sol gel method, an appropriate ratios of aluminium tri-sec-butylate ($C_{12}H_{27}AlO_3$) and magnesium methoxide $(CH_3O)_2Mg$ were mixed with hot ethanol respectively. The Mg/Al atomic ratio in the solution was selected as 3:1. It would be wise to hydrolyze the alkoxides separately for approximately 30 minutes to optimize the hydrolyzation process of the solution, under vigorous stirring at 70-90 °C to form sol (Huang et al. 1997 and Prinetto et al. 2000). Then, 9.5ml 1M potassium carbonate (K_2CO_3) was added to the mixture, followed by peptization of the sol using molar composition of the alkoxide, acid and water at 1:0.07:100 (Yoldas, 1975 and Huang et al. 1997), and be stirred until homogeneity. For binder addition, polyvinyl alcohol (PVA) (4g PVA/100ml H_2O) was added. The peptized sol is allowed to cool steadily for prolongation of hydroxylation,

alkoxilation or condensation. The solution was refluxed at 353 K up to 16 hours until the gel was formed. The mixture was then filtered using a vacuum pump. Subsequently, the filtrate was dried in an oven at 90 °C for 4 hours and then calcined in programmable carbolite furnace and heated from 450-850 °C with 6-15 hours (Egger et al., 1991) to obtain mixed oxides.

Extraction and the properties of jatropha oil

Prior to the extraction process, jatropha oil seeds were dried over night at 60 °C in an oven to remove excess moisture. The dried seeds were then weighed and grounded into fine particles. The oil was then extracted using Soxhlet extractor with *n*-hexana as solvent. The duration for each batch of extraction was fixed at 8 h while the volume of solvent per kilogram of seed was fixed at 5 L. The oil was recovered using rotary evaporator. Then, the properties of the oil such as fatty acid composition (%), moisture content (%w/w), acid value (m_{KOH}/m_{oil}, mg/g), saponification value (m_{KOH}/m_{oil}, mg/g) and density of jatropha oil were analyzed according to Malaysian Palm Oil Board, MPOB standard by My CO_2 Sdn. Bhd., Malaysia. The average molecular weight was calculated from the acid value and saponification value of jatropha oil using the following formula; M = 56.1 x 1000 x 3(SV – AV), where AV is the acid value and SV is the saponification value.

Characterization

Base strength of the samples (H_) was determined by using Hammett indicators [Xie, 2006]. About 300 mg of the sample was shaken with 1 mL of a solution of Hammett

indicators diluted in 10 mL methanol and left to equilibrate for 2 h after which no further colour changes were observed. The colour on the catalyst was then noted. The following Hammett indicators were used: bromthymol Blue (H_=7.2), phenolphthalein (H_=9.8), 2,4-Dinitroaniline (H_=15.0). The base strengths are quotes as being stronger than the weakest indicator that exhibits a colour change, but weaker than the strongest indicator that produces no colour change.

The crystallization phases were studied using XRD. The analysis was carried out using Philips Goniometer PW 1820 diffractometer, PW 1710 diffraction controller and X-ray generator PW 1729. The diffractometer was used with monochromatized CuK_{α} radiation and taken in the range of 10-70° (2θ). The X-ray tube was operated at 40 kV and 120 mA.

The surface morphology of the hydrotalcite powder was analyzed by SEM from Germany, model Leo Supra 50 VP Field Emission. Samples were placed in the sample grid for electron reflection and vacuumed (5 min) before analysis.

An infrared (IR) spectrum of hydrotalcites was obtained using FTIR spectrophotometer (Perkin Elmer FTIR 2000, USA). Samples were prepared by mixing the powdered solids with potassium bromide, KBr (the blank) in a 15:85 ratio to get transparent pellet auto supported on the different solids at 8 ton pressure. The infrared spectra were recorded both over the wave number range from 500 to 4000 cm^{-1}.

The surface area, pore volume and pore size distribution of the hydrotalcite catalyst (sample) were determined using Micromeritics ASAP 2000 V2.05. Prior to this analysis, the sample was degassed (2 hours) under vacuum at 300 °C. After degassing, the sample was transferred to the analysis system where it was cooled in liquid nitrogen (-196 °C). A 21-points analysis was carried out to obtain the nitrogen adsorption-desorption isotherm by admitting successive known volumes of nitrogen in and out of the sample and measuring the equilibrium pressure.

Biodiesel production

Jatropha *curcas* oil and an appropriate volume of methanol with HT catalysts were placed into a 500 ml three-angel necked flask equipped with reflux condenser and Teflon stirrer. The reaction mixture was blended for a period time at 55-75 °C temperature under atmospheric pressure. Molar ratio of methanol to oil was taken at 3-15:1. After reaction, the methanol was recovered by a rotary evaporator in vacuum at 45 °C. Subsequently, the catalyst was separated by filtration and the ester layer was separated from the glycerol layer in a separating funnel. The upper layer of the sample was separated from the bottom layer and immediately quenched with *n*-hexane (dilution) prior to analysis of FAME content. Methyl heptadecanoate was used as internal standard.

Analysis

The analysis of jatropha FAME in the samples and references were carried out using Gas Chromatography Flame Ionization Detector (GC-FID) which was equipped with Nukol^{TM} column (15 mm x 0.53 mm, I.D. 0.5 μm film). Helium was used as the carrier

gas. Oven temperature at 110 °C was initially hold for 0.5 min and then increased to 220 °C (hold 15 min) at a rate of 10 °C min^{-1}. The temperatures of the injector and detector were set at 220 °C and 250 °C, respectively. A quantity of 1 µl from each sample was injected into the column. FAME obtained was calculated using the EN 14103 application note (the recommended standard for obtaining total FAME content in biodiesel).

Result and discussion

Properties of jatropha oil

The characterization results of jatropha oil revealed that it contains 0.161 %w/w moisture content and acid value 20.8 m_{KOH}/m_{oil}. The density of the oil was 0.9037 g/ml and it contains 14.2% palmitic acid, 0.7% palmitoleic acid, 7.0% stearic acid, 44.7% oleic acid and 32.8% linoleic acid. The saponification value (193.55 m_{KOH}/m_{oil}) was found to be small, indicating high concentration of triglycerides, and therefore jatropha oil can be a suitable feedstock for the production of biodiesel. Experimental result showed that jatropha oil seeds have free fatty acid content 6.34%. The very high free fatty acid content of the jatropha oil pre-indicates that homogeneous transesterification method is unsuitable to convert jatropha oil to fatty acid methyl esters (biodiesel).

Catalyst characterization

The crystallization degree and purity of sol-gel LDHs strongly depended on the synthesis conditions, which should be more strictly controlled than in the coprecipitation method. By thermal decomposition of the LDHs, homogeneous mixed oxide structures

can be achieved, exhibiting peculiar properties, such as high specific surface areas and narrow pore size distributions. These features can deeply influence the catalytic properties [Prinetto, 2000].

The X-ray diffraction patterns for the calcined HT products are shown in **Figure 1**. As can be seen, calcination destroyed the layered structure, yielding a periclase MgO phase from all samples. The diffraction pattern of the HT shows the characteristic diffraction peaks of hydrotalcite (JCPDS 22-0700) and small diffraction peaks corresponding to the brucite-type phase (JCPDS 7-239). This result confirms that this sample has a double layered structure with a low degree of crystallization. On the other hand, the XRD pattern corresponding to HT calcined to 450 °C exhibited strong peaks corresponding to the hydrotalcite type material and weak signals of the brucite-type phase. Finally, the diffraction pattern of the HT calcined at 650 °C shows the presence of the periclase (JCPDS 4-0829) and hydrotalcite phases. Thus, the as-obtained product contains a hydrotalcite phase mixed with a small amount of brucite phase.

The infrared spectra of the aforementioned HT solids are shown in **Fig. 2**. In the HT spectrum the band at 3700 cm^{-1} can be attributed to a high energy stretching vibration of the hydroxyl groups of brucite [Zhang et al., 2005]. The broad absorption band centered at 3436 cm^{-1} is due to the stretching vibration of the hydroxyl groups from water and residual ethanol. The medium intensity band at 1607 cm^{-1} corresponds to the hydroxyl bending mode of adsorbed water. A scissor type vibration of C-H bonds is present at 1523 cm^{-1} and can be attributed to alkoxide residues still occluded in the fresh sample.

The characteristic vibrations of the interlayer CO_3^{2-} ion are found at 1471 and 657 cm^{-1} and that of residual free CO_3^{2-} ion is found at 1400 cm^{-1}. Three additional bands at 1195, 1095 and 1019 cm^{-1} can be assigned to Mg-O and Al-O stretching vibrations. The low intensity band at 928 cm^{-1} can be attributed to stretching vibrations of hydroxyl groups [Kloprogge et al., 2004; Labajos et al., 1992]. The band at 614 cm^{-1} can be assigned to the superposition of deformational vibration of Al-OH or Mg-OH and the characteristic condensed $[AlO_6]^{3-}$ band is observed at 414 cm^{-1} [Valcheva, 1993].

The FTIR spectrum of the solid calcined at 550 °C shows the same bands as the HT. At this temperature, the solid maintains its chemical structure. On the other hand, the spectrum of the solid calcined at 650 °C exhibits low intensity and broad absorption peak, indicating that the structure of the HT has changed. The broad band of the hydroxyl groups of brucite and the stretching vibration of hydroxyl groups from the sheet structure can be observed at 3700-3436 cm^{-1}. The medium intensity band at 1606 cm^{-1} corresponds to the hydroxyl bending mode of adsorbed water. The low intensity peak at 1398 cm^{-1} is characteristic of the interlayer CO_3^{2-} ion. Therefore, it can be concluded that carbonate is the interlaminate anion in the HT and that this anion is eliminated at temperatures up to 450 °C. At 450 °C the structure of the HT changes. These results are confirmed by XRD analysis (fig. 1).

Catalytic activity measurements

During calcination the decomposition of hydrotalcites occurs resulting in formation of mixed Mg-Al oxides phases. The influence of calcination temperature on the catalyst

activity is shown in **Figure 4**. The FAME content was found to range from 60.8% to 91.2%. From the results obtained, it is shown that calcination temperature affected significantly the catalytic activity. With the rise of calcination temperature from 450 to 500 °C, the FAME content increased gradually and came up to the maxima of 91.2% when the calcination temperature was 500 °C. However, when calcination temperature was higher than 500 °C, the FAME content dropped considerably. Almost zero FAME content of jatropha FAME was obtained using catalysts prepared at calcination temperature of 850 °C. This indicated that the catalytic properties of catalyst began to lose after calcination temperature at 500 °C. This behavior could be due to the lost of active components in the catalyst prepared at higher calcination temperature. Other factor that could contribute to the decreased catalytic performance of the catalysts prepared at higher calcination temperature is the deformation of the catalyst.

The calcination period also affected the catalytic performances of the catalyst but less significant compared to that of calcination temperature (data not shown). Nevertheless, it was observed that catalysts prepared at longer period produced slightly higher FAME content than those catalysts prepared at shorter calcination period. The highest content was produced using catalysts prepared at calcination period between 12 to 15 hours. The FAME content was decreased at shorter calcination period (less than 12 hours) could due to phase change of the catalysts, which eventually alter and reduce its catalytic performance.

Transesterification reaction

The molar ratio of methanol to oil was one of the important factors that affected the methyl esters content. Stoichiometrically, 3 mole of methanol were required for each mole of jatropha oil. However, in practice, methanol to oil molar ratio should be higher than that of stoichiometry in order to drive the reaction toward completion and produce more methyl esters. Because jatropha oil was immissible with methanol, the reaction was incomplete and limited by diffusion and thermodynamic process. So, excessive methanol should be used to promote the reaction. Higher molar ratio over the stoichiometric value resulted in a high rate of esters formation and could ensure complete reaction (Leung and Guo, 2006). However, it was observed that at molar ratio above 9:1, excessive methanol had no significant effect on the FAME content. Conversely, a longer time was required for the subsequent separation stage because separation of the esters layer from glycerol was difficult due to the fact that methanol with one polar hydroxyl group could emulsify the products (Liu, et al., 2010).

Several synthesis were tested with increasing values of mass catalyst (1-4wt.%), with molar ratios methanol to oil of 6:1 to 12:1. This series of tests was performed using hydrotalcite calcinated at 500 °C, a reaction temperature of 65 °C and reaction time 6 h. The results are shown in **Figure 5**, where it can be noticed that an increase of the molar ratio methanol to oil favors the transesterification reaction with a minimum amount of catalyst of 1wt.% of oil mass, with a molar ratio of 12:1. When a lower amount of methanol is used, it is necessary to compensate with more amount of catalyst, but the mixture inside the reactor shows higher viscosity, thus providing more resistance to

mass transfer and diminished the yield of the reaction. With a molar ratio methanol to oil of 6:1, the yield increases with the increase of catalyst loading, but for a molar ratio of 12:1, the yield is favored with a lower amount of catalyst. The molar ratio of 9:1 showed the best results as yielded 91.3% FAME, using only 3wt.% mass of catalyst.

Interaction between reaction temperature and reaction time (molar ratio of methanol to oil was fixed at 9, catalyst loading was fixed at 3wt.%) was found to significantly affect the FAME content. The results are shown in **Figure 6.** At shorter reaction time (2h), when the transesterification reaction was carried out at 55 °C, the yield was only 44.8%. However, the conversion increased to 66.1% when the reaction temperature was increased to 65 °C. The same trend was observed at 6h of reaction time but the magnitude of the increase in FAME content was more pronounced at this longer reaction time which is from 66.5% to 91.4%. In another words, reaction time has a more significant effect on the conversion at higher reaction temperature. At lower reaction temperature, there is no sufficient energy to promote extensive collisions among reactant particles. Therefore, increasing the reaction time did not contribute to any significant increase in the FAME content. However, at higher reaction temperature, the possibility of collision among the reactant particles became greater since now reactants can easily obtain the necessary activation energy. Thus if given longer contact time, most of the reactants will collide and react to give higher conversion.

The interaction between reaction temperature and molar ratio of methanol to oil molar ratio (reaction period was fixed at 6 h, catalyst loading was fixed at 3wt.%) are shown in

Figure 7. The FAME content was found to increase with increasing reaction temperature and molar ratio of methanol to oil. However, the effect of molar ratio of methanol to oil is greater at higher reaction temperature. Hence, at lower reaction temperature (60 °C), the yield obtained was only 63.7 and 70.8 wt.% (only 7.1 wt.%) for increasing molar ratio of methanol to oil at 3 to 9. However, the FAME content increased sharply as temperature rose and reached 67.8% and 91.2% at 65 °C by increasing molar ratio of methanol to oil from 3:1 and 9:1. There is a 23.4wt.% increase in the yield of biodiesel. At lower reaction temperature, again there is no sufficient energy to promote extensive collision among the reactants. Therefore, even by increasing the amount of reactants available by increasing the molar ratio of methanol to oil do not bring much benefit to the conversion. However, at higher temperature, most of the reactants have more energy, resulting to more collisions and reaction and therefore increasing the amount of reactants now have more positive effect on the FAME content.

The calcined hydrotalcite as catalyst exhibited high activity because they possessed strong basic sites and a large surface area. The transesterification reaction was strongly affected by catalyst concentration. Without adding catalyst, little reaction occured. When the catalyst concentration increased from 1 to 3wt.%, the FAME content was raised from 35.5% to the maximum yield of 91.2%. The reason was that catalyst concentration rose from 1 to 3wt.% could increase contact between reactants and catalyst. However, when the catalyst concentration increased further above 3wt.%, biodiesel conversion dropped, which was possibly due to a mixing problem involving

reactants, products and solid catalyst. Furthermore, when excessive catalyst was used, the transesterification process was easily emulsified and resulted in hard separation of products.

Apart from that, the FAME content of biodiesel was also affected by the interaction between reaction duration and catalyst loading (reaction temperature was fixed at 65 °C, molar ratio methanol to oil was fixed at 9). The results are shown in **Figure 8.** The yield increases more significantly by increasing catalyst loading as compared to increasing reaction time. It was noticed that at shorter reaction time (2h), FAME content was significantly increased from 68.3 to 83.8 wt.% (increase by 15.5 wt.%) when increasing catalyst loading from 1 to 3 wt.%, respectively. However, the increase was less pronounced (only increase by 12.2 wt.%) at longer reaction time (6h). In another words, the effect of catalyst loading reduced with the increament of reaction time.

This finding can be explained as follows: the solubility of methanol in jatropha oil is limited and thus transesterification reaction can only occur at the interface of the two-phases or on the catalyst active sites. Therefore, at shorter reaction duration, there is not sufficient time for all the reactants to access the active sites especially at low catalyst loading. Thus, when the catalyst loading was increased, the FAME content significantly increases as now the reactants have better access to the active sites. However, at longer reaction time, the amount of catalyst is no longer the limiting factor, as the reactants have more time to access the active sites. Therefore, increasing the catalyst loading at longer reaction time, do not cause that much significant effect on the FAME content.

Conclusion

Hydrotalcite with Mg/Al = 3 was synthesized by sol-gel method. The obtain product contained a hydrotalcite phase mixed oxide with a small amount of brucite phase. The hydrotalcite-like compound and products calcined at 450-850 °C were used for transesterification of jatropha oil with methanol. The conversion of the FAME did vary significantly with the calcination temperature. The maximum conversion of 91.3% was found at the following conditions; 6 h reaction time at 65 °C, methanol to oil molar ratio of 9:1, 3wt.% for catalyst loading.

Acknowlegdements

The authors gradefully acknowlegde the University Sains Malaysia for providing the University Research for this project.

References

Othman MR, Helwani Z, Martunus, Fernando WJN. Synthetic hydrotalcites from different routes and their application as catalysts and gas adsorbents: a review. Applied Organometallic Chemistry 2009;23;335-46.

Cavani F, Trifiro F, Vaccari A. Hydrotalcite-type anionic clays: preparation, properties and application. Catalysis Today 1991;11;173–301.

Xie WL, Peng H, Chen LG, Calcined Mg–Al hydrotalcites as solid base catalysts for methanolysis of soybean oil. Journal of Molecular Catalysis A: Chemistry 2006;246;24–32.

Cantrell DG, Gillie LG, Lee AF, Wilson K. Structure-reactivity correlations in MgAl hydrotalcite catalysts for biodiesel synthesis. Applied Catalysis A: General 2005;287;183-90.

Zeng HY, Feng Z, Deng X, Li YQ. Activation of Mg-Al hydrotalcite catalysts for transesterification of rape oil. Fuel, 2008;87(13-14);3071-6.

Zeng HY, Deng X, Wang YJ, Liao KB. Preparation of Mg-Al hydrotalcite by urea method and its catalytic activity for transesterification. AICHE, 2009;55(5);1229-35.

Othman MR, Rasid NM, Fernando WJN. Effect of thermal treatment on the micro-structures of co-precipitated and sol-gel synthesized Mg-Al hydrotalcites. Microporous and Mesoporous Materials 2006;93;23-8.

Jitianu M, Zaharescu M, Balasoiu M, Ivanov A, Jitianu A. Comparative study of sol-gel and coprecipitated Ni-Al hydrotalcites. Journal Sol-gel Science and Technology 2000;19;453-7.

Prinetto F, Ghiotti G, Graffin P, Tichit D. Synthesis and characterization of sol-gel Mg/Al and Ni/Al layered double hydroxides and comparison with co-precipitated samples. Microporous and Mesoporous Materials 2000;39;229-47.

Brito M, Borges ME, Gari M, Hernandez A. Biodiesel production from waste oil using Mg-Al layered double hydroxide catalysts. Energy & Fuels 2009;23;2952-8.

He J, Wei M, Li B, Kang Y, Evans DG, Duan X. Preparation of layered double hydroxides. Structure Bonding 2006;119;89-111.

N.K. Lazaridis, T.A. Pandi, K.A. Matis, Chromium (VI) removal from aqueous solutions by Mg–Al–CO_3 hydrotalcite: sorption–desorption kinetic and equilibrium studies, Ind. Eng. Chem. Res. 43 (9) (2004) 2209–2215.

G. Fetter, E. Ramos, M.T. Olguin, P. Bosch, S. Bulbulian, Sorption of 131I− by hydrotalcites, J. Radioanal. Nucl. Chem. 6 (1997) 221–223.

E. Ramos, T. Lopez, P. Bosch, M. Asomoza, R. Gomez, Thermal stability of sol–gel hydrotalcites, J. Sol–Gel Sci. Technol. 8 (1997) 437–442.

M. Jitianu, M. Zaharescu, M. Balasoiu, A. Jitianu, New SnO2 nano-clusters obtained by sol–gel route, structural characterization and their gas sensing applications, J. Sol–Gel Sci. Technol. 26 (2003) 483–487.

D. Tichit, O. Lorret, B. Coq, F. Prinetto, G. Ghiotti, Synthesis and characterization of Zn/Al and Pt/Zn/Al layered double hydroxides obtained by sol–gel method, Micropor. Mesopor. Mater. 80 (1–3) (2005) 213–220.

Y. Wang, W. Yang, J. Yang, A Co–Al layered double hydroxides nanosheets thinfilm electrode fabrication and electrochemical study, Electrochem. Solid-State Lett. 10 (10) (2007) 233–236.

M. Jitianu, M. Zaharescu, M. Balasoiu, A. Jitianu, The sol–gel route in synthesis of Cr (III)-containing clays. Comparison between Mg–Cr and Ni–Cr anionic clays, J. Sol–Gel Sci. Technol. 26 (2003) 217–221.

S. Paredes, G. Fetter, P. Bosch, S. Bulbulian, Sol–gel synthesis of hydrotalcite-like compounds, J. Mater. Sci. 41 (11) (2006) 3377–3382.

Barakos, N., Pasias, S., and Papayannakos, N. (2008). Transesterification of triglycerides in high and low quality oil feeds over an HT2 hydrotalcite catalyst. *Bioresource Technology,* **99**, 5037-5042.

Aramendia, M. A., Borau V., Jimenez C., Marinas J. M., Ruiz J. R., and Urbano F. J. (2002). Comparative study of Mg/M (III) (M=Al, Ga, In) layered double hydroxides

obtained by coprecipitation and the sol-gel method. *Journal of Solid State Chemistry*, **168**, 156-161.

Bolognini, M., Cavani, F., Scagliarini, D., Flego, C., Perego, C., and Saba, M. (2003). Mg/Al mixed oxides prepared by coprecipitation and sol-gel routes: a comparison of their physico-chemical features and performances in m-cresol methylation. *Journal of Microporous and Mesoporous Materials*, **66**, 77-89.

Leung, D. Y. C., and Guo, Y. (2006). Transesterification of neat and used frying oil: optimization for biodiesel production. *Fuel Processing Technology*, **87**, 883–890.

Lopez, D. E., Goodwin, Jr J. G., Bruce, D. A., and Lotero, E. (2005). Transesterification of triacetin with methanol on solid acid and base catalysts. *Applied Catalysis A: General*, **295**, 97-105.

Ma, F., and Hanna, M. A. (1999). Biodiesel production: a review. *Bioresource Technology*, **70**, 1-15.

Silva, C. C. C. M., Ribeiro, N. F. P., Souza, M. M. V. M., and Aranda, D. A. G. (2010). Biodiesel production from soybean oil and methanol using hydrotalcites as catalyst. *Fuel Processing Technology*, **91(2)**, 205-210.

Shumaker, J. L., Crofcheck, C., Tackett, S. A., Santillan-Jimenez, E., Morgan, T., Ji, Y., Crocker, M., and Toops, T. J. (2008). Biodiesel using calcined layered double hydroxide catalysts. *Applied Catalysis B: Environmental*, **82**,120–130.

Jitputti J, Kitiyanan B, Rangsunvigit P, Bunyakiat K, Attanatho L, Jenvanitpanjakul P. Transesterification of crude palm kernel oil and crude coconut oil by different solid catalysts. Chemical Engineering Journal 2006;116;61-6.

Ramos-Ramirez, E., Ortega, NLG., Soto, CAC., Gutierrez, MTO., Adsorption isotherm studies of chromium (VI) from aqueous solutions using sol-gel hydrotalcite-like compounds, Journal of Hazardous Materials, 172 (2009) 1527-1531.

List of Figure:

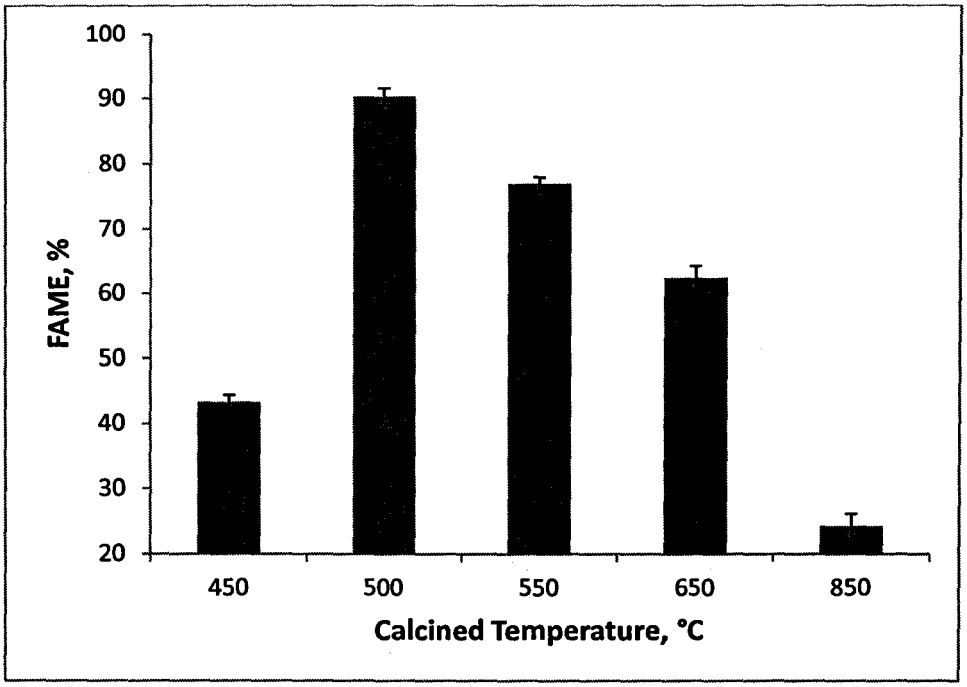

Figure 4 Effect of calcination temperature on % FAME.

Reaction conditions : methanol to oil molar ratio 9:1, catalyst amount 3wt.%, reaction temperature 65 °C and reaction time 6 h

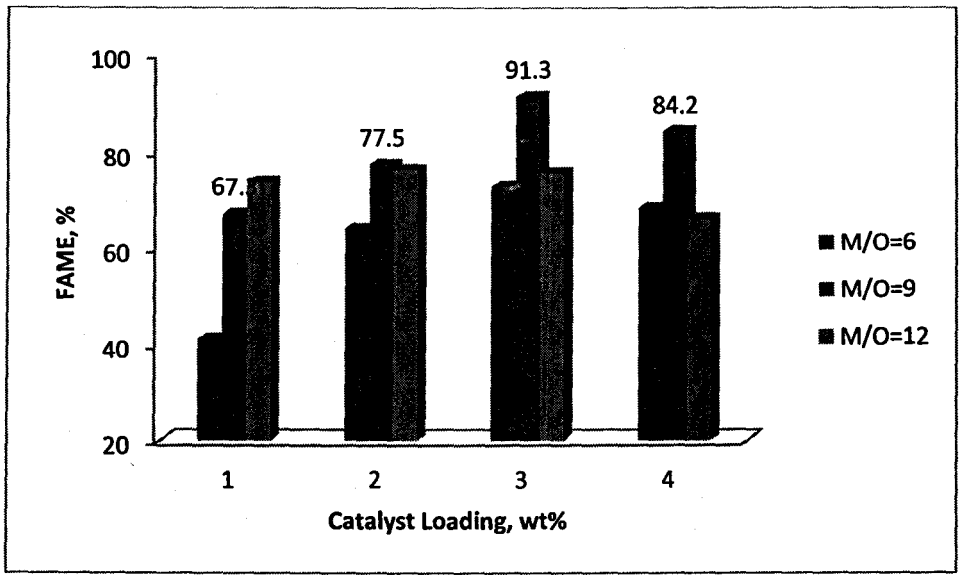

Figure 5 Effect of methanol to oil molar ratio and mass of catalyst on % FAME

(Reaction temperature = 65 °C, reaction time = 6h)

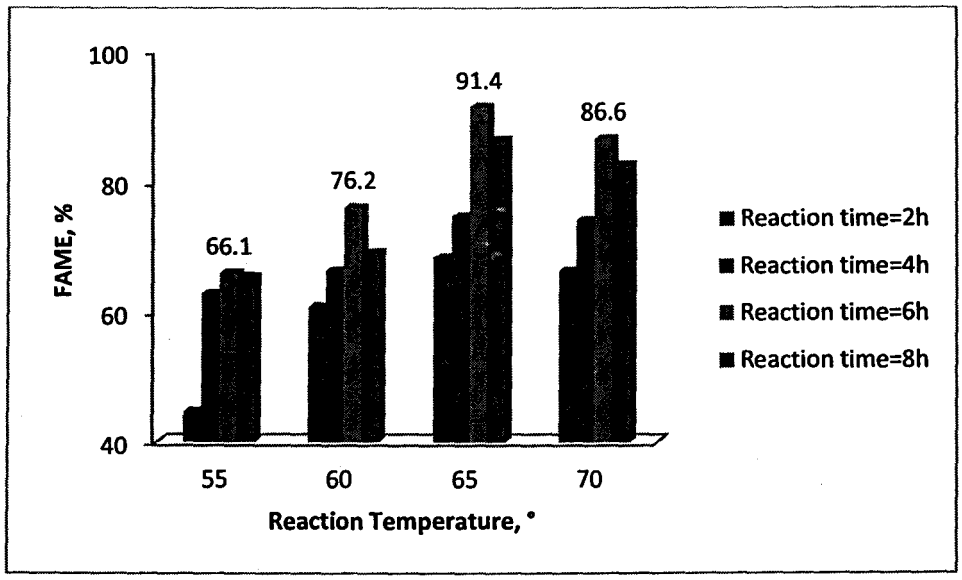

Figure 6 Effect of reaction temperature and reaction time on % FAME

(Molar ratio of methanol to oil = 9, catalyst loading = 3wt.%)

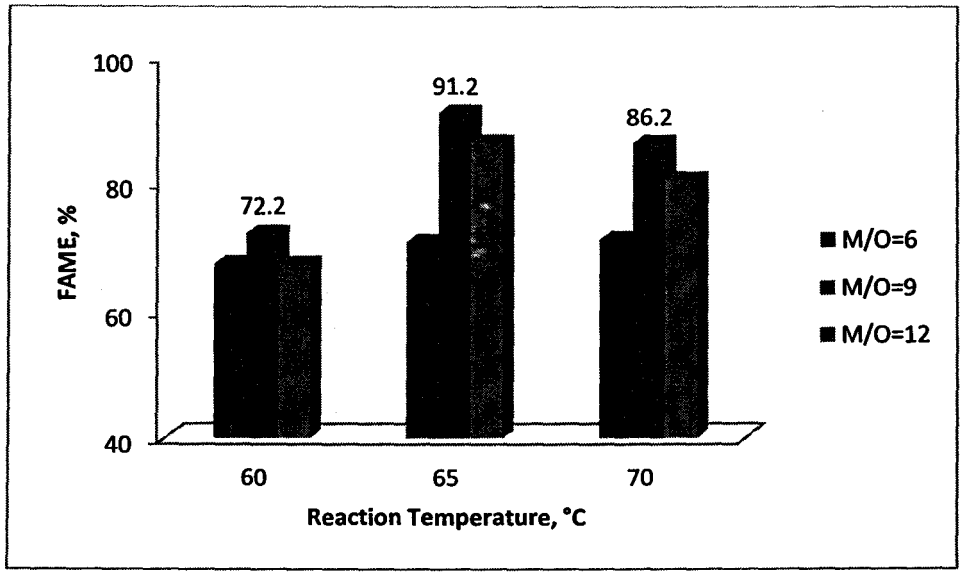

Figure 7 Effect of reaction temperature and molar ratio of methanol to oil on % FAME

(Reaction time = 6h, catalyst loading = 3wt.%)

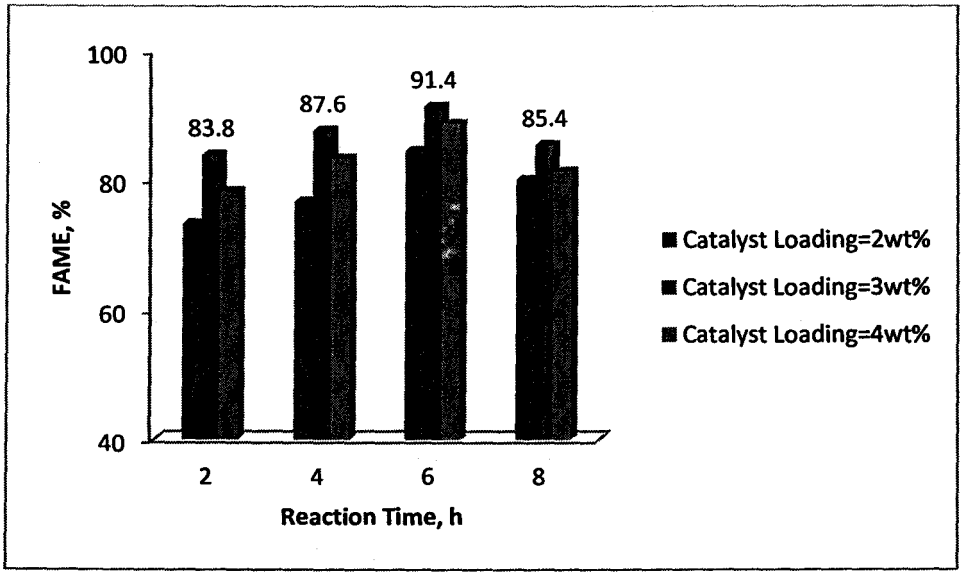

Figure 8 Effect of reaction time and catalyst loading on % FAME

(Reaction temperature = 65 °C, molar ratio of methanol to oil = 9)

Selectivity on different parameters of solid catalysts for biodiesel production: A Review

Z. Helwani[a,b], M.R. Othman[*,b], N. Aziz[b]

[a]Department of Chemical Engineering, Riau University

Pekanbaru 28293, Indonesia.

[b]School of Chemical Engineering, Universiti Sains Malaysia

14300 Nibong Tebal, Penang, Malaysia.

[*]Corresponding author

Email: chroslee@eng.usm.my

Tel: 60)-45996426

Fax: 60)-45941013

Abstract

Heterogeneous catalysts are promising for the transesterification reaction of vegetable oils to produce biodiesel. Unlike homogeneous, heterogeneous catalysts are environmentally benign and could be operated in continuous processes. Moreover they can be reused and regenerated. However a high molar ratio of alcohol to oil, large amount of catalyst and high temperature and pressure are required when utilizing heterogeneous catalyst to produce biodiesel. In this paper, the selectivity of several solid base and acid catalysts, particularly metal oxides and supported metal oxides, was reviewed. The selectivity depended on several factors such as methanol to oil molar ratio, reaction time and temperature, amount of catalyst and type of alcohol. Basically, base catalysis is a better choice than acid catalysis in terms of the reaction rate and biodiesel productivity. If the process needs to be heterogeneous, the reaction rate will be inevitably be decreased and the process requires a high reaction temperature, methanol and catalyst amount to maintain the productivity. Solid acid catalysts were able to do transesterification and esterification reactions simultaneously and convert oils with high amount of FFA (Free Fatty Acids). However, the reaction rate in the presence of solid base catalysts was faster.

Keywords: biodiesel, selectivity, solid base catalyst

1. Introduction

Biodiesel material, mono-alkyl esters of fatty acids derived from vegetable oils or animal fats, is a prime candidate as an alternative fuel for compression–ignition diesel engines [1]. Biodiesel has superior cetane number and lubricity characteristics compared to petroleum middle distillates, with comparable heat of combustion and kinematic viscosity values, and is also non-flammable, making it safer to store and handle. Mono-alkyl esters, particularly mono-methyl esters, are blended with gas oil for use as fuel in diesel engines [2,3].

Different varieties of vegetable oils such as, canola [4], palm [5], *jatropha* [6], palm kernel [7], sunflower [8], and coconut [9] have been studied as precursors for biodiesel production. The main concern about biodiesel production is the high price of vegetable oils compared to that of fossil based diesel fuel. As a result, in some countries, non-edible oils such as *jatropha* or waste cooking oils [10] are preferred from the motivation to use cheap oil sources or meet the regional oil availability, but their irregular chemical composition makes application difficult. In chemical terms, each oil source has a specific composition of fatty acids, as shown in Table 1. The chemical features of fatty acid are collectively described by the carbon number and degree of unsaturation. These features affect the reactivity toward transesterification and, as a result, the properties of the produced biodiesel (alkyl ester). For instance, the fuel properties for biodiesels, melting point and viscosity, increase with increasing carbon number and unsaturation degree [19]. Therefore, the properties of biodiesel will probably be improved by genetic engineering of the parent oil, thereby enriching the fuel with specific fatty acid [20].

Transesterification is one of the most commercially useable methods to produce biodiesel and the process involves a reaction between ester (here triglyceride) and alcohol to form new ester and alcohol. Different types of alcohols such as methanol, ethanol, propanol and buthanol have been used. However, methanol and ethanol are the most widely used,

particularly methanol owing to its low price and availability [21]. The reaction is commonly carried out in the presence of homogeneous and heterogeneous base or acid catalysts, enzymes such as lipase are also used as biocatalysts [22], but the reaction also proceeds under supercritical conditions of methanol without using a catalyst [23]. Sulfonic acid and hydrochloric acid are often used as acid catalysts [24,25], base catalysts include NaOH, KOH, their carbonates, and sodium and potassium alkoxides such as $NaOCH_3$ [24,26,27]. Basically, the reaction will proceed if methoxide ions are present in the reaction solution. Therefore, sodium and potassium methoxides dissolved in methanol can be used as the catalysts. However these compounds are expensive [28]. Figure 1 shows the reaction of triglyceride with alcohol in the presence of a catalyst producing biodiesel (mixture of alkyl esters) and glycerol [29].

Enzymatic base production of biodiesel has attracted many attention in recent years since enzymes tolerate free fatty acid and water contents in the oil to avoid soap formation and thus purification of biodiesel and glycerol is easier [30,31]. Lipases isolated from microorganism catalyze the transesterification of triglycerides, resulting in high-purity biodiesel. In general, it is difficult to reuse such biocatalysts. However, lipase immobilized on a solid material such as porous kaolinite functions as a reusable heterogeneous catalyst [32]. One of the main stumbling blocks for enzymatic transesterification is the deactivation of the enzyme due to the formation of glycerol by the transesterification of triglycerides which blocks the active sites of lipase. This deactivation markedly decreases the activity of lipase and inhibits the reuse of the biocatalyst. Recent studies showed that the active sites of lipase are not blocked by glycerol in the transesterification between triglycerides when methyl acetate is used as an acyl acceptor [33]. The reaction does not produce glycerol but triacetylglycerol, and lipase therefore maintains a high catalytic performance even after repeated reuses. Although the synthesis of acyl acceptors consumed energy, enzymatic

biodiesel production using acyl acceptors appears to be a promising process. However, enzymes are expensive to be used in a commercial production of biodiesel.

The search for new catalysts has been intensely pursued by researchers. The catalyst employed has a direct impact on the purity of the feedstock required, the kinetics of the reaction, and the extent of postreaction processing required. Unfortunately, the prevailing commercial process (base catalyzed batch reactor) has serious limitations and inefficiencies [34] and is prone to unwanted byproduct formation, especially when free fatty acids are present in the lipid feedstock. Furthermore, in both the acid and base catalyzed approaches, conversion efficiency is highly dependent upon the water and free fatty acid content of the feedstocks [35]. The predominant base catalyzed production process requires the use of high quality, high purity virgin oils. The chemistry of the base transesterification reaction in use limits feedstock flexibility due to unwanted side reactions (neutralization reactions) [36,37], and furthermore the currently employed catalysts are not reused so they must be neutralized and discarded as an aqueous salt waste stream. Homogeneous base catalysts provide much faster reaction rates than heterogeneous catalysts in transesterification. However, a large amount of water is required to transfer the catalysts from the organic phase to a water phase [26,33,38]. Therefore, it is considerably costly to separate homogeneous catalysts [39].

Heterogeneous catalysis is an economically and ecologically important field in catalysis research because these catalysts have many advantages: they are non-corrosive, environmentally benign and present fewer disposal problems. They are also much easier to separate from liquid products and they can be designed to give higher activity, selectivity and longer catalyst lifetimes [28,40]. In transesterification reaction, heterogeneous method eliminates the formation of soap, thus omitting the need of wash water. By eliminating the formation of soap, heterogeneous method further prevents formation of emulsion in the mixture which could complicate the separation and purification processes [41]. The catalysts

are not consumed or dissolved in the reaction and therefore can be easily separated from the products. As a result, the products do not contain impurities of the catalyst and the cost of final separation could be reduced. The catalysts can also be readily regenerated and reused and it is more environmentally benign because there is no need for acid or water treatment in the separation step [42].

Attempts to use heterogeneous catalysts in methanolysis have been made by Peterson and Scarrach (1984) [43]. The most recognized problem with the heterogeneously catalyzed process is its slow reaction rate compared with the homogeneous process. Because of the presence of heterogeneous catalysts, the reaction mixture constitutes a three-phase system, oil-methanol-catalyst, which for diffusion reasons inhibits the reaction. For this reason, the reaction conditions of heterogeneous catalysis are intensified to enhance its sluggish reaction rates by increasing reaction temperature (100–250 °C), catalyst amount (3–10 wt.%) and methanol/oil molar ratio (10:1–25:1). In the homogeneous system, the catalyst (NaOH) also acted as a miscibility enhancer between soybean oil and methanol. However, in the heterogeneous system, the reactants were separated into two phases, which seriously retarded the transesterification rate. This problem was effectively solved by the addition of an appropriate co-solvent. Among the hydrocarbons tested, n-hexane, tetrahydrofuran (THF), dimethyl sulfoxide (DMSO), and ethanol were the most effective co-solvent, which transformed the immiscible phases into a homogeneous state and increased the biodiesel yield by 10% [44]. Gryglewicz et al. used CaO as a solid base catalyst for transesterification of rapeseed oil with methanol and after 170 min of reaction time methyl ester yields of 93% were obtained. However, by adding certain amount of THF into rapeseed oil/methanol mixture the same yields of 93% were observed after 120 min of reaction time [28]. However, it should be noted that when co-solvent is used, the processing cost is higher due to the extra processing equipment required for the separation of the co-solvent. Other schemes for

improving oil-alcohol miscibility such as increasing the agitation speed were not as effective as the addition of co-solvent for increasing biodiesel yield. In other studies, the adoption of ultrasonic radiation was reported to be also effective for improving the miscibility between oil and alcohol. Another way to promote mass transfer problems associated with heterogeneous catalysts is using structure promoters or catalyst supports which can provide more specific surface area and pores for active species where they can anchor and react with large triglyceride molecules [45-47].

Another problem of the heterogeneous process is the dissolutions of active species into liquids, which makes the catalysis partly 'homogeneous' and then causes problems in biodiesel quality and limits the repeated utilization of catalyst. Many studies about the use of heterogeneous catalysts for transesterification treated anti-leaching performance as issue of equal importance to catalytic activities. The deactivation mechanism of heterogeneous catalysts towards transesterification can be classified into the leaching of active species and the adsorption of acidic hydrocarbons onto basic sites. The deactivation tests usually take the form of repeating the reaction cycle several times and measuring the catalytic activity in the interval between each cycle. If the deactivation of the catalyst is unavoidable, a method for regenerating its initial activity was suggested in most cases [44]. Nevertheless, the use of heterogeneous catalysts simplifies greatly the technological process by facilitating the separation of the postreaction mixture [28].

Heterogeneous catalysts are of two types–acids and bases. The advantage of using acid heterogeneous catalysts is that they are capable of esterifying the fatty acids in vegetable oil. However, acid catalysts generally exhibit weak catalytic activities and require high reaction temperatures and long reaction times. Another disadvantage is that the reaction is very sensitive to water content in the reaction system. The mechanism of acid-catalyzed transesterification starts from protonation of the carbonyl group of triglyceride and generates

a carbocation intermediate [29], which is readily converted to carboxylic acids in the presence of water [20]. Since this depresses the biodiesel (alkyl ester) yield, the acid-catalyzed transesterification should be operated in the absence of water, in order to slow down the competitive parallel reaction to carboxylic acids. Many acid heterogeneous catalysts have been reported, such as sulfated metal oxide [48,49], heteropolyacid [20], sulphonated amorphous carbon [50], acid ion exchange resin [51,52], etc. On the other hand, base catalysts exhibit high catalytic activities, and a number of basic heterogeneous catalysts have been developed, e.g., metal oxides [53,54], zeolites [55], hydrotalcites [56-61], and anion exchange resins [62]. The solid base catalyst system eliminates the corrosion problems and unwanted waste product formation. However, research studies dealing with the use of solid acid catalysts for biodiesel production have been limited due to the expectations on reaction rates and unfavorable side reactions. An ideal or a model of solid acid catalyst should possess interconnected large porous texture with moderate-to-high concentration of acid sites and a hydrophobic surface. A hydrophobic surface is essential to promote preferential adsorption of oily hydrophobic species on the catalyst surface and to avoid possible deactivation of catalytic sites by the strong adsorption of polar byproducts such as water and glycerol [63]. From the commercial point of view, solid base catalysts are more effective than acid catalysts and enzyme catalyst.

Lee et al [44] claimed that the activity of the heterogeneous catalyst could be increased to that of the homogeneous catalyst by changing the following three reaction conditions: 1) Improvement of oil-methanol miscibility by adding proper hydrocarbon co-solvent; 2) Feeding methanol in the over-stoichiometric amount; 3) Optimization of solid catalyst amount. The research and development on heterogeneous base catalysis for biodiesel synthesis have focused mainly on improving its slow reaction rate up to the level of its homogeneous counterpart. Generally, a higher reaction temperature (100-250 °C) and/or

methanol amount are required for performance of the heterogeneous process to equal that of its homogeneous counterpart, as evidenced in the commercialized Esterfip-H process [64].

A good catalyst must possess both high activity and long-term stability. The selectivity of the reaction product is also important, which reflects its ability to direct conversion of the reactant(s) along one specific pathway. The reaction should produce as much fatty acid methyl ester as possible while minimizing production of mono- or di-glycerides. This paper will review the selectivity and the influence of reaction parameter on selectivity of some solid catalysts for transesterification of triglycerides.

2. Selectivity

The selectivity is the amount of desired product divided by the amount of reactant consumed. This ratio often changes as the reaction progresses, and the selectivity based on the final mixture composition should be called an average selectivity. The selectivity is a very important parameter for many reaction systems. The proper design of a catalytic reactor requires the knowledge of the rate of reaction and the selectivity as a function of the operating conditions [65]. On scaleup from laboratory reactors to pilot-plant units to industrial reactors, slight decreases in selectivity often occur, and these are generally more important than changes in conversion. Decreases in conversion on scaleup may be corrected for by small changes in reaction time or temperature. However, it is not easy to correct for greater byproduct formation, which may mean more difficult product purification as well as greater raw material cost. A few percent decrease in selectivity may be enough to make the process uneconomic. Factors affecting selectivity changes, such as heat transfer, mass transfer and mixing pattern. With consecutive reactions that are affected by mass transfer rates, the selectivity depends on reaction conditions and may change on scaleup [66].

In describing reactor performance, selectivity is usually a more meaningful parameter than reactor yield. Reactor yield is based on the reactant fed to the reactor rather than on that which is consumed. Clearly, part of the reactant fed might the material that has been recycled rather than fresh feed. Because of this, reactor yield takes no account of the ability to separate and recycle unconverted raw materials. Reactor yield is only a meaningful parameter when it is not possible for one reason or another to recycle unconverted raw material to the reactor inlet. By constrast, the yield of the overall process is an extremely important parameter when describing the performance of the overall plant. Unconverted material usually can be separated and recycled later. Because of this, the reactor conversion cannot be fixed finally until the design has progressed much further than just choosing the reactor. The choice of reactor conversion has a major influence on the rest of the process. Nevertheless, some decisions must be made regarding the reactor for the design to proceed. Thus we must make some guess for the reactor conversion in the knowledge that this is likely to change once more detail is added to the total system. Unwanted byproducts usually cannot be converted back to useful products or raw materials. The reaction to unwanted byproducts creates both raw materials costs due to the raw materials which are wasted in their formation and environmental costs for their disposal. Thus rnaximun selectivity is wanted for the chosen reactor conversion [66].

Transesterification consists of a number of consecutive, reversible reactions [67,68]. The triglyceride is converted stepwise into diglyceride, monoglyceride, and, finally, glycerol (Eqs 1–3) in which 1 mole of alkyl esters is removed in each step. The reaction mechanism for alkali-catalyzed transesterification was formulated as three steps [69]. The formation of alkyl esters from monoglycerides is believed to be the step that determines the reaction rate since monoglycerides are the most stable intermediate compound [26].

$$TGs + MeOH \leftrightarrow DGs + MEs \quad (1)$$

$$DGs + MeOH \leftrightarrow MGs + MEs \quad (2)$$

$$MGs + MeOH \leftrightarrow GL + MEs \quad (3)$$

The maximum conversion in reversible reactions is limited by the equilibrium conversion, and the conditions in the reactor are usually chosen to increase the equilibrium conversion. *Le chatelier's principle* dictates the changes required to increase equilibrium conversion. If the system in equilibrium an excess of one of the feeds is added, then the effect is to shift the equilibrium to decrease the feed concentration. In other words, an excess of one feed can be used to increase the equilibrium conversion. Selectivity for consecutive reactions is increased by low concentrations of reactants involved in the secondary reactions. A significant reduction in selectivity is likely as the conversion increases [70].

The overall reaction is also characterized by three control stages: mass transfer, kinetic and equilibrium controlled. The mass transfer stage is the slowest of the three stages due to the poor immiscibility of the two reactants (i.e. methanol and triglycerides). At the completion of the mass transfer stage the process is controlled by the kinetic stage [68,71]. A higher reaction rate can be obtained when higher alcohol to oil ratio is used. However, at higher alcohol/oil ratios the separation of glycerol from ester becomes difficult [72,73]. Both kinetic and mass transfer stages can be improved through the use of higher reaction temperatures and vigorous mixing [71,74,75]. As in any reaction, the increase in temperature increases reaction rate exponentially. An increase in temperature also allows the reactants to be more miscible, thus allowing a higher rate of reaction to take place [76]. In the study of the kinetics of palm oil transesterification in a batch reactor, it was demonstrated that, while the overall conversion of the process did not change with temperature, the rate of the transesterification process was increased with temperature [75]. The overall reaction kinetics is dependent on the individual rate constants for the conversion of triglyceride to diglyceride, monoglyceride and alcohol ester. The conversion of triglyceride to diglyceride was reportedly [74,75] the slowest

reaction in transesterification based on the rate constants. The time needed for the mass transfer to occur was shortened as temperature was increased, leading to a higher rate of transesterification.

3. Influence of reaction parameter on selectivity

Transesterification is the general term used to describe the important class of organic reactions where an ester is transformed into another through interchange of the alkoxy moiety. The transesterification is an equilibrium reaction, and the transformation occurs essentially by mixing the reactants. However, the presence of a catalyst (acid or base) could accelerate and control the equilibrium, to achieve the high yield of the ester [63].

As concerns the operating variables, the alcohol/oil molar ratio, the type of catalyst (acid/base), concentration of the catalyst, purity of the reactants, mainly water content and free fatty acids content in the oil are among the most important. Among these issues, the determination of catalyst is the first step for designing a transesterification system [44]. In a recent study [34,77] using triacetin, they have pointed out that catalyst surface hydrophobicity may play a key factor governing product selectivity in triglycerides transesterification. Temperature has also a strong effect although at atmospheric pressure its value is limited to the normal boiling point of the alcohol used, around 338 K in the case of methanolysis reactions. Because of the transesterification reactions are reversible, an excess of alcohol has to be used with relation to the stoichiometric alcohol/oil molar ratio (3:1). The most suitable alcohol amount may be different from case to case since whereas the biodiesel yield increases with the excess of methanol, production costs rise, reaction volume increases notably and the separation of glycerol becomes more difficult [29,78]. The selectivity of some solid catalyst on different parameter are summarized in Table 2.

3.1. Molar ratio of alcohol to oil

The molar ratio of alcohol to vegetable oil was one of the most important variables that affect ester formation because the conversion and the viscosity of produced ester depended on it. Stoichiometrically, three moles of alcohol are required per mole of triglycerides to produce three moles of mono-alkyl fatty esters and one mole of glycerol. But when mass transfer is limited due to problems of mixing, the mass transfer rate seems to be much slower than the reaction rate, so the conversion can be elevated by introducing excess amount of the reactant methanol to shift the equilibrium to the right-hand side. Theoretically, raising the molar ratio of methanol to oil favors the reaction. Higher molar ratios result in greater ester conversions in a shorter time [68]. But excessive methanol is not favorable for the purification of the as-synthesized biodiesel. Because glycerol, a co-product species of methyl ester, is highly soluble in methanol, the removal of glycerol becomes very difficult with an excessive amount of methanol, which reverses the transesterification progress according to *Le Chatelier's* principle [20]. In addition, much energy is needed to recover the large amount of unreacted methanol. Moreover, methanol can increase the dissolution of vegetable oil, intermediates, and biodiesel, resulting in the wastage of the materials. Increasing the alcohol molar ratio has very limited effect on the conversion rate and fuel properties, but if the viscosity and density of the feedstock are high, the usage of molar alcohol ratios may be useful because more alcohol increases the solubility of the oil in the alcohol and improve the contact between feedstock and alcohol molecules and therefore maximized the yield [79].

The molar ratio is associated with the type of catalyst used. Acid-catalyzed reactions require the use of high alcohol-to-oil molar ratios in order to obtain good product yields in practical reaction times. However, ester yields do not proportionally increase with molar ratio. For instance, for soybean methanolysis using sulfuric acid, ester formation sharply improved

from 77% using a methanol-to-oil ratio of 3.3:1 to 87.8% with a ratio of 6:1. Higher molar ratios showed only moderate improvement until reaching a maximum value at a 30:1 ratio 98.4%) [80].

Zeng (2008) transesterified rape oil at 65 °C with hydrotalcite as a catalyst and found that the ester conversions increased considerably (methanol/oil molar ratio = 3.0: 61.2%, 4.0: 66.8%, 5.0: 79.3%, 6.0: 90.2%, 7.0: 90.8%, 9.0: 90.4%) with increasing the methanol loading amount. The optimum molar ratio of methanol to rape oil was found to be 6.0. Beyond the molar ratio of 6.0, the excessively added methanol had no enhance significantly on the ester conversion [60]. And high molar ratios such as 9.0 or 15.0 were used in the literatures [39,57,58,81]. But, given that transesterification is a reversible reaction, the use of a large excess of alcohol should benefit the conversion of triglycerides from the standpoint of thermodynamics. However, high alcohol-to-lipid molar ratios have been reported to slow down the reaction owing to a diminution in catalyst concentration by the large excess of alcohol [68]. Besides its effect on activity, using a larger excess of methanol should also drive triglycerides transesterification to a greater degree of completion from the standpoint of thermodynamics [77]. However, it is worthy to mention that the use of a large excess of methanol may not be the only or the most efficient way to increase fatty acid methyl ester selectivity.

3.2. Influence of alcohol

Lower alcohols such as methanol, ethanol, propanol, etc. can be employed for transesterification reaction without any significant difference in the yield of the product. The most commonly preferred one is methanol because of its low price than any other commercial alcohols, the reaction rate is higher and physical and chemical advantages (polar and the shortest chain alcohol). It can easily react with triglycerides, and catalyst, can be dissolved

inside it faster compared with the other alcohols. Since the acidities of ethanol and especially branched chain alcohols are low, the reactivities of their reactions with catalysts in order to produce alkoxide anion, which is the real active catalyst in transesterification, are low as well [82]. Because of this, extremely high molar alcohol ratios such as 66:1 need to be used. Moreover, in spite of these unacceptable high alcohol values in terms of the economical point of view, the ester yield is low as well as the amount of contaminants inside the produced ester (biodiesel) fuel such as mono- and diglycerides showing that the reaction is not complete [83-87].

The sort of alcohol used in transesterification is very important since it influences both the reaction kinetics and the fuel properties of the obtained biodiesel. The ester fuel produced contains, in its structure, the bonds of the alcohol used in the transesterification. Thus, both the fatty acid chain and the alcohol portions comprising biodiesel contribute to the overall properties of a fatty ester, and it is whortwhile to consider the properties imparted by other alcohols that could be used for producing biodiesel [88]. However, methanol has a lower boiling point of 64.7 °C and the transesterification reaction is carried out at a temperature which is near to this temperature. Vapours of methanol, which are highly toxic and can cause permanent blindness, are likely to be present near the site of reaction set up. Hence, appropriate measures have to be ensured for the safety of personnel working around. A new technique has been developed by the researchers [89] where alcohol in supercritical condition is used for the completion of transesterification reaction in shorter period of time without using any catalyst. The reason for the shorter time span is that the oil and supercritical alcohol exist in the same phase. In the supercritical transesterification method, a conversion of 50–95% was achieved in first 10 min. Presence of water was a source of interference in catalytic transesterification, whereas, the presence of water had shown a positive affect in methyl ester conversion by supercritical method [87]. In the catalytic supercritical methanol

transesterification method, the yield of conversion rises to 60–90% for the first 1 min. The reaction between sodium methoxide in methanol and a vegetable oil is very rapid; for example, completely transesterified in 4–6 min at room temperature [90]. However, base-catalyzed production of biodiesel requires the use of absolute ethanol because water consumes the catalyst and markedly reduces conversion efficiency of the transesterification reaction. Absolute ethanol is also very hygroscopic and for these reasons it is not widely used for large-scale biodiesel production [91,92]. Furthermore, the use of longer chain alcohols such as ethanol, n-propanol, and n-butanol in biodiesel production has shown to lower the cloud-point of the resulting biodiesel [85,87]. Sreeprasant et al (2008) have used methanol, ethanol, propanol, buthanol, hexanol and octanol to transesterified rubber seed oil and margarine oil at 70 °C with DMC as a catalyst (Fig. 2). While the fatty acid methyl, ethyl, propyl and butyl esters belong to the category of biodiesel, the hexyl and octyl esters are constituents of biolubricants [92].

The fuel qualities of alkyl esters have received varying evaluations in terms of alcohol used. Huber et al. [93] and Saraf and Thomas [94] commented that higher or branched alcohols can produce biodiesel with better fuel characteristics. In contrast, Tyson [95] reported that methyl ester and ethyl ester are similar in heat content, but that the former is slightly less viscous than the latter. Knothe [88] also concluded that methyl ester was better than ethyl ester from the standpoint of engine performance: higher power and torque were achieved from the engine when methyl ester was used as fuel. Narasimharao et al. [20] claimed that higher alkyl esters cause more injector clogging than methyl ester and that their industrial uses are hindered by some technological problems [44].

Canakci and Van Gerpen [86] investigated the effect of different alcohol types on acid-catalyzed transesterification of pure soybean oil. They obtained yields from 87.8% to 95.8% after 48 and 96 h of reaction. Results obtained are summarized in Table 3.

3.3. Reaction temperature and time

Temperature is known to play an important role in biodiesel synthesis. Increasing reaction temperature not only leads to better reaction kinetics, but also improves phase miscibility, important in a potentially diffusion-limited process. Accordingly, one can expect a faster kinetic process and shorter residence times for a batch operation upon increasing reaction temperature. However, the use of higher temperatures requires not only greater energy consumption, but also higher system pressure to keep methanol in the liquid phase, which leads to increased reactor cost [96].

Transesterification can occur in different temperatures depending on the type of oil employed [19,26,54]. Huaping et al (2006) have transesterified *jatropha* oil with CaO as a catalyst. As shown in Fig. 3, raising the reaction temperature favored the transesterification. However, for the reaction system that operated at ambient pressure, it is impossible to raise the reaction temperature further. Therefore, the reaction at 70 °C is appropriate, at which methanol keeps boiling [96].

Lijing Gao et al. (2008) have done the experiment with the reaction temperature was varied between 318 and 348 K. For the same final reaction time, the yield of fatty acid methyl ester (FAME) increased with the increase of the reaction temperature. Being an equilibrium reaction, the equilibrium constant is influenced by temperature and pressure. In addition, their experiments, which were carried out under atmospheric pressure, the former factor, reaction temperature, affected the equilibrium constant. Therefore, as the temperature rose, the conversion of the oil went up. Moreover, because of the solid catalyst used in this reaction, the mass-transfer effect should be concerned. A high temperature is a benefit to the mass transfer. On the basis of the two reasons, in which a high temperature benefit shifted the balance of the reaction to FAME and mass transfer, a higher temperature could obtain a higher yield. However, when the temperature exceeded 338 K, the FAME yield dropped

obviously. The fact that voluminous methanol gasified and reduced the amount of it in the liquid, when the temperature rose over 338 K (the boiling point of methanol), might be the reason of lower yield [81].

The conversion rate increases with reaction time. Because it is a heterogeneous reaction and the mass transfer is slow, no reaction was observed within 30 min. Huaping et al. (2006) have reported that the conversion was low in the first 1 h, however, the conversion increased rapidly afterwards and reached about 92% quickly, as can be seen in Fig. 4. The reaction reached equilibrium after 2.5 h with a conversion of 93%. Too long reaction time resulted in the appearance of a white gel in the product, which increased the viscosity of the product and affected the purification process. Here, one could say that the poor performance of solid base catalyzed vegetable oil or animal fat transesterification at low temperature was more likely associated with the nature of the solid base catalyzed reaction itself rather than with the type of feedstock used. For instance, catalysis by solids of reactions using large molecules can be restricted by limited surface site concentration and steric hindrance of the reactants. The limited surface concentration may be offset by increasing catalyst loading [96].

. However, as pointed out by Di Serio et al. (2006) in their recent study on biodiesel synthesis from soybean oil, metal oxides have a non-uniform distribution of sites with different base strengths on the surface, and basic sites of different strength demand different temperature thresholds to be involved in transesterification [97]. The higher the reaction temperature, the more basic sites are involved in the catalysis. Moreover, the use of high temperature should also help the dynamic equilibrium of triglycerides conformations giving rise to conformers more apt to react [77].

3.4. Catalyst dogase

Generally, a higher concentration of catalyst drives the reaction equilibrium to the product side. It also increases the rate of reaction, thus resulting in higher productivity [98]. The amount of solid catalyst should be balanced between the reactivity and viscosity of the reaction system [44]. Increasing catalyst amount did not guarantee a monotonous increase of production yield, because the fluid became heavily viscous at some point, which inevitably handicapped the system in terms of reaction efficiency, giving rise to a problem of mixing and a demand of higher power consumption for adequate stirring. On the other hand, when the catalyst amount is not sufficient, maximum conversion can not be reached [99,100]. Huaping et al. (2006) have found the effect of the catalyst dosage on the conversion of *jatropha curcas* oil. The results showed that the conversion was over 83% with the catalyst dosage from 0.5% to 2.5%. The dosage of 1.5% peaked the conversion. When the dosage of the catalyst was too much, more products were adsorbed, and the yield of biodiesel decreased [96].

Leclerg et al. (2001) have done the experiment under the following operating conditions: catalyst weight from 0.25 to 2 g, 63 mL of methanol, 5 g of rapeseed oil, methanol-to-oil molar ratio of 275, 22 h of reaction time at methanol reflux, the experimental results concerning the influence of the catalyst weight on ester molar fraction, mass balance, oil conversion, and ester selectivity for the transesterification of rapeseed oil with methanol in the presence of Cs-exchanged NaX are reported in Table 4. The ester molar fraction increases proportionally with the catalyst weight and then reaches a plateau representative of near completion of the reaction. A nearly quantitative yield in ester is obtained after 22 h of reaction for about 2 g of catalyst [101].

Zeng et al. (2008) found that the reaction profiles indicated that the ester conversion increased with the increase of catalyst amount from 0.5% to 1.5% 0.5% w/w of oil: 68.2%, 1.0: 79.5%, 1.5: 90.5%) [60]. However, the conversion decreased with further increase of

catalyst amount (2.0: 85.0%, 2.5: 83.7%), which was possibly due to mixing problem of reactants, products and solid catalyst [57]. The maximum ester conversion reached to 90.5% when 1.5% catalyst was added.

3.5. Mixing

Mixing is very important for the transesterification of vegetable oil, because vegetable oil and methanol solution are immiscible and the reactants and the solid catalyst are separated in the heterogeneous system. Once the two phases are mixed and the reaction is started, stirring is no longer needed. Reaction time was the controlling factor in determining the yield of methyl esters. This suggested that the stirring speeds investigated exceeded the threshold requirement of mixing [53]. Basically, since methanol and vegetable oil are immiscible, the reactants initially form a three-phase system, oil/methanol/catalyst. Accordingly, the methanolysis reaction is diffusion-controlled and poor diffusion between the phases results in a slow rate. Generally, the faster stirring speed causes better contact among the reactants and solid catalyst, resulting in the increase of reaction rate [57,60]. Not much information on mode of stirring is available. However, a better yield with mechanical stirring has been reported than with magnetic mode of stirring [79,102]. In a study on the effect of impeller speed (300–700 rpm) and reaction temperature (25 and 65 °C) on the transesterification of sunflower oil over a 1-min period, it was found that the formation of methyl ester increased as the impeller speed was increased from 300 to 600 rpm. The triglyceride conversion reached its maximum value at 600 rpm. The rate of methyl ester formation was also increased as the reaction temperature increased from 25 to 65 °C [71].

Xie et al (2006) carried out the methanolysis reaction at two randomly chosen stirring speeds (100 and 600 rpm). At lower stirring speed, the oil conversion reached only 34.8% after 9 h of reaction, whereas at 600 rpm the oil conversion reached 65.8% at the same

reaction conditions. This results showed that an efficient mixing of the reagents was essential to reach a high conversion of the oil [57].

Generally, a more vigorous stirring speed causes better contact among the reactants and solid catalyst, resulting in the increase of reaction rate. Zeng et al (2008) have transesterified rape oil with hydrotalcite as a catalyst at 70 °C and the results showed there was no reaction without stirring and stirring had a significant effect on transesterification of oil and methanol (100 rpm: 19.5%, 200: 60.2%, 300: 90.2%, 400: 90.2%, 500: 90.3%). Adding solid catalyst to the reactants while stirring facilitated the chemical reaction, the reaction started quickly. It quickly established a very stable emulsion of oil, methanol and catalyst. The ester conversion increased rapidly with an increase of stirring speeds from 100 to 500 rpm. When the stirring speed was over 300 rpm, there was no significant enhancement in the conversions about (90.2%) [60].

3.6. Basicity Determination of the Catalysts

The activity of a base catalyst may be hypothesized to depend predominantly upon the number and strength of the basic sites. To gain some insight into this effect for the catalysts using different supports, their relative basicity was investigated using a CO_2 chemisorption method. The amount of CO_2 adsorbed per gram of catalyst at 5 and 760 mmHg provides an indication of the relative basic strength and total basic sites, respectively. Although the CO_2 adsorption value does not reflect an actual quantitative basicity of the catalyst, it provides a common comparative measure of basicity among the various catalysts [103]. According to Di Cosimo et al. [104] and Bolognini et al. [105], the weak basic sites correspond to OH^- groups on the surface, the medium strength sites are related to the oxygen in both Mg^{2+}–O^{2-} and Al^{3+}–O^{2-} pairs and the strong basic sites correspond to isolated O^{2-} anions.

Eugena Li and V. Rudolp (2008) investigation the correlation between the conversion and basicity of the catalysts presented in Figure 5. It shows that the activity of a base catalyst does not predominantly depend upon its basic properties. Furthermore, no correlation is found between the activity of the catalysts and any particular one of their properties listed in Table 5. These results suggest that the activity of a base catalyst cannot be attributed to its basicity or any isolated characteristic alone but is likely to be determined by the combined effects of the various attributes of the support material [103]. Ebiura et al. [38] have investigated the methanolysis of triolein over a variety of Li, Na and K salts supported on alumina. They found that the selectivities did no depend on the type of solid-base catalysts, which suggested that the basic strength of the catalysts does not influence the selectivity.

The strongest basic sites (superbasic) promote the transesterification reaction also at very low temperatures (100 °C), while the basic sites of medium strength require higher temperatures to promote the same reaction. The experimental data reported show a correlation not only with the catalyst basicity but also with its structural texture [97]. However, the structural texture of the catalysts examined is dependent on both the precursor and the preparation method [97,106]. Hydrotalcites and their derivatives have attracted much attention recenly, as a good example of catalyst design strategy for basic catalysis [107,108], including catalytic transesterification [109-111]. The main reason for this interest is that the basicity and surface area of the hydrotalcites can be tuned by modifying the chemical composition and preparation procedure. The calcined Mg-Al is prominently featured in the studies, because its catalytic activity for transesterification has been confirmed positively and consistently [56,57,110,112]. The Li-Al hydrotalcites being dehydrated in a proper way under CO_2 free condition have been reported to have stronger Bronsted basicity than the Mg-Al hydrotalcites [112] and some seminal studies implied that Li-Al hydrotalcites are also very promising for biodiesel synthesis [112,113], although more future research is required. The

determining factors for the base-catalyzed activities of hydrotalcites are the Mg/Al ratio and calcination temperature. Mg/Al at a molar ratio of 3 is generally chosen in order to maximize the basic activity, and most calcined hydrotalcites have a medium porosity and surface area due to the decomposition of interlayer carbonates and water. Despite not having a prominent activity, hydrotalcite offer the significant advantage of maintaining their activity in the presence of FFA and water. The incorporation of other active species into the hydrotalcite lattice is expected to hold promise if the activity increases while maintaining the resistivity against FFA and water.

Silva et al (2009) evaluating the effect of Mg/Al ratio on the basicity and catalytic activity for biodiesel production from soybean oil. The basicity of the samples was evaluated from the difference between the CO_2 desorption profile and the decomposition profile (reference). The sample with the highest content of Mg (HT0.20) exhibited the largest number of basic sites. As Al is more electronegative than Mg, with increasing Al/(Mg+Al) ratio there is an increase in the average electronegativity of the catalyst, reducing the electron density of oxygen atoms and consequently reducing the total basicity of the catalyst. It should be emphasized that the HT0.33 sample, although showing the lowest total basicity, was the only one with basic sites of medium strength showing that basic sites of medium strength play a vital role in transesterification reaction [114]. This tendency differs from that observed by Xie et al (2006) [57] using mixed oxides derived from hydrotalcites in methanolysis of soybean oli at methanol reflux temperature. They observed an increase in catalytic activity with increasing Mg/Al ratio up to 3, after that the activity decreased, which was associated with the variation of the catalyst basicity. Di Serio et al (2006) [97], studying calcined hydrotalcites in transesterification of soybean oil, observed that, while at the reaction temperature of 100 °C only strong basic sites are involved, at 180 °C the sites of medium strength are also operative.

3.7. Free fatty acid

The properties of the triglyceride and the biodiesel fuel are determined by the amounts of each fatty acid that are present in the molecules. Chain length and number of double bonds determine the physical characteristics of both fatty acids and triglycerides [115]. Transesterification does not alter the fatty acid composition of the feedstocks and this composition plays an important role in some critical parameters of the biodiesel, as cetane number and cold flow properties [116].

Studies about the influence of the triglycerides composition in the biodiesel quality are scarce. Muniyappa et al. (1996) reported density, viscosity and cloud point of two biodiesels synthesized by soybean and beef tallow oil. The high cloud point of methyl esters from beef tallow oil was indicative of a high concentration of saturated fatty esters [117]. Lang et al. (2001) tested several oils (rapeseed, sunflower, canola and linseed oil) on the biodiesel production and compared some physical and fuel properties of biodiesels with those of conventional diesel fuels [88]. Cardone et al. (2003) reported a comparison of the performance of *B. Carinata* oil-derived biodiesel with a commercial biodiesel and petroleum diesel fuel. This study was centred in the oxidation stability on the basis of linolenic acid content [118]. Dmytryshyn et al. (2004) performed the transesterification of four vegetable oils, comparing properties like density, viscosity, cloud point and pour point, and establishing differences between them. The fatty acid composition suggests that 80–85% of the ester was from unsaturated acids. Substantial decrease in density and viscosity of the methyl esters compared to their corresponding oils suggested that the oils were in their mono or di glyceride form [119]. The feedstock for the synthesis of biodiesel must have a suitable combination of saturated as well as unsaturated fatty compounds to achieve improved oxidation stability and low temperature properties. Sarin et al. (2007) reported some blends of biodiesel from *jatropha* and palm oils to study their physico-chemical properties in order to improve the

oxidation stability. *Jatropha* biodiesel has poor oxidation stability with good low temperature properties. On the other hand, palm biodiesel has good oxidative stability, but poor low temperature properties. The combinations of *jatropha* and palm give an additive effect on these two critical properties of biodiesel [120].

Ramos et al (2009) have study the influence of the raw material composition on biodiesel quality, using a transesterification reaction. Some critical parameters like oxidation stability, cetane number, iodine value and cold filter plugging point were correlated with the methyl ester composition of each biodiesel, according to two parameters: degree of unsaturation and long chain saturated factor. Low cetane numbers have been associated with more highly unsaturated components (C18:2 and C18:3). Polyunsaturated fuels that contain high levels of these components include soybean, sunflower and grape seed oils. In addition, these biodiesels showed high iodine values. Furthermore, the oxidation stability decreased with the increase of the content of polyunsaturated methyl esters. This was not the case for the cold filter plugging point: biodiesels rich in long carbon chain saturated methyl esters showed the worst cold filter plugging point (CFPP) values. Biodiesel of almond, olive, corn, rapeseed and high oleic sunflower oils had the global better properties because they have the greater monounsaturated content [116].

4. Conclusion

Heterogeneous base catalysis is the most viable process for the transesterification of triglyceride into biodiesel. The heterogeneous catalysis features lower corrosiveness, environmental friendliness, easy catalyst recovery and high process integrity, all at levels superior to those of homogeneous catalysis. The research and development on heterogeneous base catalysis for biodiesel synthesis have focused mainly on improving its slow reaction rate up to the level of its homogeneous counterpart. The reaction performances were usually

evaluated in the following respects: what level of FAME yield can be achieved within a given time frame, how low the reaction temperature is and how the methanol/oil molar ratio and catalyst amount can be reduced. Generally, a higher reaction temperature (100–250 °C) and/or methanol amount are required for the performance of the heterogeneous process to equal that of its homogeneous counterparts, as evidenced in the commercialized Esterfip-H process. The selectivity of the reaction product is also important. The reaction should produce as much FAME as possible while minimizing production of mono- or di-glycerides. The selectivity depended on several factors such as methanol to oil molar ratio, reaction time and temperature, amount of catalyst and type of alcohol.

Acknowledgement

The authors acknowledge financial supports from the University Research grant, Universiti Sains Malaysia.

References

[1]. Dunn RO, Knothe G. Alternative diesel fuels from vegetable oils and animal fats. J Oleo Sci 2001;50 415-26.

[2]. Korbitz W. Biodiesel production in Europe and North America, an encouraging prospect. Renewable Energy 1999;16:1078-83.

[3]. Knothe G, Bagby MO. Recent Res Dev Oil Chem 1997;1:63.

[4]. Dalai AK, Kulkarni MG, Meher LC. Biodiesel productions from vegetable oils using heterogeneous catalysts and their applications as lubricity additives, IEEE EIC Climate Change Technology Conference EICCCC art 4057358, **2006**.

[5]. Baroutian S, Aroua MK, Raman AAA, Sulaiman NMN. Density of palm oil-based methyl ester. Journal of Chemical and Engineering Data 2008;53:877–80.

[6]. Tiwari AK, Kumar A, Raheman H. Biodiesel production from jatropha oil (Jatropha curcas) with high free fatty acids: an optimized process. Biomass and Bioenergy 2007;31:569–75.

[7]. Li H, Xie W. Transesterification of soybean oil to biodiesel with Zn/I2 catalyst. Catalysis Letters 2006;107:25–30.

[8]. Arzamendi G, Arguiñarena E, Campo I, Zabala S, Gandía LM. Alkaline and alkaline-earth metals compounds as catalysts for the methanolysis of sunflower oil Catalysis Today 2008;133–135:305-13.

[9]. Tan RR, Culaba AB, Purvis MRI. Carbon balance implications of coconut biodiesel utilization in the Philippine automotive transport sector Biomass and Bioenergy 2004;26:579–85.

[10]. Wang Y, Liu SO, Zhang Z. Preparation of biodiesel from waste cooking oil via two-step catalyzed process Energy Conversion and Management 2007;48:184–88.

[11]. Kumar A, Sharma S. An evaluation of multipurpose oil seed crop for industrial uses (*Jatropha curcas L.*) : A review. Ind Crops and Products 2008;28:1-10.

[12]. Ramadhas AS, Jayaraj S, Muraleedharam C. Biodiesel production from high FFA rubber seed oil Fuel 2005;84:335–40.

[13]. Karmee SK, Chadha A. Preparation of biodiesel from crude oil of *Pongamia pinnata.* Bioresour Technol 2005;96:1425–29.

[14]. Saka S. Production of biodiesel: current and future technology. In: JSPS/VCO Core University program seminar, Universiti Sains Malaysia, September 2005.

[15]. Cocencao M, Candeia R, Silva F, Bezerra A, Fernandez Jr. V, Souza A. Thermoanalytical characterization of castor oil biodiesel Renew. Sustain. Energy Reviews 2007;11:964-75.

[16]. Wikipedia. Soybean: Wikipedia, November 2007. See also: **/http://en.wikipedia.org/wiki/Soybean_oil#OilS.**

[17]. Malaysia palm oil council MPOC). The palm oil. Selangor: MPOC; 2007. See also: /http://www.mpoc.org.my/main_palmoil_02.asp#palmoilS.

[18]. Demirbas A. Biodiesel from vegetable oils via transesterification in supercritical methanol Energy Convers Manage 2002;43:2349–56.

[19]. Pinto AC, Guarieiro LLN, Rezende MJC, Ribeiro NM, Torres EA, Lopes WA, de Pereira PA, de Andrade JB. Biodiesel: an overview Journal of the Brazilian Chemical Society 2005;16:1313–30.

[20]. Narasimharao K, Brown DR, Lee AF, Newman AD, Siril PF, Tavener SJ, Wilson K. Structure-activity relations in Cs-doped heteropolyacid catalysts for biodiesel production. J Catal 2007;248:226–34.

[21]. Xie W, Yang Z. Ba-ZnO catalysts for soybean oil transesterification Catalysis Letters 2007;117:159–65.

[22]. Formo MW. Ester reactions of fatty materials. J Am Oil Chem Soc 1954;31:[redacted]

[23]. Kusdiana D, Saka S. Methyl esterification of free fatty acids of rapeseed oil as treated in supercritical methanol. J Chem Eng Jpn 2001;34:383-87.

[24]. Cotevon A, Vicente G, Martinez M, Aracil J. Biodiesel production from vegetable oils. Influence of catalysts and operating conditions. Recent Res Dev Oil Chem 1997;1:109-14.

[25]. Shimada Y, Watanabe Y, Samukawa T, Sugihara A, Noda H, Fukuda H, Tominaga Y. Conversion of vegetable oil to biodiesel using immobilized Candida antarctica lipase. J Am Oil Chem Soc 1999;76:789-93.

[26]. Ma F, Hanna MA. Biodiesel production: a review. Bioresour Technol 1999;70:1-15.

[27]. Krisnangkura K, Simamaharnnop R. Continuous transmethylation of palm oil in an organic solvent. J Am Oil Chem Soc 1992;62:166–69.

[28]. Gryglewicz S. Rapeseed oil methyl esters preparation using heterogeneous catalysts. Bio Tech 1999;70:249-53.

[29]. Schuchardta U, Serchelia R, Vargas RM. Transesterification of vegetable oils: a review. J Braz Chem Soc 1998;9:199-10.

[30]. Dizge N, Aydiner C, Imer DY, Bayramoglu M, Tanriseven A, Keskinler B. Biodiesel production from sunflower, soybean, and waste cooking oils by transesterification using lipase immobilized onto a novel microporous polymer. Bioresource Technology 2009;100:1983–91.

[31]. Sivozhelezova V, Bruzzeseb D, Pastorinoa L, Pechkova E, Nicolini C. Increase of catalytic activity of lipase towards olive oil by Langmuir-film immobilization of lipase. Enzyme and Microbial Technology 2009;44:72–6.

[32]. Iso M, Chen B, Eguchi M, Kudo T, Shrestha S. Production of biodiesel fuel from triglycerides and alcohol using immobilized lipase. J Mol Catal B: Enzyme 2001;16:53–8.

[33]. Du W, Xu Y, Liu D, Zeng J. Comparative study on lipase-catalyzed transformation of soybean oil for biodiesel production with different acyl acceptors. J Mol Catal B 2004;30:125-29.

[34]. Lopez DE, Goodwin JG, Bruce DA, Lotero E. Transesterification of triacetin with metahnol on solid acid and base catalysts. Appl Catal A: Gen 2005;295:97-105.

[35]. Kusdiana D, Saka S. Effects of water on biodiesel fuel production by supercritical methanol treatment. Bioresour Technol 2004;92:289-95.

[36]. Lotero E, Liu Y, Lopez DE, Suwannakarn K, Bruce DA, Goodwin JG. Synthesis of biodiesel via acid catalysis. Ind Eng Chem Res 2005;44:5353-63.

[37]. Haas MJ, McAloon AJ, Yee WC, Foglia TA. A process model to estimate biodiesel production costs. Bioresour Technol 2006;97:671-78.

[38]. Ebiura T, Echizen T, Ishikawa A, Murai K, Baba T. Selective transesterification of triolein with methanol to methyl oleate and glycerol using alumina loaded with alkali metal salt as a solid-base catalyst. Appl Catal A : Gen 2005;283:111-16.

[39]. Kim HJ, Kang BS, Kim MJ, Park YM, Kim DK, Lee JS, Lee KY. Transesterification of vegetable oil to biodiesel using heterogeneous base catalyst. Catal Today 2004;93:315-20.

[40]. Tanabe K, Hoelderich WF. New Solid Acids and Bases. Appl Catal A : Gen 1999;181:399-34.

[41]. Kansedo J, Lee KT, Bathia S. Biodiesel production from palm oil via heterogeneous transesterification. Biomass and Bioenergy 2009;33:271-76.

[42]. Dossin TF, Reyniers M-F, Berger RJ, Marin GB. Simulation of heterogeneously MgO-catalyzed transesterification for fine-chemical and biodiesel industrial production. Applied Catalysis B 2006;67:136–48.

[43]. Peterson GR, Scarrah WP. Rapeseed oil transesterification by heterogeneous catalysis. J Am Oil Chem Soc 1984;61:1593–97.

[44]. Lee DW. Heterogeneous base catalysts for transesterification in biodiesel synthesis. Catal Surv Asia 2009;13:63-77.

[45]. Ji J, Wang J, Li Y, Yu Y, Xu Z. Preparation of biodiesel with the help of ultrasonic and hydrodynamic cavitation. Ultrasonics 2006;44:e411-e414.

[46]. Stavarache C, Vinatoru M, Maeda Y, Bandow H. Ultrasonically driven continuous process for vegetable oil transesterification. Ultrason Sonochem 2007;14:413-17.

[47]. Hanh HD, Dong NT, Okitsu K, Nishimura R, Maeda Y. Biodiesel production through transesterification of triolein with various alcohols in an ultrasonic field. Renew Energy 2009;34:766-68.

[48]. Furuta S, Matsuhashi H, Arata K. Biodiesel fuel production with solid superacid catalysis in fixed bed reactor under atmospheric pressure. Catal Comm 2004;5:721–23.

[49]. Jitputti J, Kitiyanan B, Rangsunvigit P, Bunyakiat K, Attanatho L, Jenvanitpanjakul P. Transesterification of crude palm kernel oil and crude coconut oil by different solid catalysts. Chem Eng J 2006;116:61–6.

[50]. Toda M, Takagaki A, Okamura M, Kondo JN, Hayashi S, Domen K, Hara M. Biodiesel made with sugar catalyst. Nature 2005;438:178.

[51]. López DE, Goodwin Jr. JG, Bruce DA. Transesterification of triacetin with methanol on Nafion acid resins. J Catal 2007;245:381–91.

[52]. Kiss AA, Dimian AC, Rothenberg G. Solid acid catalysts for biodiesel production – towards sustainable energy. Adv Synth Catal 2006;348:75–81.

[53]. Xie W, Peng H, Chen L. Transesterification of soybean oil catalyzed by potassium loaded on alumina as a solid-base catalyst. Appl Catal A: Gen 2006;300:67-74.

[54]. Meher LC, Kulkarni MG, Dalai AK, Naik SN. Transesterification of karanja Pongamia pinnata) oil by solid basic catalysts. Eur J Lipid Sci Technol 2006;108:389–97.

[55]. Suppes GJ, Dasari MA, Doskocil EJ, Mankidy PJ, Goff MJ. Transesterification of soybean oil with zeolite and metal catalysts. Appl Catal A: Gen 2004;257:213–23.

[56]. Cantrell DG, Gillie LJ, Lee AF, Wilson K. Structure-reactivity correlations in MgAl hydrotalcite catalysts for biodiesel synthesis. Appl Catal A: Gen 2005;287:183-90.

[57]. Xie WL, Peng H, Chen LG. Calcined Mg–Al hydrotalcites as solid base catalysts for methanolysis of soybean oil. J Mol Catal A: Chem 2006;246:24–32.

[58]. Trakarnpruk W, Porntangjitlikit S. Palm oil biodiesel synthesized with potassium loaded calcined hydrotalcite and effect of biodiesel blend on elastomer properties. Renew Energy 2008;33:1558-63.

[59]. Antunes WM, Veloso CO, Henriques CA. Transesterification of soybean oil with methanol catalyzed by basic solids. Catal Today 2008;133-135:548-54.

[60]. Zeng H-Y, Feng Z, Deng X, Li Y-Q. Activation of Mg-Al hydrotalcite catalysts for transesterification of rape oil. Fuel 2008;87(13-14):3071-76.

[61]. Zeng H-Y, Deng X, Wang Y-J, Liao K-B. Preparation of Mg-Al hydrotalcite by urea method and its catalytic activity for transesterification. AICHE 2009;55(5):1229-35.

[62]. Shibasaki-Kitakawa N, Honda H, Kuribayashi H, Toda T, Fukumura T, Yonemoto T. Biodiesel production using anionic ion-exchange resin as heterogeneous catalyst. Bioresour Technol 2007;98:416–21.

[63]. Helwani Z, Othman MR, Aziz N, Kim J, Fernando WJN. Solid heterogeneous catalysts for transesterification of triglycerides with methanol: A review. Appl Catal A – Gen 2009;363(1-2):1-10.

[64]. Di Serio M, Tesser R, Pengmei L, Santacesaria E. Heterogeneous catalysts for biodiesel production Energy and fuel 2008;22:207-17.

[65]. Schuurman Y. Aspect of kinetics modelling of fixed bed reactors. Catalysis Today 2009;138(1-2):15-20.

[66]. Harriot P. *Chemical Engineering Design*, Marcel Dekker, Inc. New York, **2003.**

[67]. Schwab AW, Bagby MO, Freedman B. Preparation and properties of diesel fuels from vegetable oils. Fuel 1987;66:1372–78.

[68]. Freedman B, Butterfield RO, Pryde EH. Transesterification kinetics of soybean oil. J Am Oil Chem Soc 1986;63(10):1375–80.

[69]. Sridharan R, Mathai IM. Transesterification reactions. Sci Ind Resource 1974;33:178-87.

[70]. Smith R. *Chemical Process Design*, Mc. Graw-Hill, Inc. New York, **1995.**

[71]. Vicente G, Martinez M, Aracil J, Esteban A. Kinetics of sunflower oil methanolysis. Ind Eng Chem Res 2005;44(15):5447–54.

[72]. Meher LC, Kulkarni MG, Dalai AK, Naik SN. Transesterification of karanja (Pongamia pinnata) oil by solid basic catalysts. Eur J Lipid Sci Technol 2006;108:389–97.

[73]. Helwani Z, Othman MR, Aziz N, Fernando WJN, Kim J. Technology for production of biodiesel focusing on green catalytic techniques: A review. Fuel proc Tech 2009;90(12):1502-14.

[74]. Noureddini H, Zhu D. Kinetics of transesterification of soybean oil. J Am Oil Chem Soc 1997;74:1457–63.

[75]. Darnoko D, Cheryan M. Continuous production of palm methyl esters. J Am Oil Chem Soc 2000;77(12):1269–72.

[76]. Ma F, Clements LD, Hanna MA. Biodiesel fuel from animal fat. Ancillary studies on transesterification of beef tallow. Ind Eng Chem Res 1998;37:3768–71.

[77]. Liu X, He H, Wang Y, Zhu S, Piao X. Transesterification of soybean oil to biodiesel using CaO as a solid base catalyst. Cat Commun 2007;8:1107-11.

[78]. Meher LC, Vidya SD, Naik SN. Technical aspects of biodiesel production by transesterification—a review. Renew Sust Energ Rev 2006;10:248-68.

[79]. Leung DYC, Guo Y. Transesterification of neat and used frying oil: optimization for biodiesel production. Fuel Proc Technol 2006;87:883–90.

[80]. Lotero E, Goodwin Jr. JG, Bruce DA, Suwannakarn K, Liu Y, Lopez DE. The catalysis of biodiesel synthesis. Catalysis 2006;19:41-83.

[81]. Gao L, Xu B, Xiao G, Lv J. Transesterification of palm oil with methanol to biodiesel over a KF/hydrotalcite solid catalyst. Energy & Fuel 2008;22(5):3531-35.

[82]. Peterson CL. *Production and Testing of Ethyl and Methyl Esters.* Department of Agricultural Engineering, University of Idaho, Moscow, ID, **1994**.

[83]. Lang X, Dalai AK, Bakshi NN, Reaney MJ, Hertz PB. Preparation and characterization of bio-diesel from various bio-oils. Bioresour Technol 2001;80:53–62.

[84]. Freedman B, Pryde EH, Mounts TL. Variables affecting the yields of fatty esters from transesterified vegetable oils. JAOCS 1984;61(10):1638-43.

[85]. Lee I, Lawrence AJ, Hammond EG. Use of branched-chain esters to reduce the crystallization temperature of biodiesel. J Am Oil Chem Soc 1995;72:1155–60.

[86]. Canakci M, Van Gerpen JH. Biodiesel production via acid catalysis. Trans ASAE 1999;42:1203–10.

[87]. Demirbas A. Recent developments in biodiesel fuels. International Journal of Green Energy 2007;4:15–26.

[88]. Knothe G. Dependence of biodiesel fuel properties on the structure of fatty acid akyl esters Fuel Process Technol 2005;86:1059–70.

[89]. Madras G, Kolluru C, Kumar R. Synthesis of biodiesel in supercritical fluids. Fuel 2004;83:2029–33.

[90]. Demirbas A. Comparison of transesterification methods for production of biodiesel from vegetable oils and fats. Energy Conv Manage 2008;49:125-30.

[91]. Roger A, Korus S, Dwight H, Narendra B, Peterson CL, Drown DC. *Transesterification Process to Manufacture Ethyl Ester of Rape Oil*, Department of Chemical Engineering, University of Idaho, Moscow, ID.

[92]. Sreeprasanth PS, Srivastava R, Srinivas D, Ratnasamy P. Hydophobic, solid acid catalysts for production of biofuels and lubricants. Applied Catalysis A: General 2008;314:148-59.

[93]. Huber GW, Iborra S, Corma A. Synthesis of transportation fuels from biomass: chemistry, catalysts and engineering. Chem Rev 2006;106:4044-98.

[94]. Saraf S, Thomas B. Influence of feedstock and process chemistry on biodiesel quality. Process Saf Environ Prot 2007;85(B5):360-64.

[95]. Tyson KS. *Biodiesel, handling and use guidelines*, NREL, Golden, **2001**.

[96]. Huaping Z, Zongbin W, Yuanxiao C, Ping Z, Shije D, Xiaohua L, Zongqiang M. Preparation of biodiesel catalyzed by solid Super base of calcium oxide and its refining process. Chinese J Catalysis 2006;27(5):391-96.

[97]. Di Serio M, Ledda M, Cozzolino M, Minutillo G, Tesser R, Santacesaria E. Transesterification of soybean oil to biodiesel by using heterogeneous basic catalysts. Ind Eng Chem Res 2006;45:3009-14.

[98]. Antolin G, Tinaut FV, Briceno Y, Castano V, Perez C, Ramirez AI. Optimization of biodiesel production by sunflower oil transesterification. Bioresour Technol 2002;83:111–14.

[99]. Vicente G, Martínez M, Aracil J. Integrated biodiesel production: a comparison of different homogeneous catalysts systems. Bioresour Technol 2004;92:297–305.

[100]. Tomasevic AV, Siler-Marinkovic SS. Methanolysis of used frying oil. Fuel Proc Technol 2003;81:1–6.

[101]. Leclercq E, Finiels A, Moreau C. Transesterification of rapeseed oil in the presence of basic zeolite and related solid catalysts. J Am Oil Chem Soc 2001;78(11):1161-65.

[102]. Sharma YC, Singh B. Development of biodiesel from karanja, a tree found in rural India Fuel 2008;87:1740–42.

[103]. Li E, Rudolph V. Transesterification of vegetable oil to biodiesel over MgO-functionally mesoporous catalysts. Energy and Fuels 2008;22:143-49.

[104]. Di Cosimo JI, Díez JV, Xu M, Iglesia E, Apesteguía CR. Structure and Surface and Catalytic Properties of Mg-Al Basic Oxides. J Catal 1998;178:499–510.

[105]. Bolognini M, Cavani F, Scagliarini D, Flego C, Perego C, Saba M. Mg/Al mixed oxides prepared by coprecipitation and sol-gel routes: a comparison of their physico-chemical features and performances in m-cresol methylation. Microporous and Mesoporous Materials 2003;66:77-89.

[106]. Choudary A, Kantam M, Reddy C, Rao K, Figueras F. The first example of michael addition catalysed by modified Mg–Al hydrotalcite. J Mol Catal A: Chemical 1999;146:279-84.

[107]. Cavani F, Trifiro F, Vaccari A. Hydrotalcite-type anionic clays: preparation, properties and application. Catal Today 1991;11:173–301.

[108]. Macala GS, Robertson AW, Johnson CL, Day ZB, Lewis RS, White MG, Iretskii AV, Ford, P.C. Transesterification Catalysts from Iron Doped Hydrotalcite-like Precursors: Solid Bases for Biodiesel Production. Catal Lett 2008;122:205-09.

[109]. Barakos N, Pasias S, Papayannakos N. Transesterification of triglycerides in high and low quality oil feeds over an HT2 hydrotalcite catalyst. Biosource Technol 2008;99:5037-42.

[110]. Corma A, Iborra S, Miquel S, Primo JJ. Catalyst for the production of fine chemicals : Production of food emulsifier, monoglycerides, by glyserolysis of fats with solid base catalysts. J Catal 1998;173:315-21.

[111]. Siano D, Nastasi M, Santacesaria E, Di Serio M, Tesser R, Minutillo G, Ledda M, Tenore T. PCT application no.WO2006/050925, **2006**.

[112]. Corma A, Abd Hamid S, Iborra S, Velty A. Lewis and bronsted basic sites on solid catalysts and their role in the synthesis of monoglycerides. J Catalysis 2005; 234: 340-47.

[113]. Shumaker JL, Crofcheck C, Tackett SA, Santillan-Jimenez E, Crocker M. Biodiesel production from soybean oil using calcined Li–Al layered double hydroxide catalysts. Catal Lett 2007;115:56-61.

[114]. Silva CCCM, Ribeiro NFP, Souza MMVM, Aranda DAG. Biodiesel production from soybean oil and methanol using hydrotalcites as catalyst. Fuel Proc Tech 2009; In Press.

[115]. Mittelbach M, Remschmidt C. *Biodiesel: The Comprehensive Handbook*, Boersedruck Ges. M.B.H., Vienna; **2004**.

[116]. Ramos MJ, Fernadez CM, Casas A, Rodriguez L, Perez A. Influence of fatty acid composition of raw materials on biodiesel properties. Bioresour Tech 2009;100:261-68.

[117]. Muniyappa PR, Brammer SC, Noureddini H. Improved conversion of plant oils and animal fats into biodiesel and co-product. Bioresour Technol 1996;56:19–24.

[118]. Cardone M, Mazzoncini M, Menini S, Rocco V, Senatore A, Seggiani M, Vitolo S. Brassica carinata as an alternative oil crop for the production of biodiesel in Italy: agronomic evaluation, fuel production by transesterification and characterization. Biomass Bioenergy 2003;25:623–36.

[119]. Dmytryshyn SL, Dalai AK, Chaudhari ST; Mishra HK, Reaney MJ. Synthesis and characterization of vegetable oil derived esters: evaluation for their diesel additive properties. Bioresour Technol 2004;9255–64.

[120]. Sarin R, Sharma M, Sinharay S, Malhotra RK. Jatropha–palm biodiesel blends: an optimum mix for Asia. Fuel 2007;86:1365–71.

List of Table

List of Figure

Table 1: Oil composition of various non-edible and edible oil

Fatty acid composition %)	Moleculer formula	Non-edible oil					Edible oil		
		Jatropha (11)	Rubber seed (12)	Castor (15)	*Pongamia pinnata* (13)	Sea mango (14)	Soybean (16)	Palm (17)	Rapessed (18)
Oleic	$C_{18}H_{34}O_2$	43.1	24.6	3.0	44.5-71.3	54.2	23.0	40.0	64.1
Linoleic	$C_{18}H_{32}O_2$	34.3	39.6	4.2	10.8-18.3	16.3	51.0	10.0	22.3
Palmitic	$C_{16}H_{32}O_2$	14.2	10.2	1.0	3.7-7.9	20.2	10.0	45.0	3.5
Stearic	$C_{18}H_{36}O_2$	6.9	8.7	1.0	2.4-8.9	6.9	4.0	5.0	0.9
Linolenic	$C_{18}H_{30}O_2$	-	16.3	0.3	-	-	7.0	-	-
Eicosenoic	$C_{20}H_{38}O_2$	-	-	0.3	9.5-12.4	-	-	-	-
Ricinoleic	$C_{18}H_{34}O_3$	-	-	89.5	-	-	-	-	-
Dihydroxystearic	$C_{18}H_{36}O_4$	-	-	0.7	-	-	-	-	-
Palmitoleic	$C_{16}H_{30}O_2$	-	-	-	-	-	-	-	0.1
Others	-	1.4	-	-	-	2.4	-	-	9.1

Table 2: Selectivity of some solid catalysts on different parameter for biodiesel production

Vegetable oil	Catalysts	Concentration of catalyst, wt.%	Ratio MeOH/Oil	Reaction time, h	Temperature, ^{O}C	Selectivity, %	Reference
Blended vegetable oil	Mesoporous silica loaded with MgO	1 gr	8	5	220	93-96	(103)
Soybean oil	WO_3/ZrO_2, Zirconia-alumina and sulfated tin oxide	4 gr	40	20	200-300	90	(48)
Sunflower oil	CaO/SBA-14		12	5	160	95	(8)
Rapeseed	NaCS(34)X	0.5 gr	275	22	Methanol refluks	90-94	(101)
Jatropha Curcas oil	CaO	1.5	9	2.5	70	92-93	(96)
Rapeseed oil	Mg-Al HT co-precipitation)	1.5	6	4	65	90.5-90.8	(60)
	Mg-Al-HT urea method)	2	6	3	65	92.7-94	(61)
Soybean oil	CaO, SrO	8 3	12	0.5-3	65	95	(77)
Soybean oil	ETS-10	0.03	6	24	120	90-92	(55)
Cotton seed oil	Mg-Al-CO_3 HT	1-3	6	12	180-210	87	(121)

Table 3: The effect of alcohol type on conversion and specific gravity of ester [Canacki van gerpen](86)

Alcohol types	Boiling point (°C)	Reaction temperature (°C)	Ester conversion (%)	Specific grafity of biodiesel
Methanol	65	60	87.8	0.8876
2-propanol	82.4	75	92.9	0.8786
1-buthanol	117	110	92.1	0.8782
ethanol	78.5	75	95.8	0.8814

Table 4: Influence of the catalyst weight for NaCsX catalysts [Leclreq, 2001](101)

Catalysts weight (g)	Catalyst	Conversion (%)	Selectivity (%)	Ester molar fraction (%)	Mass balance (%)
0.25	NaCs34)X	34	90	61	89
0.5	NaCs34)X	70	96	88	96
0.5	NaCs43)X	55	94	82	90
1.0	NaCs43)X	76	93	91	92
2.0	NaCs34)X	-	-	99	-

Table 5 : Physical Data for All Tested Catalysts (before and after Mg Loading)(103)

catalyst	Surface area (m^2/g)	Pore size, (Å)	Pore volume, (cc/g)	Mg (atomic %)
Pure mesoporous silica				
MCM-41	1172	36.7	1.08	
KIT-6	661	60.7	1.00	
SBA-15	679	50.3	0.85	
Mesoporous silica impregnated with MgO				
M/MgO(A)	391	27.0	0.26	10.96
K/MgO(A)	112	46.8	0.13	8.44
S/MgO(A)	252	37.6	0.24	15.41
S/MgO(N)	315	25.7	0.20	15.26
SBA-15 with insitu coating of MgO				
MgO(A)-S	531	69.6	0.92	4.58
MgO(N)-S	524	69.4	0.91	1.45

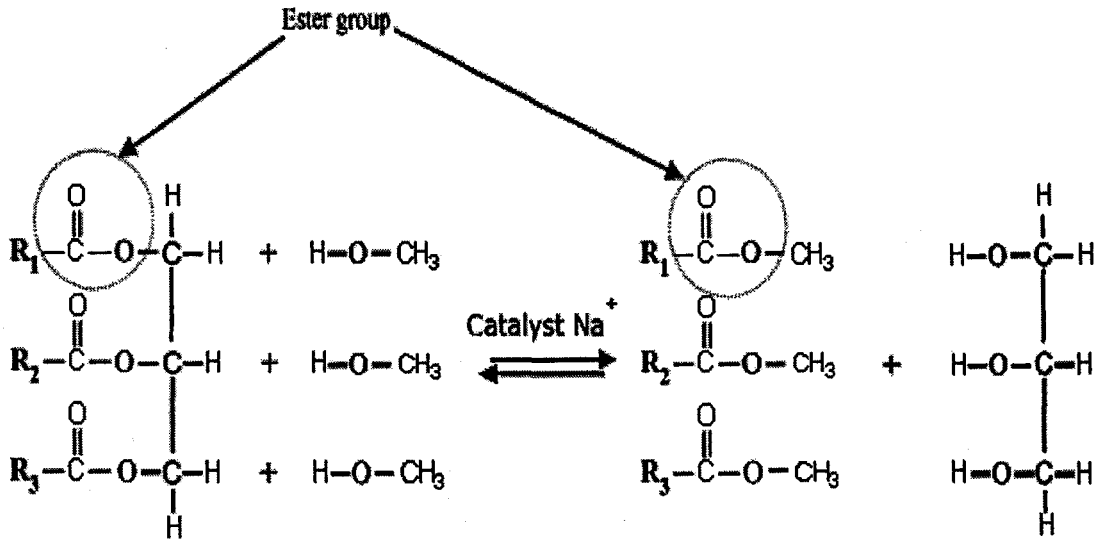

Figure 1: Overall scheme of the triglycerides transesterification (29)

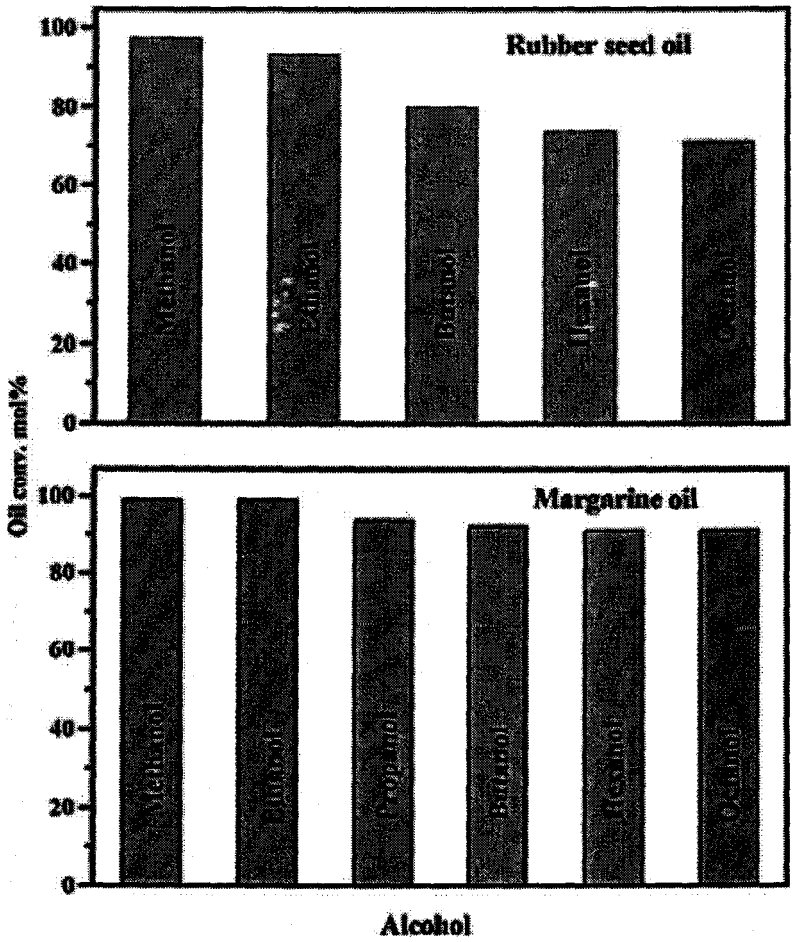

Figure 2: Influence of the type of alcohol on the tranesterification of rubber seed and margarine oils over Fe–Zn-1 catalyst. Reaction conditions: catalyst, 3 wt% of oil; oil, 5 g; oil:alcohol = 1:15 mol/mol; temperature, 443 K; reaction time, 8 h. (92).

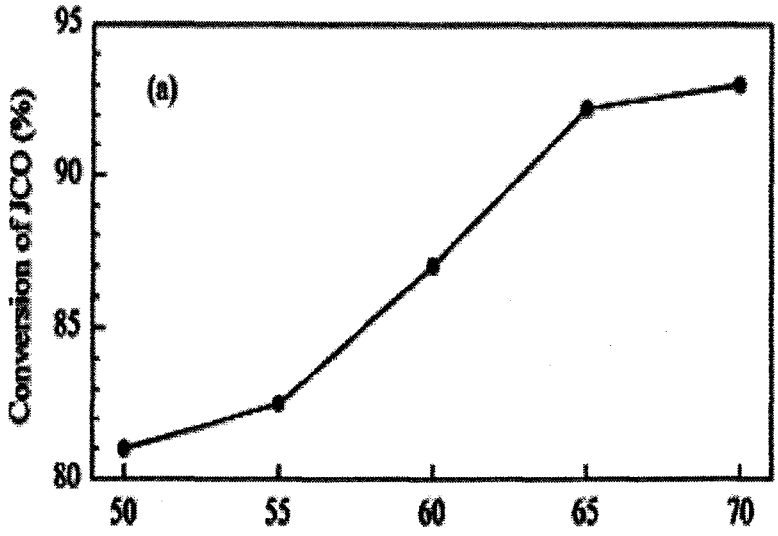

Figure 3: Influence of reaction temperature on the transesterification of JCO (*n* methanol:*n* JCO) = 9:1, catalyst dosage 1.5%, reaction time 2.5 h (96)

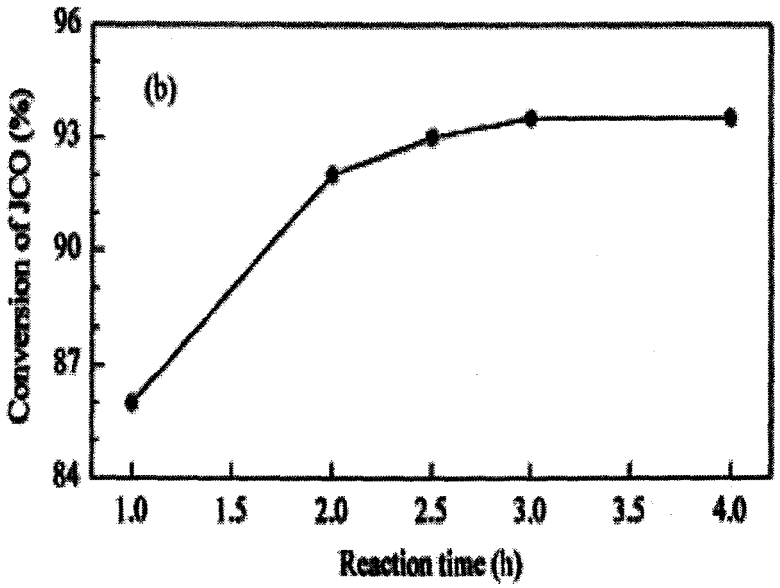

Figure 4: Influence of reaction time on the transesterification of JCO (*n* methanol:*n* JCO) = 9:1, catalyst dosage 1.5%, reaction temperature 70 °C (96)

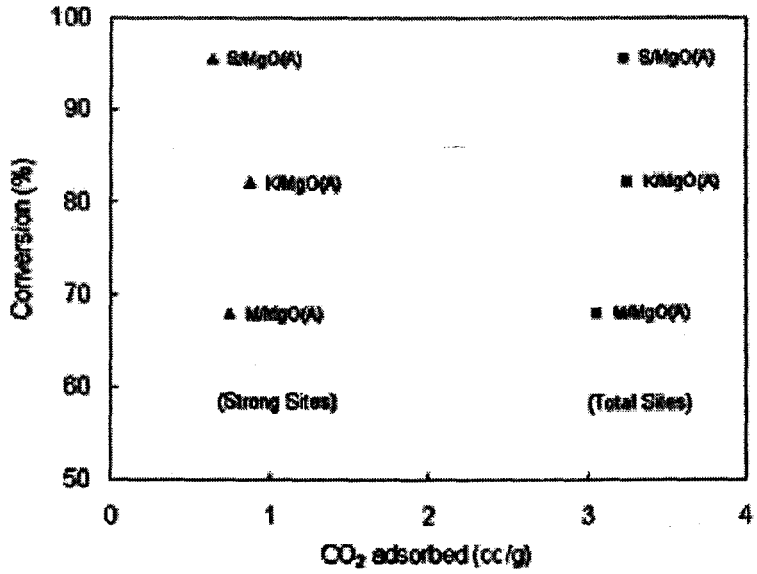

Figure 5: Correlation between the basicity of the catalyst and ester conversion (▲, CO_2 adsorption at 5 mmHg; ■, CO_2 adsorption at 760 mmHg) (103).